The Dissertation Committee for Sarah Margaret Mayes Certifies that this is the approved version of the following dissertation:

HYALURONIC ACID AND ALGINATE BLEND HYDROGEL FILMS FOR THE PREVENTION OF POSTSURGICAL ADHESIONS

Committee:

Jeanne Stachowiak, Supervisor

Christine E. Schmidt, Co-Supervisor

Laura Suggs

Krishnendu Roy

Thomas Jozefiak

Timothy George

HYALURONIC ACID AND ALGINATE BLEND HYDROGEL
FILMS FOR THE PREVENTION OF POSTSURGICAL ADHESIONS

by

Sarah Margaret Mayes, B.S. Ch.E; M.S.E.

Dissertation

Presented to the Faculty of the Graduate School of

The University of Texas at Austin

in Partial Fulfillment

of the Requirements

for the Degree of

Doctor of Philosophy

The University of Texas at Austin

May 2013

Dedication

This work is dedicated to my family: Eric Mayes, Henry Mayes and Wyatt Mayes. To Eric, for letting me go first, for your insane guitar skills, and for raising our children to respect the art of education. To Henry, for giving me a "door to happiness" that I walk through every single day. To Wyatt, for gripping and shaking the snot outta life. We're gonna have fun, and we'll like it!

P.S. Eric, it's your turn.

Acknowledgements

I would like to thank my supervisor, Christine Schmidt, for having faith in me and for having a vast appreciation for science, motherhood, and all things in between. Your vision is a driving force for those around you. Thank you to Laura Suggs for tossing me a lifesaver, more than once. I am indebted to you for your recommendations and redirection. To Krishnendu Roy for your frank, but kind, consideration. I never left your office feeling less than awesome. Thomas Jozefiak, thank you for your insightful questions that both prevented and allowed much sleep. Your perspective brought invaluable direction.

There are several colleagues who have assisted with this research. Scott Zawko, who enlightened me of my strengths and faults, and challenged my abilities with endless patience. To John Hardy, for schooling me in the art of chemistry, and for calming me. To Richelle, for being my rock and my inspiration, girl; to Ryan and Hieu, for 90's jams and whole foods and for teaching the boys to box. Thanks for keeping this journey real. To Julie, Erica, and Cheng, who listened and nodded patiently to hours of pointlessness and made me believe that I could be a scientist. To Daniel Peterson, who dreamed the dream, made things happen, and for having mad surgical skills. Thank you for building this ship. To John Joyoprayitno, for blinding me with science, for Pearl Jam, and for steering this ship. To Jessie and Jessie, who allowed me to guide them in their pursuit of science. Of all my accomplishments, mentoring you two was my greatest. It has been a tremendous honor to be a part of your education. I expect great things from both of you.

Finally, to my parents, for providing the confidence that I could reach the shore, as long as I set sail. To Henry and Wyatt, for providing both the anchor and the wind. And Eric, for providing neverending humor that makes me laugh until I fall off my chair.

HYALURONIC ACID AND ALGINATE BLEND HYDROGEL FILMS FOR THE PREVENTION OF POSTSURGICAL ADHESIONS

Sarah Margaret Mayes, Ph.D.

The University of Texas at Austin, 2013

Supervisor: Jeanne Stachowiak

Co-supervisor: Christine E. Schmidt

Postoperative adhesions form as the body's natural response to injury in an effort to temporarily protect and supply nutrients to these tissues. However, adhesions can remain permanent, and fail otherwise successful surgeries by tethering tissues together that are normally separated. An ideal anti-adhesive device reduces unwanted adhesions and leaves the patient in a state most similar to before surgery. This dissertation introduces a novel, robust hydrogel film consisting of two hydrophilic polydisaccharides, hyaluronic acid (HA) and alginate. To address the challenge of retaining HA in alginate-rich hydrogels, we methacrylated the HA (GMHA), creating hydrophobic moieties. These hydrophobic interactions shift the percolation threshold, allowing for greater concentrations of GMHA to be retained in resulting films. UV crosslinking retains GMHA beyond the percolation threshold and widens the possibilities of usable films. To enhance the mechanical properties of these alginate/GMHA films, we employed a previously developed method for creating thin, branched, interconnected fibers using urea crystal templating. Templated films are softer and, yet, tougher than films that have not been templated. This toughness is a result of increased density of polymer in the fibers. These films were selected as most conformable and most robust by surgeons in a blinded

handling study. In a rat peritoneal abrasion model for adhesion formation, the films successfully prevented adhesions with statistical equivalence to the leading anti-adhesion device commercially available. Finally, future recommendations are suggested for the development of a bilayer construct with a collagen/alginate blend bound to an alginate/HA layer for an anti-adhesive and regenerative strategy. This construct addresses the need for opposing strategies in the dynamic environment of wound healing. Further research is needed to develop the usefulness of this bilayer system, as preventing unwanted adhesions is merely a first step in achieving a blemish-free healed wound.

Table of Contents

List of Tables

List of Figures

Chapter 1: Introduction

1.1 ADHESIONS AND CURRENT TECHNOLOGIES

Postoperative adhesions have long been established as a major complication to otherwise successful surgeries (Harris 1904, Ellis 1971). Despite tremendous efforts to resolve this unwanted scar formation there exists no consistently efficacious and safe solution (Brochhausen *et al* 2011). Adhesions form in the normal, acute phase of injury, and resolve in an equilibrium state between fibrin deposition and fibrinolysis until the injury site has healed (Sulaiman 2001, Ward & Panitch 2011). However, these fibrinous strands may remain well beyond the healing period and tether tissues that are normally separated (**Figure 1.1**), causing chronic pain, loss of function, infertility, and bowel obstruction (Menzies & Ellis 1990, DiZerega 1994, Cui *et al* 2009). Adhesion formation occurs in over 90% of abdominopelvic procedures (Ellis *et al* 1999), generating the need for additional procedures in over 33% of patients (Yeo *et al* 2007). An annual $3.45 billion (US) is spent in hospitalization costs associated with adhesion-related complications (Wiseman *et al* 2010).
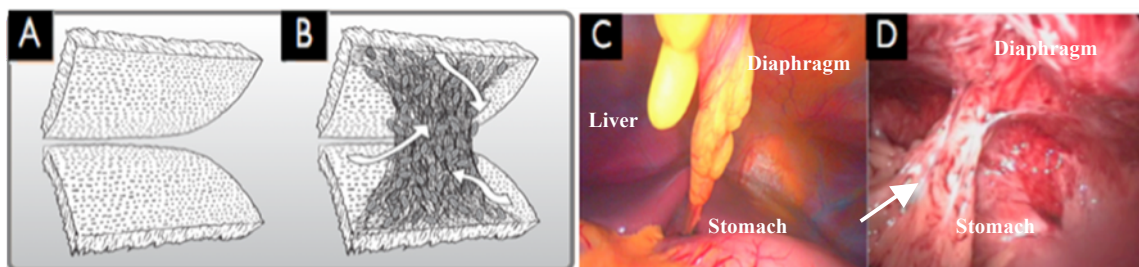
Figure 1.1 Adhesion formation. A) A diagram illustrating two healthy tissues normally separated. B) A diagram illustrating the aberrant response to surgical trauma with fibrous band formation. C) A laparoscopic view of a normal peritoneal cavity with liver, diaphragm, and stomach indicated. D) An endoscopic view of adhesions formed between the stomach and diaphragm. Aberrant adhesion caused by abdominal surgery indicated by the white arrow.

Efforts to resolve unwanted adhesions have included improvements in surgical techniques (Holmdahl *et al* 1997), pharmaceutical methods (Liu *et al* 2005), and barrier devices to mechanically separate tissues. Barrier devices have had the greatest success of any adhesion prevention method (Gago *et al* 2003, Ward & Panitch 2011). These devices include sprays, gels, solutions, *in situ* gelling polymers, and pre-formed membranes. Many attractive liquid-based technologies have failed due to dilution with bodily fluids and migration from the injury site (Ward & Panitch 2011). Gels and *in situ* gelling formulations initially received much enthusiasm because they conform to tissue geometries and can be laparoscopically delivered. However, these gels are unable to provide sustained mechanical separation to prevent adhesions. (Park *et al* 2010)

Many sophisticated technologies have reached FDA approval for adhesion prevention, and have greatly enhanced our understanding of guiding scar formation. **Table 1.1** outlines the attributes of the four FDA-approved anti-adhesion pre-formed membranes. Arguably, the most effective is Genzyme's Seprafilm®, a pre-formed membrane consisting of chemically modified hyaluronic acid (HA) and carboxymethylcellulose (CMC). Although SurgiWrap, Interceed, and REPEL-CV are elegant in design, Seprafilm® is particularly clever because of its incorporation of modified HA, a natural polysaccharide known to aid in repair. SurgiWrap and REPEL-CV rely on synthetic materials, which offer reduced costs, yet synthetics have been known to cause infection or to be ineffective in the presence of infection. Interceed has mixed reviews with some studies indicating adhesion induction (Kayaoglu *et al* 2005). Despite its efficacy, Seprafilm® is highly underutilized because it has little conformability and toughness, components necessary for robust handling properties and overall efficacy. When wet, the membrane loses mechanical integrity and cannot be manipulated. When dry, the membrane is brittle. Medical professionals are recommended

to take precautions such as changing into new, dry gloves and fully desiccating the surgical area. Often multiple units are wasted because of difficulty in handling. Currently, there are no commercially available devices that safely prevent adhesion formation and are easy to use within the operating room setting.

No commercially available sutureless anti-adhesion barrier is approved by the FDA for use in laparoscopic procedures. Procedures such as prostatectomy, oopherectomy, hysterectomy, and bowel resection are now being performed regularly through minimally invasive incisions. Over 96% of the one million cholecystectomies performed annually in the United States are conducted laparoscopically (Riall *et al* 2011). Previously unthinkable feats are accomplished via laparoscope or da Vinci™ robot. Therefore, an effective anti-adhesion pre-formed membrane with adequate handling characteristics that allow laparoscopic manipulation could be revolutionary for surgical outcomes.

Barrier Device (Company)	Interceed (Ethicon)	Seprafilm (Genzyme)	Surgiwrap (MAST Biosurgery)	REPEL -CV (SyntheMed)
Model				
FDA approval and indication	PMA approved in 1993 for gynecological adhesion prevention	PMA approved in 1996 for abdominal adhesion prevention	510K approved in 2007 for abdominal reduction of soft tissue attachments	PMA approved in 2009 for pediatric cardiothoracic adhesion prevention
Material constituents	Oxidized regenerated cellulose	Hyaluronic Acid / Carboxymethylcellulose	70:30 Poly (L-lactide-co-D, L-lactide)	Polylactide and polyethylene glycol (PEG)
Properties	• Thin, paper-like membrane shipped dry • Forms a gelatinous mass that covers injured surfaces upon application	• Thin sheet similar to Listerine patch • Forms a viscous gel if hydrated • Bioabsorbed in 28 days	• Lactic acid derivatives in a sheet form are delivered to injured area, then secured with staples or sutures • Degrades into water and CO_2 by bulk hydrolysis	• Biodegradable sheet that is shipped dry, but applied wet, and is then secured with staples or sutures • Hydrolyzes in 28 days
Advantages	• Naturally based materials • Significant clinical data with efficacy up to 50% (Franklin et al 1995)	• Naturally based materials • Significant clinical data with efficacy up to 48% (www.seprafilm.com)	• Repositionable when wet • Laparoscopically delivered • Transparent • High tensile strength	• Repositionable when wet • Laparoscopically deliverable • Transparent • High tensile strength
Disadvantages	• Limited effectiveness with blood and fluids • Difficult to handle • Cannot be used in laparoscopic applications	• Brittle / weak • Difficult to handle • Not repositionable • Cannot be used in laparoscopic applications	• Synthetic material - not resistant to infection (cases of protrusion, collections due to infection) • Requires fixative	• Synthetic material - not resistant to infection (cases of protrusion, collections due to infection) • Requires fixative
What we have learned from this technology	• Some natural materials serve as procoagulant and are not rendered effective at preventing adhesions in the presence of blood or blood proteins (Al-Jabri & Tulandi 2011)	• Seprafilm is effective as an adhesion barrier because of mechanical separation of tissues not through biological interference (Gago et al 2003)	• Some synthetic materials that are biocompatible in small amounts may actually be harmful in large amounts • No clinical data (DeWilde et al 2007) • 510k approval for soft tissue attachment barrier	• Because FDA did not approve broader market indications, SyntheMed's limited sales severely impaired corporate viability

Table 1.1   Current FDA approved pre-formed anti-adhesion devices.

1.2 AN IDEAL ANTI-ADHESION DEVICE

An ideal adhesion barrier is in the form of a pre-formed membrane, not a gel or in-situ formed film or instillate. Pre-formed membranes are controlled sit-specific care and remain in the injury site throughout wound healing. An ideal adhesion barrier has the following properties:

- Conformable and tough to withstand manipulations and laparoscopic delivery
- Briefly repositionable to allow clinical placement within the surgical field
- Tissue adherent to avoid requiring sutures or tacks to keep implant in place
- Rapidly resorbable after critical healing period

However, these criteria are often in contradiction with one another (**Figure 1.2**). An implant with robust mechanical properties may not be easily resorbed or dissolved. Similarly, a repositionable implant is not likely to be tissue adherent. Barriers of natural polymers, such as hyaluronic acid and cellulose, satisfy the criteria for tissue adherence and rapid dissolution but are often weak, difficult to handle, and not repositionable within the surgical site. Barriers of synthetic polymers, such as polylactide and polytetrafluoroethylene, satisfy the criteria for toughness and repositionability but are slow to resorb and require sutures or staples to hold them in place, making them cumbersome for the laparoscopic environment. This dissertation describes a film that combines the attractive properties of both natural and synthetic barriers by being initially conformable and tough, allowing for repositioning, and by becoming tissue adherent and resorbable shortly after implantation. This film can be passed through laparoscopic trocars and secured in place without sutures, thus making it ideal for use in a laparoscopic environment.

The overall strategy for an adhesion barrier is to provide preventative care during the critical healing period. Therefore, a "less is more" approach should be taken in the

development of any device for this space. In other words, the minimum amount of material that can provide a satisfactory amount of toughness will resorb the fastest.
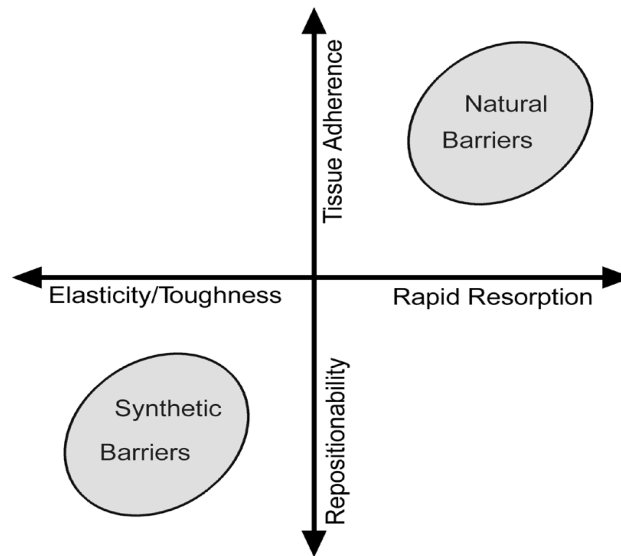
Figure 1.2 Requirements of an adhesion barrier. The critical barrier to progress in adhesion prevention is that neither the current natural nor synthetic adhesion barriers have satisfied all the ideal criteria desired by surgeons. (Acknowledgement: unpublished by Zawko, SA)

There is no standardized universally accepted "handleability" concept for implantable tissue-engineered devices. In fact, many devices are commercialized without widespread assessment for usability or for pairing with tools commonly available to surgeons. However, the ease-of-use of a device is paramount to its success. Thin films are attractive biomimetic devices because of their high surface area-to-volume ratio that maximizes tissue surface impact and minimizes foreign body response. Many thin film devices are currently available to provide soft tissue support during wound healing and/or locally deliver drugs. Assessing the mechanical properties of thin films can be challenging because of practical limitations. This dissertation correlates conformability of

6

thin films to stiffness measurements, and overall handling to toughness measurements. Most importantly, these parameters can be obtained through straightforward tensile testing that does not require specialized equipment or skills. Furthermore, this dissertation presents dynamic mechanical testing as a method useful in assessing the performance of thin films during tacking and peeling, which can be correlated to how the film is handled.

1.3 FABRICATION OF A TRANSLATABLE FILM

To address handling issues for surgical use, films need to be of appropriate clinical size and consistency. Frequently throughout this work we invited local surgeons for assessment. It was decided that a 72 mm by 72 mm (3 in by 3 in) film was adequate for these assessments (**Figure 1.3**). Duragen, a collagen-based product used for dural repair, is marketed at this size. The smallest FDA approved adhesion barrier, Surgiwrap, is 50 mm by 70 mm (2.00 in by 2.75 in) (www.mastbio.com). The smallest tensile specimen dogbone size dictated by tensile standard ASTM D638 can be used to obtain 6 samples from a 72 mm by 72 mm form (ASTM D638 2010). Standard petri dishes were not used because of the inherent slight gradient on the bottom of the dish, which imparts a thickness change that has significant impacts on mechanical testing consistency. Thickness testing is detailed in Chapter 3. The forms used were custom-built by the aerospace engineering machine shop at The University of Texas at Austin. Forms are clear polycarbonate and are machined with wall thicknesses of 3 ± 0.0127 mm and flat-bottom leveling within $0.25°$ ($\pm$ 15 min). For all experiments discussed in this dissertation, the 72 mm by 72 mm size is used, unless specified. Furthermore, the shelves in the environmental chamber were custom-built by the aerospace engineering machine

shop. Each shelf has three leveling screws, and were checked for levelness before each batch of films were cast, to ensure film thickness was as consistent as possible across each film.
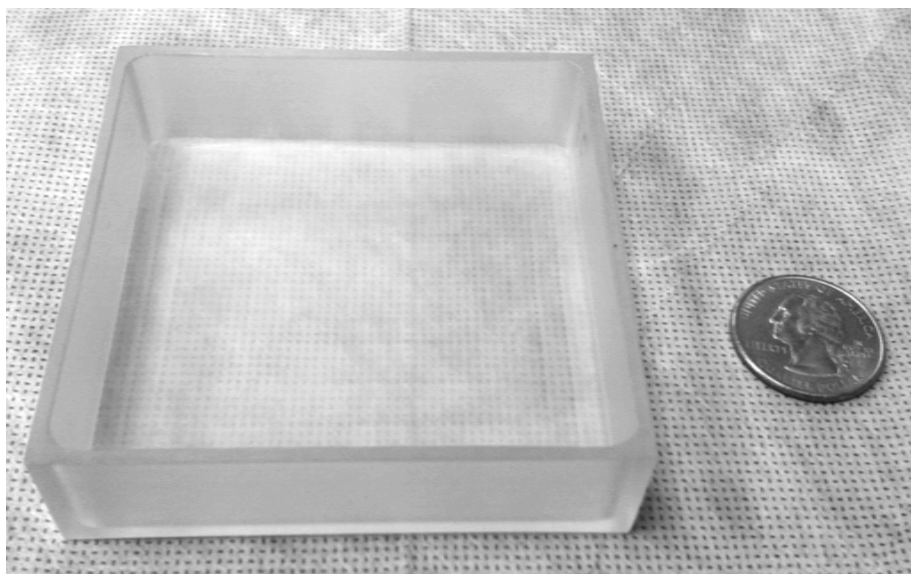
Figure 1.3 **Scale-up form for film casting**. All films in this dissertation were fabricated in a 72 mm by 72 mm form. This form fabricates films with consistent, clinically-relevant dimensions. This form is level and produces films of even thickness.

1.4 ORGANIZATION AND GOALS

This project takes on the challenge of improving the handling characteristics, utility, and efficacy of a hyaluronic acid-based film as a surgical implant and, specifically, as an anti-adhesive barrier in abdominopelvic indications. The approach involves exploration of a blend of modified HA and alginate(s) in a variety of compositions that define a range of physical properties for this blend. Secondly, this approach is to explore a processing technique to impart fibers into the hydrogel blend for

the direct consequence of improved mechanical properties. The ultimate aim of this project, therefore, is the development of a biocompatible, hydrophilic, natural polysaccharide-based thin film that has physical properties optimized for use in laparoscopic surgical procedures. Furthermore, this project aims to capture handling properties with mechanical testing techniques, to support design rules of future materials to be used in an operating room setting. These goals are achieved through physical characterization of various HA/alginate compositions, accompanied by surgeon handling to validate mechanical test results, and finally, implantation of the film into the well-known rat cecal/sidewall abrasion model. There has been much work documented for anti-adhesion devices utilizing HA or alginate, yet few studies with both polymers as a blend. Those studies regarding blended HA and alginate are limited to beads or gels with significantly different physical and chemical properties than the present work. Furthermore, ease of use is not quantified by these studies. This project introduces a film to be used as a surgical adjunct that is novel both in composition and in fabrication.

This dissertation comprises seven chapters, including this introduction. Chapter 2 reviews the rationale for use of HA in anti-adhesion environments, modification for photopolymerizable HA, and handling issues with photocrosslinked HA films. Chapter 3 reviews the rationale for strategic use of alginate in anti-adhesion environments, modifications for photocrosslinkable alginate, the purification of alginate for biomedical applications, and the characterization of alginate films. Chapter 4 details film synthesis and physical characterization. The films explored in Chapter 4 are modified HA/alginate blends. This exploration offers a unique perspective in bringing these two polymers together, in a way that has not previously been documented. The conclusions from Chapter 4 explain the fundamental materials science behavior of HA/alginate blended films. Chapter 5 presents mechanical testing of these thin hydrogel films and how these

results relate to real-world handling. To improve upon handling characteristics, a previously developed method to impart fibers in a hydrogel is added to the film fabrication technique. The details of improved handling are described in Chapter 6. Chapter 7 presents both *in vitro* and *in vivo* data for the use of the improved films as an anti-adhesion membrane. Cell studies provide impetus for conducting animal studies. The rat cecal/sidewall abrasion model for adhesion formation is detailed and results are presented. Finally, Chapter 8 provides recommendations for future work.

Chapter 2: Glycidyl Methacrylated Hyaluronic Acid

2.1 HYALURONIC ACID

Hyaluronic acid (HA) is a linear, long-chain glycosaminoglycan synthesized by every cell in every animal. HA is comprised of two residues, D-glucuronic acid and D-N-acetylglucosamine, that alternate repeatedly. HA is the only glycosaminoglycan synthesized in the hydrophobic core of the cell membrane, and is a very hydrophilic polysaccharide. This hydrophilicity is due to its polyanionic charge, which causes water to bind to its surface very tightly. This feature allows HA the ability to provide compressive support such as in knees and joints, to lubricate surfaces such as the eyes, and to remove debris from injury sites during wound healing. Its ubiquitous presence and biological utility, and its uniquely high hydrophilicity make HA well known for wound healing applications both natively and as a component of tissue-engineered devices. Of particular interest is the use of HA in anti-adhesive environments because its strong attraction of water prevents the adherence of proteins and cells.

The average healthy adult has approximately 15 g of HA present at any given time. Not template-directed, HA is polydisperse and has a wide range of native molecular weights from <10kDa to 8 MDa. The natural state of HA is as a viscous aqueous solution as in synovial fluids and extracellular fluids. HA has a high turnover rate, with replacement every 24-72 hours. Thus, unmodified HA solutions are used commercially as short-term bolus injections to hydrate joints and to reduce stiffness and pains associated with injury. And it follows that unmodified HA solutions are not reasonable for longer-term applications that require in vivo residency on the order of days or weeks.

Hyaluronic acid has several available functional groups that can be used to crosslink these long chains. Methacrylation is a popular method for crosslinking HA

because this method is relatively straightforward and occurs upon exposure to UV, which can be highly tailored. (Zhao *et al* 2013) Photocrosslinking is attractive because degree of crosslinking or time of crosslinking or patterned crosslinking can be controlled for specific applications, durations, and uses. Thus, photocrosslinking offers a simple and relatively inexpensive method for tunable HA-based constructs. Previously developed protocols for methacrylating HA using glycidyl methacrylate have been well described (Reis *et al* 2009, Li *et al* 2003, Bencherif *et al* 2009, Leach JB & Schmidt CE 2005, Zawko 2008). From this point forward GMHA refers to HA that has been methacrylated by the method described here. The advantages and disadvantages of this technique over other techniques, such as methacrylic anhydride modification, are well documented (Seidlits *et al* 2010). However, spectroscopic investigation of resultant modification of HA is largely controversial.

This chapter provides more specific details regarding the resulting GMHA synthesized from our protocol, and the issues associated with scale-up of pure GMHA films. The structure of HA, triethyl amine, glycidyl methacrylate, and an assumed product structure of GMHA are in **Figure 2.1**.

2.2 GLYCIDYL METHACRYLATE MODIFIED HYALURONIC ACID

Previously in the Schmidt lab, GMHA was dissolved in deuterium oxide and solution-state ^{1}H NMR was utilized to determine the degree of methacrylation by comparing the methyl peaks at 1.95 ppm and 1.85 ppm. (Baier 2003) Specifically, the peak at 1.95 ppm was interpreted as the methyl located on the amine group of the glucosamine residue. The peak at 1.85 ppm, that is not present in spectra of as-received HA, was interpreted to be the methyl group associated with a conjugated methacrylate

moiety. Since there is one methyl group for each disaccharide unit, and one methyl group for each methacrylate moiety, a ratio of these peaks were taken to represent the degree of methacrylation. However, the relative intensity of these two peaks is quite disparate, and they overlap, making even deconvoluted spectra of questionable value.

Several other studies have attempted to elucidate the end products arising from the reaction of glycidyl methacrylate with carboxylic acid and hydroxyl groups. These studies use model polymers to represent HA, such as polyethylene glycol, polyvinyl alcohol, or polyacrylic acid (Reis *et al* 2009, Bencherif *et al* 2009). Both studies recognize two reactions between HA and GM: transesterification and epoxy ring-opening. Of particular interest are the results reported by Reis *et al* because pH was taken into consideration to determine which reactions were occurring. This work presents model molecules that react differently at low versus high pH, the latter being most pertinent as our reactions are conducted at pH 10.5. According to Reis *et al*, the peaks at 6.18, 5.74, 5.67, 5.36 ppm correspond to methacrylate groups conjugated to hydroxyl groups. According to Reis *et al*, at high pH we should not expect methacrylation of the carboxylic acid group (although it does occur at low pH), and methacrylation occurs preferentially on the hydroxyl groups of the HA. The specific location of the methacrylate functionalization is important when considering the long-term stability of the resulting GMHA, because a functionalized carboxylic acid group is less stable than a functionalized primary hydroxyl group (Bencherif *et al* 2009).

Hyaluronic acid

Triethylamine

Glycidyl methacrylate

Glycidyl methacrylated hyaluronic acid
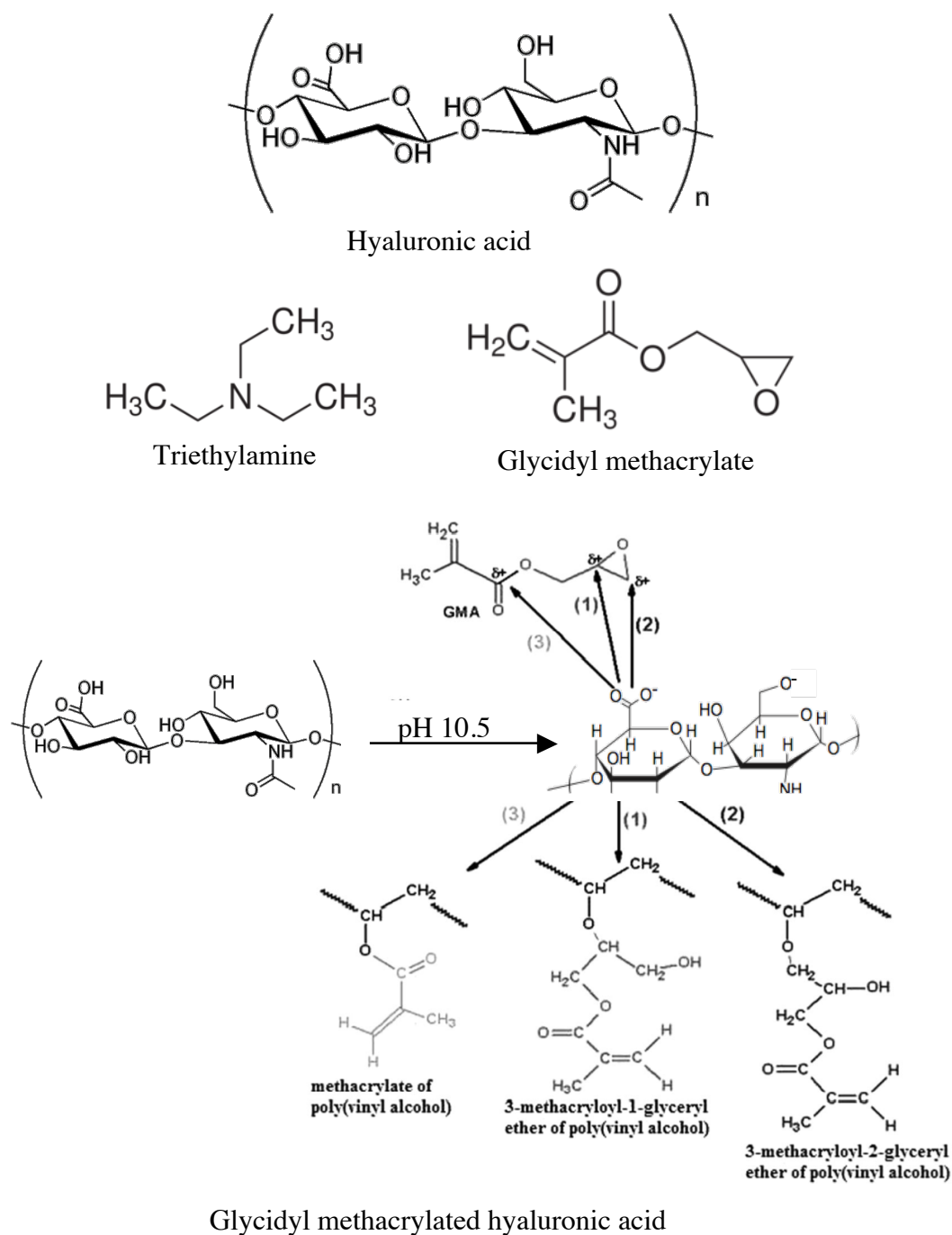
Figure 2.1 Chemical structures of methacrylation reactants and products. (Projected formula for glycidyl methacrylated hyaluronic acid reproduced without permission, Reis *et al* 2009).

14

2.2.1. Viscosity testing. Due to such a hydrophilic nature, aqueous HA solutions greater than 2% are avoided because they are too viscous to assure adequate mixing and the production of a homogeneous solution. However, the process of methacrylating HA results in GMHA solutions that have a significantly lower viscosity than HA solutions (**Figure 2.2**). This reduction of viscosity could be attributed to reduction in molecular weight due to hydrolysis of the polysaccharide backbone at high pH. Alternatively, this reduction could be attributed to conformational changes as a result of the functionalization of the hydrophilic backbone of the HA with less hydrophilic methacrylate groups. To help clarify what happened to the HA molecule upon methacrylation, we prepared a null-GMHA where all steps were taken in the methacrylation process except adding the GM. Rheological characterization compared the viscosity of null-GMHA to unmodified HA, and little difference in viscosity was found. This result suggests that conformational changes occur upon the methacrylation of the HA due to the hydrophobic nature of these moieties. More specifically, water hydrogen bonds strongly to itself and to unmodified HA; therefore, hydrophobic interactions between the methacrylate groups cause the GMHA to have a less extended conformation in solution and the solution viscosity decreases. (Dais *et al* 2005)
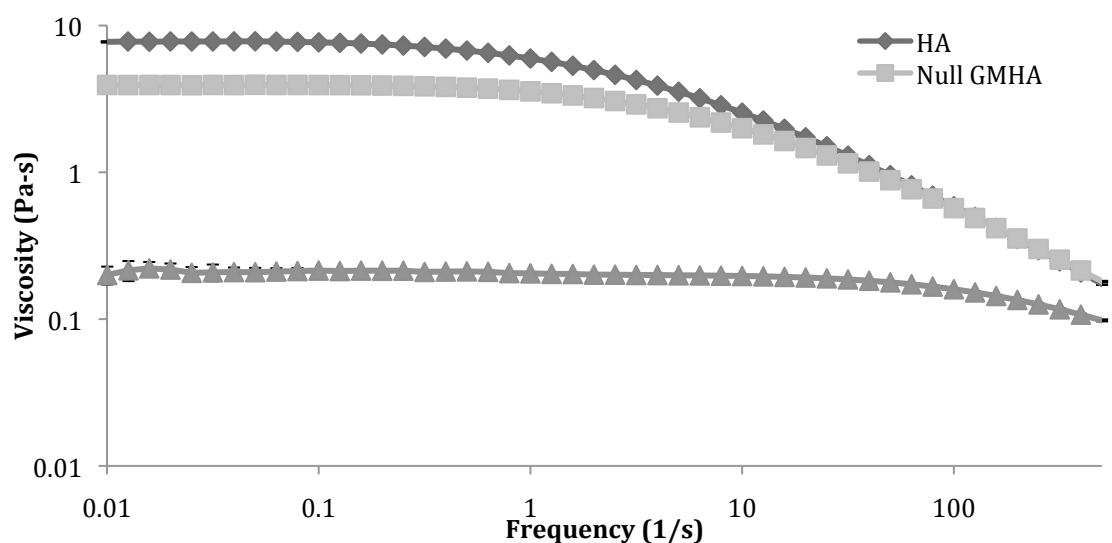
Figure 2.2 **Viscosity of methacrylated HA**. A rheometer was used to determine the viscosity of methacrylated (GMHA), non-methacrylated (Null GMHA), and as-received (HA) 1% solutions in parallel plate construction. The Null GMHA and HA follow the same profile. There is a significant difference in the profile between the HA and Null GMHA vs. the GMHA. The GMHA solution has a significantly lower viscosity than the non-modified HA solutions. Tests were run in triplicate.

2.2.2. NMR. Nuclear magnetic resonance (NMR) is a very powerful method of structure determination and is routinely used for this purpose. Proton NMR is used for the determination of degree of methacrylation of HA because the methyl groups on the HA and the methacrylate can be easily identified. (Reis *et al* 2009, Li *et al* 2003, Bencherif *et al* 2009, Leach JB & Schmidt CE 2005, Zawko 2008) We aimed to determine not only the extent of methacrylation of HA, but also the specific molecular structure of the resultant GMHA. There is a discrepancy between published reports of the resulting products of HA and glycidyl methacrylate. The most thorough investigation previously conducted was by Reis *et al*. This study considered the role of the solution pH in the reaction mechanism leading to various end products. Their results suggested that HA methacrylation conducted at high pH (10.5) produces three different products, and we were curious to know which of these products we were generating in our reactions.

Solution state NMR was conducted similarly to previous Schmidt lab members. Interpreting the spectra in the same manner indicates that we have methacrylated the HA (**Figure 2.3**). There are characteristic peaks present for the methacrylated product, as just described. This result is expected, because when we expose solutions of this GMHA product to UV irradiation, we obtain a self-supporting gel that can be manipulated (as opposed to a viscous solution). Analyzing the spectra further, we hypothesize that the triplet at 1.2 ppm and the quartet at 3.1 ppm are from the triethylamine (TEA) salt of the GMHA. Characteristic TEA spectra have a triplet at 0.99 ppm and a quartet at 2.6 ppm in deuterated water, with an integral ratio of 3:2. (Gottleib *et al* 1997) We hypothesize that a shift in TEA peaks occurs as a result of protonation of the TEA by the carboxylic acid groups on HA (HA-CO2$^-$.HN$^+$Et$_3$). Our conclusion is supported with the strong similarities between the null-methacrylated and GMHA spectra because TEA was the only chemical added to the null methacrylated HA. (**Figure 2.4**) The peak ratio in

GMHA does not correlate as well as the null-methacrylated, most likely due to impurities, as suggested by Bencherif and coworkers. Future recommendations include either adding a step in the GMHA protocol for further dialyzing in sodium chloride to remove any unwanted TEA, or perhaps omitting the TEA altogether and using sodium hydroxide (Reis *et al* 2009).
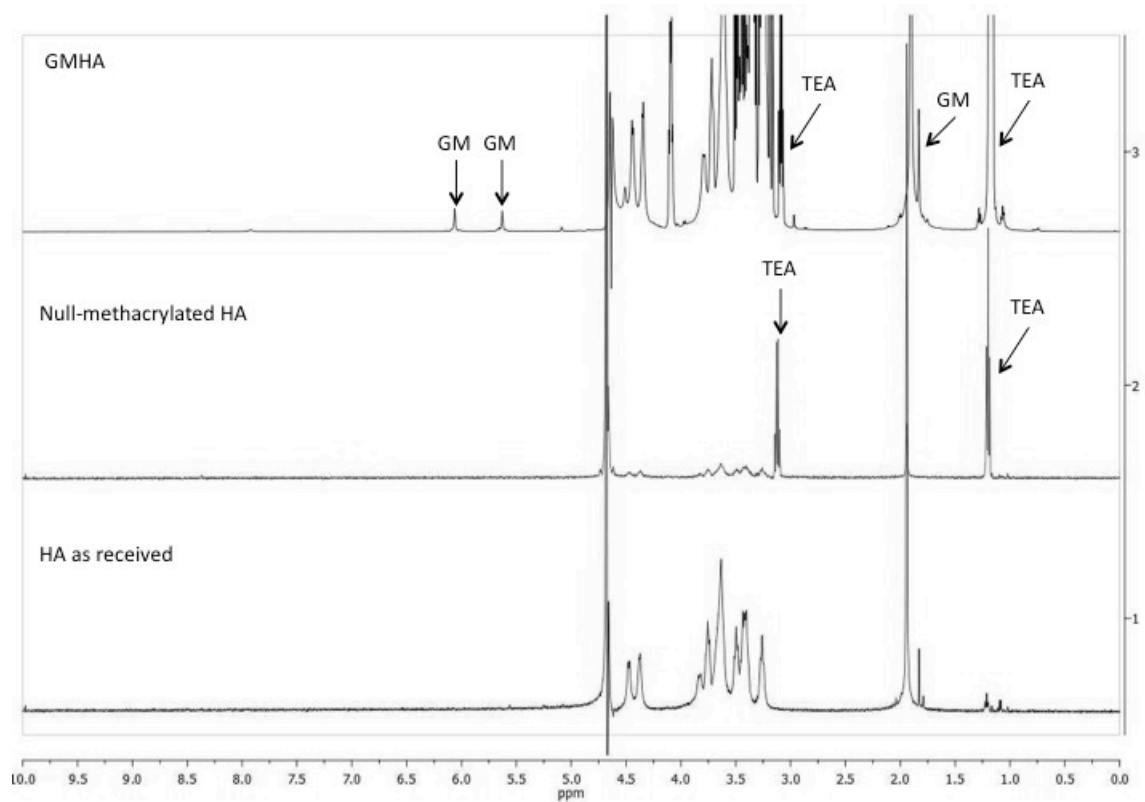
Figure 2.3 Solution state ^{1}H NMR spectra in D$_2$O. As received HA, null-methacrylated HA, and GMHA(32) were analyzed for hydrogens on the methacrylate group of glycidyl methacrylate. There is clear evidence of methacrylation from the solution state proton NMR spectra.
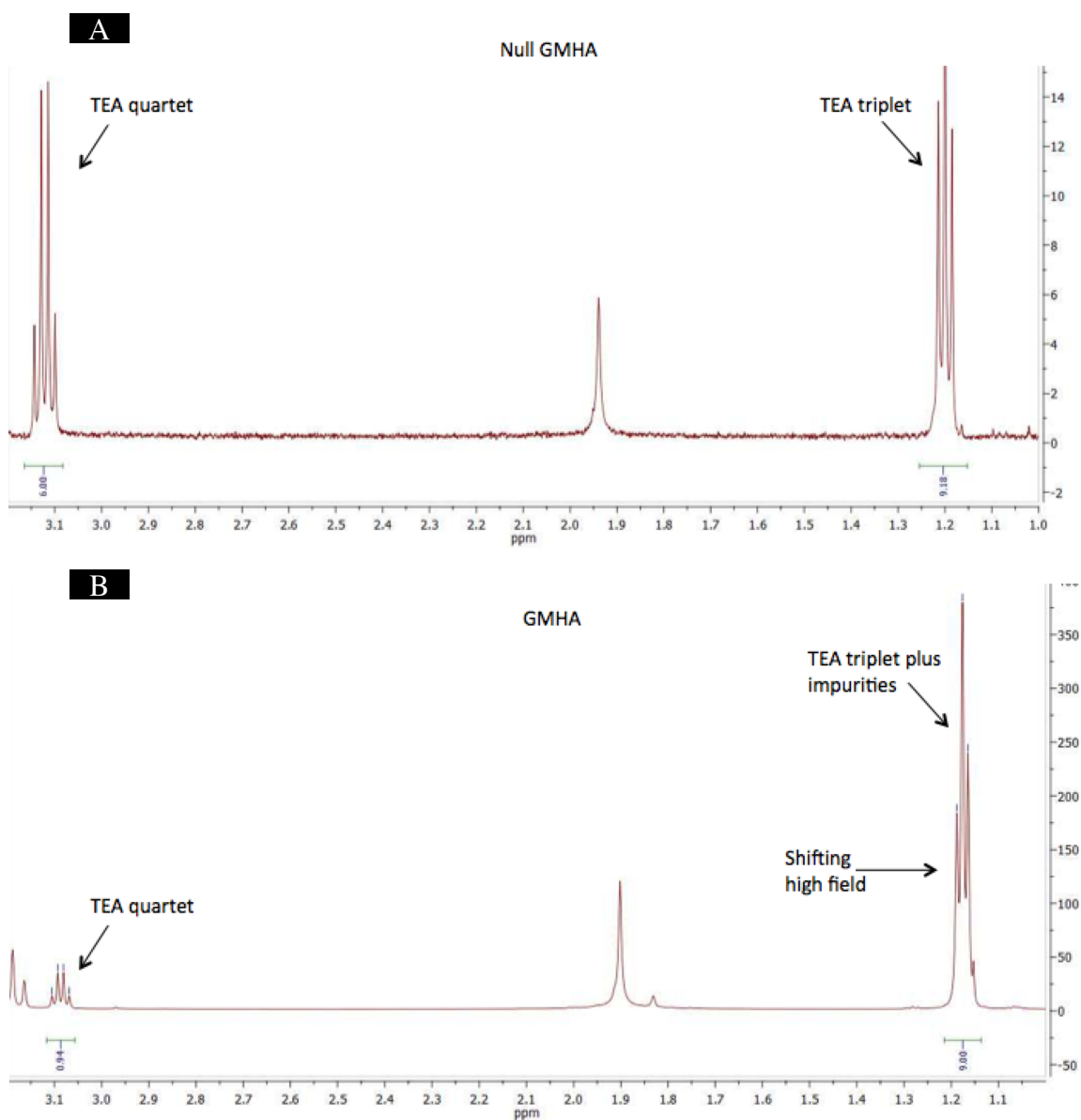
Figure 2.4 ¹H NMR evidence of TEA. A) Null-methacrylated HA spectra indicate that TEA is bound to the HA by the shifted characteristic TEA triplet at 1.2 ppm and quartet at 3.1 ppm. Furthermore the integral ratio is 3:2. B) GMHA spectra indicate that TEA may also be present as there is the characteristic quartet at 3.1 ppm, and perhaps the TEA triplet has been shifted slightly from an impurity (Bencherif *et al* 2009). The integral ratio is 9:1, which indicates there are impurities present, and not just TEA.

2.3 HANDLING ISSUES WITH GMHA FILMS

Previous members of the Schmidt lab adequately documented the synthesis and characterization of GMHA films. (Zawko 2008) These 2.2 cm diameter films were evaluated by surgeons for use as an anti-adhesion nerve wrap (**Appendix A**). The results of this evaluation indicate that GMHA films are useful because they can be applied while hydrated, and are translucent, allowing the surgeon to visually see the surgical field during placement. However, the GMHA films were too weak for manipulation or suturing, and had a persistent tendency to roll into a tube upon hydration.

2.3.1. Film Curling. Rolling into a tube-like form is referred to as curling and is common to thin films and the thin plastics industry. (Goetz 2002) Curling is typically a result of non-uniform crystallization or crosslinking. Commercially available plastic sheets typically have more than one layer, which can lead to unwanted layer-to-layer variations in crystallization rate or extent. These variations can cause one layer to shrink faster or greater than another layer, resulting in physical curling of the film towards the more crosslinked layer. Efforts to reduce curling include slowing down curing time, increasing humidity while curing, and assuring uniform curing. We hypothesized that the tendency for GMHA to curl into a tube was the result of uneven photocrosslinking. There are two ways that non-uniform crosslinking could occur. The UV spot-lamp (365 nm wavelength) used to photocure the smaller films had a peak intensity diameter of about 1cm. Mercury UV lamps traditionally have peak intensities directly parallel to lamp direction, with intensity rapidly decreasing at small angles from lamp direction. A radiometer placed directly under the spot lamp measures radiation of 22 mW/cm^2, with intensity quickly dropping to 12 mW/cm^2 at a location 2 cm radial to the first measurement. Thus, there could be variable rate of crosslinking. Also, there may be a slight gradient across the thickness of the film with greater crosslinking on the side closer

to the UV lamp. When placed in water, these gradients may induce a slight difference in swelling, with greater swelling corresponding to lower crosslinking. This reduced swelling causes curling to occur in the direction of greatest crosslinking. (Liu *et al* 2013)

To overcome this issue we obtained a custom-built UV chamber that uses mirrors to reflect and to direct lamp output uniformly across an area 12.7 cm by 12.7 cm (5 in by 5 in). Furthermore, the radiation power of the lamp was measured at 201 mW/ cm^2 at a distance 30 cm from the lamp at several places within the chamber even outside the designated 12.7 cm by 12.7 cm area. (This measurement was taken while lamp was in standby mode; lamp output exceeded the radiometer capabilities when in full mode.) The lamp requires about 30 min to reach maximum output, so the chamber was turned on 30 min prior to use for all experiments in this dissertation. To determine correlation between exposure time of the spot lamp vs. the chamber, we used a GMHA hydrogel with known properties, and ran a "gel test". For every batch of GMHA and GMHA films, we ran a "gel test" to ensure that the lamp, the photoiniator, and the GMHA were capable of satisfactory gelation. A GMHA hydrogel has the same qualitative properties after 5 min of exposure to the spot lamp as with 30 seconds of exposure to the chamber lamp. Therefore all "gel tests" and films in this dissertation were exposed to 30 seconds of UV in the chamber unless otherwise noted.

We placed 3.5 cm diameter films within the 12.7 cm by 12.7 cm area of greatest power output and exposed the top, the bottom, or both sides to UV light. Despite the efforts to provide uniform crosslinking, we did not solve the curling tendency of the films because this issue is not a result of variable intensity when full crosslinking is achieved. Rolling could be a result of the anisotropic orientation that HA takes in aqueous solutions. (Dais *et al* 2005) Although HA is a linear molecule, hydrogen bonds are responsible for a secondary worm-like coil structure when in water. In a film, unlike a

22

non-cast gel, the HA molecules are very densely packed. This dense packing may cause the hydrated film to take on the overall structure of the anisotropic GMHA molecules, causing the film to coil or roll. Also, HA has a large radius of gyration in water. Perhaps the GMHA molecules wanting to expand cause the curling. Perhaps curling is a result of edge effects.

2.3.2. Scale-up and Mechanical Weakness. Ultimately we had great difficulty making GMHA films of the 72 mm by 72 mm larger size. These films were too weak to be easily lifted from the form surface. Furthermore, the films appeared to swell significantly more than those films made in the 2.2 cm or 3.5 cm diameter wells. Most likely this difference is due to the edge-to-area ratio. As a solution casts, water is evaporated. As water is removed, the viscosity increases, which subsequently causes an increase in surface tension, particularly when a surface is present. This phenomenon causes a thickening of film at the edges of its casting container. In a 2.2 cm diameter, the edge-to-area ratio is 1.82. In a 72 mm diameter film, the edge-to-area ratio is 0.06. Therefore a GMHA film cast in a 2.2 cm well has handling properties not observed with larger films. It is important to note that film-handling properties previously discussed regarding smaller films (Zawko 2008) are not the same as the larger films. Despite increasing the amount of polymer cast and degree of methacrylation, we were unable to obtain a large film of GMHA-only that could be adequately removed from the form and handled. Other issues noted were visibility and the slippery surface of the films. Although it is advantageous to see the surgical field while implanting a device, a clear film has hindrances when attempting to pull it from water. The index of refraction of these films is too similar to water to visualize. Also, the surface of the GMHA films are so well hydrated that utensils (tweezers) have difficulty grasping and subsequently holding onto the film.

2.4 CONCLUSIONS

Hyaluronic acid (HA) can be modified by a variety of methods. Glycidyl methacrylation is a method that results in multiple end products with varying stability. Suggested end products are modeled by conjugation of polyvinyl alcohol and polyacetic acid, but are less defined with HA. Ultimately, HA can be conjugated with methacrylate groups that provide photocrosslinking capability of HA derivatives. However, at even high degrees of modification of HA, resulting films do not have mechanical integrity for applications such as an implantable device for laparoscopic delivery. We conclude that a support system is required to deliver HA to the body, whether that support system is a removal component or a mesh or a blend.

2.5 MATERIALS AND METHODS

2.5.1. Materials. High molecular weight sodium hyaluronate from *Streptococcus equi* of molecular weight $1.6x10^6$ Da was obtained from Sigma-Aldrich (St. Louis, MO). Low molecular weight sodium hyaluronate from bacterial fermentation of molecular weight $3.1x10^4$ Da was obtained from Lifecore (Chaska, MN). Photoinitiator Irgacure 2959 (I2959) was obtained from Ciba Specialty Chemicals (Basel, Switzerland). All other chemical reagents were obtained from Sigma-Aldrich. A longwave UV lamp filtered around 365 nm was used to initiate photopolymerization of films 2.2 cm in diameter (Blak-Ray B-100A, UVP, Upland, CA). A longwave UV chamber with a mercury bulb filtered around 365 nm was used to initiate photopolymerization of films greater than 2.2 cm in diameter and for the 3" x 3" films (TOTAL-CURE UV Power Shot 1100 Curing Station, SPDI, Delray Beach, FL). A radiometer with 40 W/cm^2 detection limit for UVA was used to measure power output of the UV lamp and chamber (Dymax, ACCU-CAL™ 50). Dialysis tubing of 3500 MWCO were purchased from Spectrum Laboratories (Rancho Dominguez, CA). Sterile filtration was conducted using 0.22 μm bottletop filters (Corning Life Sciences, Tewksbury, MA).

2.5.2. Methacryloyl modification of hyaluronic acid. High molecular weight and low molecular weight HA were conjugated with photocrosslinkable methacryloyl groups based on two protocols (Zawko 2008, Bencherif *et al* 2008). A 1% w/v solution of HA was prepared in a 50:50 mixture of acetone:water and stirred for 24 hours at room temperature. Twenty molar equivalents of both triethylamine as base catalyst and of glycidyl methacrylate were added to the solution and stirred for 1,2,5,7, or 10 days at room temperature. For null-methacrylated GMHA solutions, the glycidyl methacrylate was not added but the solution remained stirring at room temperature for the same duration as the other GMHA solutions. High molecular weight modified HA (GMHA)

was precipitated into a 20-fold volumetric excess of acetone and then subsequently dissolved in water for 24 hours at room temperature. Low molecular weight modified HA (GMHA) was not precipitated. Both high molecular and low molecular weight GMHA's were then dialyzed against distilled, deionized (ddI) water in 3500 MWCO for 72 hours. Samples were lyophilized after filter sterilization and stored in dessicators at -20 °C. The average degree of methacrylate substitution was determined by solution state H[1] NMR and found to be 0.22 moles of methacryloyl groups per mole of HA disaccharides. Previous studies reported 0.32 moles of methacryloyl groups per mole of HA disaccharides, but had a slightly different protocol. (Zawko 2008)

2.5.3. Null-GMHA modification of hyaluronic acid. High and low molecular weight HA was subjected to processing of 2.4.2 without the addition of glycidyl methacrylate. A 1% w/v solution of HA was prepared in a 50:50 mixture of acetone:water and stirred for 24 hours at room temperature. Twenty molar equivalents of triethylamine as base catalyst was added to the solution and stirred for 5 days at room temperature. Null-GMHA was precipitated into a 20-fold volumetric excess of acetone and then subsequently dissolved in water for 24 hours at room temperature. Null-GMHA was dialyzed against ddI water in 3500 MWCO for 72 hours. Samples were lyophilized after filter sterilization and stored in dessicators at -20 °C. The average degree of methacrylate substitution was determined by solution state H[1] NMR and found to be 0 moles of methacryloyl groups per mole of HA disaccharides.

2.5.4. Solution state NMR. ^{1}H NMR samples were dissolved in deuterium oxide at 2.5 mg/mL and the spectra recorded on a Varian Unity +300 spectrometer. The degree of methacrylation (DM) was calculated by integration of HA methyl protons (1.90 ppm) and methacrylate methyl protons (1.85 ppm).

26

2.5.5. Viscosity testing. Viscosity is a measurement of the resistance to flow. Resistance to flow can be determined with resistance to shear forces. Rheological measurements were taken with an AR-G2 Rheometer from TA Instruments (New Castle, DE) to obtain resistance to shear forces of HA, GMHA, and null-methacrylated GMHA. Viscous properties were measured as Pa-s of 1mL of solution using parallel plate geometry diameter of 60 mm, gap size of 1 mm, and inducing a frequency sweep from 0.01 to 1000 Hz. All measurements were performed in triplicate at room temperature.

2.5.6. Gel test. To ensure that all components of the photocrosslinking system were functioning properly, a "gel test" was conducted before using a batch of GMHA, photoinitator solution, and the UV chamber. This test was a simple, quick, and practical method for ensuring gelation. A 1% w/v aqueous solution of photoinitiator Irgacure 2959 was sonicated for 30 min and allowed to cool to room temperature. GMHA was then added to this solution to resolve a 2% w/v mixture, and stirred overnight in the dark at room temperature. Parafilm was placed in a 3.5 cm petri dish, and a 200μL droplet was placed on the parafilm surface. The droplets were exposed to either UV from the spot lamp or the chamber for 30 seconds or until gelation depending on the experiment. Gelation was determined qualitatively by picking the droplet up with a spatula (**Figure 2.5**). If the droplet has properly reached gelation, then the droplet will be cohesive and will not drip from an inverted spatula. If droplet was runny or dripped from the spatula, the gel test was considered a fail. All tests were done in triplicate at room temperature.

2.5.7. Synthesis of photocrosslinked GMHA films. A 1% w/v aqueous solution of photoinitiator Irgacure 2959 was sonicated for 30 min and allowed to cool to room temperature. GMHA was then added to this solution to resolve a 1% w/v mixture, and stirred overnight in the dark at room temperature. Amount of polymer cast was based on area of form, for 0.068 mg/cm^3. A 2.2 cm diameter well had 26 mg of polymer cast. A

3.5 cm diameter well had 65 mg of polymer cast. A 72 mm by 72 mm form had 350 mg of polymer cast. Forms were placed in a temperature and humidity controlled environmental chamber from Cincinnati Sub-Zero (Cincinnati, Oh). Temperature was held at 25 °C and humidity was held at 70% Rh during the casting period of 48 hours. Forms and solutions were kept from light at all times. Cast films were then subjected to UV light from the spot lamp or the chamber, depending on experiment. Crosslinked films were removed from molds, when possible, and transferred to petri dishes with large volumes of ddI water.

2.5.8. Curling tests. GMHA films were cast in 3.5 mm diameter petri dishes per the method described in Section 2.4.5. Cast films were removed from the environmental chamber and immediately exposed to UV in the UV chamber. Petri dishes were placed in the center of the chamber, one at a time, and exposed to 30 sec of UV. Films were exposed to either 30 sec on the top surface, flipped over for 30 sec on the bottom surface, or were exposed to 15 sec on top and 15 sec on bottom. Films were then placed in large petri dishes with ddI water and curling was observed. Orientation was maintained and noted by video recording. All tests were done in triplicate at room temperature.

2.5.9 Statistical analysis. All data are presented as mean ± standard deviation.
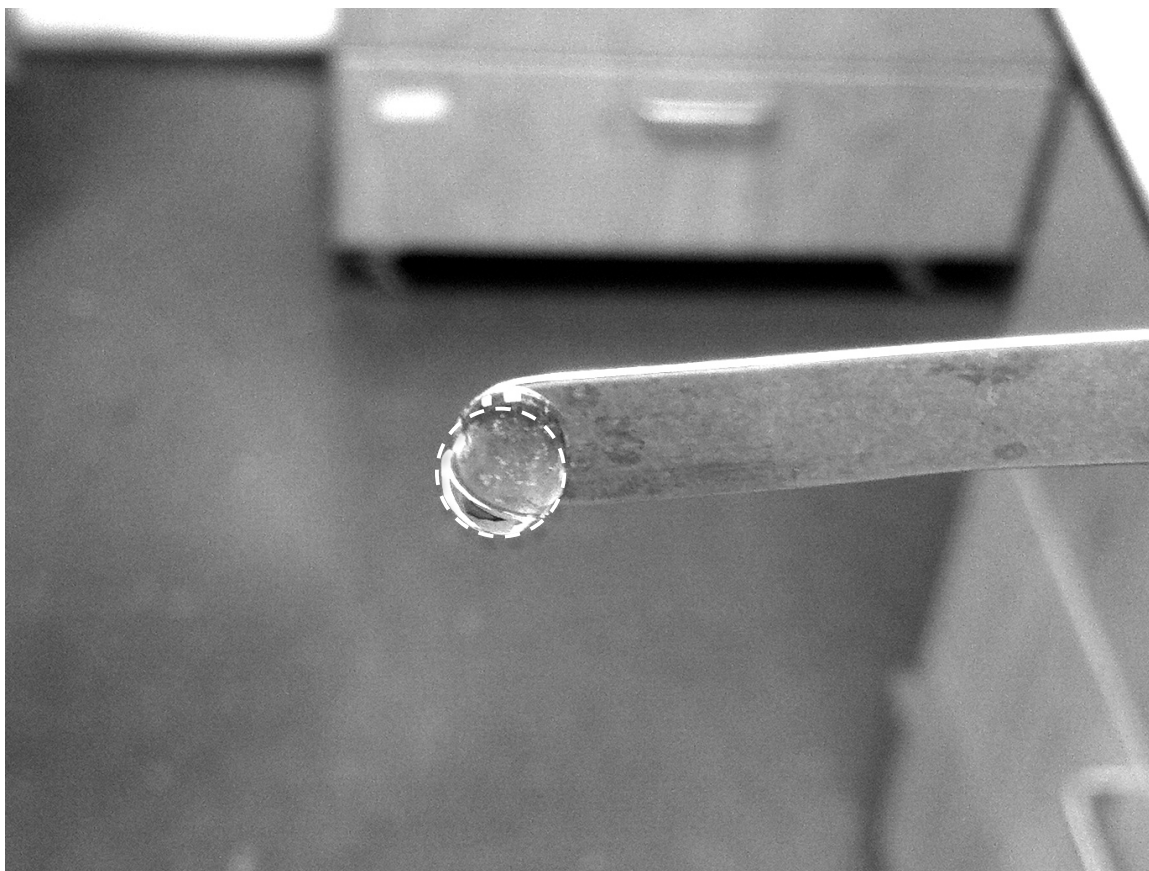
Figure 2.5   Gel test. A test to validate that all parts of the UV crosslinking system were working, was conducted on every batch of UV crosslinked films. This test ensured that the GMHA was methacryated to a useful degree of methacryalation, that the photoinitatior solution was properly mixed and functioning, and that the lamp output of the UV chamber was able to produce a predictably firm gel based on qualitative observation. Shown here is a droplet of GMHA UV crosslinked from a 2% solution in 1% irgacure 2959. The dotted white circle indicates the edge of the gel that is not dripping from the inverted spatula.

Chapter 3: Gelled Alginate Films

3.1 ALGINATE

Alginate is a long-chain polyanionic polydisccharide derived from deep ocean brown algae. Products derived from alginate permeate almost every area of life from textiles to food to biofuels. Alginate gels and beads are the subject of much research for cell encapsulation and drug delivery. (De Vos *et al* 1997, Becker *et al* 2000) The use of alginate in wound healing devices dates back to 1200 BC. Many commercially available wound dressings to treat second and third degree burns are alginate-based. Like HA, alginate provides a lubricious environment that supports healing through tissue hydration. In fact, many of alginate's properties are similar to HA, validating alginate's reputation as the plant version of hyaluronic acid.

A feature unique to alginate is its ability to gel in the presence of divalent cations. This phenomena has been the subject of intense research for over half a century. (Smidsrod & Haug 1965). Although simple in description, the ability for alginate to associate strongly with divalent cations such as calcium is complex and is depicted by an "egg-box" model. (Grant *et al* 1973) (**Figure 3.1**) Each alginate disaccharide unit is made up of two covalently linked residues, a (1-4)-linked β-D-mannuronate (M) or its C-5 epimer α-L-guluronate (G), in any combination. Any alginate monomer can appear in homopolymeric blocks of consecutive G (GG) or M (MM) units, or alternating M and G (MG) units. In the "egg-box" model, a calcium ion will associate with four carboxylic acid groups from each of four G units, typically modeled from two sets of GG sequences from two monomers. The more GG sequences in a batch of alginate, the more opportunities are generated for calcium to associate or to bind. When the calcium ion binds to the G residues it replaces water, and induces a reorientation of the polymer chain. The affinity for G residues to bind to calcium is much greater than the affinity for

G residues to bind to water. This replacement of water, subsequent change in molecular orientation with binding to calcium causes the alginate to go through a sol-gel transition. It is important to note that this gelation is unlike typical polymerization or crosslinking. Alginate gelation occurs through favorable associations with divalent cations and is not a step-wise or chain reaction. There are no required initiators or catalysts or toxic intermediate byproducts. Furthermore this gelation can be highly tailored by many variables including M/G unit ratio, polymer concentration, calcium concentration, and exposure duration to calcium-rich solution. The ability to tailor gelation in predictable ways makes this safe, natural, non-immunogenic polymer attractive for tissue engineering applications.

3.2 ALGINATE FILMS

Alginate films were previously characterized in the Schmidt lab, and provided the baseline for understanding alginate behavior for this project. (Zawko & Schmidt 2010) Calcium was selected as the binding ion because calcium is easy to obtain, is native to most tissues in the body, is nontoxic, and provides a stable gelation. (Becker *et al* 2000) Alginate's unique binding features rely on several variables such as purity, M/G ratio and sequence, molecular weight, and exposure to calcium. Previous work conducted in the Schmidt lab utilized research-grade alginate with M/G ratio of 2.23, 88kDa molecular weight, and gelled with 1.3 M $CaCl_2$ solution. To study the mechanics of films resulting from blends of GMHA and alginate, it was of great interest to identify variables that could be rationalized or reduced. A full factorial design was not going to be cost effective with scaled-up films. This section details each variable and how and why decisions were made to optimize the experimental design.

31

Sodium alginate
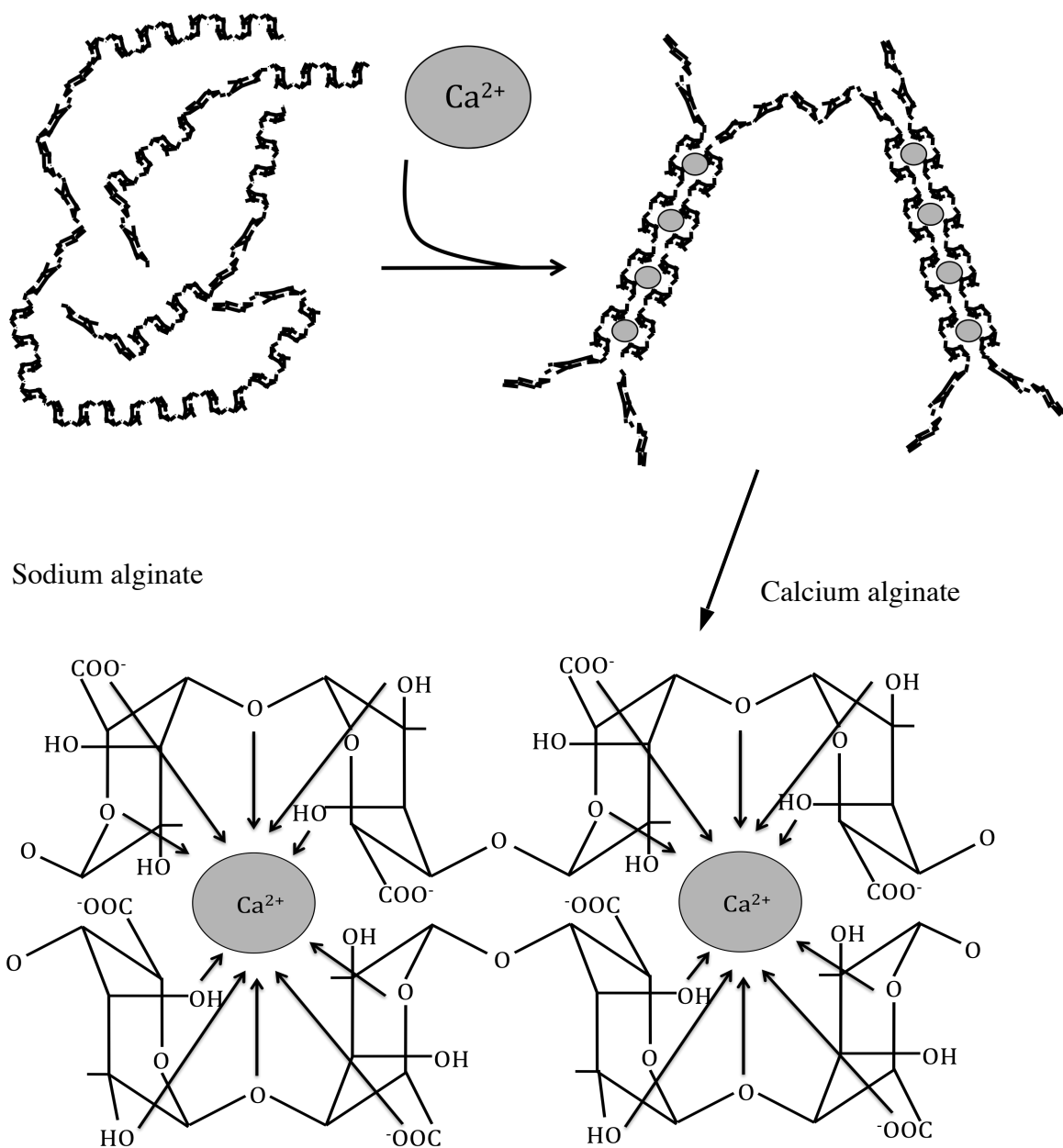
Calcium alginate

Figure 3.1 Egg-box model. When calcium ions are presented to sodium alginate, sodium ions associated with the glucuronate units are replaced by calcium ions. The association of calcium ions with the glucuronate units is facilitated by the orientation of the carboxylic acid groups. The binding of these available groups to calcium is very strong because the calcium ions can stabilize the glucuronic acid units while also creating tunnels of travel for the calcium ions. The association of calcium to alginate causes precipitation of the alginate and calcium alginate is not water-soluble.

3.2.1 Alginate grade. Generally speaking, the bulk of our understanding of alginate film behavior stems from food science. (Julian *et al* 1988) Alginate's hydrophilicity provides water permeable coatings for many common foods, which maintains or alters texture and taste, and can act as a preservative. Grade is important to consider when comparing results or procedures to previous work because food-grade alginate, research grade, and medical grade alginate all have different levels of purity. Purity plays a significant role in the mechanical properties of alginate gels and films. (Becker *et al* 2000) There are three well-known purification methods that differ slightly but each entail removing endotoxins and polyphenols at various pH and temperatures (Klöck *et al* 1994, DeVos *et al* 1997, Menard *et al* 2009). For practical purposes at the academic level, verification that unwanted impurities have been removed is often conducted merely by colorimetry. A pure alginate will appear clear, water-like in aqueous solutions whereas an impure alginate will appear murky and/or yellow in tint. (**Figure 3.2A,B**) Resulting films also have a different appearance. Purified alginate films are smooth where crude alginate films appear mottled. (**Figure 3.2C,D**)

Based on the Klöck and DeVos methods, we developed an in-house method for purifying alginate to better understand the property changes in the resulting films. Films were fabricated from both purified and as-received versions of food grade and research grade alginate. We conducted tensile tests based on ASTM D638 to compare mechanical property differences observed with purification. (**Figure 3.3**) We could not compare the grades to one another. Confounding factors that have great effects on the mechanical properties of alginate films are the M/G ratio and the molecular weight. Typically ^{1}H NMR is used to determine the M/G ratio and is reported by the manufacturer. Molecular weight is determined by fractionation. Both of these tests are expensive and are not conducted on food grade (crude) alginate. Also, research grade alginate easily obtainable

was 88 kDa molecular weight and medical grade alginate easily obtainable was either 40 kDa, 120 kDa or 220 kDa molecular weight. Therefore, we can only compare a purified alginate to its unpurified counterpart. For each alginate, the purified film is less brittle than its impure counterpart, indicated by a decrease in modulus. This change in modulus could be a result of polymer chain untangling. With fewer impurities, polymer chains may have the opportunity to untangle to a greater degree and stretch father prior to failure. Furthermore, a decrease in modulus could be a result of increased water absorption, since water acts as a plasticizer in hydrogels. This increase in water absorption may also explain the decrease in tensile strength of purified alginate films vs. crude counterparts. Purified films had decreased strength compared with crude films.

Further studies were not conducted since it was determined that the cost of in-house purification was not as cost effective as purchasing medical grade alginate. This distinction was important to establish because overall material cost consideration was relevant since each film would be scaled-up to the 72 mm by 72 mm size. Furthermore, an extensive study by Menard *et al* suggests that the patented purification method conducted by FMC Novamatrix is superior to all other methods in the removal of unwanted endotoxins and polyphenols. FMC Novamatrix also has FDA-approved quality control and related documentation, upon request. All other films referred to in this dissertation are comprised of FMC medical grade alginate purified by the manufacturer to > 99% purity.
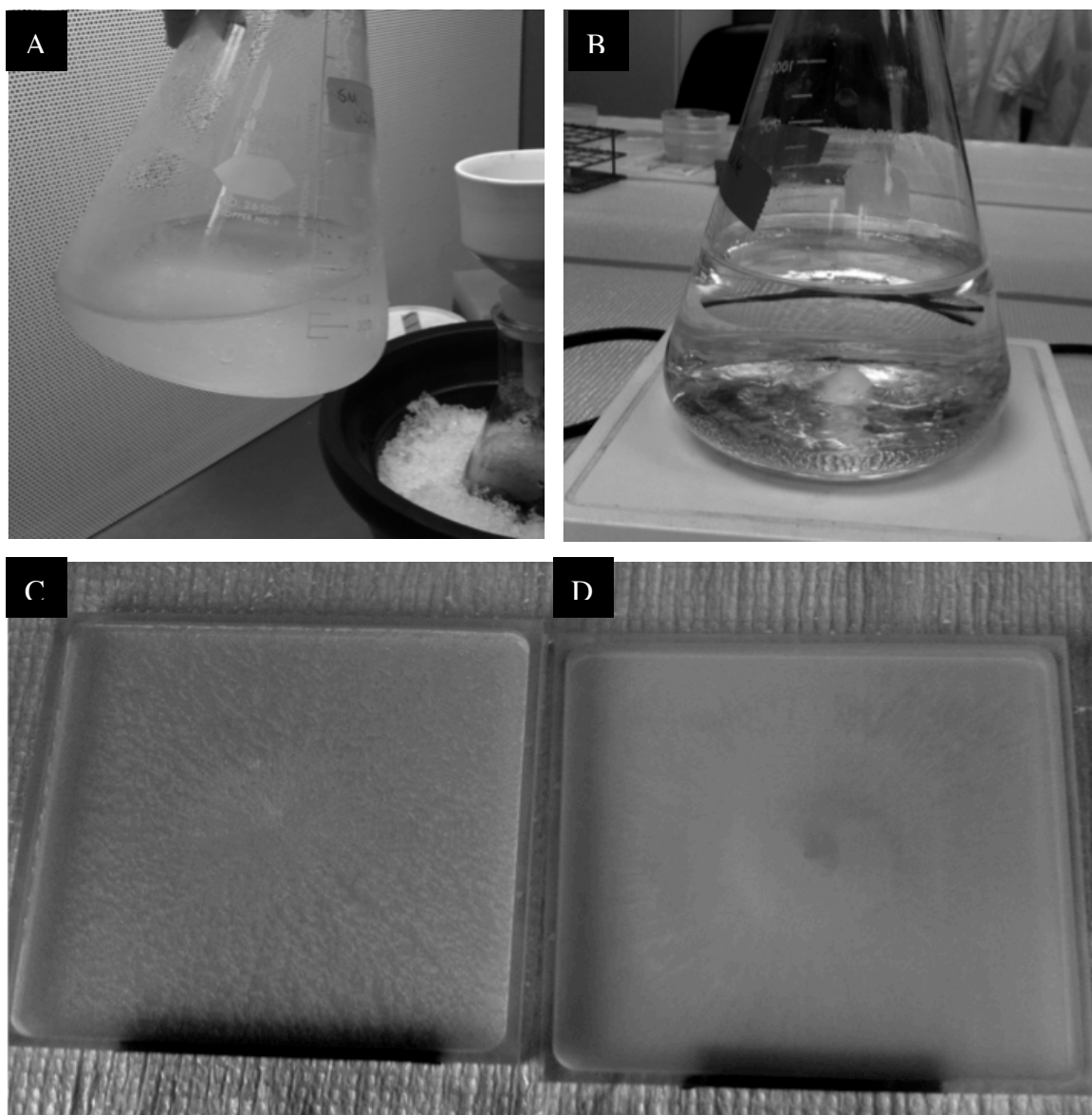
Figure 3.2 **Purification of alginate**. A) Crude alginate makes a murky solution even at dilute conditions. Crude alginate contains many polyphenols and endotoxins and proteins that are unwanted. B) Purified solutions appear clear and have a similar index of refraction as water. C) Crude alginate solutions cast mottled films that are uneven and inconsitent. D) Purified alginate solutions cast smooth films that are consistent in appearance and opacity.
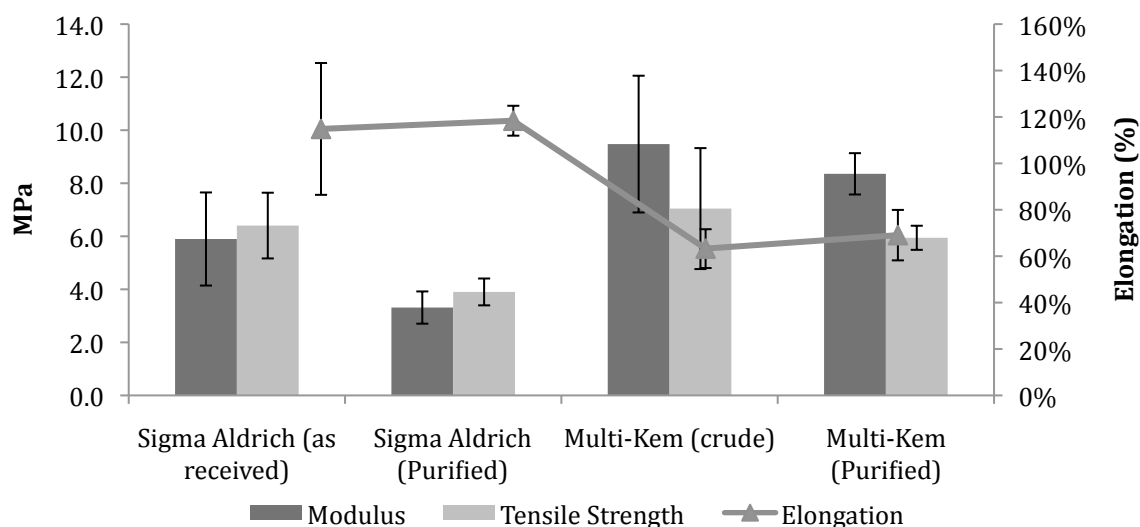
Figure 3.3 **Mechanical changes in alginate films with purification**. Two crude alginates were tested against their purified versions. The films were pulled in tensile guided by ASTM D638. The Sigma Aldrich alginate is 88 kDa average and has an M/G ratio of 2.23. The appearance of as-received Sigma Aldrich alginate solutions (2% w/v) was lightly foggy, pale yellow. The appearance of in-house purified Sigma Aldrich alginate solutions (2% w/v) was clear, water-like. The modulus decreased with purification, indicating a softer, less brittle film. The tensile strength also decreased with purification, indicating a film with less plastic deformation before failing. This same trend was found with an alginate from Multi-Kem. The alginate from Multi-Kem was much cruder and no molecular weight information is known. However the M/G ratio is approximately 1.0. The appearance of as-received Multi-Kem alginate solutions (2% w/v) was very murky and dark yellow. The appearance of in-house purified Multi-Kem alginate solutions (2% w/v) was clear, pale yellow. The modulus decreased with purification, indicating a softer, less brittle film. The tensile strength also decreased, however not statistically.

3.2.2 M/G residue ratio. Typically alginates with higher M/G ratios are derived from the leaves of brown algae, whereas lower M/G ratios are derived from the stems of brown algae. (Haug & Larsen 1962, Haug & Smidsrod 1965) Both the M/G ratio and the M/G sequence (block or random) dictate the mechanical properties of resultant films. (Lee *et al* 1996) Although both types of alginates are used in wound healing devices commercially, high G alginates are more prevalent because of the gelling capabilities. It is well-known that high G calcium-alginate beads and gels are stronger than their high M calcium-alginate counterparts. This increased strength widens the range of possible molecular weights that could produce a strong film. Also, high G alginate gels degrade more slowly than high M alginates. Since HA is known to degrade on the order of hours, it was of interest to increase the residence time of the films at the injury site prior to degradation. Furthermore, sterilization techniques such as gamma radiation or e-beam typically have a negative impact on crosslinking density and may cause an overall decrease in the strength of the films. Unless otherwise stated films consisted of medical grade high G alginate.

3.2.3. Molecular weight of alginate. Polysaccharides are not template-directed and, therefore, are polydisperse. Although fractionation techniques are used to segregate molecular weights, these aggregates retain relatively wide ranges. Mechanical properties of alginate are highly dependent on molecular weight, and these effects are well-documented. (Draget *et al* 1994, Smidsrod & Haug 1972) With increasing molecular weight, there is increased entanglement of polymer, which increases both stiffness and strength of resultant gels and films. Commercially available medical grade alginates commercially available are easily obtainable at median values of 40 kDa, 120 kDa, and 220 kDa. The actual range of polymer molecular weight around these values is quite large. According to the manufacturer, 120 kDa alginate ranges from 20 kDa to 200 kDa.

We attempted to make films of all three of these medical-grade alginates. The 40 kDa alginate did not make a film that could be removed from the form at any calcium chloride concentration, and was not considered for further study. The 120 kDa and the 220 kDa alginates crosslinked with 100 mM calcium chloride made films that could be handled, and were pulled in tension based on ASTM D882. (**Figure 3.4**) An increase in molecular weight has a trend of increasing the brittleness and overall strength of the film, which follows what is found in literature. (Draget *et al* 1994) This increased strength most likely is a result of increased entanglement of longer polymer chains.

Although higher molecular weight alginate produces stronger films, the degradation profile *in vivo* may be inadequate. Sodium alginate greater than 48 kDa are not renally cleared. (Al-Shamkhani *et al* 1995) According to Al-Shamkhani et al, intraperitoneal injections of molecular weight ranging from 108 kDa to under 40 kDa were radiolabeled and tracked for 24 hours. Over 63% of the alginate was recovered from the urine. However, the average molecular weight of alginate found in the urine was 48 kDa. This suggests that higher molecular weights may take much longer to be hydrolyzed and cleared from the body. Although 24 hours is too short a duration, an anti-adhesion device should be fully dissolved within 28 days of implantation. Molecular weight of alginate may play a significant role in the dissolution rate of anti-adhesion films *in vivo*. Many studies in this dissertation were conducted comparing 120 kDa to 220 kDa alginate-based films to optimize handling properties with required dissolution rate.
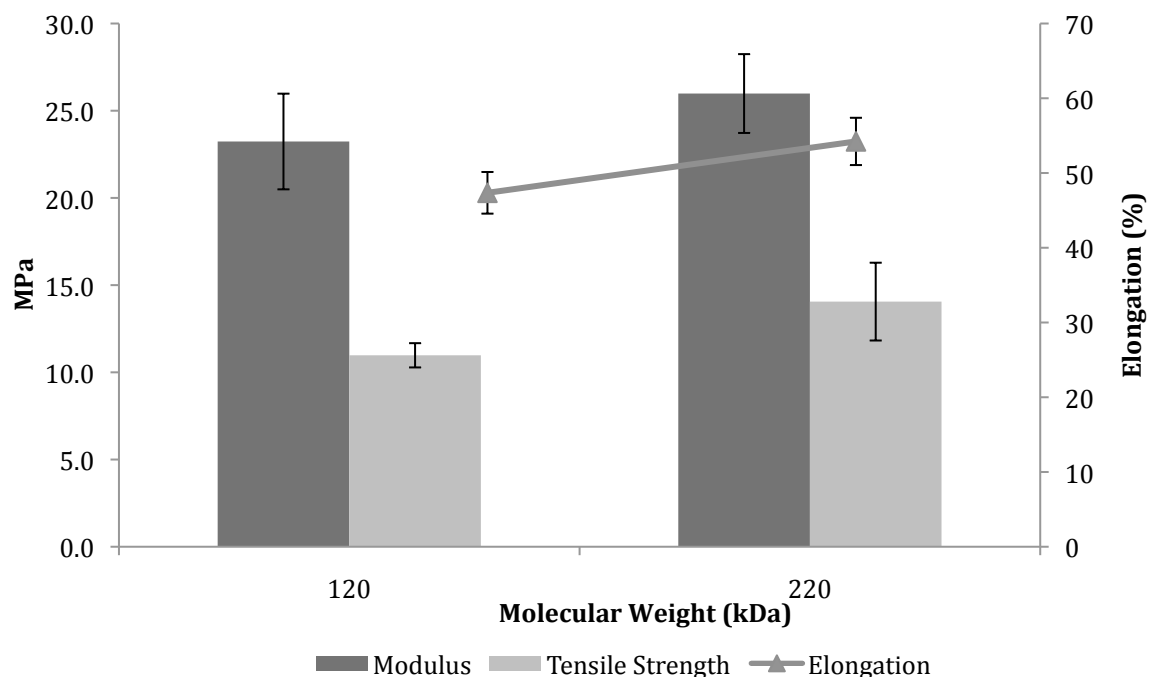
Figure 3.4 **Tensile properties of low vs. high molecular weight alginate**. Medical grade, high G (M/G ratio of 0.67) alginate was pulled in tensile in accordance with ASTM D882. Films with low molecular weight (120 kDa) had a Young's modulus of 23.24 ± 2.74 MPa, tensile strength of 10.98 ± 0.7 MPa, and elongation of 47.35% ± 2.79. Films with high molecular weight (220 kDa) had a Young's modulus of 25.99 ± 2.26 MPa, a tensile strength of 14.06 ± 2.23 MPa, and elongation of 54.23% ± 3.16. The modulus is statistically similar with increased molecular weight but there is a trend of increasing modulus with molecular weight. Higher molecular weight polymers entangle more and resist elastic deformation in comparison to lower molecular weight counterparts. The tensile strength was statistically similar for both molecular weights. Tensile strength is a measure of how much a material deforms before breaking. The overall deformation is influenced by ability to plastically deform. This increase in molecular weight does not significantly change the plastic deformation ability of resulting thin alginate films. Elongation is not statistically different.

3.2.4. Calcium gelation of alginate films. There are two methods for calcium gelation of sodium alginate: internal and external. The internal method involves mixing alginate with an insoluble calcium salt, acidifying the solution to release the calcium for alginate gelation, then extrusion of gelled alginate into oil. (Draget 1994) Resultant gels are more homogenous than those externally gelled gels. However, internally gelled gels are weaker due to significantly larger pore size and subsequent swelling. (Chan 2006)

External calcium gelation involves exposure of sodium alginate to calcium solution, and is simpler than internal gelation because no acidification is required. External gelation differs significantly from internal gelation because the process is a time-dependent balance of gelation and dissolution (**Figure 3.5**). When a cast solution of alginate is exposed to calcium rich aqueous solutions, the water redissolves the alginate while, simultaneously, the calcium associates with the G residues and causes gelation. The higher the calcium concentration in the gelling solution, the less time the water has to swell the alginate before gelation occurs. With less swelling, there is increased density of calcium ion associations that gel alginate chains together. Therefore, resultant films from various calcium concentrations of external gelling solutions have significantly different physical, and resulting mechanical, properties.

It is important to note that the number of calcium ions in the resultant films does not change with varying concentration of calcium chloride. The association that alginate has with calcium is strong and stable. However, these associations may be further apart from one another with lower concentrations of calcium chloride.
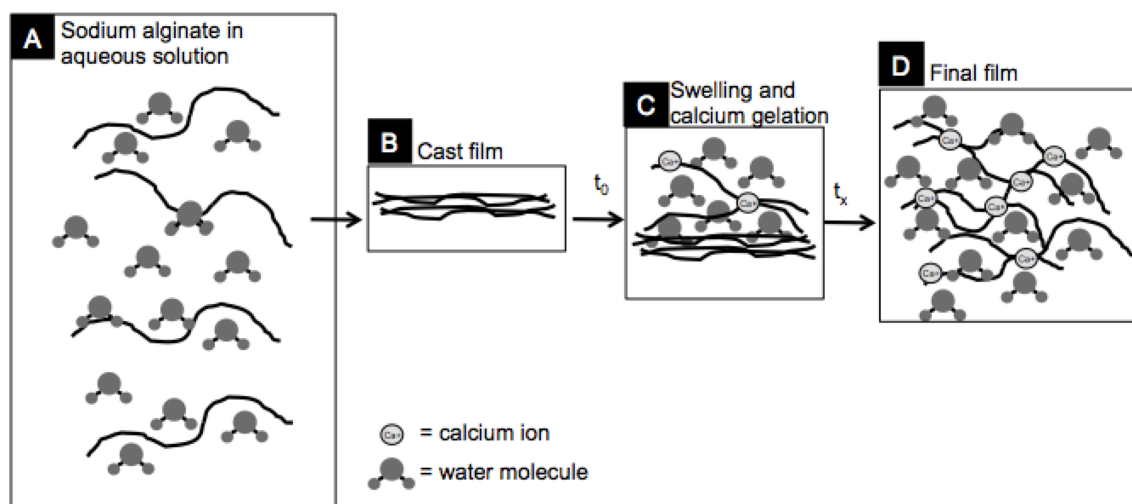
Figure 3.5 Re-swelling cast alginate films in calcium chloride solution. A) Sodium alginate is very soluble in water. Chain movement is free and water molecules surround alginate chains. The water molecules require alginate chain expansion and the chains take up as much volume as possible. B) When in the cast form, alginate chains are densely packed, as water is no longer present in the system. A cast alginate film is very thin and takes up minimum volume. C) When aqueous calcium chloride solution is first introduced to the cast film (t_0), the water causes solvation of the alginate, while the calcium ions cause precipitation of the alginate via glucuronate junctions. These competing processes occur simultaneously. Therefore, the final volume of the resultant film is dependent on calcium concentration, as more calcium ions will allow less solvation from water. The boxes in this diagram are loosely representative of volume but are not drawn to scale.

Previously Schmidt lab researchers characterized alginate films gelled with 1.3 M calcium chloride. Biologically relevant calcium levels are approximately 8.5 to 10.2 mg/dL with a maximum nontoxic concentration of 17 mg/dL. (Allbritton *et al* 1988) Calcium levels are responsible for many conditions such as appetite, hormone release, and blood clotting. Although excess calcium quickly reaches renal clearance, it is important to not jeopardize this balance. Therefore it is of great interest to minimize calcium ions required. Many alginate constructs used for biomedical engineering purposes are gelled with 100 mM calcium chloride, and are cytocompatible when degraded remnants and fluids are exposed to cells.

To determine the optimal concentration of external gelation solution, we compared films of 150 mg alginate (medical grade, high G, 120 kDa) resulting from 10 mM, 50 mM, or 100 mM aqueous calcium chloride solutions. Films were left to gel for 60 min. Thickness and swelling measurement results are tabulated in **Table 3.1** and visually represented in **Figure 3.6**. As expected, the lower the calcium concentration in the gelling solution, the thicker the resulting film. It then follows that a lower calcium concentration in the gelling solution correlates to a film with greater swelling ratio. This increase in thickness and swelling ratio is a result of the balance of gelation and redissolution timing. Water is attracted to the monomers, and rushes into the film, swelling each residue as it binds. Simultaneously, calcium ions are attracted to the carboxylic acid groups on the G units, and binds as the water opens up and expands the next alginate monomer layer. With fewer calcium ions, monomer expansion increases before a calcium ion can lock the monomer's orientation. The 100 mM solution was selected as optimal because the swelling ratio is similar to GMHA films and the thickness was minimized.

CaCl2 molarity	Thickness (mm)	Swelling Ratio (g water/g polymer)
10 mM	0.86 ± 0.19	38.57 ± 2.30
50 mM	0.20 ± 0.02	6.31 ± 0.53
100 mM	0.06 ± 0.02	2.79 ± 0.66

Table 3.1   Effect of calcium chloride molarity on alginate films. Calcium chloride molarity plays a significant role in resultant film swelling ratio and thickness. All films cast were 150 mg of medical grade, high G, low molecular weight alginate (LVG). Films were exposed to calcium chloride solutions for 60 min. There were significant differences in both thickness and swelling of resultant films. With decreased molarity of calcium chloride solution, there was a significant increase in thickness and swelling ratio due to the solvation increase with greater concentrations of water.
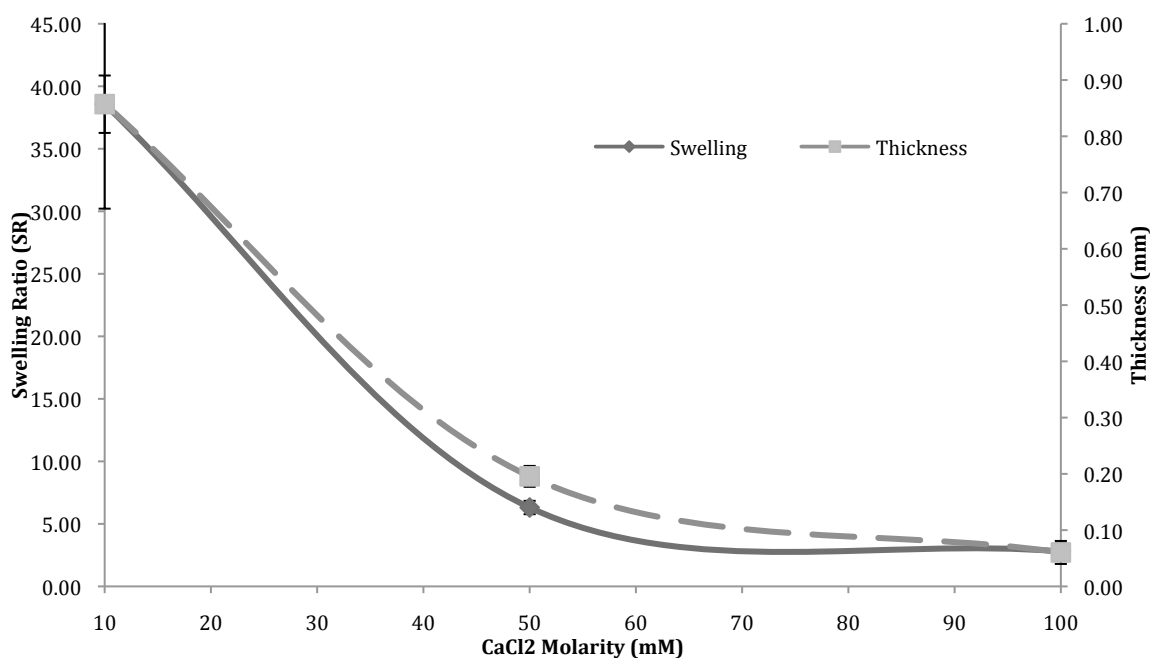
Figure 3.6   Effect of calcium chloride molarity on alginate films. This graph visually represents the data in Table 3.1. Swelling ratio and thickness increase significantly with decreasing calcium concentration in the gelation solution.

3.2.5. Film thickness. Mechanical properties of thin hydrogel films are dramatically dependent upon thickness. (Jansson & Thuvander 2004) Thickness is dependent on the amount of polymer cast and how level the casting conditions are. We optimized the minimum amount of polymer cast with the consistency of thickness across a film. Previously characterized films cast in 2.2 cm diameter wells had 26 mg of polymer, which is analogous to about 300 mg of polymer in our 72 mm by 72 mm forms. Films of 50 mg, 150 mg, and 300 mg were cast and gelled with varying calcium chloride concentrations from 10 mM to 1300 mM. Subsequently, local surgeons manipulated these films to provide input for optimal thickness.

Three blinded local surgeons were asked to handle the films as they would in an operating room setting. Two of the surgeons were general surgeons; one was a neurosurgeon. They were asked to specifically consider the thickness with regards to handling. Before handling the films, they stated that minimal thickness was preferred. The consensus of their comments is tabulated in **Table 3.2**. Films denoted "*N/A*" were too weak to be lifted from the form. Films denoted with "*Thick*" could not be rolled into tubes very easily for simulated laparoscopic insertion. Films denoted "*Thin*" stuck to itself similar to plastic food wrap. The 50 mg film gelled in 1.3 M calcium chloride cracked when folded and was termed "*Brittle*". The films denoted "*Stiff*" were said to feel "plasticy" and "not conformable". The films that were most well liked were 150 mg of polymer gelled in 100 mM calcium chloride. It is important to note that none of these films were considered very conformable. This exercise was solely to narrow the range for target thicknesses that would be comfortable for surgeon insertion.

Calcium Conc. (mM)	Polymer cast (mg)		
	50	150	300
10	N/A	Thick	Thick
50	N/A	Thick	Thick
100	Thin	Good	Good
500	Thin	Good	Stiff
1300	Brittle	Stiff	Stiff

Table 3.2. Surgeons' assessment for handling of films with varying thickness. These films were evaluated for overall handability. Films that are denoted as "Thick" were not suitable for laparoscopic insertion because they could not easily be rolled or had too much shape memory. Films that are denoted "Thin" stuck to themselves and were difficult to manipulate. Films denoted "Stiff" cracked when rolled or folded. The film denoted "Brittle" cracked when folded.

To assess the target thickness range, thickness measurements were taken at 169 points per film and plotted in Matlab. (**Figure 3.7A-C**) Films that were deemed to have good handling were included in thickness measurements, along with one that was too thin. These measurements helped to define the desired and undesirable ranges. The results are plotted in **Figure 3.7D**. Films with thicknesses below 50 μm or above 120 μm were deemed not acceptable by surgeons. The acceptable thickness range is denoted by the shaded region in Figure 3.7D. These results had significant influence on further development of films. There were two important findings from this study. The first finding was how relatively small fluctuations in thickness can cause changes in handling that are recognized by surgeons. Therefore, the range of thicknesses acceptable was between 65-90 μm. The second finding was the determination of thickness consistency across the area of one film. The colormaps in Figure 3.7A-C indicate thickness by color. Darker squares are thicker and lighter squares are thinner. These maps provide a visual representation of thickness changes found across each film, which indicates the levelness of the casting equipment and of the casting technique. The percent variation in thickness was indirectly proportional to film thickness average. Therefore, the target thickness for all films was 90 μm. At least three thickness measurements were taken for all films used in the experiments presented in this dissertation. Films with any measurement below 50 μm or above 120μm were not considered in experiments.
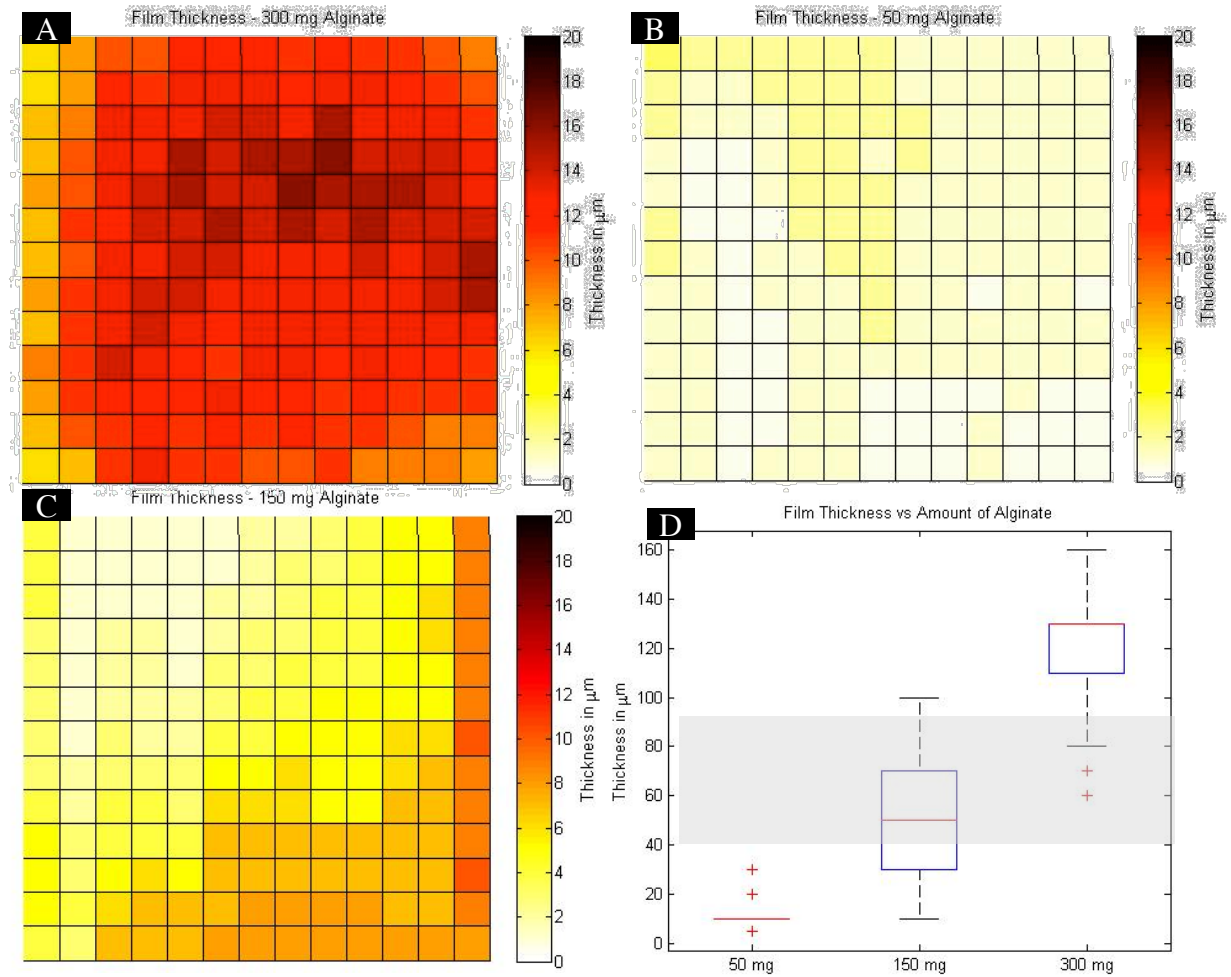
Figure 3.7. Thickness of alginate films. Matlab colormaps were used to visually observe consistency of thickness across films of varying overall thickness and polymer content. A) Films with 300 mg of alginate had many areas greater than 120 μm, which was too thick. B) Films with 50 mg of alginate had many areas less than 50 μm, which was too thin. C) Films with 150 mg of alginate were primarily between these values and were used in future studies. D) A boxplot provides the median and upper and lower quartiles of thickness measurements. The gray shaded area represents the thickness most liked in a survey of surgeons.

3.3 CONCLUSIONS

Calcium alginate films have the potential to create devices that can be handled for use as surgical adjuncts. However, purification must be ensured before any mechanical assessment. For use as an anti-adhesion barrier we used medical grade sodium alginate, with a low M/G ratio to maximize gelation capability. We selected the lowest molecular weight that would provide mechanical integrity, which was 120 kDa. We selected the lowest calcium chloride concentration that provides minimal swelling but maximum flexibility, which was 100 mM. Based on surgeon's advice, we selected 150 mg of polymer per 72 mm by 72 mm form, as this provided an optimal thickness between 50-120 μm. These selections greatly reduced variables for characterization of alginate/GMHA-blended films.

3.4 MATERIALS AND METHODS

3.4.1. Materials. Crude (food grade) sodium alginate was obtained as a generous gift from Multi-Kem Corp (Ridgefield, NJ). Research grade alginate was purchased from Sigma-Aldrich (88 kDa, M/G ratio 2.23). Medical grade alginate was purchased from FMC Novamatrix (Pronova UP VLVG: 40 kDa, M/G ratio 0.67. Pronova UP LVG: 120 kDa, M/G ratio 0.67. Pronova UP MVG: 220 kDa, M/G ratio 0.67. Pronova UP LVM: 120 kDa, M/G ratio 1.5. Pronova UP MVM: 220 kDa, M/G ratio 1.5.) Ethylene glycol tetraacetic acid (EGTA) and sodium hydroxide purchased from Sigma-Aldrich. All other chemicals purchased from Fisher Scientific. Hand mallet dogbone steel die in accordance with ASTM D638 Type V was purchased from Ontario Die Company (Port Huron, MI). Tensile tests were conducted on an Instron 3345 universal testing unit equipped with a BioPuls bath, smooth grip faces, and a 100 N load cell. Extension was measured with a video extensometer. Thickness measurements were taken with a Vernier micrometer, digital, with 1/100 mm tolerance (BGS, Germany).

3.4.2 Purifcation of alginate. A 1% solution of sodium alginate was stirred at 4°C overnight with 0.04% w/v EGTA. Solution was poured over a 5 μm filter and pH was lowered to 3.0 with 2M HCl at 4°C. Alginate pKa value is about 3.65 (Haug & Smidsrod 1965), so the alginic acid precipitate was collected. Filtrate was discarded. At room temperature, the precipitate was added to 100 mL of chloroform and 25 mL of 1-butanol and stirred for 2 hours. Alginate precipitates were again collected on a Buchner funnel and washed with several portions of chloroform. Alginate was redissolved at 1% w/v ddI water overnight at room temperature. Then 0.5M NaOH was added very slowly, over an hour or more, until alginate was fully dissolved and the pH was 12.5. At room temperature, 100 mL of chloroform and 25 mL of 1-butanol were added and solution stirred for 30 min. Solution was centrifuged at 3500 rpm for 10 min. Effluent was

aspirated into 2:1 ratio of ethanol: effluent and allowed to rest for 10 min. Precipitates were filtered again over Buchner funnel with intermittent vacuum and then lyophilized and stored at -20 °C for later use. It was observed that high G alginates were more difficult to purify than high M alginates, requiring several more rinses with ethanol to purify.

3.4.3. Synthesis of a calcium alginate film. A 2% w/v solution of sodium alginate in ddI water was stirred at room temperature overnight. Between 5 – 15 mL were cast in a 72 mm by 72 mm form, depending on the experiment. Forms were placed in a temperature and humidity controlled environmental chamber from Cincinnati Sub-Zero (Cincinnati, Oh). Temperature was held at 25 °C and humidity was held at 70% Rh during the casting period of 48 hours. Forms and solutions were kept from light at all times. Cast films were crosslinked with aqueous solutions of 1.3 M – 10 mM calcium chloride for 5 – 60 min, depending on experiment. This crosslinking occurred by pouring 50 mL of calcium chloride solution on top of the cast solution, while still in the 72 mm by 72 mm form. Some films were pulled from the bottom of the form after 15 min of crosslinking and left to further crosslink for an additional 15 min in the form. Films were rinsed excessively in ddI water for 48 hours before use.

3.4.4. Film thickness and swelling ratio measurements. After synthesis and rinsing, films were cut with a six-inch blade into four equally sized pieces, with ribbing discarded. (**Figure 3.8**) Three thickness measurements were taken of the film, one at the top, one in the middle, and one at the bottom, with a micrometer. The average of these values was taken as the thickness. The swelling ratio was determined by Equation 1. To obtain swollen weight, each piece was placed on a surgical glove and scooted around until excess water was removed. This step was conducted three times for each piece. The average of these three values gives Ws [mg] in **Equation 1**. Film pieces were then placed

into 15 mL conical tubes and lyophilized for 48 hours. Dry weight gives Wd [mg]. All tests were conducted in triplicate.

$$SR = \frac{W_S - W_D}{W_D} \qquad [1]$$

3.4.5. Film thickness for colormaps. After synthesis and rinsing, films were cut with a six-inch blade into 13 equally sized strips, 5 mm wide, with ribbing discarded. (**Figure 3.9**) Thirteen thickness measurements were taken of each strip, every 5 mm, with a micrometer. Measurements were inputted into MATLAB as 13 vectors for a 13 x 13 matrix. "pcolor" command was used to generate the color plots.

3.4.6. Tensile testing of hydrogel films. Two ASTM methods were used to test the tensile properties of the films. The first method, ASTM D638, uses specimens cut into the dogbone shape (**Figure 3.10**) Tensile testing was conducted according to ASTM D638 with minor modifications. After synthesis and rinsing, films were die-cut with a size V handled die and rubber mallet. Per the standard, specimens have a 9.53 mm gage length and 3.18 mm gage width. Three thickness measurements are taken per strip. In accordance with ASTM D638, specimens with thickness changes greater than 10% were discarded. Furthermore, any test strip with a thickness measurement less than 50 μm or greater than 120 μm was discarded. Test samples were prepped with at least 24 hours of soaking in water at room temperature. Pneumatic submergible grips were placed at the edge of the necking region, about 25.4 mm apart. Slack was compensated with pre-test conditions of 0.2 N load. Specimens are pulled in tensile at 5 mm/min strain rate until failure. Proper test completion was considered any failure that occurred in the necking region and did not occur at a nick, tear, or other defect. Most defects were a result of die cutting. The second test method used was ASTM D882. After synthesis and rinsing, films were cut with a six-inch blade into 13 equally sized strips, 5 mm wide, with ribbing

51

discarded. Three thickness measurements are taken per strip. In accordance with ASTM D882, strips with thickness changes greater than 10% were discarded. Furthermore, any test strip with a thickness measurement less than 50 μm or greater than 120 μm was discarded. Test samples were prepped with at least 24 hours of soaking in water at room temperature. Pneumatic submergible grips were placed 25.4 mm apart. This distance was used as the gage length. Specimens were marked at the grips with a paint pen, for video extensometer recognition. An aqueous bath, maintained at 25 °C, is lifted to submerge the specimen, and tests were started immediately. Specimens are pulled in tensile at 5 mm/min strain rate until failure. Proper test completion was considered any failure that did not occur at a nick, tear, or other defect. Most defects were a result of improper cutting. The Young's modulus, a measure of intrinsic film stiffness (Cao *et al* 2007), was calculated according to ASTM D638 (and D882) as the slope of the force–extension curve multiplied by the distance between the tension grips and divided by the initial area of the specimen (length x thickness), and was expressed as MPa (**Equation 2**). The elongation at break (E, % of the original length) (**Equation 3**) and tensile strength (TS, MPa) (**Equation 4**) were also calculated according to the ASTM D882 method. Toughness was taken as the area under the true stress vs. true strain curve. All film types were tested in triplicate, at least.

$$\text{Young's Modulus (MPa)} = \frac{\text{Tensile Strength (N/mm}^2)}{\text{Elongation at break}} \qquad [2]$$

$$E(\%) = \frac{(L - L_0)}{L_0} \times 100\% \qquad [3]$$

$$TS(\frac{N}{mm^2}) = \frac{F}{A} \qquad [4]$$

3.4.7 Statistical analysis. All data are presented as mean ± standard deviation.
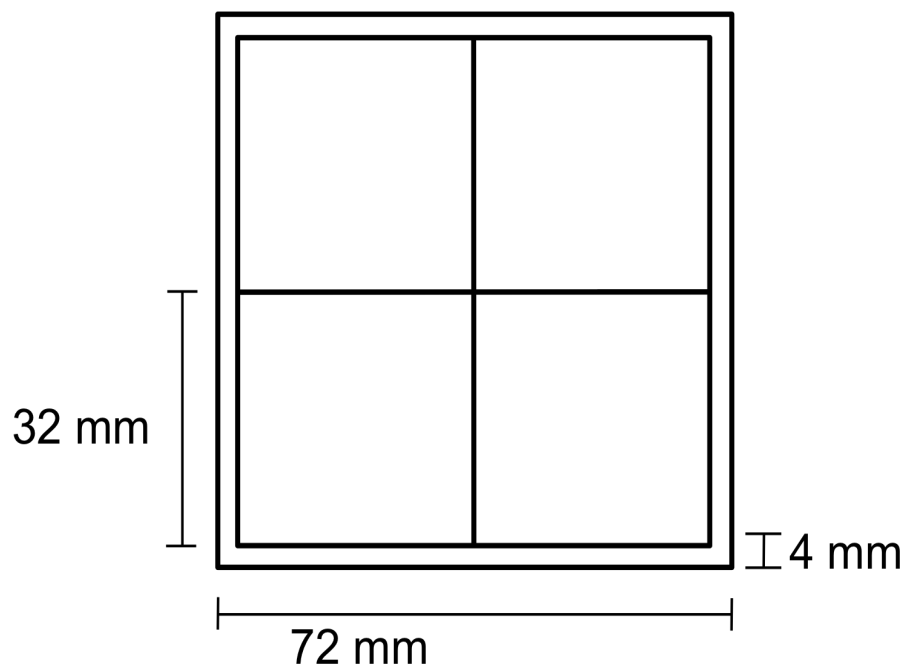
Figure 3.8. Film preparation for swelling and thickness studies. All films were cast in 72 mm by 72 mm forms. Before conducting any experiment, ribbing was removed as selvage, indicated by the 4 mm gap between edge of film and smaller square. This ribbing is different than the rest of the film because of casting effects. Films were then cut into four equal pieces. Films were cut with a six-inch blade so that tears or defects from cutting were minimized. Photograph indicates typical square used for testing.
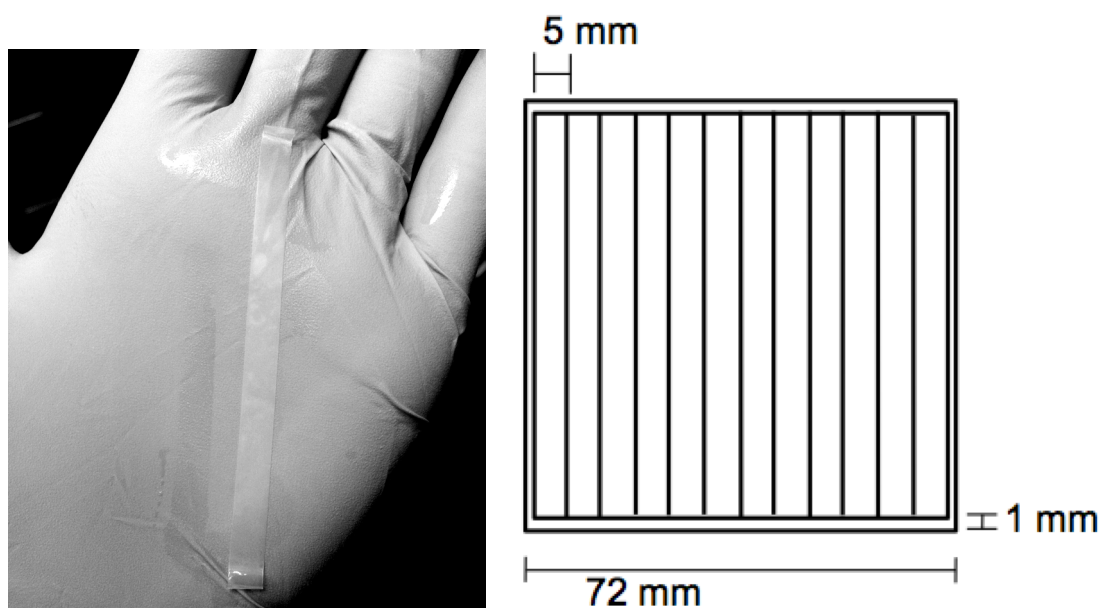
Figure 3.9. Film preparation for thickness studies. All films were cast in 72 mm by 72 mm forms. Before conducting any experiment, ribbing was removed as selvage, indicated by the 1 mm gap between edge of film and smaller square. This ribbing is different than the rest of the film because of casting. Films were then cut into thirteen equal strips. Films were cut with a six-inch blade so that tears or defects from cutting were minimized. Photograph indicates typical strip used for testing.
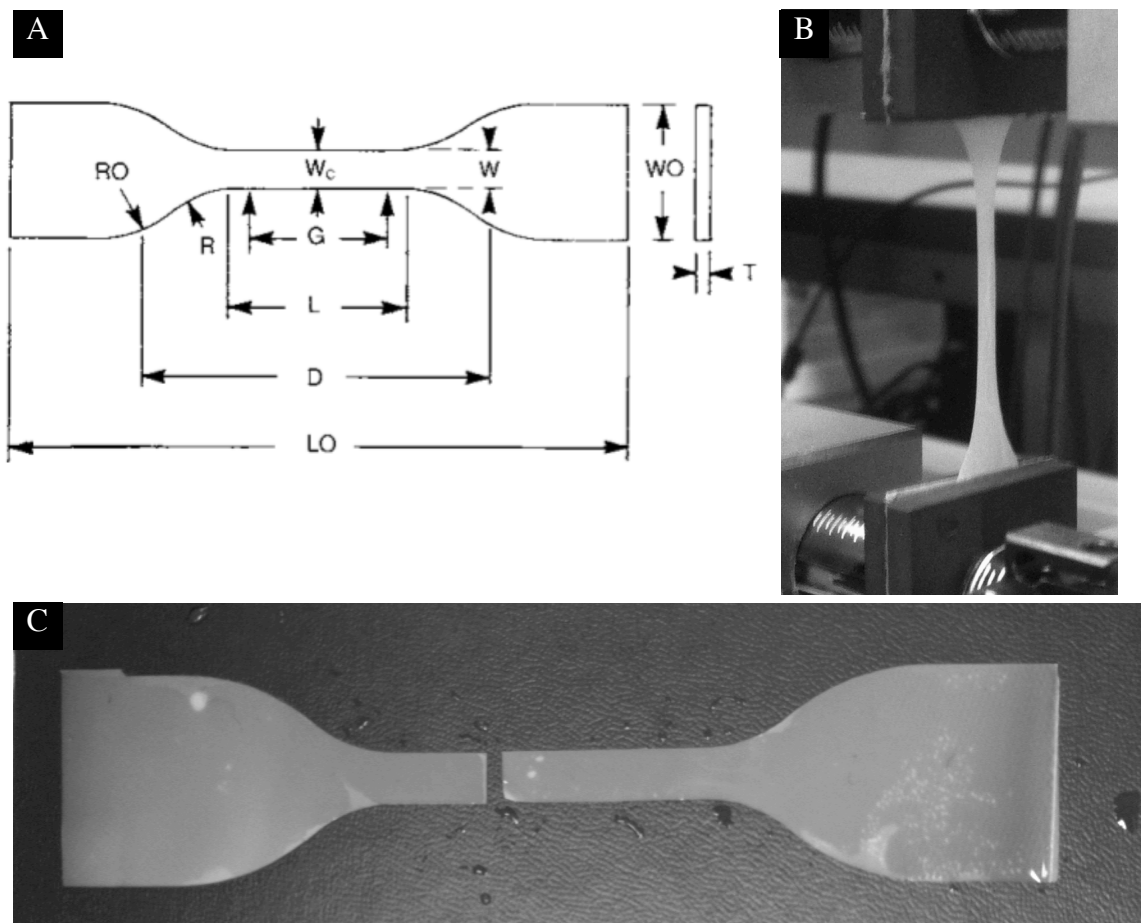
Figure 3.10. "Dogbone" die cut ASTM D638 V. After film synthesis and rinsing, films were placed onto a cork surface in between two pieces of foil. A) A rubber mallet was used to provide pressure to a dogbone die cut with the following dimensions: D = 65 mm, W = 6.35 mm. WO and LO varied with specimens as allowed by the standard. (ASTM D638 2010) B) Die cut film loaded on Instron for tensile testing. C) Proper failure of test specimen.

Chapter 4: GMHA and Alginate Blend Films

ABSTRACT

We have characterized thin, planar hydrogel films cast from GMHA/alginate blends of varying composition. GMHA and alginate are highly hydrophilic, linear polydisaccharides that can be cast from aqueous solutions. Cast films are first exposed to UV to photocrosslink the GMHA. Films are then exposed to an aqueous solution of calcium chloride to cause alginate gelation. Once gelation is complete, films are rinsed exhaustively in ddI water. Resultant films are translucent and smooth. Swelling ratios vary with composition while thickness remains uniform. Although macroscopically homogenous, we hypothesize that GMHA and alginate are phase separated and form two phases during the casting process. Resultant films exhibit behaviors that follow the theory of percolation. At low GMHA concentrations, resultant films are alginate-rich, with a coarse GMHA phase. When a greater amount of GMHA is added, the GMHA reaches a continuous phase through clustering mechanisms. Without photocrosslinking, this continuous GMHA phase leaches from the alginate gel with exposure to water. We hypothesize that leaching is energetically favorable for chain orientation and for water association. Photocrosslinking prevents this continuous phase from leaching, despite water exposure and time. The presence of GMHA does not interrupt alginate gelation with calcium. Dissolution studies show that calcium removal causes complete dissolution of films that do not have a continuous phase of photocrosslinked GMHA. Percolation is polymer-specific and is highly dependent on composition, molecular weight, and the degree of methacrylation. To our knowledge, no previous work elucidates the percolation phenomena of HA/alginate gels or films.

4.1 BACKGROUND: ALGINATE AND HA TOGETHER

Limited research has been conducted on blends of HA and alginate. In most studies, these two polymers are studied separately (Rubert *et al* 2012). Perhaps the similar charge on both polymers is a deterrent. However, there are studies that incorporate both polymers, primarily for the same reasons presented here. Alginate provides mechanical integrity and HA provides significant healing properties recognized by the body. Intended for cartilage repair, HA was incorporated into alginate-rich beads with fibrin and chondrocytes (Lindenhayn *et al* 1999). In this study, fibrin supported chondrocyte attachment, which then supported HA retention by binding HA to cell receptors. According to Lindenhayn and coworkers, the reason for HA loss was a result of larger pore size with lower alginate concentration and the disruption of the association of calcium with alginate. Thus it is presented that HA leaches from an alginate-rich system as a result of pore size or inability for alginate to gel, and is only retained by chondrocyte-led interactions. Na and coworkers combined alginate and HA in similar concentrations for the development of a hydrogel to prevent abdominal adhesions. (Na *et al* 2012) The polymers were combined in the solution state, for an injectable solution. In this study, the HA is not crosslinked and the alginate is mildly gelled with calcium. No attempt to determine retention of HA in final solution is made. Another study investigates a hydrogel of GMHA and alginate as an interpenetrating network (IPN). (D'Arrigo *et al* 2012) This IPN is 67% calcium alginate and 33% GMHA per their protocol. D'Arrigo *et al*. methacrylate GMHA to 20%. They present these polymers in a thick hydrogel for drug delivery. The mechanical properties and protein release profile are presented but no investigation of solubility, or polymer retention, is presented. Other studies present alginate and HA blended *in-situ* gelling solutions where either the alginate or HA have been modified by a hydrazide or aldehyde or are modified with tyramine, and covalently

crosslink upon mixing. (Dahlmann *et al* 2012, Ganesh *et al* 2013) The HA and alginate are covalently bound and, therefore, are retained within the same system.

4.2 CHARACTERIZATION OF GMHA AND ALGINATE FILMS

The most important attribute to maintain in alginate/GMHA blended films was overall handling under hydrated conditions. The pure GMHA films were too weak and tended to curl. The pure alginate films were too stiff and not conformable. Therefore, it was projected that a blended film would produce a combination of these two extremes, which could provide a complementary advantage. To explore resultant films from alginate/GMHA blends, there were three variables to be investigated: composition, molecular weight of alginate, and Degree of Methacrylation (DM) of GMHA. Low molecular weight alginate is denoted LVG. High molecular weight alginate is denoted MVG. Low DM GMHA is denoted GMHA(11). High DM GMHA is denoted GMHA(32). Before any characterization, it was critical to establish which compositions of films could be handled. A film that can be handled is one that can be removed from the form without tearing or otherwise breaking. Films that could not be handled were not considered for further testing (**Figure 4.1**). Films were fabricated at several intervals between the extremes of pure alginate and pure GMHA. These films of varying composition were fabricated with high or low molecular weight alginate, high or low DM, and with or without UV. Handleability results are tabulated in **Table 4.1**. Films that could be pulled from the form are represented with a ✓. Film composition is denoted as alginate/GMHA %w/v. Low molecular weight, high G alginate (LVG) was mixed with either low methacrylated GMHA(11) or high methacrylated GMHA(32). High molecular weight, high G alginate (MVG) was mixed with high methacrylated GMHA(32). All films with at least 67% w/v of alginate were able to be removed from the form and

handled. Higher molecular weight alginate extended the range of handleable films. Eliminating UV exposure decreased the range for handleable film fabrication.
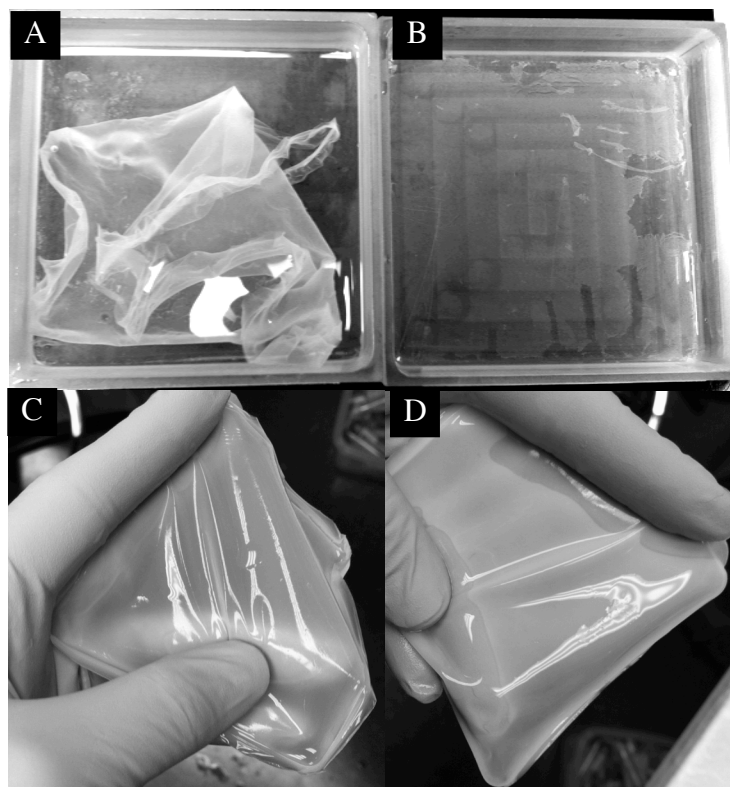
Figure 4.1: **Handleability**. A) Film was cast from a 30/70 w/v blend of alginate/GMHA(32) with exposure to UV. This film has the consistency of mucous in aqueous solutions and could not be picked up from the form easily. B) Film was cast from a 30/70 w/v blend of alginate/GMHA(32) with no exposure to UV. Scrape marks can be seen from an attempt to gather film from form. Neither of these films were considered for study. C) Film was cast from a 60/40 w/v blend of alginate/GMHA(11) with no exposure to UV. Film is soft and pliable. D) Film cast from a 67/33 w/v blend of alginate/GMHA(32) with exposure to UV. Film is sturdy but pliable. Film can be removed from form and was tested.

Alg/GMHA	LVG/11		LVG/32		MVG/32	
	No UV	UV	No UV	UV	No UV	UV
100/0	✓	✓	✓	✓	✓	✓
83/17	✓	✓	✓	✓	✓	✓
67/33	✓	✓	✓	✓	✓	✓
50/50	✓	✓	✓	✓	✓	✓
40/60				✓	✓	✓
30/70						✓

Table 4.1. **Film Handleability**. Films that could be removed from the form are represented with a ✓. Shaded boxes denote films that were slimy. LVG = low viscosity high G medical grade alginate. MVG = medium viscosity high G medical grade alginate. 11 = low degree of GMHA methacrylation. 32 = high degree of GMHA methacrylation.

Of the films that could be handled, there was a noticeable difference in texture. Some films were very slippery, or had a mucinous surface, while others were slick but dry. The ones that felt mucinous are denoted by a shaded box in Table 4.1. This slimy surface was reminiscent of the surface of a GMHA-only film. To understand the consequences of blending alginate and GMHA for film fabrication, we conducted several studies that are detailed in this section.

4.2.1 Polymer retention studies Percolation is a random phenomenon that describes the movement of material into clusters, and the behavior of material at each stage of clustering. (Stauffer & Aharony 1994) The theory of percolation can be categorized into early, late, and final stages (Furukawa 2003, Siggia 1979). The early and late stages can be visualized in **Figure 4.2**. Early stage refers to small concentrations of material B added to a host material A, where the resulting blend appears homogenous. Motions are driven by chain diffusion, but the materials are phase-separated. Late stages of percolation refer to concentrations of material B added to host material A such that material B begins to cluster. These cluster formations are no longer chain diffusion driven but are motion driven within each phase domain. Thus, as the clusters form in the phase with material B, the chains will move within these clusters. We hypothesize that it is energetically favorable for the chains in the clusters to be able to move, and this movement is facilitated by increased clustering. As more material B is added, more clusters form and/or grow, and chains have a greater area to move within. At a critical composition, these clusters form one continuous phase. Chains within this continuous phase can move within and throughout this phase. Final stages of percolation refer to a dramatic change in structure kinetics such that the rate of structure change of at least one phase increases considerably and a bilayer forms. Final stage percolation will not be addressed in this dissertation.

61

The point at which the added material B reaches a continuous phase is often referred to as the percolation threshold. The percolation threshold between two materials is composition-dependent in isothermic reactions. Furthermore, percolation is polymer-specific, and is affected by factors such as molecular weight and crosslinking density. (Andradi & Hellmann 1993) Historically, percolation theory is applied to a two-phase system that follows predictable behavioral patterns of phase separation. (McMaster 1975) When applied to hydrogel blends, these theoretical prediction values are complicated by the presence of the solvent, water, which plays a significant role in hydrogel properties. Thus a two-phase system is actually a three-phase system. Furthermore, water can provide additional chain movement, which complicates predictive percolation approximations. Therefore, hydrogel percolation studies often involve determination of a critical composition for a desired result such as electrical conductivity (Ferris & Panhuis 2009), gelation point (Aufderhorst-Roberts *et al* 2012), or degradation pattern (Schultz *et al* 2012).

To investigate the possibility of phase separation of alginate and GMHA we quantified the amount of polymer retained after alginate/GMHA-blended film fabrication. At every stage of percolation, there is a significant dependence on compositional equilibrium. Therefore, the amount of polymer retained in final films would reveal an equilibrium trend in composition. Furthermore, we would observe a sharp compositional shift at or near the percolation threshold. Although the film fabrication protocol is calculated to cast 150 mg of polymer in a 1% w/v solution into each form, the dry weight, W_D, was determined in order to verify the amount cast. The W_D determined was remarkably consistent across several compositions at 144 ± 0.6 mg. Results are tabulated in **Table 4.2**. Per the manufacturer, there is 0.5% w/v moisture in the as received alginate and HA powder which accounts for all of the "lost" weight (~ 4-5 mg). Therefore, 144

mg was used as the W_D for all films. Final film weights, W_R, were obtained after fabrication, subsequent rinsing in water, and lyophilization. To determine if there was a time dependency on polymer loss, one set of films (LVG/32) were rinsed for 24 hrs, 48 hrs, or 10 days in ddI water with daily water replacement, and then lyophilized. It was determined that any polymer lost occurred in the first 24 hours, so timepoints for this set were compiled for higher N (N = 9). Polymer retention results are tabulated in **Table 4.3**.

To establish the retention of alginate during the film fabrication process, we fabricated alginate-only films. After synthesis and rinsing, alginate-only films weighed 144 ± 1.2 mg. Alginate-only films did not lose any polymer during film fabrication. Using 144 mg as amount of starting polymer, an alginate-only film was considered to have 100% polymer retention. We concluded that loss of polymer observed was loss of GMHA and not loss of alginate. **(Figures 4.3-4.5)**

One of the most remarkable and useful observations with polymer retention results was the effect of UV. When the GMHA made a continuous phase, the UV exposure crosslinked this continuous phase, and the film retained its GMHA component. When the GMHA made a continuous phase and the film was not exposed to UV, this GMHA phase leached from the film and little to no GMHA was retained. For example, LVG films cast with 45% GMHA(32) that were exposed to UV retained 83% ± 1.9 of the polymer cast. Conversely, LVG films cast with 45% GMHA(32) without UV exposure had a final weight equal to the amount of cast alginate, 53% ± 2.2 of polymer cast. Thus, films with 45% GMHA(32) that were not exposed to UV did not retain GMHA(32). Therefore, we concluded that GMHA(32) makes a continuous phase in LVG films when between 40-50% of the film is GMHA(32).

63

This discussion will now be broken into two segments: films with GMHA concentrations below the percolation threshold, and films with GMHA concentrations at or above the percolation threshold.

Retention of GMHA is statistically similar for all films with GMHA concentrations less than the percolation concentration. (**Figure 4.6**) For example, LVG films with 17% GMHA(32) retained 67% ± 4.1 and 62% ± 4.7 of the initial GMHA(32) with and without UV, respectively. LVG films with 17% GMHA(11) retain 67% ± 3.1 and 69 ± 7.3% of the initial GMHA(11) with and without UV, respectively. Similarly, MVG films with 17% GMHA(32) retain 60% ± 5.4 and 64% ± 3.4 of the initial GMHA(32) with and without UV, respectively. Results are similar to these for all films with 33% GMHA, and other concentrations of GMHA below the percolation point for each film type. These results suggest that the amount of GMHA retained before the percolation point is largely a result of how much exposure there is to water. Because the thickness of the films is kept constant, water exposure through the surfaces of the films is the only variable held constant. This conclusion is supported by the theory that the mechanism for leaching is through the effect of water, and the attraction water has for GMHA. In concentrations lower than percolation, the GMHA clusters do not have access to the water, unless they are near the surface. Simply put, there is no direct path for the GMHA clusters to escape to the large volume of water, so the clusters do not escape the film. If retention of GMHA before the percolation threshold were a result of entanglement in alginate, then the molecular weight of alginate would have an effect on this retention. The results in Figure 4.6 also suggest that UV exposure did not impact the retention of GMHA below the percolation threshold. We theorize that the reason UV exposure did not play a role was because the clusters of GMHA did not form a continuous phase. A continuous phase would provide a film-wide network for

64

photocrosslinking to connect all GMHA in the film. In this situation, this GMHA network would be a fully interpenetrating network with the alginate, and UV would connect the clusters, minimizing leaching. However, in films with GMHA concentrations below the percolation threshold, the clusters have not yet made a continuous phase and, therefore, there is no path for photocrosslinking to connect the clusters. GMHA clusters are not connected whether or not there is photocrosslinking attempted. Finally, the study of GMHA retention below the percolation threshold suggests that GMHA and alginate can be retained within the same film if the concentration of GMHA is below the percolation threshold.

Our data supports this theory because films with compositions at or above the percolation threshold retained the majority of the GMHA originally cast, when exposed to UV. When GMHA concentrations were at or above the percolation threshold, and the film was not exposed to UV, the GMHA phase was not retained in the film. The method by which GMHA leached from the film, when not UV crosslinked, was due to exposure to water. We theorize that at least a portion of this continuous GMHA phase was exposed to water during the rinsing step that follows exposure to calcium chloride solution. This exposure, caused the GMHA to leave the film because of increased chain movement afforded in more dilute conditions. The GMHA is attracted to the large water volume because the polymer chains can move more freely than in the film matrix. Furthermore, bound water is immobilized by the negative charges on the backbone of the HA molecule. The mutual desire for the GMHA to unfold or to relax and for the water to interact with the GMHA is strong enough to attract the GMHA into the water from the film. Most importantly, the connection of water to the GMHA phase can be small because there is a direct path for any chain in this phase to reach the large volume of

65

water. Thus, all chains that can move within the GMHA-rich phase can move within this phase into the large volume of water.

The percolation point of GMHA in alginate-rich films shifts with DM of GMHA. (**Figure 4.3 and 4.4**) The percolation threshold for GMHA(11) is between 33 and 40%. The percolation threshold for GMHA(32) is between 45-50%. This shift in percolation is supported by the viscosity data presented in Chapter 2. As previously discussed, the decrease in viscosity with increasing DM is due to the hydrophobic moieties added to the backbone of HA. Water is not attracted to the methacrylate moieties on GMHA. Therefore, water excludes these moieties causing a change in polymer conformation so that water has greatest access to the hydrophilic, negatively charged moieties. Therefore, higher DM causes increased conformational changes and the GMHA molecules are less stretched. This conformation is important when considering the percolation threshold since percolation is the point at which a continuous phase is reached. If GMHA molecules are less spread out, then a greater concentration of GMHA is required to reach a continuous phase. This supports the result that the percolation threshold of GMHA(11) occurred at a lower concentration than GMHA(32).

The percolation point of GMHA in alginate-rich films does not shift with molecular weight of alginate. (**Figure 4.4 and 4.5**) In either high or low molecular weight alginate, GMHA(32) reaches a continuous phase between 40 and 50% GMHA(32). Percolation is polymer specific and dependent on concentration when pH and temperature are held constant. Increasing the molecular weight of alginate does not effect either of those factors. In fact, the only effect that increasing molecular weight had on the leaching properties of the films was the increase in range of concentrations that fabricated a film that could be handled. Concentrations of MVG below the handlability threshold of LVG could be handled. This result suggests that the alginate polymer chains

are entangled more at increased molecular weights. However, this entanglement has no effect on the ability for GMHA to cluster or to make a continuous phase. That said, perhaps an increase from 120 kDa to 220 kDa is not significant enough to prevent GMHA from being exposed to the surface. It would be interesting to observe any percolation threshold changes with very high molecular weights of alginate.

A recent study of HA retention in alginate beads concludes that retention is concentration-dependent. (Lindenhayn *et al* 1999) However, this conclusion is based on theoretical pore size of alginates, and suggests that HA is retained in higher concentrations of alginate because of decreased pore size. The authors conclude that increasing alginate concentration will increase HA retention because more HA will be entrapped in the alginate matrix. Lindenhayn *et al* also concluded that leaching of HA was a result of repulsion of the two negatively charged polymers. While these conclusions are founded, based on our findings, this leaching of HA was more than likely occurring because of a percolation mechanism.

The theory of percolation is applicable to films of alginate/HA blends. Awareness of the percolation threshold at various HA modifications is a powerful tool in understanding the film composition, the processing requirements for film fabrication, and the film's ability to dissolve or to degrade. Based on our findings, HA of varying modification can be retained in alginate films without further crosslinking, as long as the percolation threshold is known. These threshold values can be plotted to predict the influence of DM of GMHA **(Figure 4.7**). The relationship between percolation threshold concentration of GMHA and DM may be a power law relationship. This type of relationship is plausible because GMHA is too weak to sustain gelled alginate in dilute concentrations; thus, invalidating a linear relationship. Using a power law relationship one could predict a percolation value for a given amount of alginate and known

modification of HA. Furthermore, knowing that release of calcium ions causes dissolution of the alginate-rich films, one could select a modification of HA that best suits a minimum amount of alginate for fastest degradation of a film. Simultaneously, the percolation threshold predicts when a fully interpenetrating network of alginate and HA is established. This concentration would provide the slowest degrading films because it would require dissolution of the alginate and enzymatic degradation of the crosslinked HA network.

Although the work presented here supports the theory of percolation, it would be of great interest to obtain image-supported evidence of this separation. We expect that separation is on a nanometer scale and would require a very thin film of cast alginate/GMHA above the percolation threshold to show clusters. Epifluorescence could be attempted but more than likely confocal with a very high objective would be required to visualize the clusters of GMHA within an alginate-rich environment. I do not think these phases could be detected by XPS or EDAX-TEM because the nitrogen signal would not be strong enough to detect in clusters. Calcium associations are more than likely very thorough throughout as GMHA will have some light associations with calcium. Therefore, it is suggested that fluorescence of each polymer would be preferred in the dry state via confocal imaging.

Alg/GMHA	Dry Weight, W_D (mg)
100/0	144 ± 0.9
83/17	144 ± 0.3
67/33	145 ± 0.6
50/50	144 ± 0.6
Average	**144 ± 0.6**

Table 4.2   **Dry weight for polymer retention studies**. Solutions were cast into 50 mL conical vials and lyophilized. Composition is denoted as alginate/GMHA %w/v. Calculated mass dispensed was 150 mg. This 6 mg difference can be explained by a 0.5% water mass in as-received polymer powder, per manufacturer.
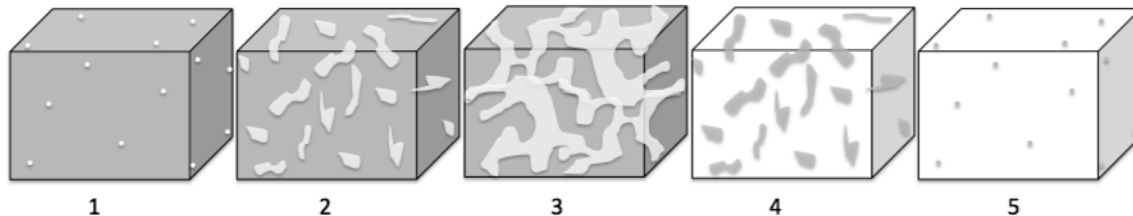
Figure 4.2.   **Percolation theory**. 1) When a material B, denoted as white, is added in small concentrations to material A, denoted as dark, the resulting blend is homogenous. Polymer chain movement is diffusion driven. 2) As concentration of B increases within A, the B chains begin to cluster. This clustering is driven by chain movement within the B phase, and is no longer diffusion driven. 3) At a critical composition of B within A, the clusters of B create a continuous phase. Any chain within this phase can move within the entire phase and these movements are driven kinetically. 4-5) Representation of percolation in a material B-rich environment.

Alg/ GMHA	% Polymer Retained					
	LVG/11		LVG/32*		MVG/32	
	No UV	UV	No UV	UV	No UV	UV
100/0	100.0 ± 0.4					
83/17	94.8 ± 3.2	94.3 ± 0.7	93.1 ± 0.9	93.9 ± 1.2	94.3 ± 1.9	95.1 ± 2.7
67/33	86.1 ± 0.5	89.9 ± 0.1	82.5 ± 2.7	82.8 ± 1.2	83.2 ± 1.0	86.9 ± 5.4
60/40	64.0 ± 1.6	85.5 ± 0.7	83.1 ± 0.8	85.1 ± 1.6	78.1 ± 2.1	85.8 ± 3.0
50/50	52.9 ± 0.7	89.9 ± 1.0	52.5 ± 1.4	83.0 ± 1.2	53.5 ± 1.5	76.5 ± 2.1
40/60				81.5 ± 3.3	43.3 ± 1.8	70.9 ± 2.9
30/70						65.6 ± 3.4

Table 4.3. **Polymer Retention**. Film were cast into 72 mm by 72 mm forms. LVG denotes low molecular weight (~100 kDa) high G (M/G ratio is 0.67) alginate. MVG denotes high molecular weight (~200 kDa) high G (M/G ratio is 0.67) alginate. Methacrylation is denoted by 11 and 32 (11% and 32% theoretical, respectively) and composition is shown as %alginate/%GMHA w/v. After casting, films were exposed to 100 mM calcium chloride aqeous solution for 30 min. Films were then rinsed for 48 hours in ddI water. Dry weight was obtained after lyophilization and results are shown as a % weight remaining of original weight. For all films, N = 3 except the LVG/32 marked * for N = 9.
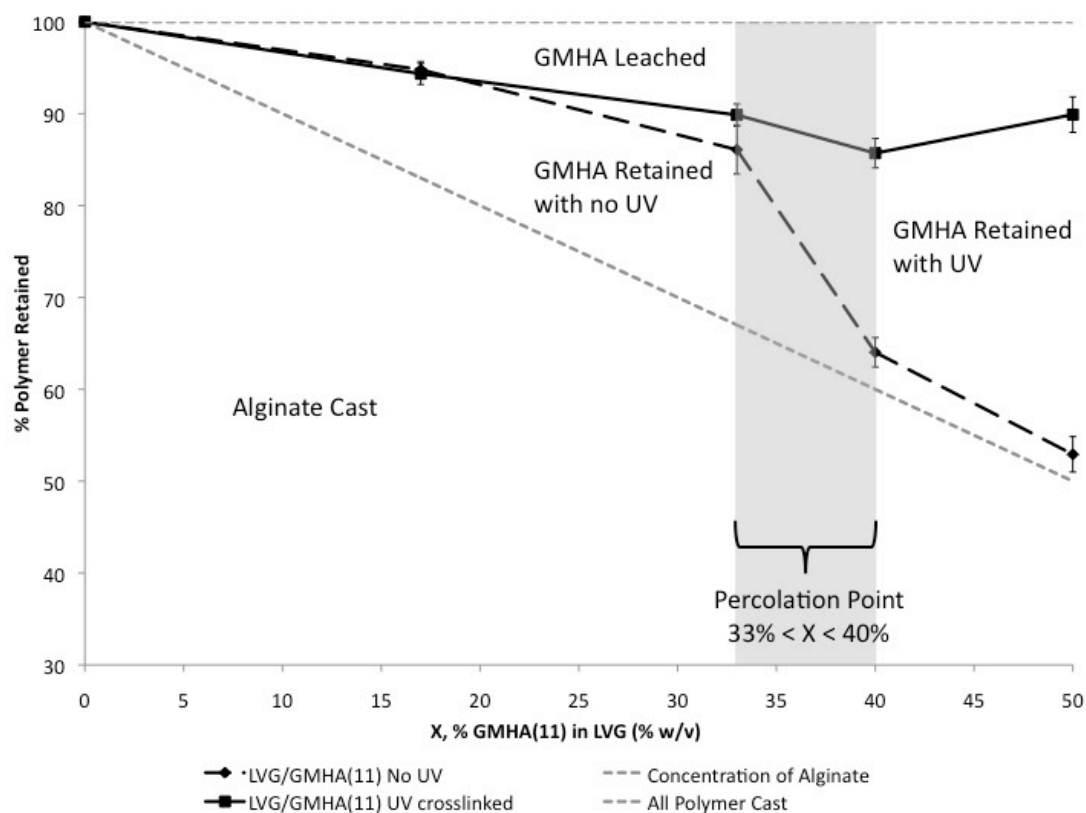
Figure 4.3. Polymer Retention in LVG/11 films. Films were cast into 72 mm by 72 mm forms. After casting, films were exposed to UV (or not), and then films were gelled in 100 mM calcium chloride aqueous solution for 30 min. Films were then rinsed exhaustively in ddI water. Dry weight was obtained after lyophilization and results are shown as a % weight remaining of original weight. This % polymer remaining is given along the y-axis. LVG denotes low molecular weight (~120 kDa) high G (M/G ratio is 0.67) alginate. Methacrylation is denoted by 11 (11% theoretical). The concentration of GMHA, X, increases along the x-axis. The gray dotted line represents the % of alginate cast. The solid black line represents the % polymer retained for films exposed to UV. The dotted black line represents the % polymer retained for films not exposed to UV. The films with 17% GMHA(11) retained the same amount of total polymer indicating the GMHA(11) is not in a continuous phase. Films with 33% GMHA(11) retained statistically similar amount of total polymer indicating the GMHA(11) is not in a continuous phase. Films with 40% GMHA(11) have dramatically different % polymer retained indicating that the GMHA(11) has reached a continuous phase and leaches from the sytem without UV crosslinking. Therefore the percolation point for GMHA(11) in an alginate-rich (LVG) system is between 33 and 40%. For all films, N = 3.
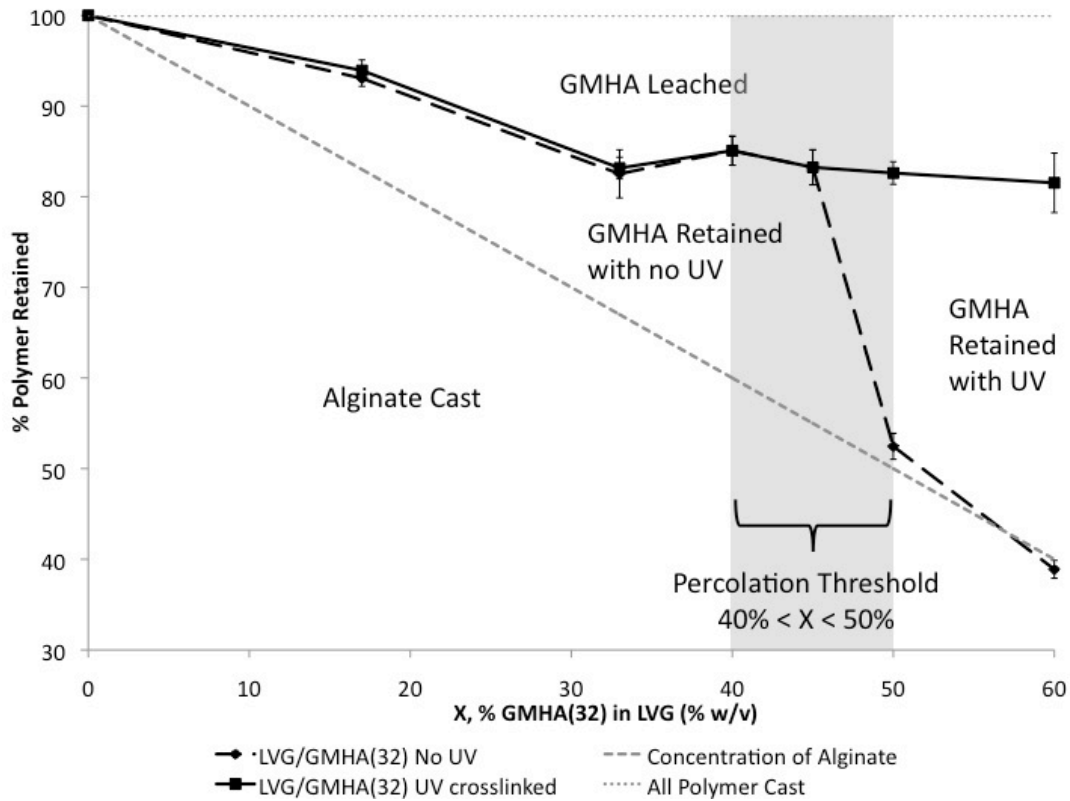
Figure 4.4. **Polymer Retention in LVG/32 films**. Films were cast into 72 mm by 72 mm forms. After casting, films were exposed to UV (or not), and then films were gelled in 100 mM calcium chloride aqueous solution for 30 min. Films were then rinsed exhaustively in ddI water. Dry weight was obtained after lyophilization and results are shown as a % weight remaining of original weight. This % polymer remaining is given along the y-axis. LVG denotes low molecular weight (~120 kDa) high G (M/G ratio is 0.67) alginate. Methacrylation is denoted by 32 (32% theoretical). The concentration of GMHA, X, increases along the x-axis. The gray dotted line represents the % of alginate cast. The solid black line represents the % polymer retained for films exposed to UV. The dotted black line represents the % polymer retained for films not exposed to UV. The films with 17-40% GMHA(32) retained the same amount of total polymer indicating the GMHA(32) is not in a continuous phase. Films with 50% GMHA(32) retained dramatically different % polymer indicating that the GMHA(32) has reached a continuous phase and leaches from the sytem without UV crosslinking. Therefore the percolation point for GMHA(32) in an alginate-rich (LVG) system is between 40 and 50%. Films with 60% GMHA(32) retain a high % polymer which suggests alginate is clustered in a GMHA-rich matrix. For all films, N = 3.
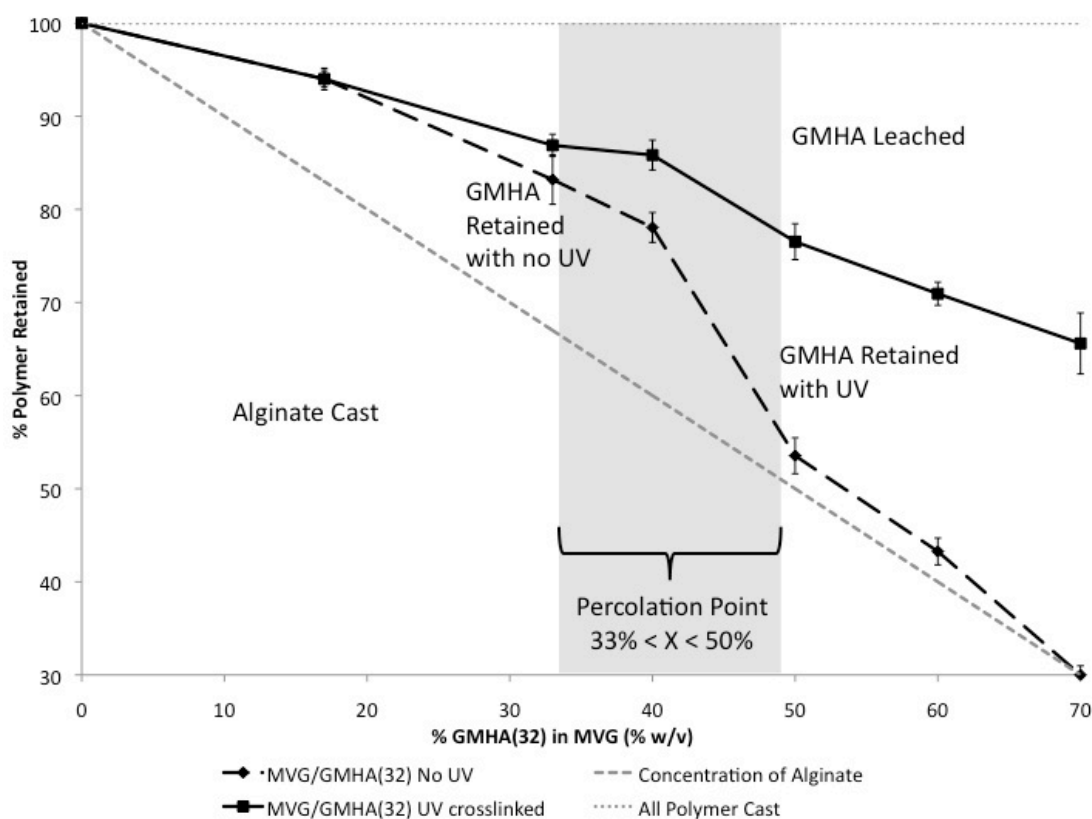
Figure 4.5. % Polymer Retention in MVG/32 films. Films were cast into 72 mm by 72 mm forms. After casting, films were exposed to UV (or not), and then films were gelled in 100 mM calcium chloride aqueous solution for 30 min. Films were then rinsed exhaustively in ddI water. Dry weight was obtained after lyophilization and results are shown as a % weight remaining of original weight. This % polymer remaining is given along the y-axis. MVG denotes high molecular weight (~220 kDa) high G (M/G ratio is 0.67) alginate. Methacrylation is denoted by 32 (32% theoretical). The concentration of GMHA, X, increases along the x-axis. The gray dotted line represents the % of alginate cast. The solid black line represents the % polymer retained for films exposed to UV. The dotted black line represents the % polymer retained for films not exposed to UV. The films with 17-33% GMHA(32) retained the same amount of total polymer indicating the GMHA(32) is not in a continuous phase. Films with 50% GMHA(32) retained dramatically different % polymer indicating that the GMHA(32) has reached a continuous phase and leaches from the sytem without UV crosslinking. Therefore the percolation point for GMHA(32) in an alginate-rich (LVG) system is between 33 and 50%. Films with 60-70% GMHA(32) retain a high % polymer which suggests alginate is now clustered in a GMHA-rich matrix. For all films, N = 3.
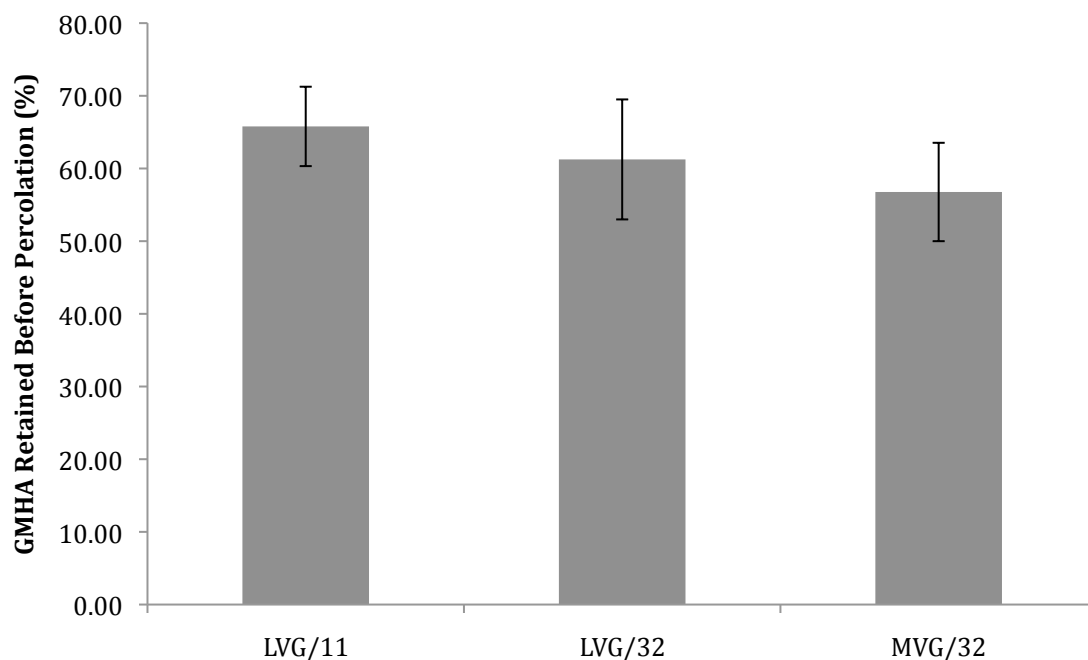
Figure 4.6. GMHA retention prior to percolation threshold. Each film type has a
different percolation point, as described in Figures 4.3-4.5. Films of each
type retain the same % GMHA with or without UV, with concentrations of
GMHA below the percolation point. These values of % GMHA retained (for
films with GMHA concentration below the percolation point), were
averaged. The average of % GMHA retained below the percolation point is
statistically similar across all film types.
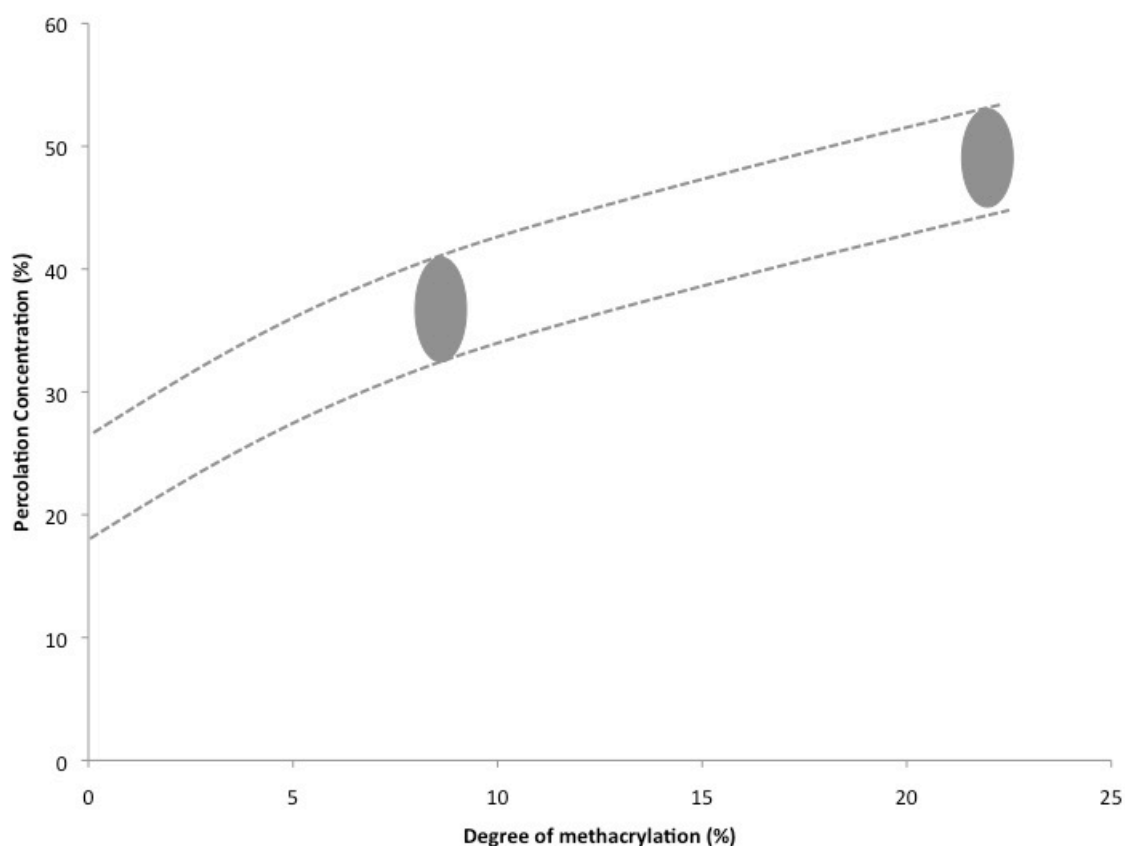
Figure 4.7. Percolation threshold versus degree of methacrylation. The concentration of GMHA(11) and GMHA(32) at the percolation threshold is plotted against the degree of methacrylation 8% and 22%, respectively. The dotted lines are drawn for the eye only but indicate that there may be a power relationship between these values. This relationship would make sense because eventually there would be a limit for alginate required to make an "alginate-rich" matrix.

4.2.2 Swelling and thickness studies The swelling ratio provides an indirect approximation of the crosslinking density of a hydrogel. (Zawko *et al* 2009) The swelling ratio is the ratio of grams of water absorbed per gram of polymer. The more a hydrogel is crosslinked or entangled, the less it swells and the less water is absorbed. Therefore lower swelling ratios are typically associated with high crosslinking density or highly entangled polymers. GMHA(32)-only films and LVG alginate-only films had similar swelling ratios (2.5 ± 0.15 and 2.6 ±.0.16, respectively). Both single-polymer films had relatively low swelling ratios compared to the swelling ratios we observed in alginate-only films gelled in lower molarity calcium chloride solution. This lower swelling ratio was a result of highly crosslinked and/or entangled polymer strands. We investigated the same variable changes in swelling ratio as with polymer retention, to infer crosslinking density of films in various states. In other words, we quantified swelling ratio changes with respect to composition while modulating the degree of methacrylation (DM) of GMHA and the molecular weight (MW) of alginate.

The swelling properties of alginate/GMHA compositions are presented in **Figures 4.8 – 4.10**. Swelling ratios across variations in composition had a similar trend, regardless of DM or MW of alginate. That is, introducing up to 33% w/v GMHA to alginate-rich films caused an increase in swelling ratio. Swelling ratios of compositions with greater than 33% w/v GMHA differed based on the percolation point of GMHA. As the composition reached percolation, there was a significant change in swelling ratio depending on whether or not the film was exposed to UV. Swelling ratio was dependent on exposure to UV for film compositions greater than 33% GMHA. Films that were exposed to UV had a significantly lower swelling ratio than similar films that were not exposed to UV.

Swelling ratios of films comprised of alginate/GMHA with GMHA concentrations below the point of percolation are significantly higher than alginate-only or GMHA-only films. This phenomenon is most likely a result of the following factors: decreased entanglement of the alginate polymer strands, the presence of non-photocrosslinked GMHA, and increased pore volume due to loss of GMHA.

We theorize that in low concentrations of GMHA, the GMHA clusters serve to interrupt either the calcium bridges formed by the crosslinked alginate, or the entangling of the alginate to itself. Similarly the alginate serves to interrupt the ability for the GMHA to create crosslinked networks or to entangle. Therefore, the overall crosslinking density is decreased with compositions of alginate/GMHA-blended films. If the swelling ratio changes were due to an interruption of calcium bridges, then changing the molecular weight would have less of an effect on the swelling ratio since M/G ratio remains the same for either molecular weight. If the swelling ratio changes were due to a decrease in the entanglement of the polymers, then higher molecular weight alginate would have lower swelling ratios than similar films of lower molecular weight alginate. We observed a significant decrease in the overall affect of compositional changes to swelling ratio in higher molecular weight alginate films. Thus, molecular weight played a significant role in the swelling ratio as a result of the ability for strands to entangle with one another and, therefore, cause an overall increase in density of the film. These results are supported by the handlability studies that indicated that higher molecular weight alginate increased the range of compositions capable of making a handleable film.

Another reason that the addition of GMHA to alginate-rich films increased the swelling ratio (below the percolation threshold) was the attraction of water to GMHA. With the addition of non-photocrosslinked GMHA, there is a driving force for more water to be bound to the film. We hypothesize that clusters of GMHA (below the

percolation threshold) are not photocrosslinked continuously to each other, and, therefore, have lower crosslinking density than the continuous phase photocrosslinked GMHA. Uncrosslinked GMHA is soluble and has much greater swelling ratios than crosslinked GMHA (Zawko *et al* 2009). Therefore, for GMHA concentrations below the percolation threshold, there was an increase in ability to retain water around the GMHA clusters. Furthermore, the pore volume of the film was most likely increased by the introduction and subsequent loss of some GMHA. As previously discussed, for GMHA concentrations less than the percolation threshold, approximately 65% of the GMHA remained in the film. Thus, between 30-40% of GMHA was leached through contact to water at the surface of the film. This 30-40% polymer loss may increase the pore volume of the film, which is subsequently replaced with water. Increased pore volume attracts more water into the hydrogel. (Malladi *et al* 1984) Exact pore volume changes were not determined.

As the concentration of GMHA reached the percolation threshold, the swelling ratio was then dependent on UV exposure. Films exposed to UV with GMHA concentrations at or beyond percolation threshold experienced a lowered swelling ratio. This decrease was a result of increased crosslinking with the network of methacrylated GMHA. With increased crosslinking, less water is absorbed into the film. Simultaneously, films with GMHA concentrations at or above the percolation threshold that were not exposed to UV experienced a continued increase in swelling ratio. This increase was a result of the loss of GMHA, and, therefore, reduced crosslinking density. This loss of material most likely increased pore volume, and this volume was subsequently replaced with water. Therefore, more water was absorbed by films that lost GMHA polymer via percolation. These results were expected and follow the results of the polymer retention studies.

The results of swelling studies were congruent with the polymer retention studies. Films that retained GMHA had a lower swelling ratio than films that did not retain any GMHA in alginate/GMHA-blended films. This decreased swelling ratio makes sense because there are more crosslinks in the films with GMHA. Thickness measurements were also taken along with swelling ratio results, and are presented in Figures 4.8-4.10. Thickness of films that have not been exposed to UV are indicated with solid gray line. Thickness of films that were exposed to UV are indicated with the dotted black line. Changes in film thickness followed a similar trend as swelling ratio. The more crosslinked a film, the thinner the film. The less crosslinked a film, the thicker the film. That said, all films primarily remained in the desired thickness bracket of 50 – 120 μm.
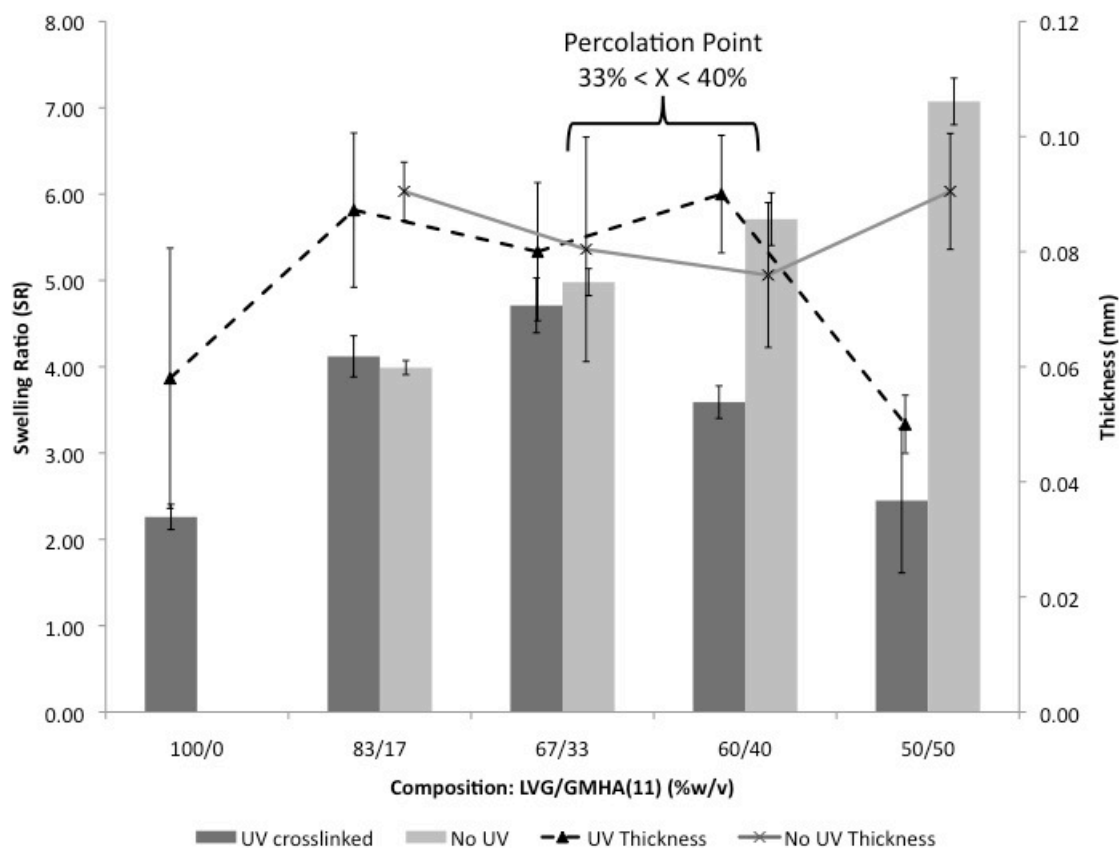
Figure 4.8. Swelling ratio and thickness of LVG/11 films. The swelling ratio of LVG/GMHA(11) films was determined between swollen weight in ddI water (24 hours) and the lyophilized weight. Hydrated weights were taken after rinsing protocol. The swelling ratios are similar between films with or without exposure to UV with GMHA(11) concentration below the percolation threshold. For films with GMHA(11) concentrations above 33%, the swelling ratios are significantly different with exposure to UV. LVG films with 40% GMHA(11) swell twice as much without exposure to UV. Films with UV exposure have a low swelling ratio, indicating an increase in crosslinking density. Films without exposure to UV have a higher swelling ratio, indicating a decrease in crosslinking density. These results indicate that the loss of GMHA decreases the overall crosslinking density. For all films N =3.
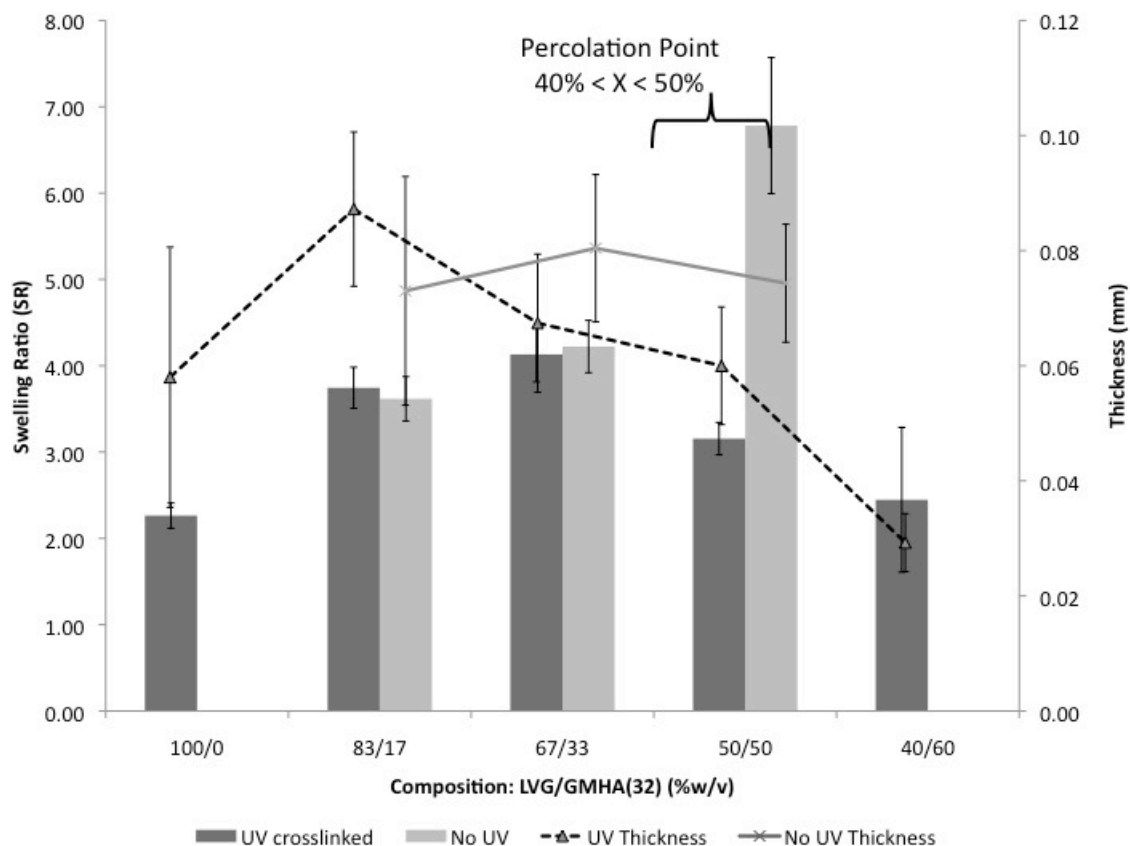
Figure 4.9. Swelling ratio and thickness of LVG/32 films. The swelling ratio of LVG/GMHA(32) films was determined between swollen weight in ddI water and the lyophilized weight. Hydrated weights were taken after rinsing for 24 hours. The swelling ratios are similar between films with or without exposure to UV with GMHA(32) concentration below the percolation threshold. For films with GMHA(32) concentrations above 33%, the swelling ratios are significantly different with exposure to UV. LVG films with 50% GMHA(32) swell more than twice as much without exposure to UV. Films with UV exposure have a low swelling ratio, indicating an increase in crosslinking density. Films without exposure to UV have a higher swelling ratio, indicating a decrease in crosslinking density. These results indicate that the loss of GMHA decreases the overall crosslinking density. We were not able to obtain test the swelling ratio of films with less than 50% alginate. For all films N =3.

81
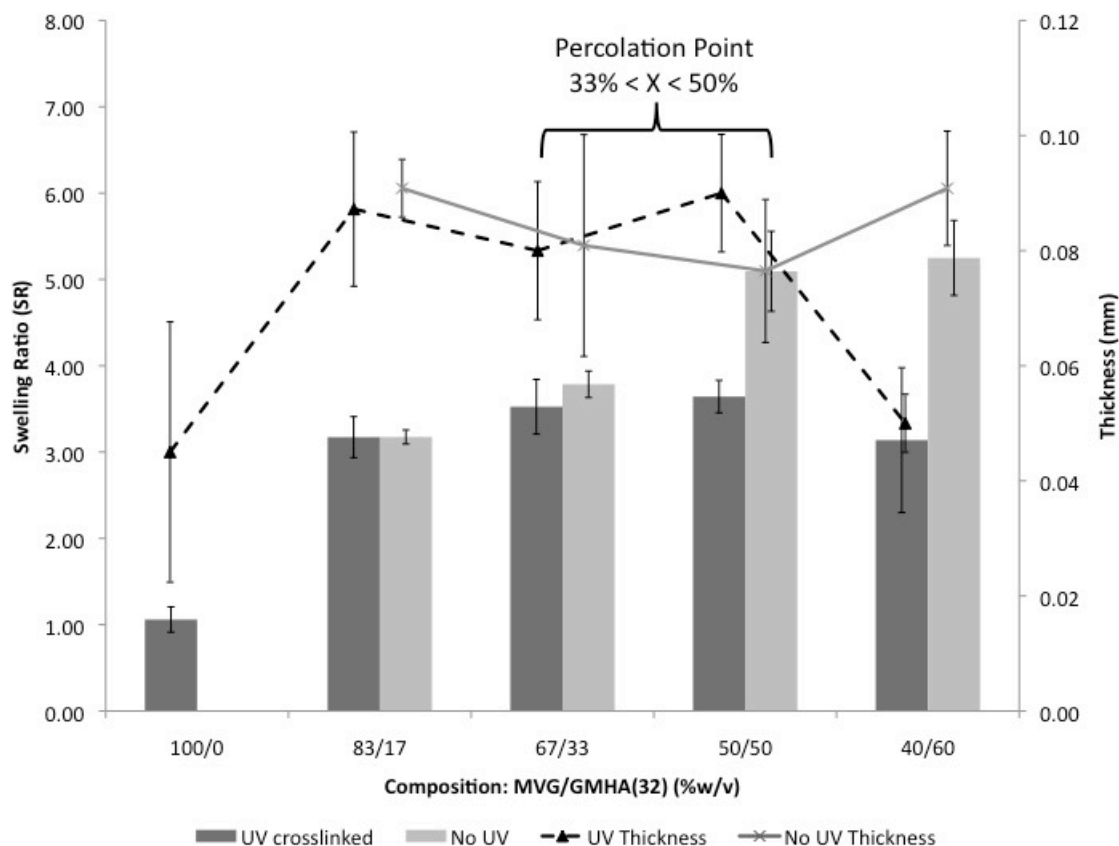
Figure 4.10. Swelling ratio and thickness of MVG/32 films. The swelling ratio of MVG/GMHA(32) films was determined between swollen weight in ddI water and the lyophilized weight. Hydrated weights were taken after rinsing protocol. The swelling ratios are similar between films with or without exposure to UV with GMHA(32) concentration below the percolation threshold. For films with GMHA(32) concentrations above 33%, the swelling ratios are significantly different with exposure to UV. LVG films with 50% GMHA(32) swell 30% more without exposure to UV. This swelling difference is not as dramatic as the LVG films because the MVG alginate chains are much more entangled. Films with UV exposure have a low swelling ratio, indicating an increase in crosslinking density. Films without exposure to UV have a higher swelling ratio, indicating a decrease in crosslinking density. These results indicate that the loss of GMHA decreases the overall crosslinking density. For all films N =3.

4.2.3. Calcium content The ability for alginate to exchange sodium ions for divalent cations is well described (Haug & Smidsrod 1965, Smidsrod & Haug 1965, Roger *et al* 2006, Sartori *et al* 1997). Although this exchange can occur with many divalent cations, calcium, in particular, causes a stronger gelation than most. Furthermore, this exchange is highly dependent on the M/G ratio of alginate residues. The selectivity coefficient for high-G alginate to associate with calcium ions has been found to be high when compared to other divalent cations (Haug & Smidsrod 1965). This exchange causes intra- and inter-chain associations with the glucuronate residues (G-units) via negatively charged oxygen atoms on the carboxyl moieties (Braccini *et al* 1999). Approximately two sodium ions are displaced for every calcium ion. These calcium ions remain associated with the G-units in an "egg crate" model (Grant *et al* 1973). This model has been verified with infrared radiation identifying COO- peak changes with calcium binding. Calcium-bound G-units make a zipper-like formation with tunnels for calcium ions to traverse. The more sequential G-units there are, the more calcium ions bind. These zipper-like formations are called calcium bridges and are the foundation for gelation and mechanical integrity of resultant alginate-based films. When the carboxyl groups of the glucuronate residues associate with calcium, they give up associations with water. This exchange is not easily reversed, and calcium-alginate gels are not soluble in water.

The ability for the alginate to form calcium-bridges is critically important for the handleability of the resulting alginate/GMHA films. As previously discussed, films with low concentrations of alginate could not be handled. From our polymer retention results, most likely the alginate forms isolated clusters within a GMHA-rich film at these low-alginate concentrations. Without a continuous phase, calcium bridges could not form a

network across all of the alginate in the film. Without these calcium bridges, the film cannot be handled.

To better understand how changes in composition would affect the amount of calcium in the films, we quantified calcium content via atomic absorbance spectroscopy (AAS). AAS is a common method for calcium determination in alginate films, and confirms the gelation reaction exchange between sodium and calcium (Roger *et al* 2006, Pereira *et al* 2013). We aimed to verify if the addition of GMHA(32) decreased the amount of calcium bridges formed by the alginate (LVG or MVG). If concentration of calcium (mmol) per weight of alginate (g) decreased with increasing GMHA(32) concentration, then the GMHA(32) may be interrupting calcium bridge formation. Alternatively, if the concentration of calcium (mmol) per weight of alginate increased with GMHA(32) concentration then the GMHA may be sequestering calcium ions. Finally, no change in calcium content would suggest that the presence of GMHA(32) has no effect on the calcium bridge formation between glucuronate residues, and was not sequestering calcium ions. Calcium causes HA chains to change from a 4-fold conformation to a 3-fold conformation, meaning that the molecule takes on a more relaxed conformation. (Sheehan *et al* 1983) This structural change causes chain relaxation, with a reduction in "stiff segment" concentration. The viscosity of calcium-HA solutions is less than equivalent sodium-HA solutions. (Napier & Hadler 1978) Biologically, this conformational change phenomenon provides synovial mucin with its diffusive properties. (Ropes *et al* 1947) Calcium ion binding is preferred over sodium ions, yet requires significant hydration. (Sheehan *et al* 1983) As long as there is significant water available (specifically, 9 water molecules for every 1 calcium ion), then the HA will prefer the 3-fold conformation with calcium binding.

The results of AAS are shown in **Figure 4.11**. The dotted line represents the theoretical value of calcium concentration (mmol) per weight of alginate (g) cast. This value is calculated based on the theoretical exchange of 1 calcium ion per 2 sodium ions using sodium content provided per manufacturer. This value does not take into consideration calcium sequestered by the GMHA(32). Calcium ions are associated with HA carboxyl and hydroxyl moieties. With GMHA, there is a significant decrease in available hydroxyl moieties and specific mmol Ca/g GMHA cannot be estimated.

From our AAS values we concluded that the presence of GMHA(32) had little impact on the overall calcium content in resulting films. Alginate-only films contained a calcium concentration near theoretical predictions. Alginate/GMHA(32) films with 17% GMHA(32) also contained a calcium concentration near the theoretical value, independently of UV exposure. Alginate/GMHA(32) films with 33% GMHA followed this same trend with values similar to theoretical, with or without photocrosslinking. We conclude that the presence of GMHA(32) does not disturb the calcium bridge formation in alginate/GMHA(32) films.
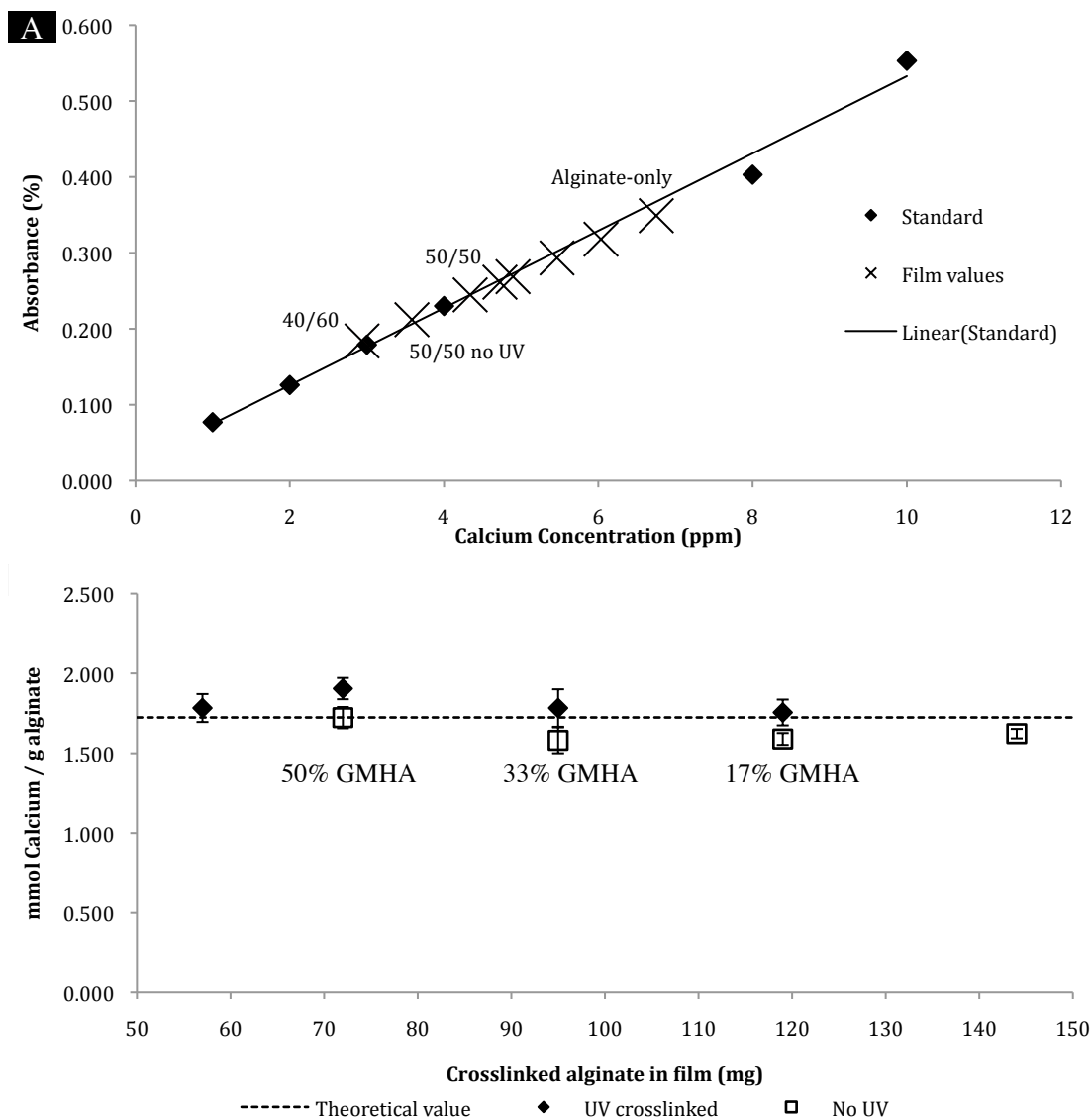
Figure 4.11. Calcium content of LVG/32 films. Films were fabricated in 12-well tissue culture plates, producing 2.2 cm diameter films that were dissolved in 0.05 M EDTA overnight. Solutions were diluted with nitric acid. A) Calcium standards were made in nitric acid. All film values fell along the linear portion of AAS standard. As expected, films cast as 100% LVG had the highest amount of calcium ions in the film. B) The calcium content for all films were at the theoretical value for an exchange of sodium for calcium per weight of alginate, except the LVG films with 50% GMHA(32) sequester more calcium ions per gram of alginate than theoretical, when exposed to UV. This suggests that there may be mutual calcium ion sequestering between both polymers at that composition. For all films N =3.

4.2.4. Dissolution studies Degradability is an essential property for tissue engineering devices. Many non-resorbable surgical devices commonly used in abdomenopelvic surgeries are often accompanied by significant scarring or foreign body response. Furthermore, FDA requires extensively more quality control for implants persisting beyond 28 days after implantation. (FDA 2002) The success of an abdominal adhesion barrier is inherently tied to its ability to bioresob quickly after the critical healing period. To determine the degradability of alginate/GMHA-blended films, we first considered the mechanisms for degradation. While hyaluronidase enzymatically degrades HA (Stern 2003), there is no enzyme to degrade the plant-based alginate. Bolus injections of solution-state alginate of molecular weight 108 kDa was shown to be primarily renally cleared. (Al-Shamkhani *et al* 1995) These injections contained non-gelled, soluble alginate able to be distributed by the lymphatic system and the blood stream. Our films contain gelled alginate, which is not water-soluble. Therefore a mechanism for reverse gelation of the alginate would need to be incorporated into degradation studies of our films.

The dissolution of calcium-alginate in sodium-rich solutions is well known. (Smidsrod & Haug 1972) Sodium ions are smaller than calcium ions, which require less energy to bind to the carboxyl groups of the G-units. Any association of calcium with M-units is quickly substituted for sodium when exposed to sodium-rich solutions. Once the M-units release the calcium, this exposes G-units to sodium ions, which subsequently causes release of more calcium. The replacement of calcium ions with sodium ions causes a reverse gelation of the alginate. The resulting sodium alginate is soluble in aqueous solutions. The timing and degree of the replacement of calcium ions with sodium ions is highly dependent on the concentration of sodium ions exposed to the gelled alginate. In summary, the alginate component of the films would dissolve in the presence

of physiological fluids, which are naturally sodium-rich; however, this dissolution would depend heavily on the amount and duration of sodium-rich fluid exposed to the film.

Although we could not replicate the dynamic biological healing environment of an abdominal injury *in vitro*, we could assess the type of mechanisms required for full dissolution of the films at various compositions and crosslinking densities. We could also observe the dissolution profile, which could support analyzing *in vivo* degradation in the future. We first attempted to dissolve the films in physiologically relevant concentrations of hyaluronidase (5 IU/dL) in phosphate buffered saline (PBS). Results were difficult to ascertain because the timeline for replacement of calcium ions with sodium ions is much shorter than the enzymatic degradation of GMHA. In fact, we were ultimately unable to degrade GMHA-only films with high levels of hyaluronidase, up to 500 IU/dL. This inability suggests that the enzyme could not physically get to the densely packed GMHA in the films. However, for the purpose of this project, GMHA-only films were not further investigated for degradation, since they do not have good handling properties.

We then approached dissolution of just the alginate component. Since exposure to sodium-rich fluids is inconsistent from person to person, there was no physiologically relevant volume of PBS to test. Therefore, it was of interest to create a dissolution study that was efficient for laboratory assessment. To speed up the removal of calcium for dissolution of the films, we used citrate, a well-known calcium chelator. At pH 7.4, citrate has three deprotonated carboxylic moieties (pKa1 = 2.79, pKa2 = 4.30, pKa = 5.65) capable of binding to divalent cations. (Roger *et al* 2006) The chelation of calcium ions can be tailored by citrate molarity. Using 0.1 M citrate caused removal of calcium ions on the order of minutes. It was of great importance that each film piece be similar to one another, thus have theoretically similar calcium ions per each film type.

The results of dissolution studies are shown in **Figure 4.12**. A film that could not be seen or found with a spatula was considered to have gone through complete dissolution. The alginate-only (LVG) films went through complete dissolution just after an hour of exposure to citrate. Films with 17% GMHA(32) and 33% GMHA(32) went through complete dissolution in less than 60 minutes and less than 30 minutes, respectively. This reduced time for dissolution was expected because there is less alginate in these films, and, thus, less calcium to replace. From the calcium content studies we know that with decreased alginate, there is an expected decreased amount of calcium to chelate from that film. We also assume that pore volume increase due to GMHA leaching may play a role in the dissolution timing of the films. Larger pores and/or pore volume allow the citrate solution greater access to polymer chains and, thus, calcium ions to chelate. Therefore, the amount of time it takes to cause dissolution of the films decreases with addition of 17% or 33% GMHA(32) to alginate (LVG) films.

Films with 40% GMHA(32) or greater, that were exposed to UV, did not go through complete dissolution in citrate. At 60 minutes, 24.7 ± 0.64 mg of films with 40% GMHA(32) remained. At 60 minutes, 29.6 ± 0.63 mg of films with 45% GMHA(32) remained. At 60 minutes, 30.0 ± 2.13 mg of films with 50% GMHA(32) remained. At 60 minutes, 40.8 ± 1.71 mg of films with 60% GMHA(32) remained. Since these films had GMHA(32) concentrations greater than the percolation threshold, we concluded that a continuous phase was reached and that UV crosslinking provided a network of GMHA. This network is not stabilized by calcium ions and therefore the removal of calcium does not effect the stability of this network.

Films with 50% GMHA(32) that were not exposed to UV went through complete dissolution the fastest, within 20 minutes in citrate. This observation was expected because there is half as much alginate as the alginate-only films. Also this result followed

our knowledge of polymer retention. These films are pure alginate (LVG) films because the GMHA(32) has reached the percolation threshold and the continuous phase leaches from the film without UV crosslinking. Therefore we expected for these films to go through complete dissolution. Furthermore, we expected this dissolution to occur more quickly than the alginate-only films because the loss of the GMHA(32) may leave behind an increased pore volume. To investigate this theory, we compared the dissolution rate of the same weight of alginate in a film cast of 100% LVG vs. a cast LVG film of 50% GMHA(32) that was not exposed to UV. Therefore the only difference between the films was any pore volume change with the leaching of GMHA(32). The cast amount of alginate was held constant. Qualitatively, the 100% LVG film went through dissolution about 5-10 minutes after the 50% LVG film, supporting the theory that leaching causes an increase in pore volume. No further studies were conducted.

As the alginate-only film contains the most grams of alginate, and therefore, the most calcium ions, the citrate required to cause full dissolution should be the greatest of any film. The more calcium ions to remove, the more citrate required to remove those ions. Theoretically, if we removed all calcium ions from the film, then it would cause full dissolution of the alginate, and there would be no alginate left in the film. If this were true, then all mass remaining after the dissolution would be a GMHA network. We compared the mass of film remaining after 60 min in 0.1M citrate to the mass of GMHA(32) retained in that film composition from the polymer retention studies. The values were within standard deviation (**Figure 4.13**).

Films that remained after an hour of exposure to citrate were films that had a continuous network of UV crosslinked GMHA. This percent mass remaining was statistically similar to the percent mass of GMHA that did not leach from the film as determined in the polymer retention studies. This result indicated that the alginate

component went through reverse gelation with release of calcium ions and the GMHA component was still intact.

The conclusions of our dissolution studies were two-fold. The most important finding was that films with GMHA concentrations lower than the percolation threshold went through complete dissolution with the loss of calcium ions. This suggests that there is only one mechanism for dissolution of this film. The GMHA clusters do not create a full network and, thus, dissolve when not caught in the alginate-rich gelled matrix. The films with GMHA concentrations greater than the percolation threshold, and exposure to UV, did not dissolve with the removal of the calcium ions. This result is due to the continuous phase of GMHA that is photocrosslinked. This continuous phase creates a network that is not stabilized by calcium ions and, thus, does not dissolve by this mechanism. The films with GMHA values close to the percolation threshold, without going over it, went through complete dissolution the fastest.
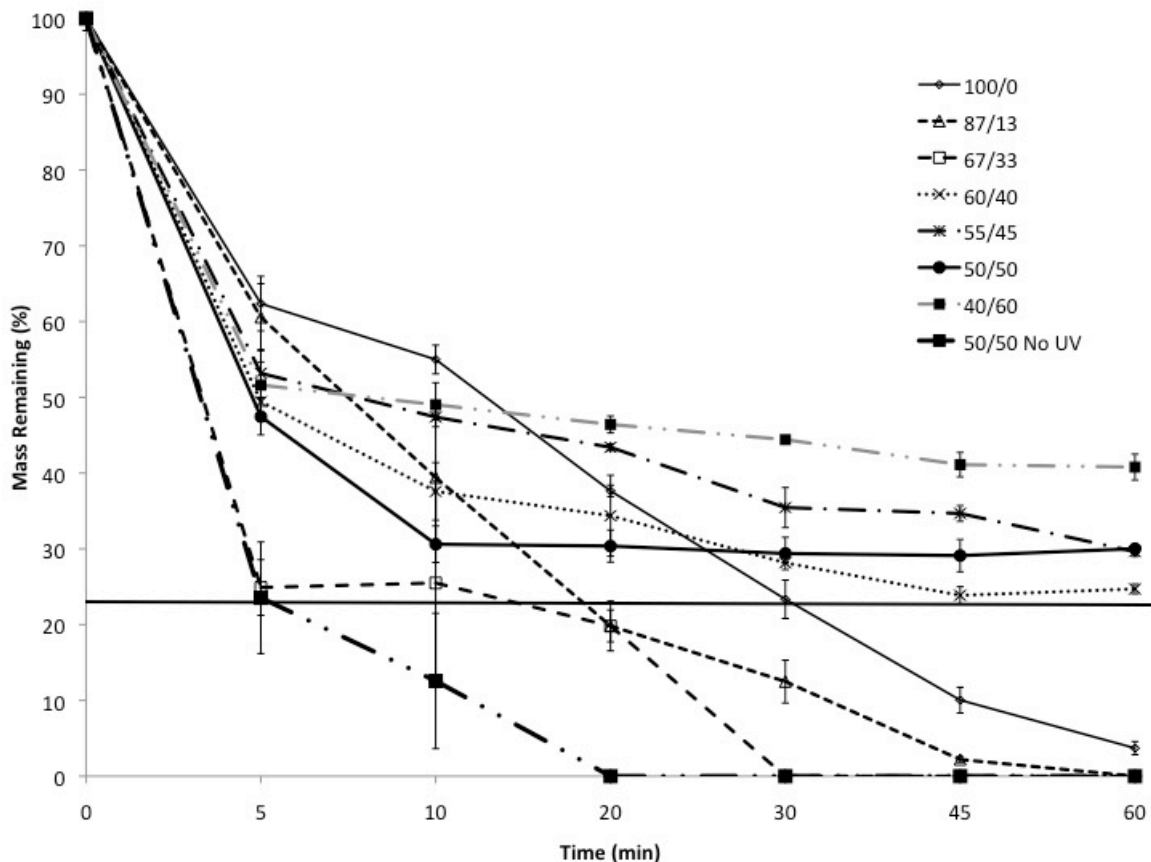
Figure 4.12. Dissolution of LVG/32 films in 0.1 M citrate. After fabrication and rinsing, films were oven-dried, weighed, swelled in ddI water, and then exposed to citrate. At given timepoints films were removed from citrate, rinsed, oven dried, and weighed. Mass remaining is given on the y-axis as a % of original weight. The flat black line indicates the break between films that fully dissolved and films that did not go through dissolution due to a GMHA network stabilized by methacrylate crosslinking. Films with GMHA concentrations below the percolation threshold went through full dissolution. The film with 50%GMHA(32) not exposed to UV went through dissolution the fastest. For each timepoint N = 3.
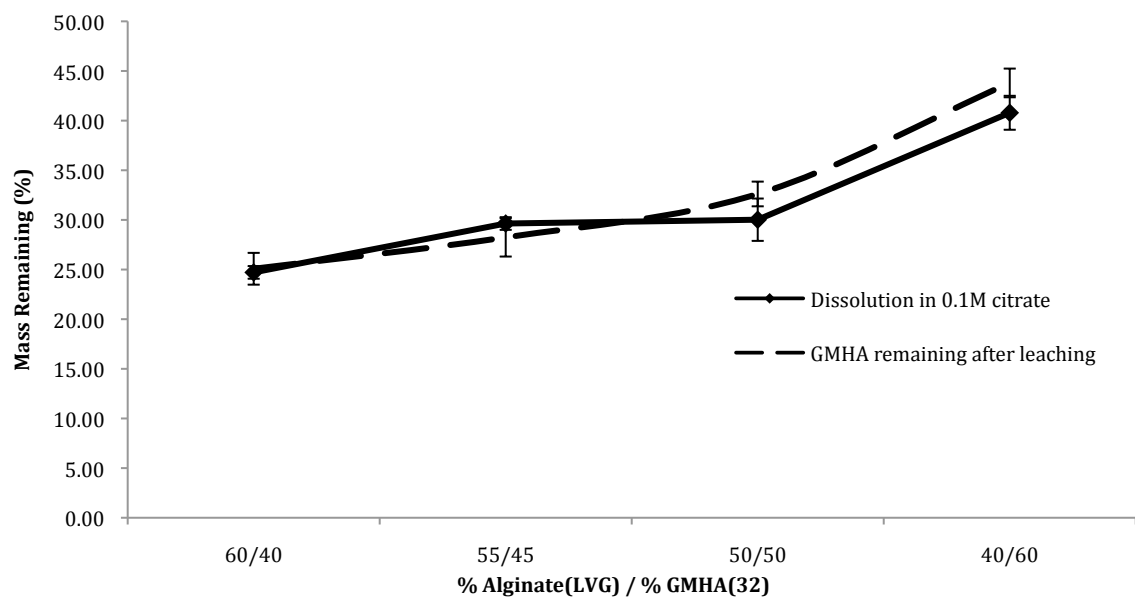
Figure 4.13. Retention of GMHA versus mass not dissolved in 0.1 M citrate. The weight of polymer lost in the polymer retention studies was assumed to be loss of only the GMHA component. Therefore, we calculated the % of GMHA retained from leaching and plotted here as % mass of the total film on the y-axis vs film composition on the x-axis. These values are represented by the dotted line. The solid line represents mass remaining as a % of original mass after exposure to 0.1 M citrate for 60 min. The two curves agree within statistical significance, which suggests that the citrate has caused dissolution of the alginate component and that only GMHA remains. N = 3.

4.2.5. Thermogravimetric analysis The results of the polymer retention studies indicated that polymer was leaching from the films during the rinsing. We sought to determine what the constituents of our films were after fabrication and rinsing, to support the assumption that GMHA was the only component responsible for this loss of polymer retention. Thermogravimetrical analysis (TGA) is widely applied for determination of constituents in hydrogels. (Caykara *et al* 2005) The decomposition temperature is the temperature at which a material experiences significant structural change and chemically decomposes. Thermal decomposition requires breaking of bonds with subsequent mass loss, which is measured with a TGA. If alginate and GMHA have different decomposition temperatures and profiles then we would see a shift in decomposition of the film with compositional changes of these two polymers. Some studies have conducted similar studies with blends of alginate and HA. (Sun & Zhitomirsky 2010) These studies conducted TGA analysis on solutions of unmodified and uncrosslinked alginate and HA. Their conclusions indicated that increasing concentration of HA in alginate-rich solutions caused increased temperature of thermal decomposition of the blended hydrogels.

We first ran TGA of the polymers as received vs. crosslinked/gelled to observe changes that crosslinking/gelation would impart. The derivative of the decomposition curve provides the ability to discern small differences in mass change. The derivative curves of alginate and GMHA are presented in **Figure 4.14**. The alginate was run as received vs. a cast film gelled with calcium ions and rinsed. The GMHA(32) was run as a powder vs. a cast film with UV exposure. While there was little difference between the UV crosslinked GMHA vs. GMHA powder with decomposition at 220 °C, there was a significant difference in calcium gelled alginate film vs. alginate powder. The effect of calcium gelation caused a flattening of the decomposition profile, shown as a removal of the sharp peak in the derivative profile. We then analyzed all compositions of

alginate/GMHA-blended films. The derivatives of these curves are provided in **Figure 4.15**. The effect of calcium crosslinking was so great that differences in composition were not discernable. Films of all compositions that were exposed to calcium had a similar decomposition profile. We hypothesize that the presence of calcium alginate stabilizes the GMHA so as to prevent decomposition at 220 °C. Thus, compositional changes were not discernable. This result prevented TGA from being a useful way to verify that alginate was not leaching from the film.

However, the decomposition of a film comprised of 50% GMHA(32) that had been exposed to 60 minutes of 0.1M citrate had a profile very similar to that of GMHA-only film. (**Figure 4.16**) This result supports earlier findings that removal of alginate leaves a GMHA-only network.
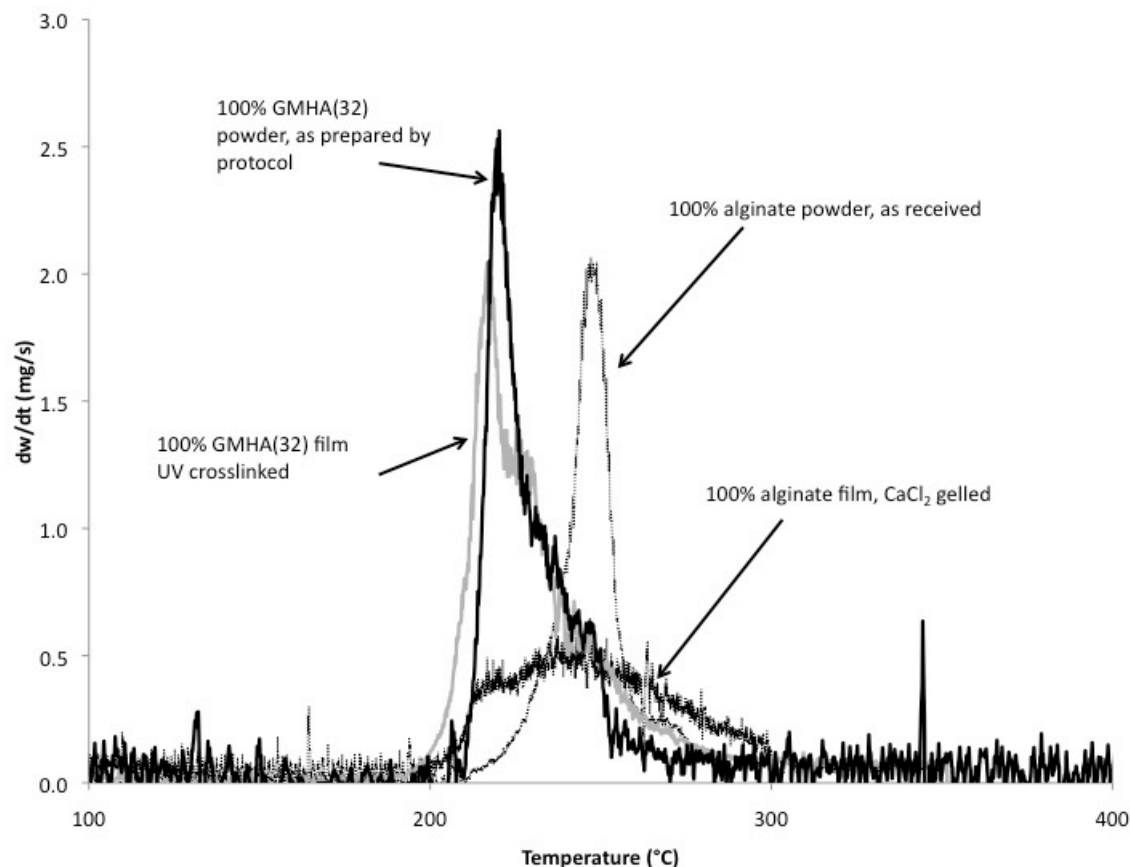
Figure 4.14. Differential TGA of alginate and GMHA powders, UV crosslinked GMHA film, and calcium gelled alginate film. Alginate powder (LVG, medical grade, M/G ratio 0.67, 120 kDa) decomposes around 250 °C with a 50% mass loss. GMHA(32) powder decomposes at around 220 °C with a 50% mass loss. A crosslinked GMHA(32) film decomposes around 210 °C with a 50% mass loss. A calcium gelled alginate (LVG) film decomposes between 210 °C and 300 °C with a 20% mass loss. The profiles of uncrosslinked and crosslinked GMHA are not very different. The profiles of alginate powder vs. gelled alginate are very different.
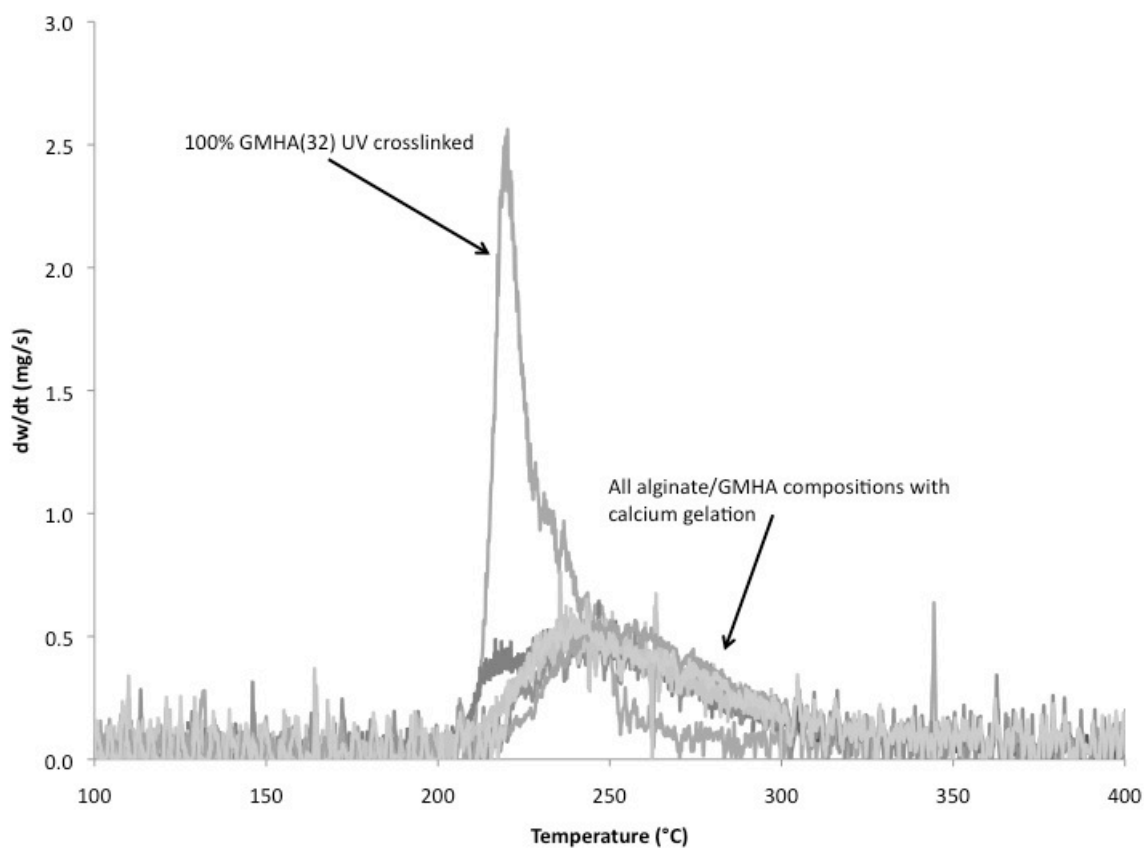
Figure 4.15. Differential TGA of LVG/GMHA(32) films of varying compositions from 100% LVG to 100% GMHA(32). Alginate (LVG, medical grade, M/G ratio 0.67, 120 kDa) and GMHA(32) blended films of the following compositions were analyzed for decomposition temperature and profile (alginate/GMHA %w/v): 100/0, 83/17, 67/33, 50/50, 40/60, 0/100). All films with calcium-gelled alginate appeared to have no identifiable change with this type of analysis.

97
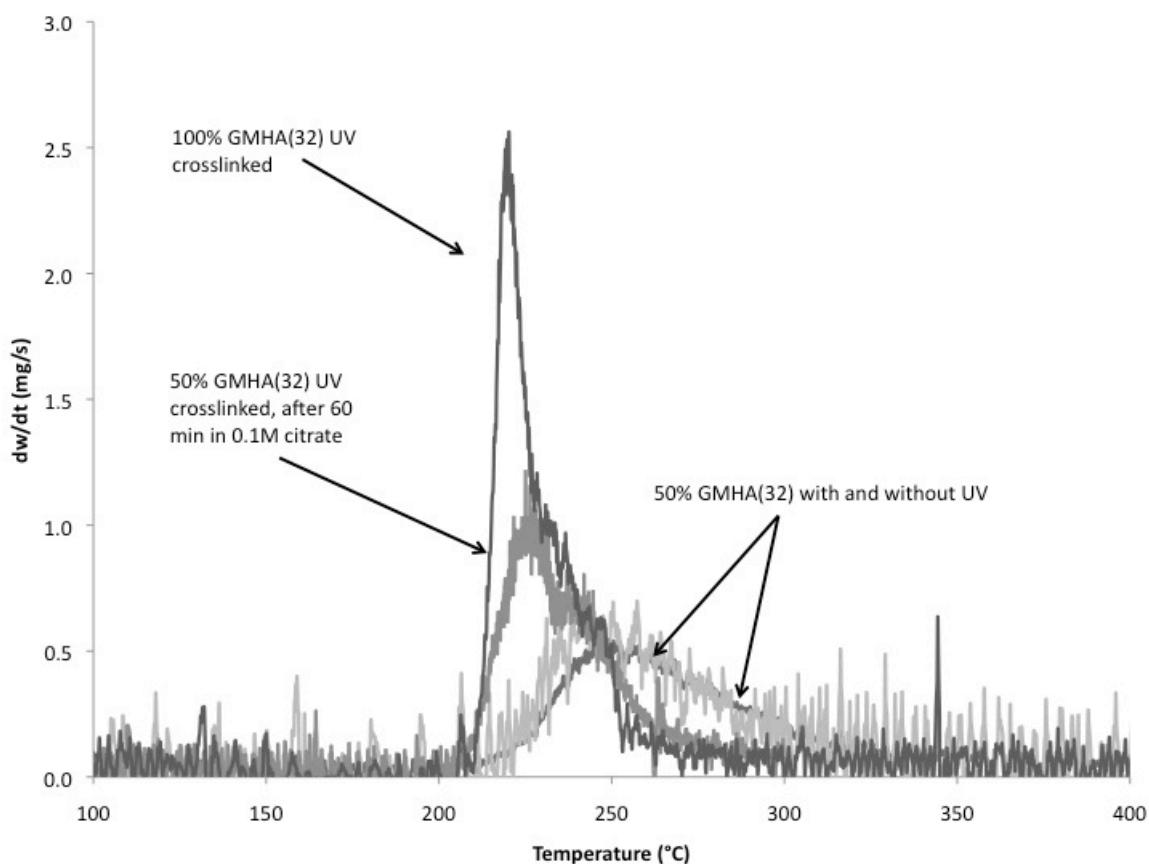
Figure 4.16. Differential TGA of LVG/GMHA(32) films at percolation threshold before and after 60 min exposure to 0.1 M citrate. Alginate (LVG, medical grade, M/G ratio 0.67, 120 kDa) and GMHA(32) films with 50% GMHA(32) were analyzed with and without exposure to UV. Since calcium gelled alginate was present in both films, there is no significant difference in the decomposition profile. However, the LVG/GMHA(32) 50/50 film exposed to UV and then exposed to 60 min of 0.1 M citrate has a decomposition temperature and profile similar to the 100% GMHA(32) film which indicates that calcium gelled alginate has been removed with citrate.

4.3 MATERIALS AND METHODS

4.3.1. Materials. Medical grade sodium alginate was purchased from FMC Novamatrix (Sandvika, Norway): Pronova UP LVG: 120 kDa, M/G ratio 0.67, and Pronova UP MVG: 220 kDa, M/G ratio 0.67. High molecular weight sodium hyaluronate from *Streptococcus equi* of molecular weight 1.6×10^6 Da was obtained from Sigma-Aldrich (St. Louis, MO). Photoinitiator Irgacure 2959 (I2959) was obtained from Ciba Specialty Chemicals (Basel, Switzerland). All other chemicals purchased from Fisher Scientific.

4.3.2. Methacryloyl modification of hyaluronic acid. High molecular weight hyaluronic acid was conjugated with photocrosslinkable methacryloyl groups based on two protocols (Zawko 2008, Bencherif *et al* 2008). A 1% w/v solution of HA was prepared in either ddI water or a 50:50 mixture of acetone:water and stirred for 24 hours at room temperature. Twenty molar equivalents of both triethylamine as base catalyst and of glycidyl methacrylate were added to the solution and stirred for five days at room temperature (pH 12.5-10.5). Modified HA (GMHA) was precipitated into a 20-fold volumetric excess of acetone and then subsequently dissolved in water for 24 hours at room temperature. GMHA solution was then dialyzed against ddI water in 3500 MWCO for 72 hours. Samples were lyophilized after filter sterilization and stored in dessicators at -20 °C. The average degree of methacrylate substitution was determined by ^{1}H NMR. For solutions prepared in ddI water, substitution was found to be 8.9% ± 0.6 substitution of methacryloyl groups per mole of HA disaccharides. For solutions prepared in 50:50 mixture of acetone:water, substitution was found to be 22% ± 1.1. These values are an average of 10 analysis.

4.3.3 Polymer retention studies. A 1% w/v aqueous solution of photoinitiator Irgacure 2959 was sonicated for 30 min and allowed to cool to room temperature. To

obtain the dry weight, W_D, 15mL of a 1% aqueous solution of alginate/GMHA was cast into a 50 mL conical vial using the same pipette system used to cast into the forms. The conical vial was lyophilized and weights were taken gravimetrically. To obtain weight retained, W_R, 15 mL of a 1% solution of alginate/GMHA with 0.05% Irgacure 2959 was cast into a 72 mm by 72 mm form. Forms were placed in a temperature and humidity controlled environmental chamber from Cincinnati Sub-Zero (Cincinnati, Oh). Temperature was held at 25 °C and humidity was held at 70% Rh during the casting period of 48 hours. Forms and solutions were kept from light at all times. Cast films were then subjected to UV light from the chamber, depending on the experiment. After photocrosslinking, if conducted, 50 mL of 100 mM calcium chloride solution was pipetted on top of the cast film in the form. Films were left to crosslink for 30 minutes. Films were removed from molds, when possible, and transferred to petri dishes with large volumes of ddI water. Films were rinsed exhaustively in ddI water for 24 hours, 48 hours, or 10 days, depending on the experiment. Films were then placed into a 15 mL conical vial, lyophilized, and weights were taken gravimetrically. All films were tested in triplicate. **Equation 5** was used to determine the amount of polymer remaining:

$$\%Polymer = \frac{W_R}{W_D} \times 100 \qquad\qquad [5]$$

4.3.4. Synthesis of a calcium alginate/GMHA film. A 1% w/v solution of alginate/GMHA in ddI water was stirred at room temperature overnight, and cast in a 72 mm by 72 mm form. Forms were placed in a temperature and humidity controlled environmental chamber from Cincinnati Sub-Zero (Cincinnati, Oh). Temperature was held at 25 °C and humidity was held at 70% Rh during the casting period of 48 hours. Forms and solutions were kept from light at all times. Cast films were then subjected to UV light from the chamber, depending on the experiment. After photocrosslinking, if

conducted, 50 mL of 100 mM calcium chloride solution was pipetted on top of the cast film in the form. Films were left to crosslink for 30 minutes. Films were removed from molds, when possible, and transferred to petri dishes with large volumes of ddI water. Films were rinsed exhaustively in ddI water for 24 hours.

4.3.5. Film thickness and swelling ratio measurements. After synthesis and rinsing, films were cut with a six-inch blade into four equally sized pieces, with ribbing discarded. (Figure 3.8) Three thickness measurements were taken of each piece, one at the top, one in the middle, and one at the bottom, with a micrometer. The average of these values was taken as the thickness. The swelling ratio was determined by Equation 3. To obtain swollen weight, each piece was placed on a surgical glove and scooted around until excess water was removed. This step was conducted three times for each piece. The average of these three values gives Ws [mg] in **Equation 6**. Film pieces were then placed into 15 mL conical tubes and lyophilized for 48 hours. Dry weight gives Wd [mg]. All tests were conducted in triplicate.

$$SW = \frac{W_S - W_D}{W_D} \qquad [6]$$

4.3.6. Calcium content by atomic absorption spectroscopy (AAS). Films were cast into 12-well tissue culture plates, rendering films approximately 2 cm in diameter. Films were fabricated in the same fashion as 72 mm by 72 mm films. After fabrication and rinsing, 2 cm diameter films were lyophilized and dry weights were obtained. This dry weight was used to determine mmol calcium / g alginate. Films were then dissolved in 10 mL 0.05 M EDTA (pH 8) overnight. Solutions were diluted with 0.1 M nitric acid to obtain values within the standard ppm range of the atomic absorption spectrophotometer (Agilent Technologies 240FS AA, Santa Clara, CA). Theoretical

values of calcium were based on amount of sodium in the as-received alginate provided by the manufacturer. Calcium quantification was carried out in the absorption mode, using an air–acetylene flame at a wavelength of 422.7 nm. Standard solutions of calcium with different concentrations were used to obtain the calibration curve, while the EDTA solution was used as a blank measurement. All tests were performed in triplicate.

4.3.7. Dissolution studies. After synthesis and rinsing, films were cut with a six-inch blade into four equally sized pieces, with ribbing discarded. (Figure 3.8) Film pieces were placed in a weighboat in a dessication oven at 50 °C overnight. Dry weights were taken gravimetrically. Film pieces were exposed to 5, 10, 20, 30, 45, or 60 minutes in 100 mM citrate (pH 7.4) in dynamic conditions. At the determined timepoint, films were removed from citrate and washed three times in ddI water. Films were then dried in a dessication oven at 50 °C overnight. Final weights were taken gravimetrically. Throughout the dissolution study the films stayed in the same weighboat except when being weighed. The dissolved film pieces did not stick to the weighboat and could be easily removed without mechanical damage or loss of material.

4.3.8. Thermogravimetric analysis (TGA). Thermal characterization was performed using thermogravimetric analysis (TGA) in order to evaluate the influence of UV crosslinking on GMHA(32) decomposition, the influence of calcium gelation on alginate (LVG) decomposition, the influence of compositional changes between 100% GMHA(32) films and 100% LVG film decomposition, and, finally, the influence of removal of LVG (via dissolution) from a 50/50 LVG/GMHA(32) film. Samples (1–4 mg) were heated in a Mettler Toledo TGA 1 (Mettler-Toledo, Columbus, OH) in a range of 40–600 °C at a constant heating rate of 10 °C/min, under a nitrogen atmosphere (50.0 mL/min). All measurements were performed in triplicate.

4.3.9 Statistical analysis. All data are presented as mean ± standard deviation.

Chapter 5: Mechanical properties of GMHA and Alginate Blend Films

ABSTRACT

Hydrogel mechanical properties are predominantly dependent on physical properties such as composition, crosslinking density, and hydration. This chapter characterizes mechanical changes in alginate/GMHA-blended films with varying composition and crosslinking density. Tensile testing provides quantification of macroscopic differences such as toughness and conformability observed during handling of the film. Dynamic mechanical analysis (DMA) provides insight into the viscoelastic properties related to overall film stability. As the concentration of GMHA is increased, film strength decreases as indicated by a decrease in Young's modulus and tensile strength. These decreases are a result of decreased alginate concentration and increased bound water to the hydrogel. Gelled alginate is the only component of the film with load-bearing capability. With less alginate content there are fewer calcium junctions to bear load. The GMHA component does not significantly contribute to the load-bearing strength of the film, even when photocrosslinked. Bound water acts as a plasticizer in hydrogels, and contributes to decreased film strength. Tensile tests also reveal an increase in film elongation with increasing GMHA concentration, as a result of long-chain GMHA untangling. Decreasing DM of GMHA further increases elongation. The overall toughness of films decreases as a result of alginate/GMHA phase separation, with great loss of mechanical integrity in films beyond the percolation threshold. Increasing molecular weight of alginate diminishes the overall effect of GMHA. DMA results indicate that increasing GMHA concentration reduces the film's ability to resist deformation as indicated by a decrease in storage modulus. This decrease is coupled with a decrease in overall gel stability as indicated by a lower gelation frequency.

103

5.1 ADDITION OF ALGINATE TO HA

The impetus for combining alginate and HA was to harness the mechanical integrity of gelled alginate with the wound healing properties of HA. A classic way to alter the mechanical properties of a material is to create blends with other materials. Since photocrosslinked HA does not have the mechanical integrity to withstand normal operating room manipulation, and since alginate is not a component of the body's natural healing process, blending these polymers intends to harness mechanical strength and anti-scarring performance. One of the major driving forces for blending polymers together is to obtain a resulting material that combines the strength of the individual components. (Paul & Bucknall 2000) Polymer blends offer enhanced mechanical properties such as improved toughness (Sun *et al* 2012), and increased plasticity (Gaillard *et al* 2013). The mechanisms for these enhanced features vary, but many include sacrificial bond breaking for the improved bulk material deformation without fracture. (Gong *et al* 2003) Since GMHA hydrogel films are weak, and alginate films are brittle, the theory for blending them was to capitalize on GMHA chain movement to allow for greater alginate chain stretching. According to a study by Sun *et al*, alginate chains are capable of "unzipping" and "rezipping" calcium associations while blended with photocrosslinked polyacrylamide (PAA). The PAA provides a lattice for the alginate to stretch farther. They proposed that calcium crosslinks broken during tensile tests are immediately recovered because the PAA allows that recovery. Since our films include a photocrosslinked GMHA network, we projected a similar method for mechanical enhancement with alginate. Together, the GMHA and alginate would complement one another in a blend.

5.2 MECHANICAL PHENOMENA WITH PHASE SEPARATED BLENDS

Alginate/GMHA-blended films are complicated by phase separation and a percolation threshold. Traditional two-component heterogeneous blends have mechanical properties that can be described by the equivalent box model (EBM) and the percolation concept of a critical volume fraction of constituents. (Kolarik *et al* 2000) The EBM for binary blends predicts that materials will respond to stresses with partly parallel and partly series components of both materials. Cocontinuous fractions behave in series while discontinuous fractions behave in parallel. These fractions shift depending on composition. A cocontinuous fraction refers to areas where the two components have interfacial adhesions that provide mechanical integrity. A discontinuous fraction refers to areas where there is no interfacial adhesion between the two components. Combining this theory with percolation, there is a critical volume fraction where the two materials are not compatible and there is no longer a cocontinuous fraction. At this composition the composite mechanical properties shift and follow predictions of parallel behavior, where each component behaves independently. Typical results of mechanical changes at these critical compositional values are shifts in toughness or modulus. In a study of synthetic blends of RTPP/ABS, the toughness of the composite at critical composition values, or near the percolation threshold, was significantly less than composite values where cocontinuous fractions were present. (Slouf *et al* 2007) A deviation in modulus is also experienced at the percolation threshold with increasingly decreasing values with higher discontinuous fractions.

Conventional models developed to describe such systems do not apply to our films because of the high water content in the films. Alginate/GMHA films are ternary complexes consisting of alginate, GMHA, and water. The films are 79% ± 6 water, as

determined by swelling tests. There are two types of associations that water has with these polyanionic polymers. Water immobilized onto the surface of the molecules is referred to as bound water. The second layer of water associated with the bound water is referred to as free water. Bound water plays a significant role in the mechanical properties of hydrogel films, and is known to act as a plasticizer in hydrogels. (Quinn *et al* 1988) As a plasticizer, the influence of water imparts reduced modulus and tensile strength, and increased elongation by favoring formation of amorphous areas, thus reducing resistance to traction. Furthermore, we hypothesize that the presence of water causes the GMHA component to leach, which has significant implications on the resulting composition of films. Therefore water plays a major role in the composition and hydration of alginate/GMHA films, both of which significantly impact the mechanical properties of hydrogels (Anseth *et al* 1996).

Armed with an understanding of resultant film composition, and the fundamental theories of polymer blends and phase separated blends, it was important to select the best method for capturing mechanical property changes while varying film composition and crosslinking density. Furthermore, it was of great interest that our methods follow ASTM standards already developed for thin film technologies, so that we could use a commonly found testing apparatus. Finally, the results of mechanical testing need to be correlated to the handling and utility of the films.

5.3 MECHANICAL TESTING OF THIN HYDROGEL FILMS

Thin film hydrogels are of great interest for biomedical applications because they offer densely packed polymers with the ability to cover large surface areas with minimal material. Thin films support the "less is more" approach to biomedical devices, which helps reduce foreign body response and unwanted scarring. Of great interest is the study

106

of polysaccharide-based films, since tissue-engineered scaffolds of natural materials evoke a more favorable *in vivo* response than synthetic scaffolds (Picart *et al* 2002). As with any tissue-engineering scaffold, mechanical properties of films are directly related to the *in vivo* response and to the utility of the device. Although hyaluronic acid and alginate, separately, were components of the first natural-based polyelectrolyte films to be investigated (Decher & Schlenoff 2012), no work has yet elucidated the mechanical properties of these two polysaccharides in a blended film.

Mechanical properties of planar hydrogel films are characterized using compressive or tensile tests. Compression tests are preferred as most planar films are too brittle to be loaded in tension. (Lin *et al* 2010) Compression tests are typically conducted on a universal testing apparatus (such as an Instron) where two flat surfaces apply equal and opposite pressure, or on a rheometer where parallel plates are used to apply shear forces to the specimen. Shear forces are particularly useful because they reveal the viscoelastic properties of the hydrogel. Typically, the lower recommended limit of allowable thickness for thin film testing on both a universal testing system or a rheometer is approximately 500 μm, which is outside the range of our film thickness. Tensile tests are typically conducted on a universal testing apparatus (such as an Instron or texture analyzer) where film ends are secured in grips and the specimen is pulled in equal and opposite directions at a constant strain rate, or on a dynamic mechanical analyzer (DMA) where high frequency oscillations are applied. Frequency oscillations are used to obtain viscoelastic properties. The geometry of our films, particularly the thickness, made them better suited for tensile analysis.

Tensile testing is used extensively to determine strength and utility of thin hydrogel films. (Febriyenti 2010, Pawde & Deshmukh 2008, Fujie *et al* 2009) Particularly, for wound dressings, it is preferable to obtain robust but pliable devices

(Khan et al 2000, Macleod et al 1997, Nagarsenker & Hegde 1999), with elasticity (Sezer et al 2007). To optimize these features, tensile test results can reveal property differences from compositional or processing changes in film fabrication. Changes in tensile strength and elongation at break, which are used to determine Young's modulus, are sensitive to macroscopic characteristics (Garcia *et al* 2009), and can be related to film handling. Alginate films have been much more extensively tested than HA films, primarily because of the mechanical integrity that follows gelation of alginate. Even crosslinked HA-based films do not have the mechanical integrity to be loaded into a tensile testing apparatus. Thin films (less than 120 μm) consisting of alginate are often developed for food preservation or for oral drug delivery (Martin *et al* 2001). This development requires the addition of a plasticizer like glycerol, to reduce brittle fracture of alginate-only films. Although mechanical property results of food grade, surfactant-blended alginate films cannot directly be compared to our results, we can follow the same method of evaluation. DMA testing was also attractive for mechanical characterization of our films, because it is a more sensitive test to the viscoelastic properties. Changes in storage modulus and loss modulus, which are used to determine tan delta, relate to shifts in the solid-like and elastic-like components of a material. These values offer insight into microscopic film characteristics and can be related to overall film stability.

The thicknesses of our films were between 50-120 μm as recommended by surgeon's handling. These thin films do not remain fully hydrated in ambient conditions, between 20-65% Rh. Under these conditions alginate-only films equilibrate to 10% ± 2 water content, while alginate/GMHA-blended films equilibrate to approximately 2%. (**Table 5.1**) There is a significant loss of film hydration after 15 minutes exposure to ambient conditions. With loss of hydration, the films dramatically change behavior because the plasticizing effects of water are diminished. Qualitative assessments of films

108

with less than 50% water content indicate plastic deformation with handling and increased stiffness. For alginate-only films, this limit is reached within 33 ± 2 min of ambient exposure. It takes about 15-20 min to prepare a sample on the tensile apparatus. Therefore, conducting tensile tests in conditions of 65% Rh does not provide a suitable environment to obtain mechanical property data. All mechanical tests were conducted in fully hydrated conditions.

LVG / GMHA(11)	Water lost at 15 minutes (%)	Time to 50% water lost (min)	Final equilibrium at 65% Rh (%)
100/0	25.9 ± 4.6	33 ± 4	9.5 ± 1.6
67/33	18.3 ± 8.6	48 ± 6	2.3 ± 1.5
50/50	16.0 ± 8.9	57 ± 5	2.2 ± 1.7

Table 5.1 Ambient film drying. Films were weighed wet and then allowed to dry in ambient conditions. Weight was taken every minute for 90 minutes. Alginate only films dried the fastest, in about a half hour. The greater the GMHA content, the more time required to reach equilibrium. When a film is in equilibrium with ambient conditions (23 °C, 65% Rh) there is significantly decreased water content in the films than in fully hydrated conditions. These results support conducting mechanical testing in fully hydrated conditions, as mechanical tests can take more than 15-30 min to complete. (N = 6)

5.4 TENSILE TESTING OF ALGINATE/GMHA FILMS

        We conducted tensile testing of films of varying composition of alginate/GMHA with both high and low molecular weight alginate and with high and low degree of methacrylation (DM). (**Figure 5.1**) The effect of molecular weight and concentration on the mechanical properties of polymer blends has long been a subject of research (Larson 1999). An increase in molecular weight is commonly associated with increase in modulus and tensile strength because of chain entanglement and crosslinking density. Degree of crosslinking has shown to be directly related to the mechanical properties of polymer gels and films (Decher & Schlenoff 2012). The effect of increased degree of crosslinking reduces swelling ratios which reduces the influence of water as a plasticizer.

        5.4.1. Tensile testing of LVG/GMHA(11) films. Low molecular weight alginate (LVG) films were varied in composition with low DM GMHA(11). (**Figure 5.2**) At 17% GMHA(11) there was a 75% ± 2.0 decrease in Young's modulus and a 65% ± 2.5 decrease in tensile strength. These decreases continue with decreasing alginate concentration, with no significant trend changes associated with the percolation threshold. Young's modulus is dependent on the film's ability to resist deformation and to withstand strain. A decrease in modulus is caused by a decrease in strength and/or an increase in elongation. We hypothesize that the decrease in alginate concentration contributes to the decrease in film strength. Both Young's modulus and tensile strength are properties that depend on the load-bearing capabilities of a material. Calcium gelation and chain entanglement of alginate are the most likely components in the ternary complex that resist deformation with load. We deduce that the GMHA component does not resist deformation since we cannot successfully apply grip load to a GMHA-only film. (The application of the grip tears a GMHA-only film.) Therefore with decreasing alginate content the resulting films have decreased strength, and deform more easily

under stress. Accompanying the decreased modulus is an increase in elongation, or the ability to withstand greater strains. The elongation has a bimodal profile with the greatest elongation correlating with the percolation threshold of 33% GMHA(11) concentration. Films with 17% GMHA(11) stretched 54% ± 5.3 farther than LVG-only films. Films with 33% GMHA(11) film can be stretched 104% ± 3.5 farther than LVG-only films. We hypothesize that the presence of GMHA attracts more water to the film. The increased presence of water allows for chains to move with less resistance to increasing stress. GMHA supports an increase in alginate chain flexibility. Films with 50% GMHA(11) exposed to UV continued the trend, suggesting that photocrosslinking of GMHA does not contribute to strength of the film. However, films with 50% GMHA(11) not exposed to UV are weaker than the 50% GMHA(11) exposed to UV, suggesting that the presence of GMHA contributes to chain flexibility and retention of strain.

5.4.2. Tensile testing of LVG/GMHA(32) films. LVG films were varied in composition with high DM GMHA(32). (**Figure 5.3**) The introduction of GMHA(32) to LVG films had a similar effect as with GMHA(11). As GMHA(32) was initially added to LVG, there was a 73% ± 1.9 decrease in Young's modulus and a 49% ± 0.8 decrease in tensile strength. The modulus and tensile strength continued to decrease with increasing concentration of GMHA(32), or, decreasing alginate concentration. Again, we hypothesize that this decrease in strength is a result of decreasing concentration of alginate. One difference between the GMHA(11) and the GMHA(32) profile in LVG blended films was elongation. The composition of greatest elongation was 33% GMHA(32) with 84% ± 3.9 greater elongation than LVG-only films. This composition is the same composition as greatest elongation for LVG/GMHA(11). However, the films stretched 20% more with GMHA(11) than with GMHA(32) with or without UV exposure. The ability for the LVG films to stretch further with GMHA(11) compared to

GMHA(32) was most likely a result of increased chain flexibility. With GMHA(11) closer to percolation, theoretically there are larger clusters of GMHA(11) than GMHA(32). Larger clusters may provide a more lubricious environment for chain movement. This movement may attract higher water content. Both of these effects may result in chains sliding past one another, which would support GMHA(11) having increased retention of strain before catastrophic failure.

5.4.3. Tensile testing of MVG/GMHA(32) films. High molecular weight (MVG) alginate was varied in composition with GMHA(32). (**Figure 5.4**) Although modulus and tensile strength decreased, the effects of GMHA(32) on MVG-rich films were not as dramatic as the effects of GMHA(32) on LVG-rich films. With addition of 17% GMHA(32) to MVG-rich films, decreases in modulus and tensile strength were 54% ± 1.8 and 42% ± 1.6, respectively. These results support the theory that film strength is a result of the alginate component. Inherent with increase in molecular weight is the increased entanglement of polymer chains. These entanglements resist deformation when stresses effort to pull the chains apart. It is reasonable to assume that there are more polymer chain entanglements in MVG than LVG. We hypothesize that alginate chain movement allowed by the lubricious GMHA is more significant in LVG-based films than in MVG-based films. There are fewer chain entanglements in the LVG-based films than in the MVG-based films. Therefore, for an equal amount of GMHA present, the effects are more significant in LVG films. The elongation profile of MVG/GMHA(32) is bimodal, but greatest elongation was only a 40% ± 3.2 increase over an MVG-only film. This elongation occurred at a composition of 33% GMHA(32), similar to the other film complexes.

All films presented a similar trend with compositional changes. Addition of 17% GMHA to alginate-rich films caused a sharp and significant decrease in modulus and

tensile strength, with an increase in elongation. Addition of 33% GMHA to alginate caused further decrease in modulus and tensile strength, as well as continued increase in elongation. LVG/GMHA(11) films have a lower modulus and tensile strength than LVG/GMHA(32) films and exhibit more elongation. We hypothesize that these trends are a result of increased allowable movement of the alginate chains with increased water content. MVG/GMHA(32) films do not elongate as much as LVG/GMHA(32) films. We hypothesize that the inability for MVG/GMHA(32) films to stretch farther before breaking is the increased entanglement of alginate chains with increased molecular weight. This entanglement resists deformation, which is supported by an increase in modulus. Ultimately the increase in alginate molecular weight plays a significant role in the mechanical integrity of the film, therefore diminishing the influence of GMHA.

The effects of DM and subsequent photocrosslinking on the mechanical properties of GMHA-only hydrogels is significant. Rheological evaluation of photocrosslinked GMHA-only hydrogels indicates that increased DM increases compressive modulus as a result of increased strength. (Seidlits *et al* 2010) Masked GMHA hydrogels with exposed and unexposed areas to UV have significantly different swelling properties and modulus. (Zawko *et al* 2009) As presented in chapter 4, the DM of GMHA in alginate/GMHA-blended films can shift the percolation threshold. The subsequent retention or loss of GMHA has an effect on the swelling ratio of the resulting films, which, in turn, has some effect on the mechanical properties. There is an inverse relationship between crosslinking density and swelling ratio. With decreased swelling ratio, there is increased crosslinking density, which increases the modulus, or stiffness, of hydrogels. The swelling ratio of low molecular weight alginate (LVG) films was greater than high molecular weight alginate (MVG) films. This difference results in less stiff films, as indicated by the decrease in modulus. Furthermore, the removal of GMHA by leaching continues this trend with

decreased modulus and tensile strength. The effect of UV crosslinking was visible and dramatic in the polymer retention studies, indicating that this step plays a major role in the ability to make a film. However, because the mechanical integrity of photocrosslinked GMHA is so low, the UV crosslinked continuous GMHA phase did not play a remarkable role in the overall mechanical characteristics of resulting films. Without UV, films continued to decrease in modulus, tensile strength, and elongation. Films with at least 50% GMHA content were weak and soft.

Ultimately, mechanical strength is owed to the calcium gelation of the alginate component of blended films. All mechanical properties related to load, such as tensile strength and Young's modulus, follow the trend in alginate composition. Loss of strength is a result of decreased concentration of calcium gelled alginate. However, the ability for the films to stretch farther, with decreased amounts of alginate, suggests that the presence of GMHA allows greater chain movement. GMHA is mucinous when not photocrosslinked. The binding strength of water to GMHA is responsible for this texture. While we hypothesize that the alginate and GMHA components are phase-separated, the water retention caused by the presence of GMHA may significantly impact alginate chain motility. The "unzipping" and "rezipping" of alginate associations with calcium may not apply, but the GMHA lattice does appear to allow greater extension of alginate-based films.

Figure 5.1. Instron universal testing apparatus equipped with a Biopuls bath.
Specimen is marked for videoextensometer. DdI water bath is maintained at
25 °C. Specimens are pulled at 5 mm/min strain in accordance with ASTM
D882.

116
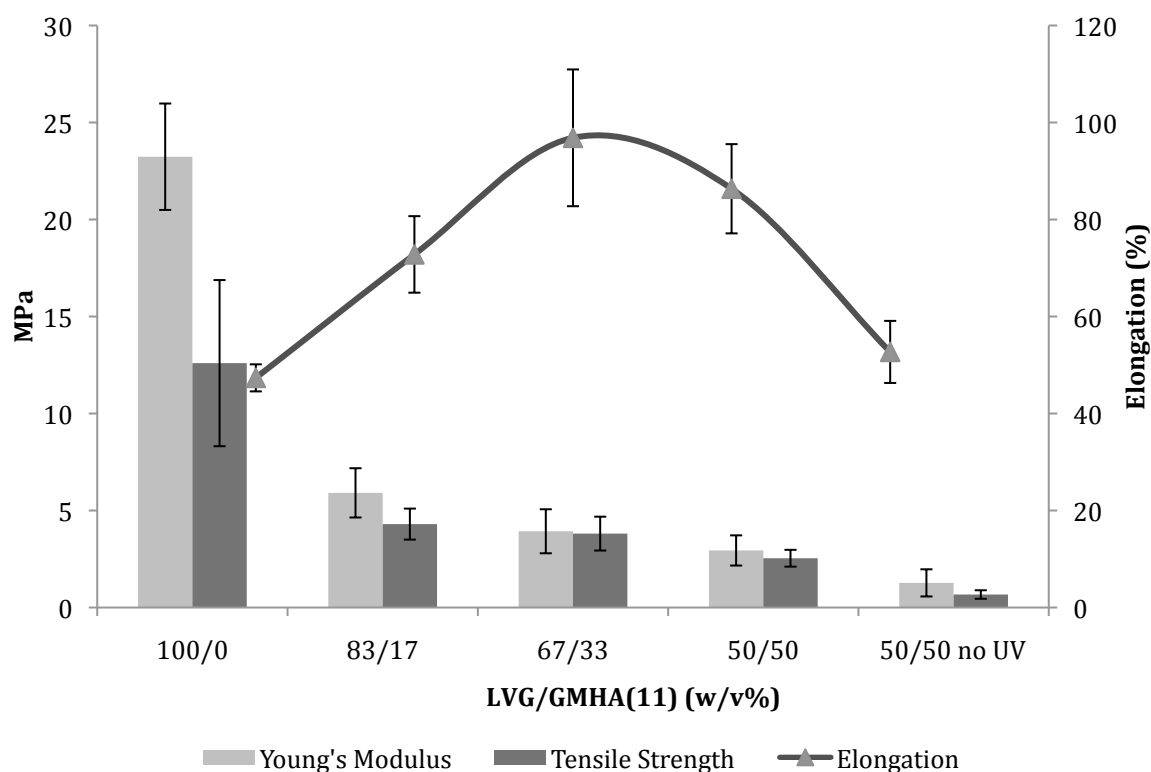
Figure 5.2. **ASTM D882 results for LVG/GMHA(11)** After fabrication and rinsing, films were cut into 5 mm wide strips and pulled in tensile at 5 mm/min until failure. LVG-alone films were brittle in comparison to those films with GMHA(11). Young's modulus and tensile strength decrease with increasing concentration of GMHA(11). The presence of a UV crosslinked GMHA(11) network at 50% GMHA(11) results in increased modulus, tensile strength, and elongation when compared to the LVG film where all GMHA has leached. Films with 33% GMHA(11) have greatest elongation with 104% ± 3.5 greater than LVG-only films. (N = 8)
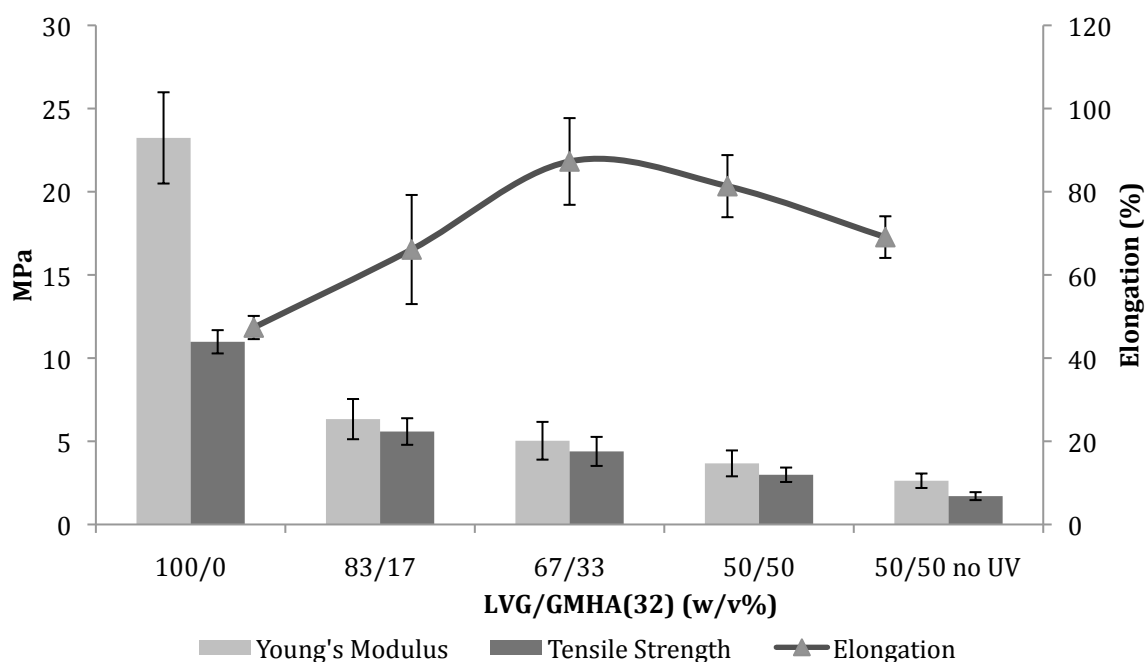
Figure 5.3. **ASTM D882 results for LVG/GMHA(32)** After fabrication and rinsing, films were cut into 5 mm wide strips and pulled in tensile at 5 mm/min until failure. LVG-alone films were brittle in comparison to those films with GMHA(32). Young's modulus and tensile strength decrease with increasing concentration of GMHA(32). The presence of a UV crosslinked GMHA(32) network at 50% GMHA(32) results in increased modulus, tensile strength, and elongation when compared to the LVG film where all GMHA has leached. Films with 33% GMHA(32) have greatest elongation with 84% ± 3.9 greater than LVG-only films. (N = 8)
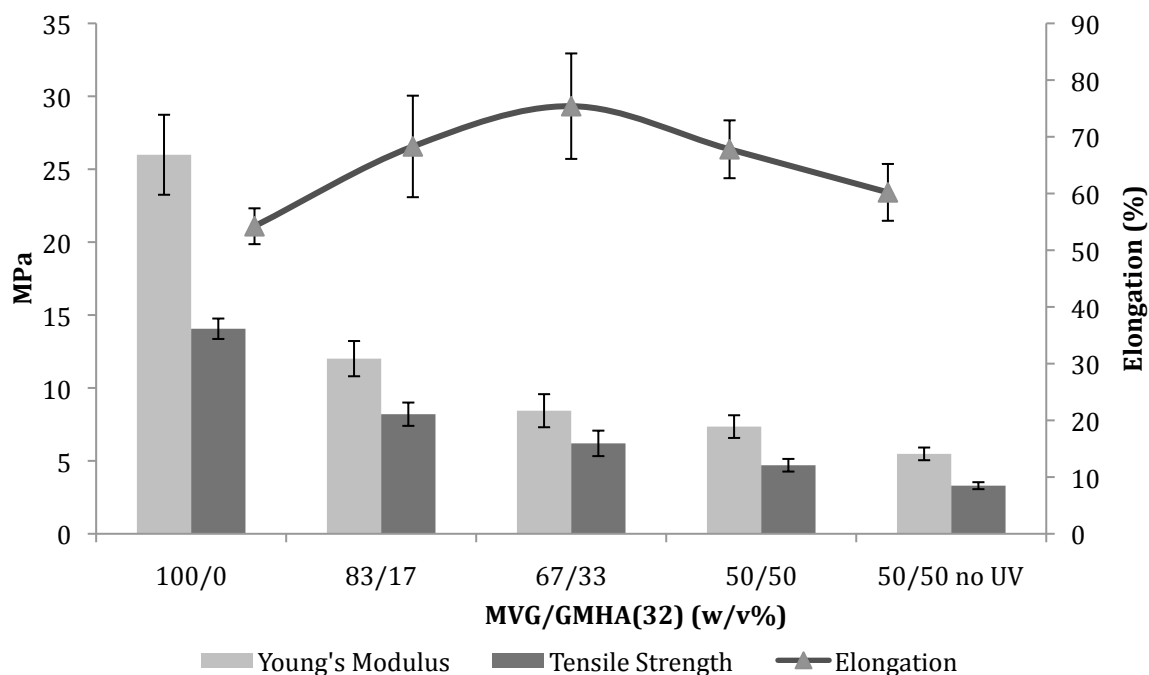
Figure 5.4. **ASTM D882 results for MVG/GMHA(32)** After fabrication and rinsing, films were cut into 5 mm wide strips and pulled in tensile at 5 mm/min until failure. MVG-alone films were brittle in comparison to those films with GMHA(32). Young's modulus and tensile strength decrease with increasing concentration of GMHA(32). The presence of a UV crosslinked GMHA(32) network at 50% GMHA(32) results in increased modulus and tensile strength when compared to the MVG film with all GMHA leached (50/50 no UV). However, there was no significant change in elongation as a result of alginate chain entanglement. Films with 33% GMHA(32) have greatest elongation with 40% ± 3.2 greater than MVG-only films. (N = 8)

5.4.4. Toughness measurements. Toughness of a material is the amount of energy absorbed before catastrophic failure, and is determined by calculating the area under the true stress-strain curve. Toughness refers to the ability of a material to resist fracture, and, unlike modulus or tensile strength, is independent of the load bearing capabilities of a material. Toughness is dependent on the amount of strain that a material can withstand. Because toughness is calculated by integration, even small fluctuations in strain behavior can cause significant increase in toughness values. Using the true stress-strain curves generated by tensile tests, we compared relative toughness values for alginate/GMHA-blended films. (**Figure 5.5**) Although alginate-only films were the toughest, films with concentrations of GMHA up to 33% were statistically similar in toughness values. The MVG films were the least tough, which is supported by a decreased ability to elongate. We hypothesize that MVG chain entanglement prevented the ability for the chains to slide past one another. The LVG/GMHA films with 33% GMHA concentration were not statistically different with GMHA(11) and GMHA(32) values at 11.6 ± 2.8 mJ and 9.7 ± 2.9 mJ, respectively. However, this trend is consistent with the ability for the chains to withstand higher strain values before failing.
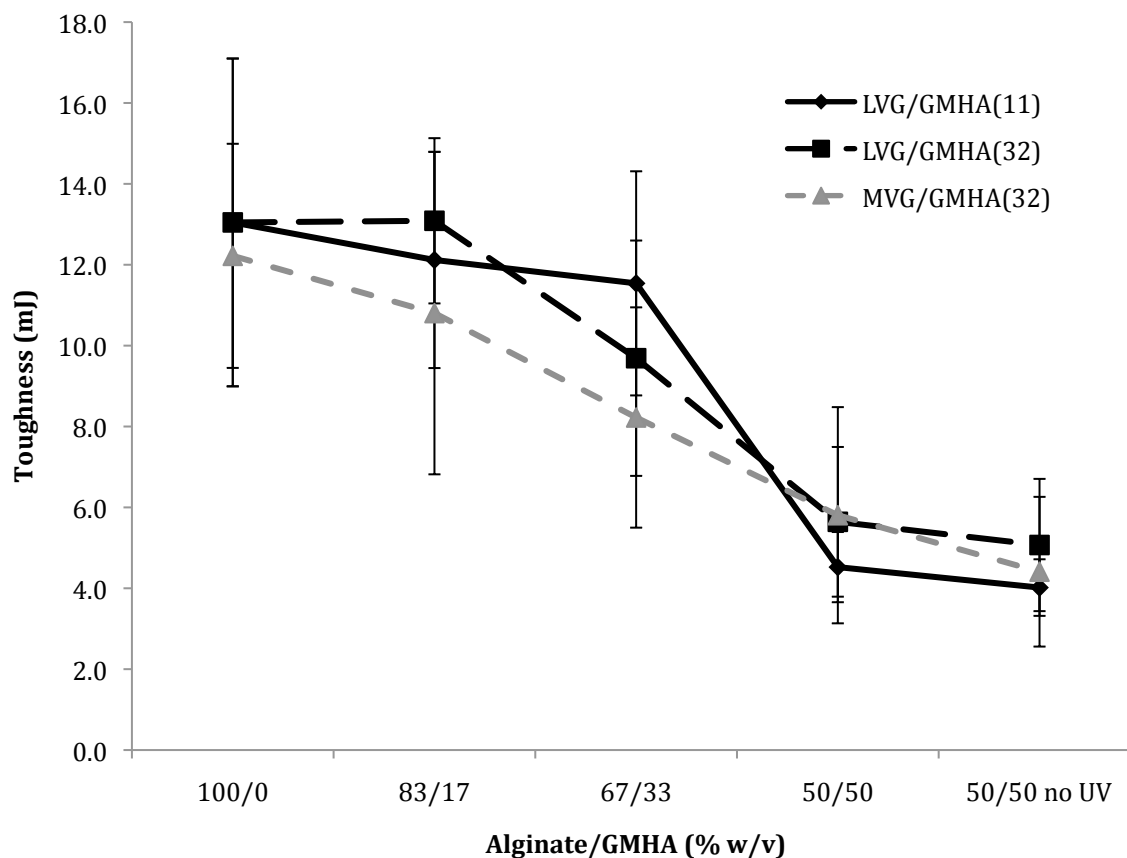
Figure 5.5 Toughness measurements from tensile tests Films were pulled in tensile in accordance with ASTM D882, until failure. BlueHill Software 2.0 calculates the area under the true stress-strain curve generated from these tests. Toughness is given in units of energy, mJ. Toughness decreased with increasing concentrations of GMHA. However, toughness decrease was not statistically significant until 50/50 blends. MVG films were the least tough as a result of increased alginate chain entanglement. (N = 8)

5.5 DYNAMIC MECHANICAL ANALYSIS OF ALGINATE/GMHA FILMS

Dynamic mechanical analysis (DMA) is the analysis of a material's response to an oscillating force. (Menard 2008) Viscoelastic materials offer interesting responses to oscillating forces because there is a time element associated with rate of deformation and corresponding rate of response. The viscous component of materials acts as a liquid, and has an immediate response to stress. The elastic component of materials acts as a solid, and resists deformation. The resistance of deformation, flow tendency, and phase lag are time-based responses of viscoelastic materials. DMA is often used to analyze mechanical properties of viscoelastic thin films. (Farris *et al* 2011) As opposed to large deformation testing such as tensile-to-failure tests, DMA testing is non-destructive and considers material response to strains well within the linear elastic region.

Alginate/GMHA films are viscoelastic hydrogels. Modulus of viscoelastic materials can be separated into storage modulus (G') that represents the solid-like component of the film, and loss modulus (G") that represents the liquid-like component of the film. The storage modulus can provide a measurement of material softness while the loss modulus can provide a measurement of unrecoverable deformation. The ratio of G" to G' is called the tan delta, δ, and gives rise to gel stability. (Menard 2008) Historically, high frequency sweeps were developed for manufacturers to determine the "liquification" of polymers for setting proper extrusion rates. The point at which δ reaches unity represents the frequency that a polymer can be extruded. Lower unity frequencies are associated with less stable polymers.

We conducted DMA analysis on LVG/GMHA(32) films of varying composition. The storage and loss moduli were determined at 1 Hz, which is commonly used as the frequency of biological processes. (Wang & Rahmatalla 2013) The results of DMA testing supports our large deformation tensile testing with decreasing modulus with

increasing concentration of GMHA(32). (**Figure 5.6**) These results suggest that adding GMHA(32) to alginate-rich films increases the softness of the film. At this frequency (1 Hz), the effect of photocrosslinked GMHA(32) is insignificant. The G' and G" are similar for films with 50% GMHA(32) that were or were not exposed to UV, at 1 Hz.

Frequency sweeps were conducted to determine the gel stability of the films. (**Figure 5.7**) As expected, the stability of the film is diminished with increasing GMHA(32) concentration. The liquification frequency of LVG-only films was 161.05 ± 5.0 Hz. This value was decreased to 96.92 ± 3.0 Hz with 33% GMHA(32). A 50% GMHA(32) film exposed to UV was more stable than the 50% GMHA(32) film not exposed to UV. The effect of photocrosslinking increased stability of the film by 42%. These results suggest that photocrosslinked GMHA provides resistance to deformation at high frequencies.
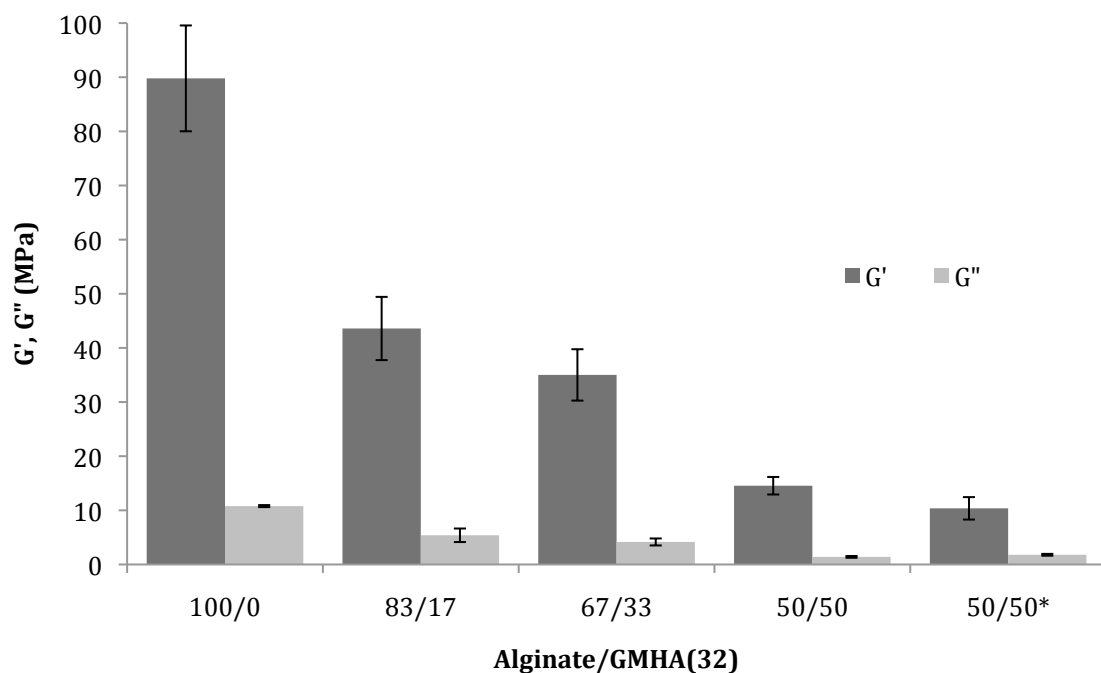
Figure 5.6 DMA tensile testing of alginate/GMHA(32) films at 1 Hz. The viscoelastic properties of alginate/GMHA(32) films were determined at 1 Hz and 25 °C in a submergible chamber of ddI water. The storage modulus (G') is greater than the loss modulus (G") indicating that the film behaves more solid-like at this frequency. The trend in decreasing storage modulus indicates that softness increases with increasing concentration of GMHA(32). Tests were conducted in triplicate.
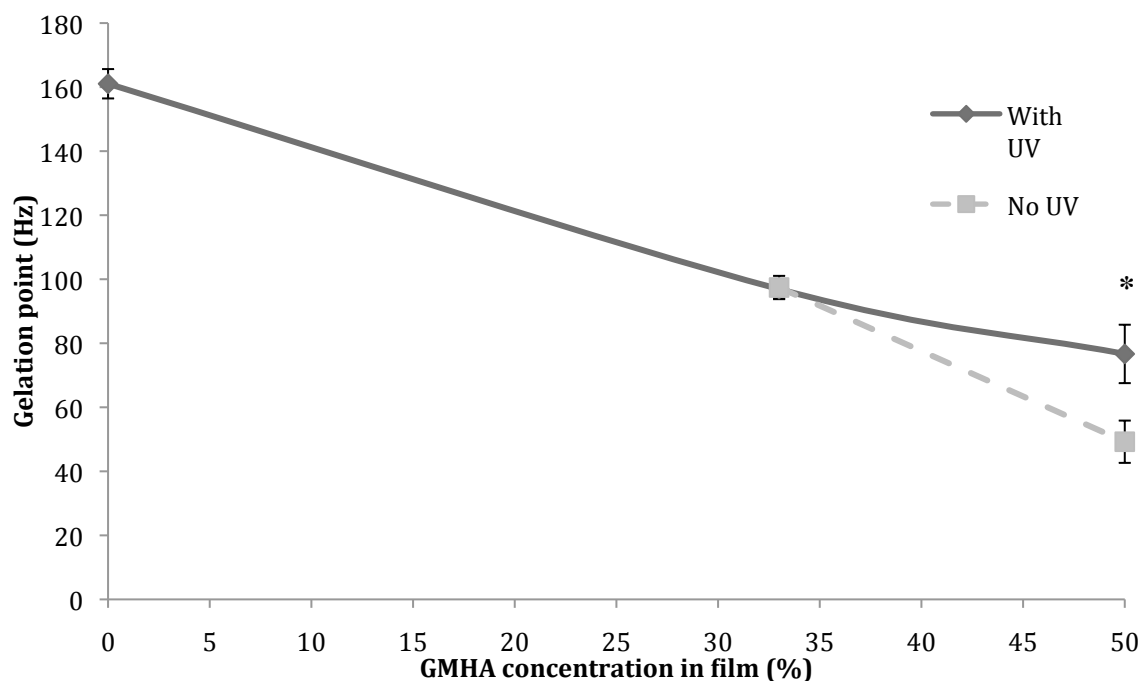
Figure 5.7 Gel stability of LVG/GMHA(32) films. The viscoelastic properties of alginate/GMHA(32) films were examined between 1 to 200 Hz and 25 °C in a submergible chamber of ddI water. The point of "liquification" of the film is determined by tan delta =1. The frequency of tan delta = 1 relates to gel stability with lower frequency values associated with less stable films. The stability of the films decrease with increasing GMHA(32) concentration. Furthermore, the presence of photocrosslinked GMHA(32) provides stability for resulting films as the absence of this network significantly decreases the frequency of liquification (p = 0.02). Therefore, for a 50/50 LVG/GMHA(32) blend, the presence of photocrosslinked GMHA(32) provides stability. All tests were conducted in triplicate.

5.6 Materials and Methods

5.6.1. Materials. Medical grade sodium alginate was purchased from FMC Novamatrix (Sandvika, Norway): Pronova UP LVG: 120 kDa, M/G ratio 0.67, and Pronova UP MVG: 220 kDa, M/G ratio 0.67. High molecular weight sodium hyaluronate from *Streptococcus equi* of molecular weight 1.6×10^6 Da was obtained from Sigma-Aldrich (St. Louis, MO). Photoinitiator Irgacure 2959 (I2959) was obtained from Ciba Specialty Chemicals (Basel, Switzerland). All other chemicals purchased from Fisher Scientific. Tensile tests were conducted on an Instron 3345 universal testing unit equipped with a BioPuls bath, smooth grip faces, and a 100 N load cell. Extension was measured with a video extensometer. Thickness measurements were taken with a Vernier micrometer, digital, with 1/100 mm tolerance (BGS, Germany).

5.6.2. Methacryloyl modification of hyaluronic acid. High molecular weight hyaluronic acid was conjugated with photocrosslinkable methacryloyl groups based on two protocols (Zawko 2008, Bencherif *et al* 2008). A 1% w/v solution of HA was prepared in either ddI water or a 50:50 mixture of acetone:water and stirred for 24 hours at room temperature. Twenty molar equivalents of both triethylamine as base catalyst and of glycidyl methacrylate were added to the solution and stirred for five days at room temperature (pH 12.5-10.5). Modified HA (GMHA) was precipitated into a 20-fold volumetric excess of acetone and then subsequently dissolved in water for 24 hours at room temperature. GMHA solution was then dialyzed against ddI water in 3500 MWCO for 72 hours. Samples were lyophilized after filter sterilization and stored in dessicators at -20 °C. The average degree of methacrylate substitution was determined by ^{1}H NMR. For solutions prepared in ddI water, substitution was found to be 8.9% ± 0.6 substitution of methacryloyl groups per mole of HA disaccharides. For solutions prepared in 50:50

mixture of acetone:water, substitution was found to be 22% ± 1.1. These values are an average of 10 analyses.

5.6.3. Synthesis of a calcium alginate/GMHA film. A 1% w/v solution of alginate/GMHA in ddI water was stirred at room temperature overnight, and cast in a 72 mm by 72 mm form. Forms were placed in a temperature and humidity controlled environmental chamber from Cincinnati Sub-Zero (Cincinnati, Oh). Temperature was held at 25 °C and humidity was held at 70% Rh during the casting period of 48 hours. Forms and solutions were kept from light at all times. Cast films were then subjected to UV light from the chamber, depending on the experiment. After photocrosslinking, if conducted, 50 mL of 100 mM calcium chloride solution was pipetted on top of the cast film in the form. Films were left to crosslink for 30 minutes. Films were removed from molds, when possible, and transferred to petri dishes with large volumes of ddI water. Films were rinsed exhaustively in ddI water for 24 hours.

5.6.4. Ambient condition film equilibrium. After synthesis and rinsing, films were cut with a six-inch blade into four equally sized pieces, with ribbing discarded. (Figure 3.8) To obtain initial weight, each piece was placed on a surgical glove and scooted around until excess water was removed. This step was conducted three times for each piece. The average of these weights was used as initial weight. To determine the equilibrium hydration of films in ambient conditions, pieces were left on the balance and gravimetric weight was recorded every 1 min for 120 min. Weights are presented as percent of initial weight. (N = 6)

5.6.5. Tensile testing of hydrogel films. Tensile testing was conducted according to ASTM D882 with minor modifications. After synthesis and rinsing, films were cut with a six-inch blade into 13 equally sized strips, 5 mm wide, with ribbing discarded as selvage. Three thickness measurements are taken per strip. In accordance with ASTM

D882, strips with thickness changes greater than 10% were discarded. Furthermore, any specimen with a thickness measurement less than 50 μm or greater than 120 μm was not included. Test samples were prepped with at least 24 hours of soaking in ddI water at room temperature. Pneumatic submergible grips were placed 25.4 mm apart. This distance was used as the gage length. Specimens were marked at the grips with a paint pen, for video extensometer recognition. An aqueous bath, maintained at 25 °C, is lifted to submerge the specimen, and tests were started immediately. Grip faces were wrapped in masking tape for tear prevention, as recommended by Instron. Specimens were pulled in tensile at 5 mm/min strain rate until catastrophic failure. Proper test completion was considered any failure that did not occur at a nick, tear, or other defect. Most defects were a result of improper cutting. The Young's modulus, a measure of intrinsic film stiffness (Cao *et al* 2007), was calculated according to the ASTM D882 as the slope of the force–extension curve multiplied by the distance between the tension grips and divided by the initial area of the specimen (length x thickness), and was expressed as MPa (**Equation 7**). The elongation at break (E, % of the original length) (**Equation 8**) and tensile strength (TS, MPa) (**Equation 9**) were also calculated according to the ASTM D882 method. Toughness (T, mJ) was taken as the area under the true stress-strain curve, until strain at break, ε_B (**Equation 10**). All films were tested in triplicate, at least.

$$\text{Young's Modulus (MPa)} = \frac{\text{Tensile Strength (N/mm}^2\text{)}}{\text{Elongation at break}} \qquad [7]$$

$$E(\%) = \frac{(L - L_0)}{L_0} \times 100\% \qquad [8]$$

$$TS(\frac{N}{mm^2}) = \frac{F}{A} \qquad [9]$$

128

$$T = \int_0^{\varepsilon_B} \sigma(d\varepsilon) \qquad\qquad [10]$$

5.6.6. Dynamic mechanical analysis (DMA). After synthesis and rinsing, films were cut with a six-inch blade into 13 equally sized strips, 5 mm wide, with ribbing discarded as selvage. Three thickness measurements are taken per strip. Any specimen with a thickness measurement less than 50 μm or greater than 120 μm was not included. Test samples were prepped with at least 24 hours of soaking in water at room temperature. Dynamic mechanical analysis was conducted on a TA Q800 with submergible chamber (TA Instruments, New Castle, DE). Films were pulled in tensile for two testing sequences. The response to sinusoidal deformation over time was measured at 1 Hz frequency, 0.1% strain, and 15 mm specimen length for 2 hours. We also conducted frequency sweeps from 0.01 Hz to 200 Hz at 25 °C. The viscoelastic properties of alginate/GMHA-blended films were quantified in terms of the storage modulus (G'), the loss modulus (G"), and tan delta (δ). G' gives the elastic or solid-like component, G" gives the viscous or liquid-like component, and δ = 1 gives the point of gelation. G' and G" were recorded when steady-state was reached at Hz = 1, and represent the softness of the film. The point of gelation represents overall gel stability. All tests were conducted in triplicate.

5.6.7 Statistical analysis. All data are presented as mean ± standard deviation. Student's t-tests were conducted for significance.

Chapter 6: Improved Film Handling with Crystal Templating

ABSTRACT

A successful anti-adhesive device demands robust mechanical behavior to facilitate handling and positioning within the patient, and, yet, optimal conformability on delicate tissues. To improve upon the film characteristics discussed in Chapter 4, we utilized a crystal templating technique that stabilizes an interconnected branched porous network as well as an interconnected fibrillar microstructure within the films. Fiber and pore formation is verified with SEM. Urea removal is confirmed with TGA. The polymer network in the fibers may be more dense than bulk polymers in nontemplated films. Templating increases polymer retention. We hypothesize that this retention is due to compression of viscous polymer during crystalline network formation, which decreases the exposure of GMHA clusters to the water-rich surface. Compression of the polymers may reduce the concentration of clusters that have a direct path for leaching into the rinsing water. Templating decreases the dissolution rate of alginate/GMHA-blended films, most likely as a result of increased density of polymers in the fibers. Templating increases film toughness as a result of increased elongation. We hypothesize that increased elongation is a result of the porous structure that acts as sacrificial defects, and of the fibrous network that allows greater elongation via compression of void volume. However, fiber direction was ultimately difficult to control, and tensile test results varied. DMA results indicated that templating decreases gel stability, with fiber alignment playing a role in that stability. Thus, templated films are tougher, yet more liquid-like. These mechanical property changes allow for improved film handling and increased flexibility, as confirmed by surgeon subjective evaluation.

6.1 INTRODUCTION

Methods to enhance the mechanical properties of biocompatible hydrogels include grafting with synthetic polymers (Nagahama *et al* 2012), creating nanocomposite gels (Wang *et al* 2012), integrating nanosheets (Fujie *et al* 2009), microgel reinforcements (Hu *et al* 2011), double networks (Haque *et al* 2012), or covalently bound composites (Chen *et al* 2010). These methods improve the toughness and durability of hydrogels by increasing load-bearing capabilities and extension. Resulting hydrogels rely on fundamental composite principles where one component of the composite introduces sacrificial bonds to allow greater strain capacity of the system. (Friedrich *et al* 2005) Most biocompatible, tough materials are developed for cartilage repair, where toughness plays a significant role in the success of the implant. However, these hydrogels have very slow degradation rates, if at all. For instance, double network hydrogels are only 25% degraded after 30 days exposure to biomimetic conditions (Haque *et al* 2012).

Microgel reinforced hydrogels (Hu *et al* 2011) are similar in design to our alginate/GMHA-blended films with concentrations of GMHA less than the percolation threshold. These reinforced hydrogels utilize small beads of crosslinked gels to sacrificially break during tensile stress. However, these microgels are more densely crosslinked than the surrounding polymer matrix, creating multifunctional crosslinking points to transfer energy across the matrix/microgel interface. In this model, the microgels serve as a cocontinuous fraction to support toughness and elongation. As discussed in chapter 5, our GMHA clusters serve as a discontinuous fraction, ultimately weakening the films. We were interested in enhancing the mechanical properties of our films. Hydrogel toughening methods similar to those just discussed have produced covalently crosslinked alginate and GMHA (Dahlmann *et al* 2012, Ganesh *et al* 2013), or introduced a synthetic reinforcement (Jeon *et al* 2007, Xu *et al* 2013). However these

methods provide mechanical properties with equal or decreased toughness, or films with long degradation rates. Therefore, we needed a method for improved toughness without the addition of synthetic polymers or increased crosslinking of alginate/GMHA-blended films.

A hydrogel templating technique developed previously in the Schmidt lab (Zawko & Schmidt 2010) utilizes a crystallizable poragen to stabilize an interconnected branched porous network within cast films. This technique exploits the property of small molecules to self-assemble into large interconnected networks via dendritic crystal formation. There are several crystallizable poragens that have been investigated for resulting hydrogel properties. (Thomas & Schmidt 2011) Propagation of the crystalline network is viscosity-driven, so the density of branching is dependent on the viscosity of the cast polymer solution at the time of poragen nucleation. The branching pattern is poragen-specific. We selected urea as our crystallizable poragen because urea is non-toxic, inexpensive, and creates dense branching networks in HA-based films. (Zawko & Schmidt 2010) As the crystalline network propagates throughout the bulk of the film, cast viscous polymer is compressed into a branched network along side the crystalline network. Polymer conformation is stabilized by UV photocrosslinking of GMHA with subsequent calcium gelation of alginate. Upon exposure to the aqueous calcium chloride solution, the crystallized urea is removed from the hydrogel. These crystal formations leave behind a dendritic pore network and fibrillar microstructure within alginate/GMHA-blended films.

This technique for creating a dense network of fibers in hydrogel films was an attractive method for providing a desired improvement in mechanical properties. Templating is void of the use of synthetic, non-degrading polymers or covalent crosslinking of alginate to GMHA, which would change the mechanism for dissolution of the resulting films. Furthermore, templating is inexpensive and does not require

sophisticated equipment. In this chapter, we explore the effect of templating on an LVG/GMHA-blended film with 33% GMHA. Blended films of 67% LVG alginate and 33% GMHA were selected for templating for several reasons. The mechanical properties of this blend were low in modulus, which was best for conformability, and they had greatest elongation. Low molecular weight alginate was selected because it favors bioresorption *in vivo*. Also, complete dissolution required only one mechanism since 33% GMHA concentration is below the percolation threshold. Finally, GMHA(11) was preferred because it was projected that lower DM favors faster bioresorption *in vivo*. These attributes place this film as a lead candidate for success as a rapidly resorbed anti-adhesion barrier.

6.2 VERIFICATION OF FIBRILLAR STRUCTURE

Seeding nucleation creates obvious crystalline networks (**Figure 6.1A**). However, resulting fibrous network after film synthesis are more difficult to see (**Figure 6.1B**). To ensure that we are imparting a fibrous and porous ultrastructure to films with the *in situ* crystallization method, we imaged alginate/GMHA-blended films fabricated with and without templating (**Figure 6.2**). Films with and without urea are processed the same, with the exception of the crystal nucleation step. Ultrastructure was visualized with scanning electron microscopy (SEM). Without crystal-templating, there are no fibers visible (Figure 6.2A). Crystal-templating imparts a fibrous polymer network in thin alginate/GMHA-blended hydrogel films. (Figure 6.2B,C)

Fibers are defined as string-like materials with high length-to-width ratios, which offer increased strength as reinforcements. (Callister 2010) This strength stems from two attributes, density (specific strength is strength divided by density) and small diameters, which minimizes defects. Natural fibers include cellulose and collagen, which provide

133

significant mechanical strength to plants and tissues, respectively. We hypothesize that the templating process compresses the viscous polymer solution into these thin fibers, which increases the density of polymer strands within the fibers. Therefore, the fibers of templated films would be denser than nontemplated bulk film. Small angle x-ray scattering (SAXS) was conducted in collaboration with the Texas Materials Institute. (**Appendix B**) SAXS conducted on templated versus nontemplated alginate-only films indicated a difference in scattering intensity at very low q (Å^{-1}) values that correspond to 5-130 nm. Radius of gyration of alginate in ionic solutions is approximately 15 nm (Andersen et al 2012). Deviation in scattering intensity below 5 nm looks similar between templated and nontemplated films. At the largest scale features of 130 nm, scattering intensity was about 140% higher for templated films at q = 0.025 Å^{-1}. Increased scattering is associated with higher density of features between 5-130 nm. These results support a denser polymer fiber in the templated films than the bulk polymer in nontemplated films.

6.3 VERIFICATION OF UREA REMOVAL

To impart a porous structure with utilization of crystal templating, the urea must be removed from the film. To ensure urea removal we conducted thermogravimetric analysis (TGA) of films with and without urea present. (**Figure 6.3**) Both nontemplated and templated LVG/GMHA(32)-blended films were prepared, with UV exposure followed by calcium chloride gelation of alginate and subsequent rinsing. Another set of films was prepared with urea remaining. These films were exposed to UV but were not calcium gelled, so that the urea could be kept in the film. Nontemplated GMHA(32)-only films were exposed to UV, but were not exposed to calcium chloride solution. The TGA curve profile of urea is fingerprinted with a three-stage decomposition from urea to biuret

to cyanuric acid. (Wakeland et al 2010) The profile of decomposition of the unrinsed and templated alginate/GMHA films with urea is very similar to the urea profile. These results indicate that urea can be detected in the films with TGA. The alginate/GMHA templated film rinsed of urea looks much like the alginate/GMHA nontemplated film. The three-stage decomposition profile of urea cannot be detected in the TGA decomposition curve of templated alginate/GMHA films that have been rinsed. These results suggest that urea is successfully removed from the films with 24 hours of rinsing in ddI water.

6.4 POLYMER RETENTION OF TEMPLATED FILMS

Templating influences the polymer retention in LVG/GMHA 67/33 (%w/v) films. (**Figure 6.4-6.5**) Templated alginate/GMHA-blended films with 33% GMHA(11) concentration increase polymer retention by 6.8% ± 0.7 compared to nontemplated similar films. Templated alginate/GMHA-blended films with 33% GMHA(32) concentration increase polymer retention by 10.6% ± 1.0 compared to nontemplated similar films. We hypothesize that this increase in polymer retention is a result of polymer compression into thin fibers. It was proposed that the loss of polymer was facilitated by exposure to water-rich environments as experienced at the surface of the film. We hypothesize that in compressed fibers, fewer GMHA clusters are exposed to the water-rich phase. In other words, there are fewer clusters with a direct path to the free water. Finally, this compression may place methacrylated GMHA clusters in closer proximity, which, in turn, could facilitate increased influence of photocrosslinking. Although there is not enough GMHA concentration to make a continuous phase, there could be higher concentrations of GMHA in individual fibers.

6.5 SWELLING AND THICKNESS OF TEMPLATED FILMS

Similar to results from templating alginate-only and GMHA-only films (Zawko 2008), templating alginate/GMHA-blended films increased the swelling ratio. (**Figure 6.6-6.7**) The swelling ratio of alginate/GMHA-blended films with 33% GMHA(32) increased by 9.4% ± 0.3. The swelling ratio of alginate/GMHA-blended films with 33% GMHA(11) increased by 14.7% ± 0.6. Swelling ratio can be described as the weight of water loaded onto the film per weight of polymer. The templated films with 33% GMHA retained a similar percent polymer as those with 17% GMHA. Therefore, the templated films can be loaded with a much greater volume of water than a nontemplated film with the same amount of polymer. This capability could be attractive for loading small molecules or drugs for future indications.

6.6 DISSOLUTION OF TEMPLATED FILMS

As presented in Chapter 4, 33% GMHA(11) or 33% GMHA(32) concentration in alginate/GMHA-blended films is below the GMHA percolation threshold. Therefore the GMHA clusters do not form a continuous phase at this concentration. We can take advantage of this feature, as only one mechanism is required for dissolution of the film, as determined by previous dissolution studies. Upon release of calcium ions, the proposed GMHA clusters are released from the alginate matrix. Since these clusters are not crosslinked, they do not form a network. For success as an anti-adhesion barrier, rapid dissolution is desired. As concluded in Chapter 4, films with GMHA concentration below the percolation threshold dissolve fastest. We exposed templated LVG/GMHA(32)-blended films with 33% GMHA(32) to 0.1 M citrate for calcium chelation. We aimed to understand the impact that templating had on dissolution, both in mechanism changes for complete dissolution and in increase or decrease of dissolution rate.

Templating reduced the dissolution rate of alginate/GMHA(32) films, extending the theoretical *in vivo* residence time. (**Figure 6.8**) At 60 minutes, the mass remaining was 25.6% ± 3.6 of original, whereas similar nontemplated films went through complete dissolution in 30 minutes. The profile of dissolution and resulting mass remaining is similar to nontemplated films with 40% GMHA(32). From previous studies, films with 40% GMHA(32) composition did not lose further mass even with exposure to citrate overnight. However, we allowed the nontemplated films with 40% GMHA(32) and the templated films with 33% GMHA(32) to stay in the citrate for an additional 60 minutes. Films were not monitored during this hour. After 120 minutes, templated films had gone through complete dissolution. These results suggest that crystal templating decreases the rate of dissolution. We hypothesize that this decrease is a result of time required to remove calcium ions and relax alginate chains from the more densely packed polymer fibers as opposed to the polymer conformation in nontemplated films. The results of this study also suggest that templating does not alter the mechanistic requirements for causing complete dissolution. This experiment demonstrates that GMHA compression into fibers does not allow the formation of a continuous network of GMHA that would necessitate additional enzymatic degradation. This effective reduction of dissolution rate could be exploited for an indication with longer-term residence or combined with semi-prolonged drug release.
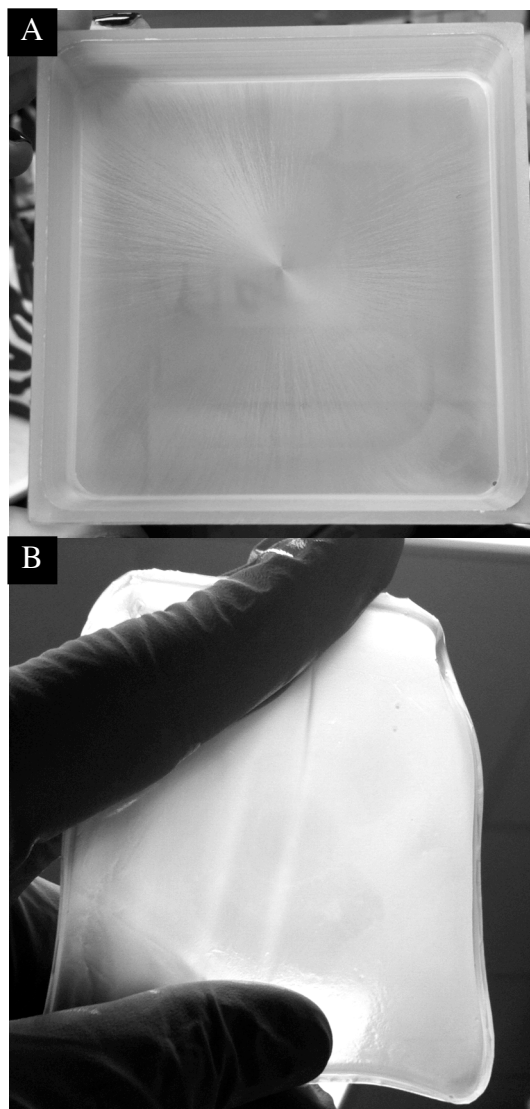
Figure 6.1. Visual verification of crystal templating. Alginate/GMHA-blended films can be crystal templated. A) Nucleation of urea crystal templating was conducted in the center of the form for a radial pattern. Film has not yet been gelled. B) After film fabrication, this pattern is more difficult to detect with the human eye.
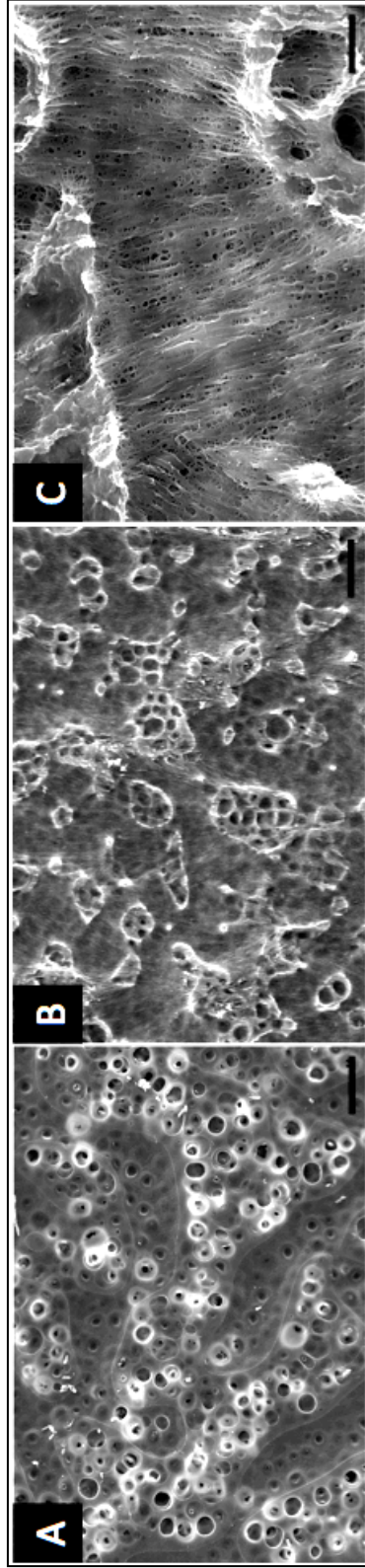
Figure 6.2. *in situ* crystal-templating imparts fibrillar ultrastructure. SEM images of glycidyl methacrylated hyaluronic acid and alginate films (A) without crystal templating (scale bar 10μm) (B) with urea crystal-templating (scale bar 10μm) and (C) with urea crystal-templating (scale bar 2μm). Fibers and pores can be observed in films that have been crystal-templated.

139
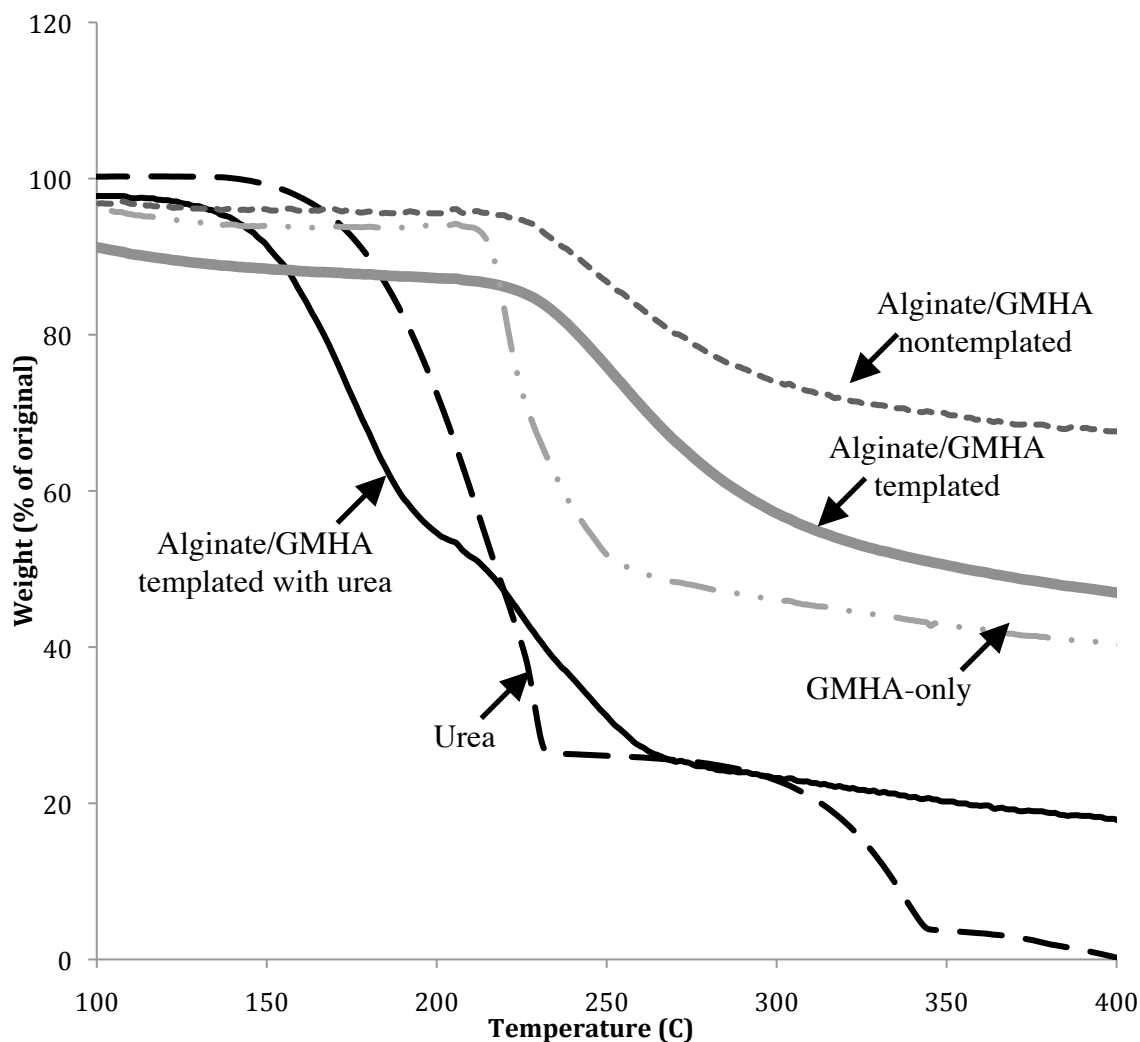
Figure 6.3. Thermogravimetrical analysis (TGA) curves of alginate/GMHA films with urea removal. Alginate (LVG) and GMHA(32) films were prepared with and without urea templating. Films that were prepared with urea remaining were not calcium gelled. GMHA(32) only films were not templated. The profile of alginate/GMHA templated with urea is much like the urea profile. The alginate/GMHA templated film rinsed of urea looks much like the alginate/GMHA nontemplated film. These results support the claim that urea is successfully removed from the films upon rinsing. All tests were conducted in triplicate.
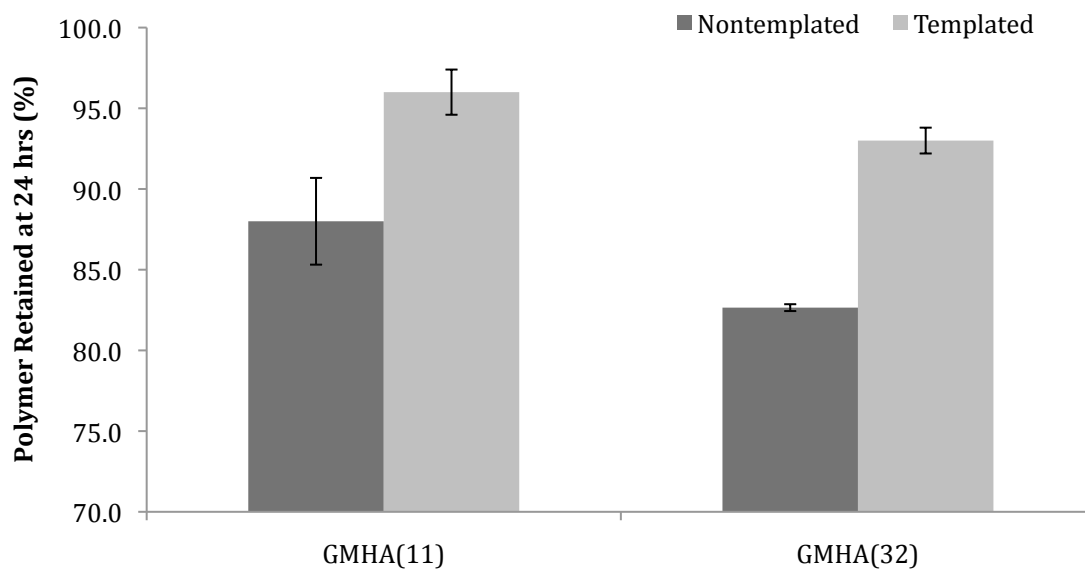
Figure 6.4. Polymer retention increased with templating. Films are 67% LVG alginate and 33% GMHA (w/v). Polymer retention is enhanced by the urea crystallization process. We hypothesize that polymer retention is increased because the templating process compresses viscous polymer together which decreases the exposure of GMHA-rich clusters to the water-rich surface environment. Thus, there are fewer clusters that have a direct path to the free water.
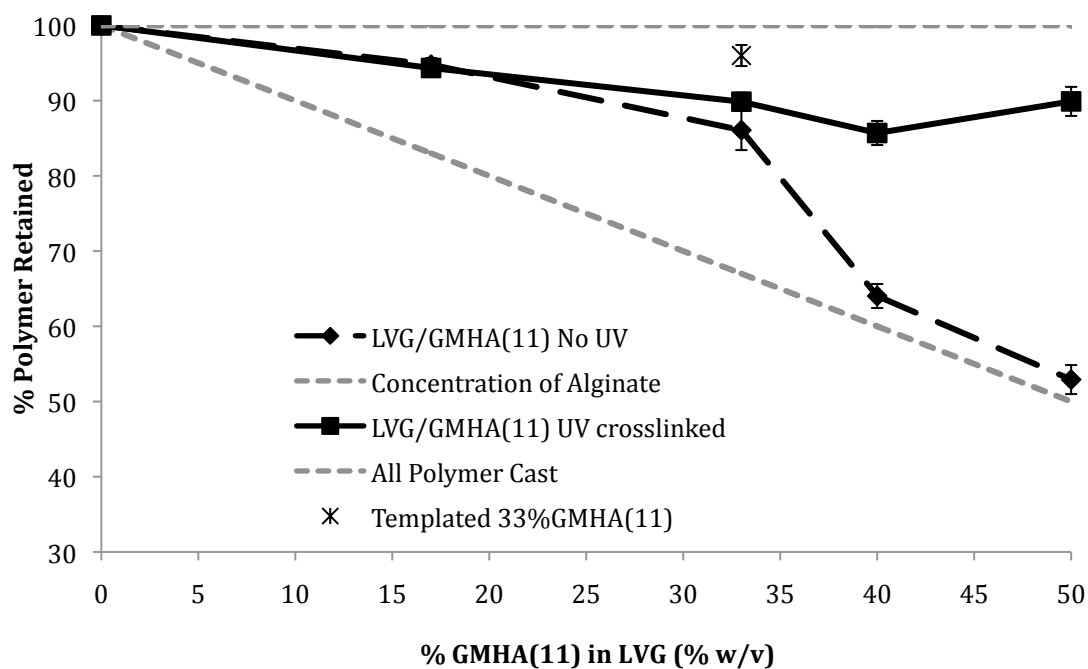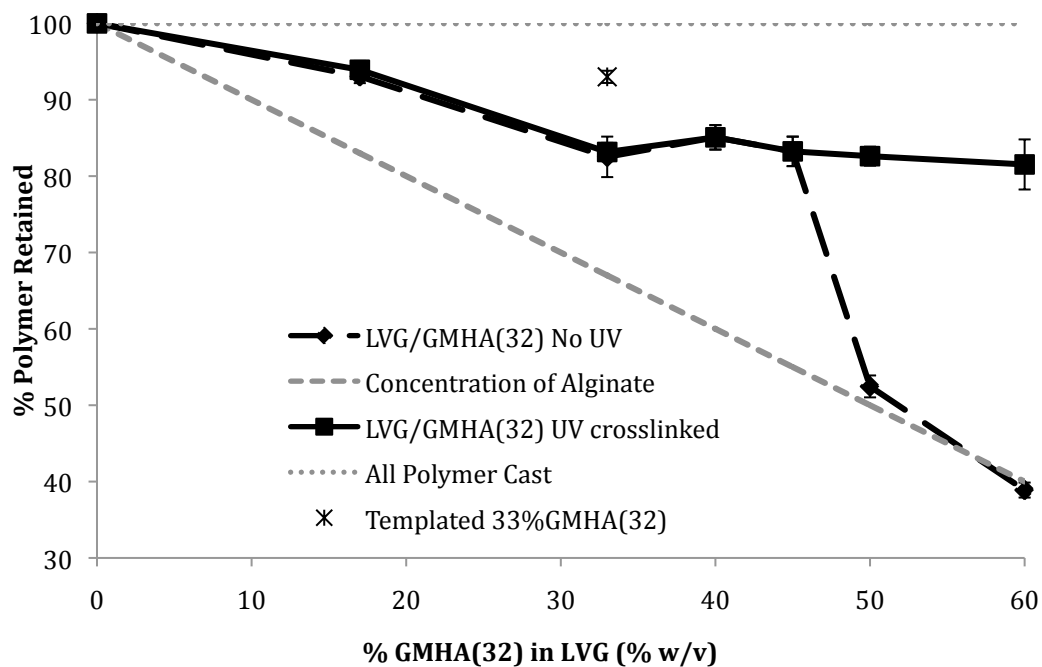
Figure 6.5 Polymer retention. Presentation of templating influence on polymer retention with data described in Chapter 4. Templated films are represented by the star at 33% GMHA concentration.
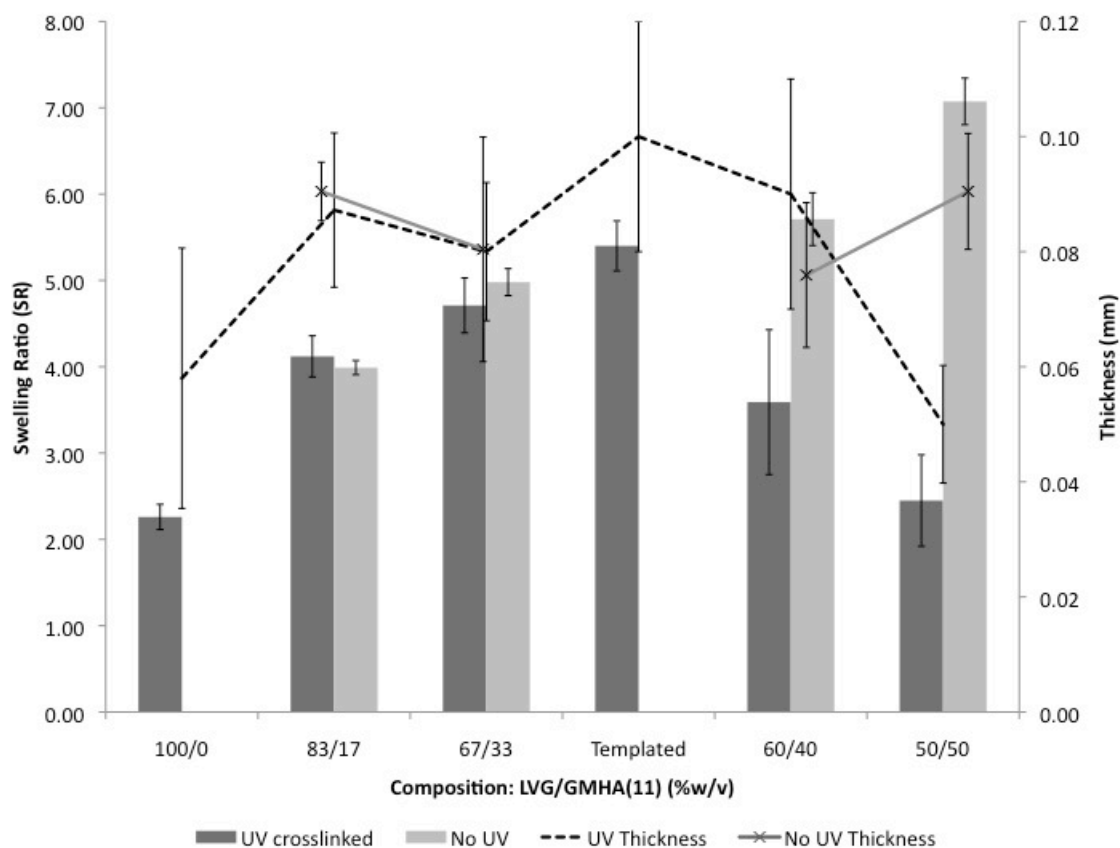
Figure 6.6 Swelling and thickness of LVG/GMHA(11) templated films. Templated LVG-rich films with 33% GMHA(11) concentration had a higher swelling ratio than nontemplated similar films. Swelling ratio can be described as the weight of water loaded onto the film per weight of polymer. The templated films with 33% GMHA(11) retained a similar percent polymer as those with 17% GMHA. Therefore, the templated films can be loaded with a much greater volume of water than a nontemplated film with the same amount of polymer.
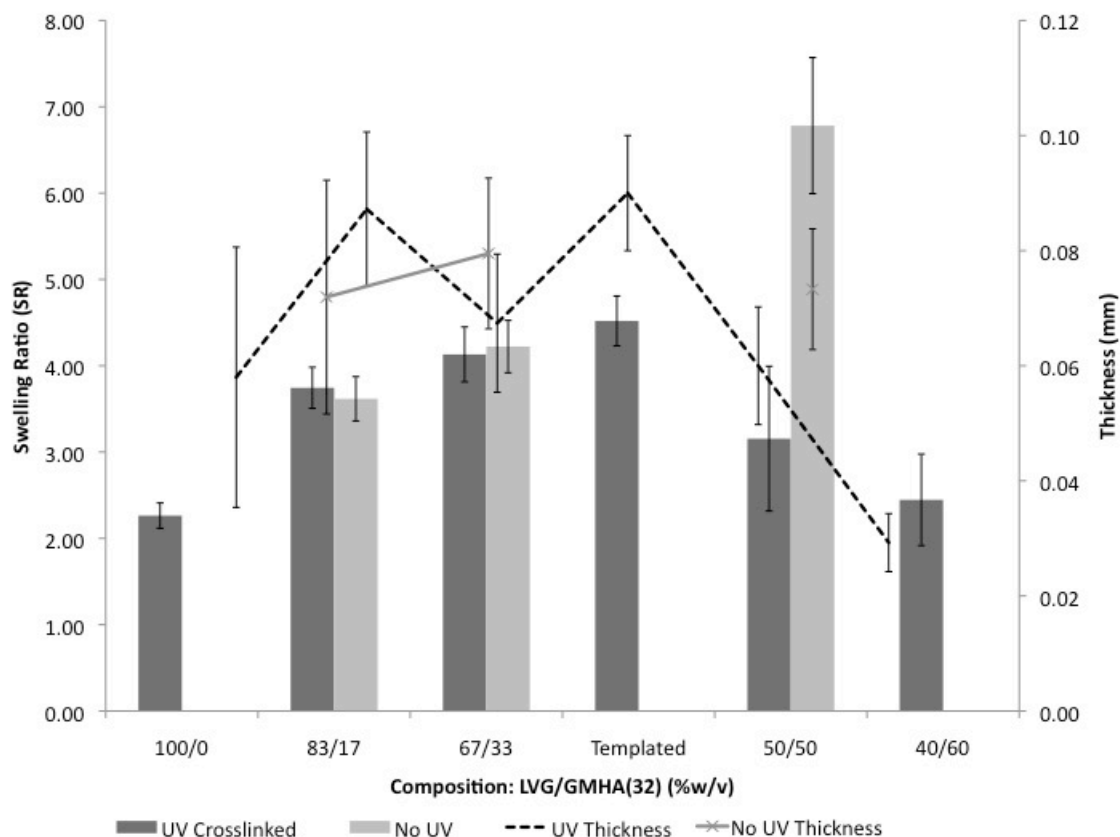
Figure 6.7 Swelling and thickness of LVG/GMHA(32) templated films. Templated LVG-rich films with 33% GMHA(32) concentration had a higher swelling ratio than nontemplated similar films. Swelling ratio can be described as the weight of water loaded onto the film per weight of polymer. The templated films with 33% GMHA(32) retained a similar percent polymer as those with 17% GMHA. Therefore, the templated films can be loaded with a much greater volume of water than a nontemplated film with the same amount of polymer.
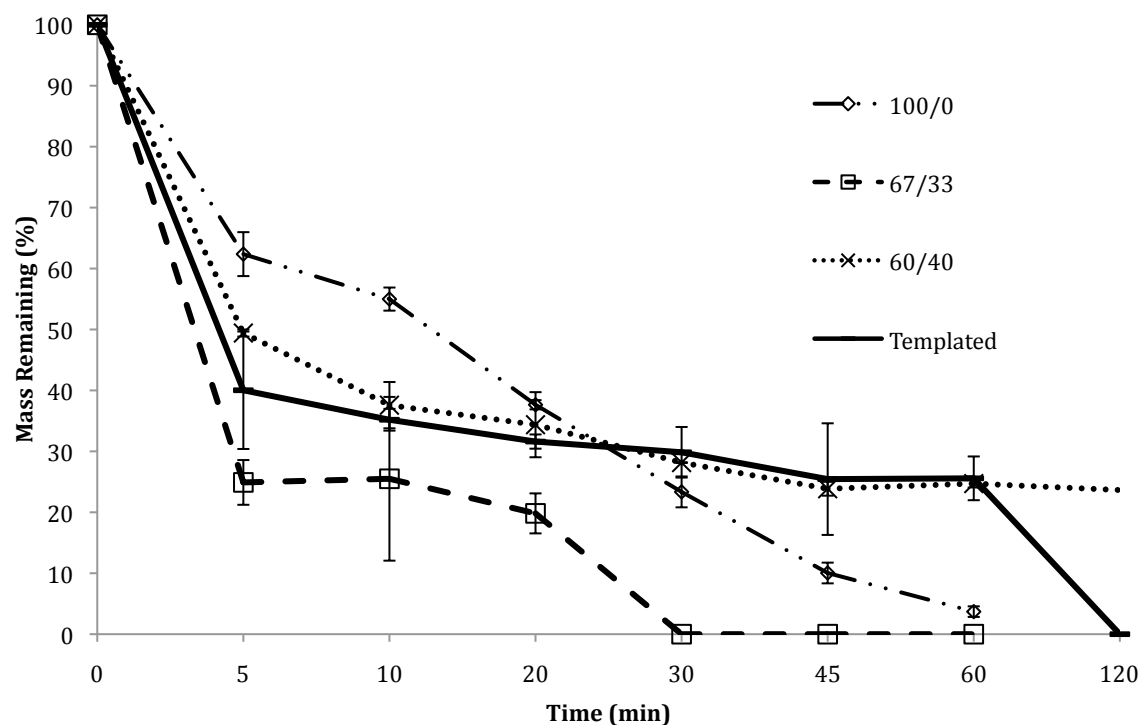
Figure 6.8 Dissolution of LVG/GMHA(32) templated films compared to nontemplated films. Templated LVG-rich films with 33% GMHA(32) concentration had a similar dissolution profile as the nontemplated films with 40% GMHA(32) with 60 min of exposure to 0.1 M citrate. However, an additional 60 min of exposure to 0.1 M citrate caused complete dissolution of the templated films. From previous studies, the films with 40% GMHA(32) exposed to UV did not further reduce in mass lost. (N = 6)

6.7 TENSILE TESTING OF TEMPLATED FILMS – "PARALLEL TO FIBER DIRECTION"

The process of urea crystal propagation creates two features: a branched crystal network, and compressed polymer fibers that are along-side the crystal network. Although there is visible overall apparent fiber direction, the polymers ultimately follow the branched, dendritic crystal patterns created by the urea. Therefore these fibers are also branched and dendritic, creating a somewhat random basket-like network. Once the urea is removed, the branched pores allow for sacrificial voids that increase elongation when pulled in tensile. The basket-like fibrous mesh of dense polymers also allows for increased elongation to decompress the polymers. A diagram illustrating this hypothesis is presented in **Figure 6.9**. In the nontemplated alginate/GMHA-blended films, pore volume is theoretically homogenous and random. The tensile strength is owed to the alginate calcium gelation. The elongation is attributable to increased water content provided by the presence of GMHA (and/or leaching of GMHA) and the ability for polymer chain movement.

Templated films were pulled in tension, in the direction of visible fibers, and compared with nontemplated films. (**Figure 6.10**) "Parallel to fiber direction" specimens were taken from radial patterned films, from the center of the film to the diagonal edge. Templated LVG-rich films with 33% GMHA(11) concentration had an insignificantly decreased Young's modulus when compared to nontemplated films with 33% GMHA(11) ($p = 0.76$). Modulus decreased by 22%, which was within standard deviation of the nontemplated film. An increase in tensile strength of templated films was unremarkable compared to nontemplated films ($p = 0.94$). Tensile strength increased by 26%, which was within standard deviation of the nontemplated film. Decrease in Young's modulus was a result of increased elongation. Elongation was significantly increased by 55% ($p < 0.05$).

As discussed in Chapter 5, toughness is the amount of energy that a material stores prior to catastrophic failure. It is ultimately a measure of allowed strain and is taken as the area under the true stress-strain curve. Due to the dramatically increased elongation, the toughness of templated films pulled in the direction of visible fibers, was as much as 500% higher than the nontemplated films ($p < 0.05$). (**Figure 6.11**) We hypothesize that the branched, porous network allows greater stretch and strain, while the compressed polymers in the fibers must undergo greater elongation (or strain) to fail. More specifically, the compressed fibers must be first pulled away from each other, and then slide past one another until failure.

6.8 TENSILE TESTING OF TEMPLATED FILMS – "NOT PARALLEL TO FIBER DIRECTION"

When fiber direction was not readily visible or if large deformation tensile stress was applied in various orientations other than "parallel to fiber direction", there was inconsistency in the resulting tensile data. Pulling a templated specimen "perpendicular to fiber direction" would give elongation values anywhere from equal to alginate-only films, to the greatest extension value obtained by films pulled "parallel to fiber direction". This inconsistency supports the theory that fiber compression imparted by the templating process is more basket-like, with several directions of fiber growth. The SEM images also depict fibers with a web- or basket-like orientation. Furthermore, large deformation tensile tests were too destructive to capture the anisotropic differences imparted by visible fiber direction.

Urea crystallization is a branched, dendritic pattern dependent on the viscosity of its environment. Although templating is a simple laboratory process, pattern consistency was difficult to maintain. (**Figure 6.12**) The films were cast in a closed environment, but seeding requires exposing the cast solutions to ambient conditions, which sometimes

147

caused self-nucleation of urea. Furthermore, controlling crystallization direction was ultimately not possible on the scale of our large films, since urea crystallizes in a branching pattern. Thus, the urea crystals were naturally trying to branch away from one another in a radial pattern. Radial patterned templated films were the most consistent and controllable for this reason.

6.9 DYNAMIC MECHANICAL ANALYSIS (DMA) OF TEMPLATED FILMS

DMA provides a non-destructive mechanical analysis of materials by oscillating force within the linear elastic region. Our aim was to utilize this more sensitive testing apparatus to reveal the viscoelastic property changes imparted by templating. Fiber direction is more visible in alginate-only films. Therefore, we hypothesized that if anisotropic mechanical behavior could not be observed where fiber direction was most visible, then most likely we would not be able to better quantify anisotropic behavior with alginate-only films.

The storage and loss moduli were determined at 1 Hz. (**Figure 6.13**) Storage modulus (G') represents the solid-like component of the film. Loss modulus (G") represents the liquid-like component of the film. Both alginate/GMHA(32)-blended films and alginate-only films were effected by templating. The G' and G" decreased when comparing the templated versus nontemplated films. However, there is no significant difference in the viscoelastic response of the material according to fiber direction at 1 Hz.

Frequency sweeps were conducted to determine the gel stability of templated versus nontemplated films. (**Figure 5.7**) As expected, the stability of the film is diminished with increasing GMHA(32) concentration. The liquification frequency of LVG/GMHA(32) films with 33% GMHA concentration was 100.01 ± 3.3 Hz when not templated. This value was decreased to 76.49 ± 3.2 Hz when pulled perpendicular to fiber

148

direction. Liquification frequency was further decreased to 62.91 ± 3.5 Hz when pulled parallel to fiber direction. Therefore, the templating process decreases the stability of an alginate/GMHA-blended film by 21% and 35% when pulled perpendicular to and parallel to fiber direction, respectively. A similar trend was found with LVG-only films. Nontemplated films had a liquification frequency of 161.05 ± 5.0 Hz. This value was decreased to 101.67 ± 5.4 Hz when pulled perpendicular to fiber direction. This value was further decreased to 86.57 ± 6.17 Hz when pulled parallel to fiber direction. Therefore, the templating process decreases the stability of an alginate-only film by 35% and 45% when pulled perpendicular to and parallel to fiber direction, respectively. The overall effect of templating and the anisotropic mechanical behavior in alginate-only films is more dramatic than in alginate/GMHA-blended films. We hypothesize that this difference is a result of the discontinuous fraction of interactions between the phase-separated polymers in blended films. An alginate-only film is significantly more uniform than the blended films, with only one viscosity. Blended films, as a result of phase separation, have fractions of different viscosities across the bulk of the film. Because templating is viscosity-driven, the fibrous networks formed in alginate-only films are more uniform than in blended films.

From these results we conclude that the effect of templating decreases the stability of the film, and that at high frequencies, there is a departure of stability with respect to fiber direction. When pulled in parallel to the direction of visible fibers, the stability of the material is decreased. When pulled perpendicular to the direction of visible fibers, the stability of the film is decreased from similar nontemplated films, but increased when compared to parallel tensile properties. High frequency testing relates to extrusion capabilities of a material, with crystalline direction contributing greatly to anisotropic mechanical properties of deformed materials. (Kasada et al 2011) Thus, it would follow

that a material with fiber directionality would present anisotropic mechanical properties. Therefore we further conclude that the templating method can impart fiber directionality that can be detected with sensitive, high frequency testing.
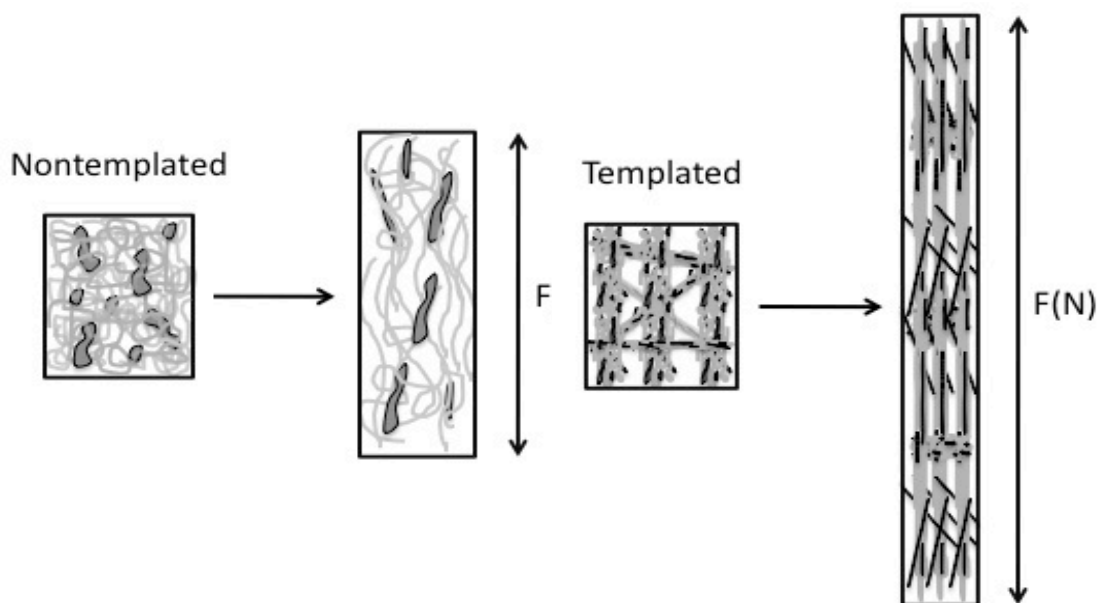
Figure 6.9. Schematic of influence of fibers and pores during tensile. A templated film is more porous than nontemplated films. Furthermore templating causes organization of polymers into compressed fibers. Although there is visible overall apparent fiber direction, the polymers follow the branched, dendritic crystal patterns created by the urea. Therefore these fibers are also branched and dendritic, creating a somewhat random basket-like network. The pores allow for sacrificial voids that increase elongation when pulled in tensile. The basket-like fibrous mesh of dense polymers also allows for increased elongation to decompress the polymers.
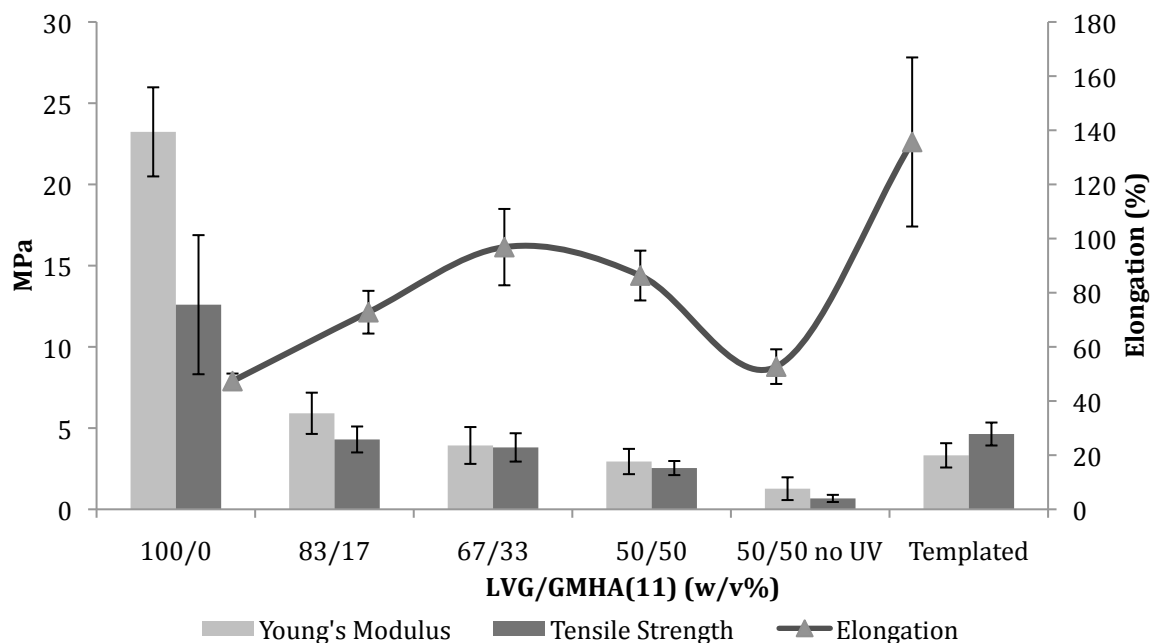
Figure 6.10 Tensile testing of templated versus nontemplated films. Templated LVG-rich films with 33% GMHA(11) concentration had an insignificant decreased modulus when compared to nontemplated films with 33% GMHA(11) ($p = 0.76$). The tensile strength insignificantly increased ($p = 0.94$). Decrease in modulus was a result of increased elongation. Increase in elongation was significant ($p < 0.05$). (N = 6)
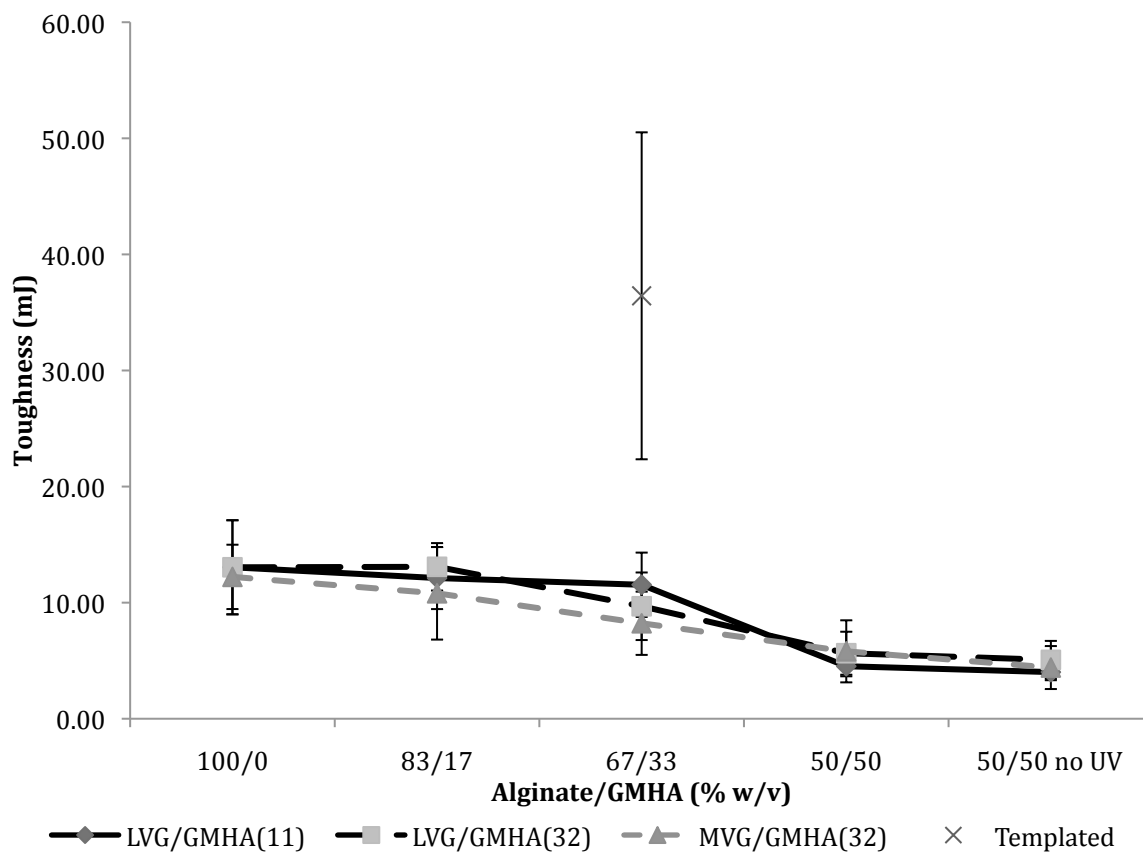
Figure 6.11 Toughness of templated versus nontemplated films. Alginate/GMHA(11) templated films are tougher than nontemplated similar films as a result of increased elongation. This elongation is a result of a fibrous and porous network imparted by templating. Toughness of templated films, when pulled in the direction of visible fibers, is 36.43 ± 14.1 mJ. Toughness of the nontemplated counterpart is 9.7 ± 2.9 mJ.
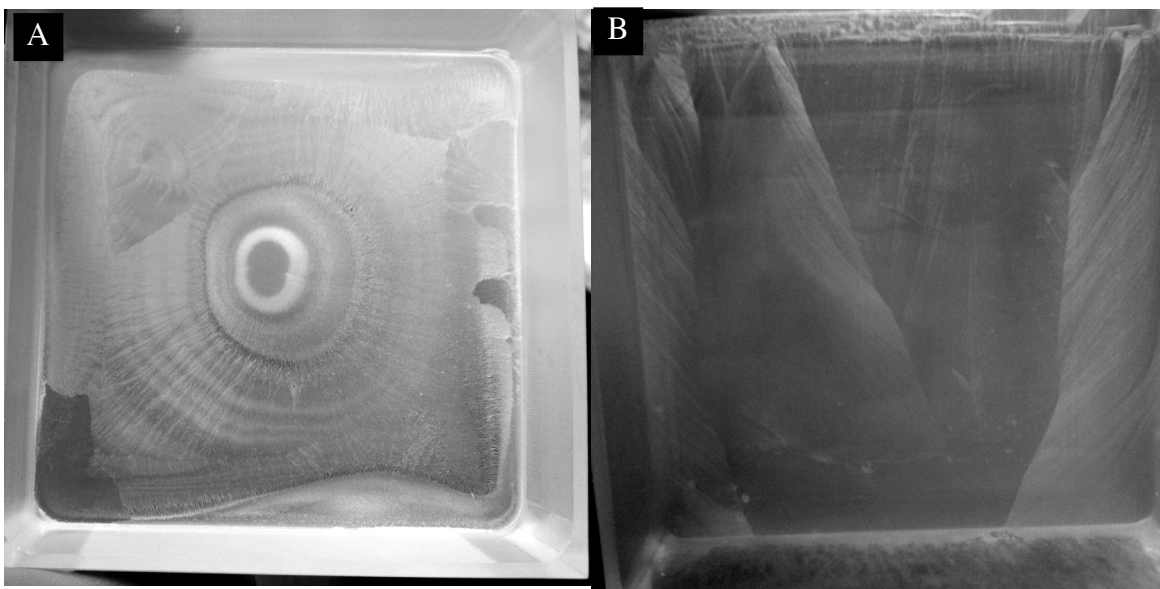
Figure 6.12 Non-ideal urea crystallization patterns. **A)** Although films of alginate/GMHA/urea blends were cast in a closed environment, opening the door to seed nucleation often caused concurrent self-nucleation of urea crystals in the cast solution. Crystals would precipitate onto the cast solution surface in white rings. B) Vertical patterns to get fiber direction across the film. The templating patterns cross over themselves in some places suggesting fiber direction could be variable from top to bottom film surface.
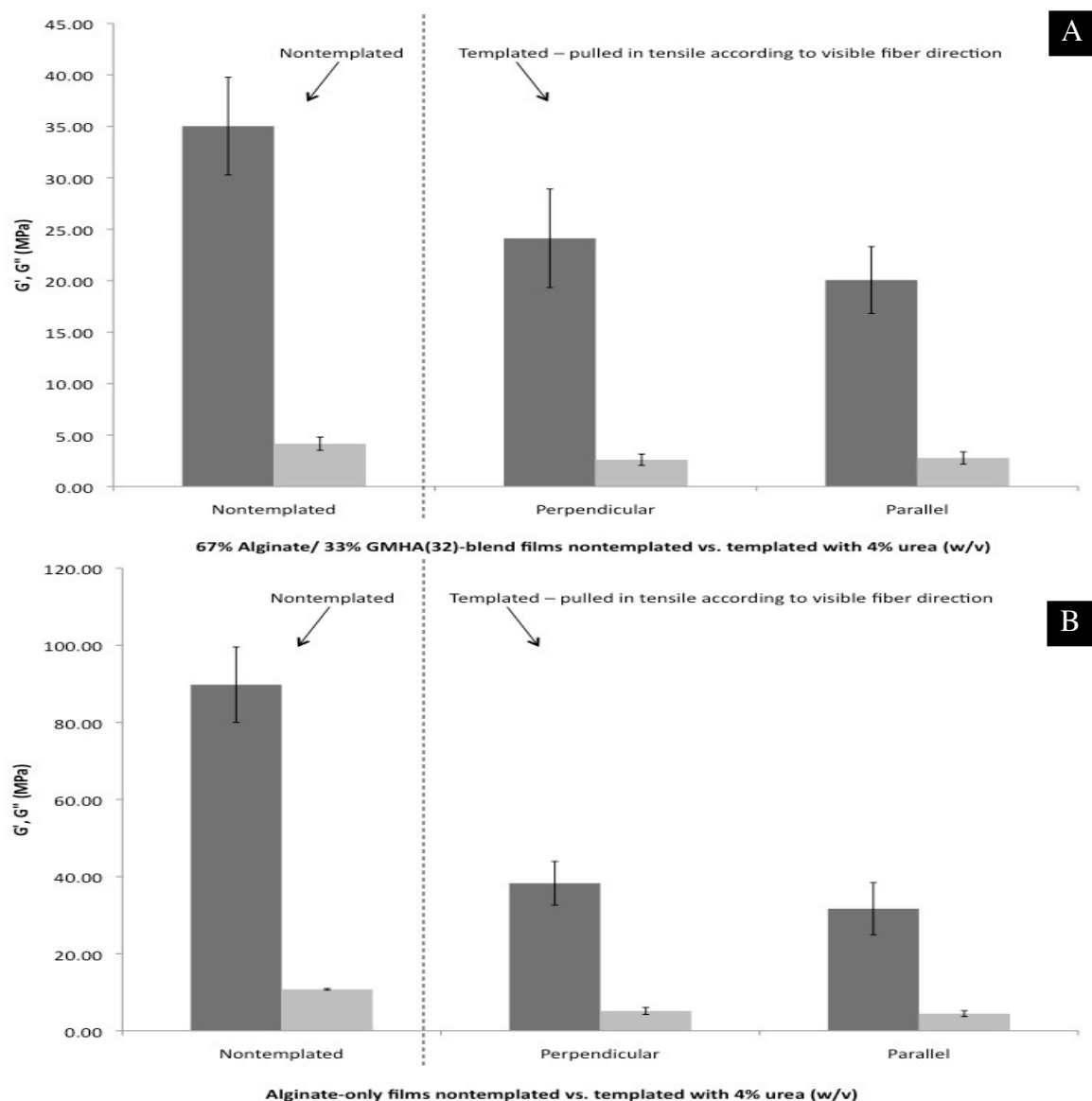
Figure 6.13 DMA tensile testing of 67/33/4 and 100/0/4 films at 1 Hz with templating. A) LVG/GMHA(32) films with 33% GMHA concentration with and without 4% urea templating. The modulus is decreased with templating, as predicted by tensile tests. There is no significant difference in G' or G" with regards to fiber direction. B) LVG-only films, both with and without templating. The storage modulus (G') is greater than the loss modulus (G") indicating that the film behaves more solid-like at this frequency. The trend in decreasing storage modulus indicates that softness increases with templating. Tests were conducted in triplicate.

155
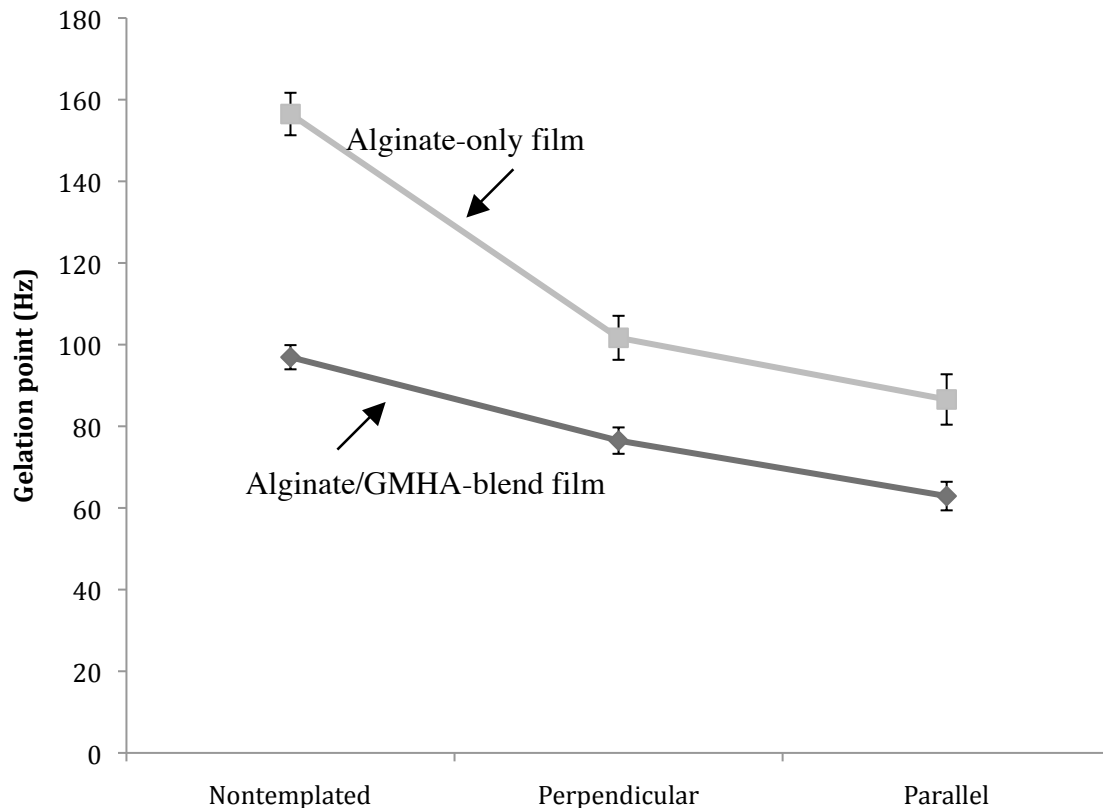
Figure 6.14 High frequency DMA tensile testing for gel stability. Gel stability was determined by tan delta values at unity during high frequency tensile oscillation. LVG/GMHA(32) with 33% GMHA concentration were templated or nontemplated. Nontemplated films were more stable than templated films depicted by a higher frequency liquification point. The templating process decreases the stability of an alginate/GMHA-blended film by 21% and 35% when pulled perpendicular to and parallel to fiber direction, respectively. Therefore there is a preferred fiber direction, and this direction plays a role in the overall stability of the films. Results for alginate-only films Tests were conducted in triplicate.

156

6.10 SURGEON HANDLING SURVEY

Objective mechanical characterization is critical to understanding the fundamentals of material behavior. This understanding drives predictive measures by which materials can be tuned to suit a particular need. However, in the case where the end user is also highly reliant on subjective metrics, ultimately, there lies the challenge of marrying objective and subjective observations. For the development of an anti-adhesive film, the end user employs the use of highly trained, yet subjective, instruments to ascertain mechanical integrity: human hands.

In medicine there are numerous examples of imperative correlation between objective and subjective data, pain being the most obvious. Assessing a patient's level of pain or performing a diagnosis can rely heavily on a person's subjectivity on how they feel and to what degree. Although objective markers such as increased range of motion or decreased swelling are helpful, these data cannot stand alone as indications of a completed treatment of the patient. Similarly, objective mechanical analysis of film behavior cannot, on its own, produce data that dictates usability or ease of use in an operating room setting. Critical to the success of any device is acceptability of the end user. If surgeons are unwilling to use the films, then efficacy is of little value. Therefore, it is of great scientific value to combine both objective and subjective data in a meaningful way, to capture what attributes would leverage success as a surgical adjunct.

We invited five local surgeons to participate in a handling study of alginate/GMHA-blended films. Each surgeon came separately and on a different day, and was unaware of other surgeon input. In addition, surgeons signed a document admitting blindedness to film composition or to film fabrication method. Surgeons were asked to select a film to handle from a set of three films. A new set of films was used for each surgeon. (**Figure 6.15**) Each film was scored for three features: conformability,

toughness, and ease of use. Each feature was scored on a scale of 1 to 5, with 1 as minimal and 5 as greatest. Optimal values were left up to discretion. Conformability was the only feature given examples of extremes. Parafilm was provided as an example of least conformable with a ranking of 1. Saran Wrap was provided as most conformable. The results of the survey are tabulated in **Table 6.1**.

Each surgeon manipulated the films to individual preference or manner. All surgeons wore gloves. All surgeons utilized an inverted spine sawbone available for conformability assessment. Conformability was gauged on the ability for the film to lay on the complex geometry of the inverted spine. A commonly used word to describe this behavior was "memory". If the film felt like it had too much "memory" then surgeons suggested that it would not lay well on soft tissues. Films with too much "memory" were scored low on the conformability scale. Although an optimal conformability score was not provided to the surgeons, they all scored films they preferred with high conformability scores. Films with high conformability scores were depicted as not having too much memory and feeling relaxed. Handling of films was conservative until asked to assess toughness. To assess toughness, all surgeons pulled films until failure. Toughness was assessed by all surgeons as how much strength it took to break the film in a two-handed, tensile-like grip. No instructions were provided; this was conducted ad hoc. Some surgeons optimized toughness to be at a score of 3. Some surgeons optimized toughness to be at a score of 5. The lower ranking was given to optimal toughness because it was estimated that a film that is too tough would probably not stay in place without significant tacking. A film that was "not tough enough" was "too soft" and it was estimated that pushing the film down a trocar for laparoscopic delivery would be very difficult. Ultimately there did not seem to be much of a consensus for what the optimal subjective toughness of a surgical adjunct film should be.

158

When asked to assess ease of use, all but one surgeon immediately rolled up the film to mock laparoscopic insertion. One surgeon used tweezers available to envision graspers and pushing the film down a trocar. If a film was too difficult to roll up, it was given a low score for ease of use. Most films received favorable scores for ease of use.

The results of the surgeon's survey suggest that there is a correlation between conformability and modulus. Alginate-only nontemplated films have high modulus according to objective mechanical testing, and would not conform to tissues well according to subjective surgeon's handling. Although not well correlated, the survey results suggest that toughness should be optimized with the ability for the film to relax, or not store "memory". To this end, there was an interest in the templated film because it required more diligence to break the film when compared to nontemplated. Simultaneously, the templated films were significantly more conformable than the alginate-only films ($p = 0.01$). The templated films have significantly higher toughness in objective tensile data, but were statistically similar to the other films in the subjective survey ($p = 0.48$). This discrepancy is more than likely a result of rate of deformation (tensile tests strain rate of 5 mm/min much slower than surgeon's "pull test") as well as what is deemed optimal for each surgeon. The alginate/GMHA-blended films scored higher for ease of use. The primary reason alginate-only films were found more difficult to use was a result of having too much "memory". Alginate-only films will retain a given position and, thus, it was mentioned that migration or additional requirements for suturing would be an issue. At the end of the survey, surgeons were asked to rank order the films. All surgeons selected the alginate-only film as last choice. All but one surgeon selected the templated film as their top choice.
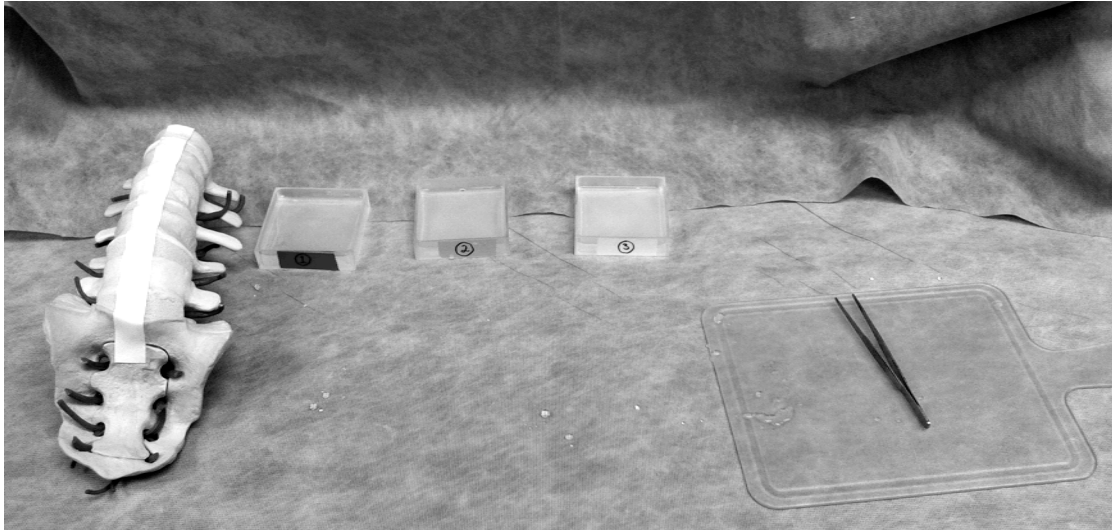
Figure 6.15 Surgeon's Handling Survey Set Up. Three films marked 1, 2, or 3 were placed on a laboratory bench. A sawbone spine model was available for conformability assessment. Surgeons were asked to assess the films for conformability, toughness, and ease of use. Surgeons were then asked to rank the films for choice.

Film	Conformability	Toughness	Ease of Use
Alginate Nontemplated	1.2	4.4	2.1
Alginate/GMHA Nontemplated	4.0 (0.01)	3.3 (0.25)	4.8 (0.01)
Alginate/GMHA Templated	4.4 (0.01)	4.1 (0.48)	4.8 (0.01)

Table 6.1 Surgeon's Handling Survey Results. All results are on a scale of 1 to 5, with 5 representing the greatest of each category. Values shown here are an average of 5 scores, values in parentheses are p-values when compared to alginate-only nontemplated film. Alginate nontemplated films were given the lowest conformability score, the highest toughness score, and the lowest ease of use score. Alginate/GMHA-blended films did not differ significantly in any category (p-values = 0.33, 0.16, 0.70 for conformability, toughness, and ease of use, respectively).

6.11 MATERIALS AND METHODS

6.11.1. Materials. Medical grade sodium alginate was purchased from FMC Novamatrix (Sandvika, Norway): Pronova UP LVG: 120 kDa, M/G ratio 0.67. High molecular weight sodium hyaluronate from *Streptococcus equi* of molecular weight 1.6×10^6 Da was obtained from Sigma-Aldrich (St. Louis, MO). Photoinitiator Irgacure 2959 (I2959) was obtained from Ciba Specialty Chemicals (Basel, Switzerland). All other chemicals purchased from Fisher Scientific. Tensile tests were conducted on an Instron 3345 universal testing unit equipped with a BioPuls bath, smooth grip faces, and a 100 N load cell. Extension was measured with a video extensometer. Thickness measurements were taken with a Vernier micrometer, digital, with 1/100 mm tolerance (BGS, Germany).

6.11.2. Methacryloyl modification of hyaluronic acid. High molecular weight hyaluronic acid was conjugated with photocrosslinkable methacryloyl groups based on two protocols (Zawko 2008, Bencherif *et al* 2008). A 1% w/v solution of HA was prepared in either ddI water or a 50:50 mixture of acetone:water and stirred for 24 hours at room temperature. Twenty molar equivalents of both triethylamine as base catalyst and of glycidyl methacrylate were added to the solution and stirred for five days at room temperature (pH 12.5-10.5). Modified HA (GMHA) was precipitated into a 20-fold volumetric excess of acetone and then subsequently dissolved in water for 24 hours at room temperature. GMHA solution was then dialyzed against ddI water in 3500 MWCO for 72 hours. Samples were lyophilized after filter sterilization and stored in dessicators at -20 °C. The average degree of methacrylate substitution was determined by ^{1}H NMR. For solutions prepared in ddI water, substitution was found to be 8.9% ± 0.6 substitution of methacryloyl groups per mole of HA disaccharides. For solutions prepared in 50:50

mixture of acetone:water, substitution was found to be 22% ± 1.1. These values are an average of 10 analyses.

6.11.3. Synthesis of photocrosslinked GMHA films. A 1% w/v aqueous solution of photoinitiator Irgacure 2959 was sonicated for 30 min and allowed to cool to room temperature. GMHA was then added to this solution to resolve a 1% w/v mixture, and stirred overnight in the dark at room temperature. Amount of polymer cast was based on area of form. A 2.2 cm diameter well had 26 mg of polymer cast. Forms were placed in a temperature and humidity controlled environmental chamber from Cincinnati Sub-Zero (Cincinnati, Oh). Temperature was held at 25 °C and humidity was held at 70% Rh during the casting period of 48 hours. Forms and solutions were kept from light at all times. Cast films were then subjected to UV light from the spot lamp, depending on experiment. Crosslinked films were removed from the wells, and transferred to petri dishes with large volumes of ddI water.

6.11.4. Synthesis of a calcium alginate/GMHA film. A 1% w/v solution of 67% alginate / 33% GMHA(11 or 32) (w/v) in ddI water was stirred at room temperature overnight with 0.05% photoinitiator. Solution was cast in a 72 mm by 72 mm form. Forms were placed in a temperature and humidity controlled environmental chamber from Cincinnati Sub-Zero (Cincinnati, Oh). Temperature was held at 25 °C and humidity was held at 70% Rh during the casting period of 48 hours. Forms and solutions were kept from light at all times. Cast films were then subjected to UV light from the chamber, depending on the experiment. After photocrosslinking, if conducted, 50 mL of 100 mM calcium chloride solution was pipetted on top of the cast film in the form. Films were left to crosslink for 30 minutes. Films were removed from molds, when possible, and transferred to petri dishes with large volumes of ddI water. Films were rinsed exhaustively in ddI water for 24 hours.

162

6.11.5. Synthesis of a templated alginate/GMHA film with urea. A 1% w/v solution of 67% alginate / 33% GMHA(11 or 32) (w/v) with 2% w/v urea in ddI water was stirred at room temperature overnight with 0.05% photoinitator. Solution was cast in a 72 mm by 72 mm form. Forms were placed in a temperature and humidity controlled environmental chamber from Cincinnati Sub-Zero (Cincinnati, Oh). Temperature was held at 25 °C and humidity was held at 70% Rh during the casting period of 48 hours. Forms and solutions were kept from light at all times. At 48 hours, nucleation of urea crystallization was conducting by seed crystal. Cast films were subjected to UV light from the chamber after completion of crystal propagation. After photocrosslinking, films were air-dried in the hood for at least 24 hours.

6.11.6. Synthesis of a urea-templated calcium alginate/GMHA film. A 1% w/v solution of 67% alginate / 33% GMHA(11 or 32) (w/v) with 2% w/v urea in ddI water was stirred at room temperature overnight with 0.05% photoinitator. Solution was cast in a 72 mm by 72 mm form. Forms were placed in a temperature and humidity controlled environmental chamber from Cincinnati Sub-Zero (Cincinnati, Oh). Temperature was held at 25 °C and humidity was held at 70% Rh during the casting period of 48 hours. Forms and solutions were kept from light at all times. At 48 hours, nucleation of urea crystallization was conducting by seed crystal. For radial patterns, one nucleation point was seeded in the center of the film. For linear patterns, a razor was used to seed nucleation along one edge. Cast films were subjected to UV light from the chamber after completion of crystal propagaion. After photocrosslinking, 50 mL of 100 mM calcium chloride solution was pipetted on top of the cast film in the form. Films were left to crosslink for 30 minutes. Films were removed from molds and transferred to petri dishes with large volumes of ddI water.

6.11.7 Scanning Electron Microscopy. Films were air-dried for 24 hours in the hood, then sputter coated with 15 nm of platinum/palladium for observation with SEM (Zeiss Supra 40 VP) with an acceleration voltage of 10 kV. Images were brightness and contrast enhanced.

6.11.8. Thermogravimetric analysis (TGA). Thermal characterization was performed using thermogravimetric analysis (TGA) in order to verify the removal of urea from crystal templated films. Samples (1–4 mg) were heated in a Mettler Toledo TGA 1 (Mettler-Toledo, Columbus, OH) in a range of 40–600 °C at a constant heating rate of 10 °C/min, under a nitrogen atmosphere (50.0 mL/min). All measurements were performed in triplicate.

6.11.9. Tensile testing of hydrogel films. Tensile testing was conducted according to ASTM D882 with minor modifications. After synthesis and rinsing, films were cut with a six-inch blade into 13 equally sized strips, 5 mm wide, with ribbing discarded as selvage. Three thickness measurements are taken per strip. In accordance with ASTM D882, strips with thickness changes greater than 10% were discarded. Furthermore, any specimen with a thickness measurement less than 50 μm or greater than 120 μm was not included. Test samples were prepped with at least 24 hours of soaking in ddI water at room temperature. Pneumatic submergible grips were placed 25.4 mm apart. This distance was used as the gage length. Specimens were marked at the grips with a paint pen, for video extensometer recognition. An aqueous bath, maintained at 25 °C, is lifted to submerge the specimen, and tests were started immediately. Grip faces were wrapped in masking tape for tear prevention, as recommended by Instron. Specimens were pulled in tensile at 5 mm/min strain rate until catastrophic failure. Proper test completion was considered any failure that did not occur at a nick, tear, or other defect. Most defects were a result of improper cutting. The Young's modulus, a measure of

intrinsic film stiffness (Cao *et al* 2007), was calculated according to the ASTM D882 as the slope of the force–extension curve multiplied by the distance between the tension grips and divided by the initial area of the specimen (length x thickness), and was expressed as MPa (**Equation 11**). The elongation at break (E, % of the original length) (**Equation 12**) and tensile strength (TS, MPa) (**Equation 13**) were also calculated according to the ASTM D882 method. Toughness (T, mJ) was taken as the area under the true stress-strain curve, until strain at break, ε_B (**Equation 14**). All films were tested in triplicate, at least.

$$\text{Young's Modulus (MPa)} = \frac{\text{Tensile Strength (N/mm}^2)}{\text{Elongation at break}} \qquad [11]$$

$$E(\%) = \frac{(L - L_0)}{L_0} \times 100\% \qquad [12]$$

$$TS(\frac{N}{mm^2}) = \frac{F}{A} \qquad [13]$$

$$T = \int_0^{\varepsilon_B} \sigma(d\varepsilon) \qquad [14]$$

6.11.10. Dynamic mechanical analysis (DMA). After synthesis and rinsing, films were cut with a six-inch blade into 13 equally sized strips, 5 mm wide, with ribbing discarded as selvage. Three thickness measurements are taken per strip. Any specimen with a thickness measurement less than 50 μm or greater than 120 μm was not included. Test samples were prepped with at least 24 hours of soaking in water at room temperature. Dynamic mechanical analysis was conducted on a TA Q800 with submergible chamber (TA Instruments, New Castle, DE). Films were pulled in tensile for two testing sequences. The response to sinusoidal deformation over time was measured at

1 Hz frequency, 0.1% strain, and 15 mm specimen length for 2 hours. We also conducted frequency sweeps from 0.01 Hz to 100 Hz at 25 °C. The viscoelastic properties of alginate/GMHA-blended films were quantified in terms of the storage modulus (G'), the loss modulus (G"), and tan delta (δ). G' gives the elastic or solid-like component, G" gives the viscous or liquid-like component, and δ = 1 gives the point of gelation. G' and G" were recorded when steady-state was reached at Hz = 1, and represent the softness of the film. The point of gelation represents overall gel stability. All tests were conducted in triplicate.

6.11.11 Statistical analysis. Kruskal-Wallis pairwise comparison was conducted on R software. Student's t-test for significance was used to obtain p-values. All other data are presented as mean ± standard deviation.

Chapter 7: Efficacy of an Alginate/GMHA Anti-adhesion Membrane

7.1 INTRODUCTION

The ideal anti-adhesion membrane must be pliable and robust to withstand operating room procedures including laparoscopic delivery; must maintain mechanical integrity while hydrated to facilitate repositioning within the surgical field; must conform to delicate tissue geometries; must be tissue adherent, obviating the need for sutures and staples; must effectively prevent unwanted adhesions during the critical healing period; and must dissolve within 14 days of implantation to avoid foreign body response. (**Table 7.1**) Our lead candidate for further development as an anti-adhesive membrane was optimized for handling and dissolution rate: a templated alginate/GMHA-blended film with low molecular weight alginate, low degree of methacrylation, and a GMHA concentration below the percolation threshold. However, it was impossible to ascertain the efficacy of the optimized film without *in vitro* and *in vivo* assessment.

7.2 *IN VITRO* CELL STUDIES

7.2.1. Cytocompatibility. Before using our films in an animal model, we examined the behavior of normal human dermal fibroblasts (HDF) *in vitro* for cytocompatiblity of the degraded film. Films were degraded in media. Human dermal fibroblasts were selected for cytocompatibility studies as these cells are relevant to adhesion formation, and are responders to injury. Cytocompatibility studies were conducted in accordance with ISO 10993-5 for *in vitro* cytotoxicity. (ISO 2009) Positive control substrates of poly-L-lysine (PLL) attached to tissue culture polystyrene supported the growth of fibroblasts. HDF were exposed to extracts of degraded films. Preliminary results indicate that degraded films are non-toxic. (**Figure 7.1**) These results are not

surprising as both alginate and HA are established nontoxic, nonimmunogenic polymers. However, the favorable cell study results indicate that the presence of TEA or unwanted methacrylate leftover products from functionalization of GMHA must be rinsed out during the film fabrication process.

7.2.2. Fibroblast attachment. Alginate and HA are highly hydrophilic and are established anti-adhesive polymers (Cho *et al* 2010, Sufiyarov 2007). We challenged the anti-adhesive behavior of our alginate/GMHA-blended films in experimental conditions that favor cellular adhesion. We selected HDFs because they are known to adhere to a variety of surfaces via secretion of thick actin bundles (Nishimura *et al* 2007). Serum-free media was used as serum can interfere with cellular adhesion. Cells were assessed at six hours after seeding, and imaged by epifluorescence at 20x magnification. Fibroblasts did not adhere to the film surface, indicating that films are non-adhesive. Positive control substrates of attached PLL supported the attachment and proliferation of HDF. Reduction of cell attachment on film surface, compared to positive control, was 96.79% ± 3.37 (**Figure 7.3**). Studies were conducted in triplicate.

7.3 *IN VIVO* RAT CECAL ABRASION MODEL

In vitro studies do not accurately represent the elegant, dynamic process of wound healing and the cascade of biological events leading to adhesion formation. An effective adhesion barrier is required to balance this complex environment with its dissolution rate. Therefore, to effectively prevent adhesion formation, a film must remain in the location of injury until the healing period is complete, yet be dissolved by 14 days postoperative, to prevent fibrous encapsulation. Live animal analysis is conventionally accepted as the most clinically relevant method for testing efficacy.

Requirement	Description	Logic
Biocompatible / non-adhesive	Examine in vitro cytocompatibility and cellular adherence with human dermal fibroblasts	Provide preliminary safe and efficacious data to support in vivo studies
Repositionable	Film must be repositionable in vivo for at least five minutes in the rat abdomen	Optimal instructions for use for ease of clinical handling and implantation of film
Tissue adherent	Film must not migrate in vivo from implanted location within 72 hours of critical healing	Provide site specific protection of injured tissues only where film implanted
Resorbable	Film must not be visible with gross observation within 14 days of implantation in vivo, and resorbed by 28 days	Reduce opportunity for foreign body response or late stage healing
Efficacious	Film must successfully prevent unwanted adhesions in vivo with statistical significance compared to untreated animals	Provide an ideal prototype anti-adhesion pre-formed barrier for clinical application in the abdomen

Table 7.1. Ideal anti-adhesion barrier criteria.
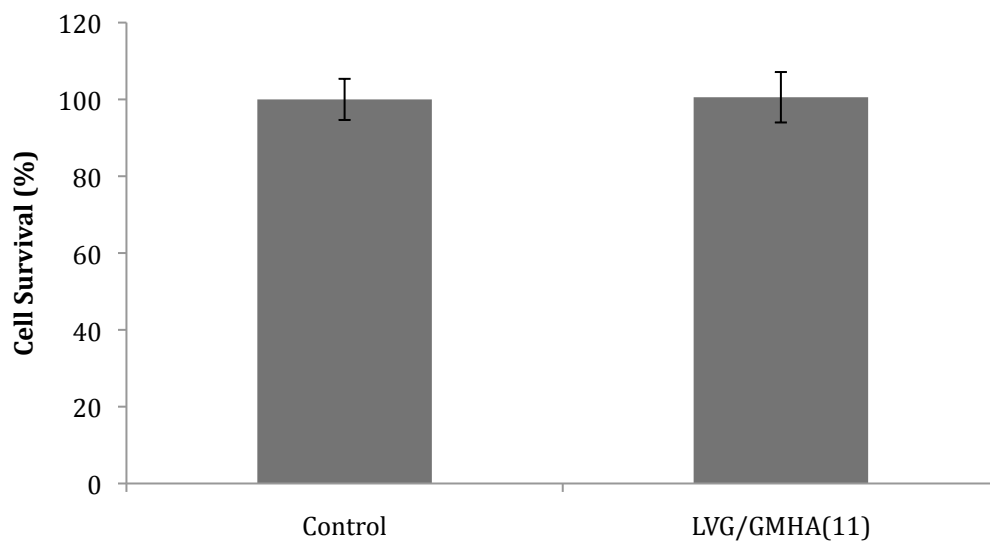
Figure 7.1. Cytocompatibility results of degraded film effluent. A PLL control surface for optimal cell survival was compared to survival of cells exposed to 0.75% concentration of extract from degraded film in media, per ISO 10933-5. Eight trials were run per film, and studies were conducted in triplicate including controls. Results are normalized per the control. The film did not cause a significant change in cell survival at 24 hours ($p = 0.98$).
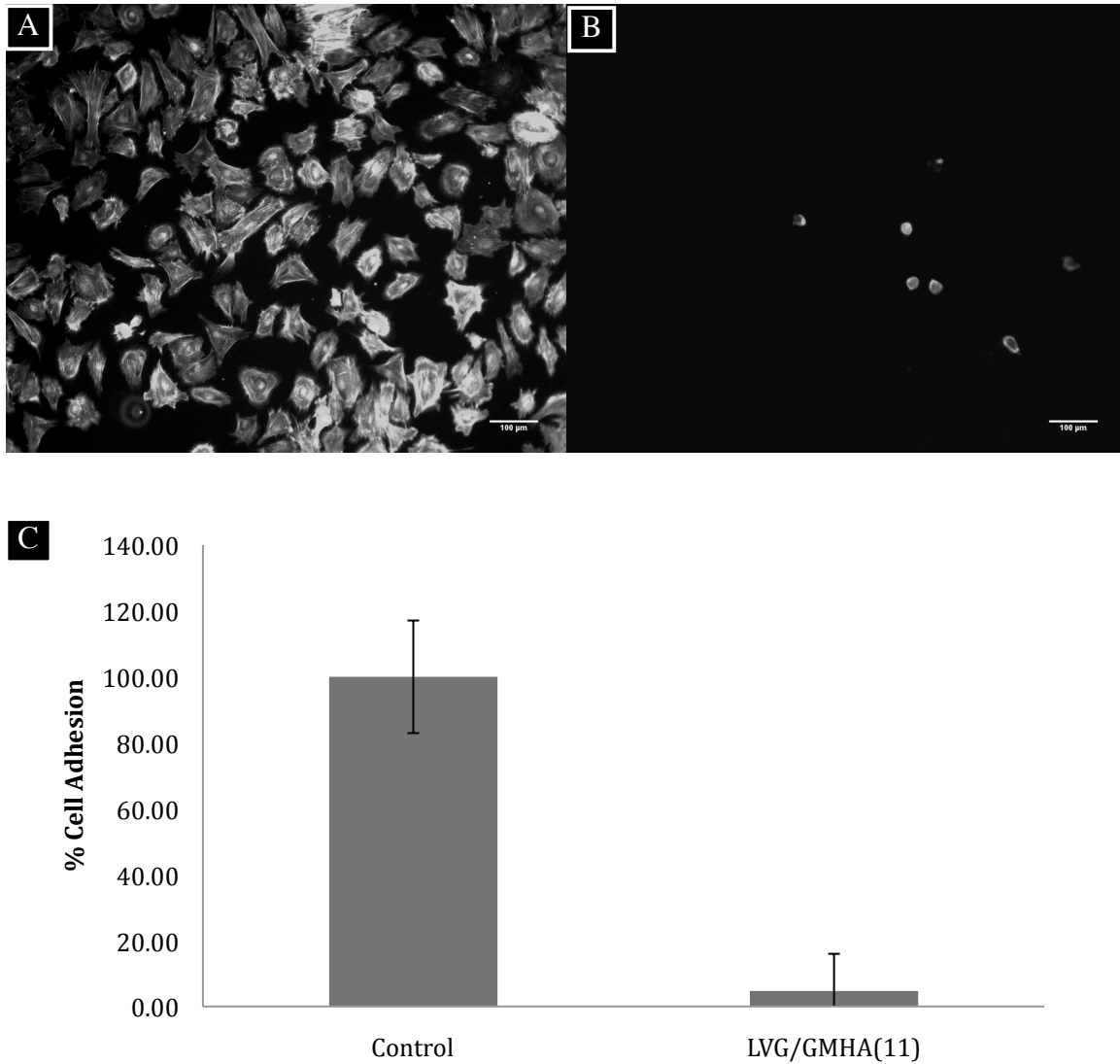
Figure 7.2. Fibroblast anti-adhesion. A) DAPI and phalloidin staining of HDF on PLL versus LVG/GMHA(11) surface. Microscopic observations of fibroblasts strongly adhered to PLL control surface for optimal cell attachment and proliferation, and B) fibroblasts minimally adhered to the LVG/GMHA(11) film. Scale bars = 100 μm. (C) A PLL control surface for optimal cell attachment and proliferation was compared to attachment of cells exposed to film surface in media with serum. Eight trials were run per film, and studies were conducted in triplicate including controls. Results are normalized per control. (p << 0.01)

The rat peritoneal abrasion model is defined, documented, and accepted as the optimal model for anti-adhesion testing. (Ersoy *et al* 2009, Lo *et al* 2010, Rajab *et al* 2010, Way *et al* 2010) Rat abdominal adhesions form quickly, can be assessed grossly on an industry-accepted subjective scale, and are most similar to human adhesion formation in both timing and placement. (Ozel *et al* 2005) Although there are slight variations of this model, primarily it involves placing two injured tissue surfaces in proximity to each other either with or without a barrier. Gross assessment evaluates adhesion formation between the two injured surfaces.

7.3.1 Rat cecal abrasion surgical procedure. Instructions of use, migration, dissolution rate, and efficacy of the LVG/GMHA(11)-blended film was tested in the rat cecal abrasion model at The University of Texas at Austin Animal Research Center (UT-ARC) under the approval of the Institutional Animal Care and Use Committee (IACUC) for protocol AUP-2010-00164. This model induces adhesion formation by injuring adjacent cecal and abdominal wall tissues. (Ozel *et al* 2005). Over 3 to 10 days post-surgery the cecum and abdominal wall become tethered with fibrotic adhesions. The efficacy of test materials is determined by inserting them between the injured cecum and abdominal wall at the time of injury to prevent physical contact between the injured tissues. At selected timepoints the animals were sacrificed and the proportion of animals in the test group with adhesions was compared to the proportion of animals in the positive and negative control groups with adhesions. An extensive description of the protocol is included at the end of this chapter. Briefly, this open surgical procedure entails accessing the abdominal cavity through a 4 cm midline laparotomy incision (**Figure 7.3**). Then a partial-thickness defect is inflicted by scalpel on a 2 cm^2 area of the abdominal wall. Next, the entire cecum surface is abraded with sterile gauze until punctate bleeding, but not perforation, is observed. In treated animals a 1.5 in^2 film is

placed between the injured tissues. In negative control animals no further treatment is provided. In positive control animals a 1 in^2 HA/CMC membrane (SepraFilm®, Genzyme) is inserted between the injured tissues. Irrigation with saline or chelating solution may or may not be conducted before closing the animal, depending on the experiment. The abdominal layers and skin incisions are closed separately with 3-0 suture and surgical clips. Animals are sacrificed at various timepoints to assess adhesion formation.

7.3.2 Gross adhesions grading scale. A number of methods for grading adhesions have been reported in the literature. The strength of abdominal-cecum tissue adhesions has been quantified with a tensiometer (Harris *et al* 1995). Most reports have utilized semi-quantitative grading scales based on the number and extent of adhesions (Nair *et al* 1974), the vascularity of adhesions (Leach *et al* 1998), the difficulty of dissecting adhesions (Yeo *et al* 2006), or combinations thereof. At selected timepoints animals were euthanized by carbon dioxide inhalation. Then the abdominal cavity is exposed by a U-shaped incision. The extent and severity of the adhesions are grossly observed and graded by three blinded surgeons not otherwise involved with this proposal. For each animal the number of adhesions and their anatomical locations were recorded. Then the severity of the adhesions is evaluated according to the tenacity or difficulty of separating the adhered tissues (Yeo *et al* 2006). A grade of 0 is assigned to animals that have no adhesions (**Figure 7.4**). Grade 1 is assigned to adhesions that are the least severe and separable by gravity alone. Grade 2 adhesions are moderately severe and are separable by blunt dissection. Grade 3 adhesions are the most severe, such as the whole of the cecum adhered directly to the abdominal wall, and are separable only by sharp dissection and unavoidable reinjury of the underlying tissue.

7.4 PREVENTING ADHESIONS

Preventing unwanted postoperative adhesions requires these features from an anti-adhesive device:

- Non-toxic, does not cause harm;
- Is tissue adherent, to prevent migration of device and to provide site specific care;
- Completely dissolved in no less than 3 days but no greater than 14 days to provide care during critical healing period and to reduce chance for fibrotic response;
- Effectively prevent unwanted adhesions.

To determine which of these features we would need to address for further film optimization, we conducted a pilot efficacy study with 40 animals. There were 4 groups with 10 animals in each group. The groups included a negative control group that received no treatment, a positive control group that received the leading commercially available anti-adhesion device, Seprafilm®, an experimental group with templated LVG/GMHA(11)-blended films with 33% GMHA(11) concentration, and an experimental group with templated LVG/GMHA(11)-blended films with 33% GMHA(11) concentration and further treatment of soaking in 0.25% HA. The final treatment group was selected because benchtop studies confirmed that templated films could be backfilled with HA, increasing the concentration of HA in the film without loss of mechanical integrity. We hypothesized that a higher concentration of HA could play a role in the overall efficacy of the film in preventing unwanted adhesions. All films were sterilized in the hood with gentamicin and sterile technique. Necropsy was conducted at 14 days postoperative. (**Table 7.2**)

Adhesions were found in 90% of untreated negative control animals (animals that were injured but received no prophylactic treatment), indicating successful implementation of this animal model. Our positive control, Seprafilm® treatment, successfully prevented unwanted adhesions in 80% of the animals. This value is statistically significant when compared to the negative control group (p = 0.002). This value also indicates that our model was not overly adhesiogenic, as we expected Seprafilm® to be effective. Templated LVG/GMHA(11) with 33% GMHA(11) concentration films successfully prevented adhesions in 90% of the animals in this treatment group. This value is statistically significant when compared to the negative control group (p = 0.004). Finally, templated films that were backfilled with HA were successful at preventing adhesions in 70% of the animals in this group. This value is statistically significant when compared to the negative control group (p = 0.026). There was no statistical significance in efficacy between the Seprafilm® group and either experimental group, or between the two experimental groups (p = 0.54, 0.56, 0.23, respectively). Effective membranes are anticipated to exhibit grade 0 adhesions in greater than 70% of the treated animals based on literature reports for HA/CMC membranes in the rat cecal abrasion model (Burns *et al* 1997). The results of this pilot study suggest that our films are effective at preventing adhesions in the rat cecal abrasion model.

However, there are several other requirements for a successful anti-adhesion device in humans, as previously mentioned. Membranes must not migrate from the injury site until after the critical healing period, and must degrade, bioresorb, or otherwise not be visibly present at <14 days postoperative. However, we recovered at least a portion of 70% of the templated films and at least a portion of 80% of the templated/backfilled films at 14 days necropsy. Films were found in the pelvis, away from the cecum or area of injury. Films were folded or balled up, but were primarily intact. Because our films were

successful at preventing adhesions, this suggests that they did not migrate from the injury site until after the critical healing period. However, they did not significantly dissolve.

There were several key conclusions from this pilot efficacy study:

1. Templated and templated/backfilled films are easy to apply and can easily be inserted into a small incision. In fact, it was noticed that a larger incision had to be made to accommodate the delivery of Seprafilm® into the peritoneal cavity.

2. Templated LVG/GMHA(11)-blended films with 33% GMHA(11) concentration were effective at preventing unwanted adhesions.

3. The backfilling process was unnecessary in the prevention of adhesions.

4. Our films did not dissolve within 14 days postoperative. Therefore we need to increase the dissolution rate of the films.

5. Our films migrated from the injury site. Therefore, we would need to address tissue adherence.

These conclusions drove subsequent optimization of our film. We were challenged to increase adherence to prevent migration, and to increase the dissolution rate so that the film is fully dissolved < 14 days. If a film was successful at preventing adhesions, and was dissolved < 14 days postoperative, then mucoadhesivity may be a transient feature requiring further investigation. Therefore, we focused on film dissolution rate.

7.4.1 *In vivo* dissolution study. Although we used sterile technique in the lab, FDA approval mandates bioburden levels that typically require more stringent techniques such as gamma irradiation. Important to the success of any FDA-approved Class III device is meeting sterilization criteria of 10-log reduction in bioburden mass. We sterilized our films using both Co-60 gamma (Phoenix Memorial Laboratory, The University of Michigan) and ebeam radiation (National Center for Electron Beam Research, TAMU), and determined that ebeam sterilization has the least impact on the mechanical properties

of our films. An assessment was conducted at TAMU Electron Beam Facility to determine the bioburden of our as received versus e-beam sterilized films at those given radiation levels. The results of this assessment indicated that an 8 kGy irradiation would be sufficient to remove bioburden to an FDA-approved level.

Exposure to irradiation can reduce the molecular weight of polysaccharides (Gryczka *et al* 2009). Molecular weight contributes significantly to the mechanical properties of our films, which directly impacts the dissolution rate. Lower molecular weight should lend itself to a faster dissolution rate. We hypothesized that sterilization could impact our *in vivo* results, and cause faster dissolution of the film. Films were e-beam sterilized at 35 kGy, 25 kGy, and 15 kGy. The films exposed to 35 kGy had no mechanical integrity and could not be removed from the plastic bag without tearing. It was determined that this radiation exposure was catastrophic to the handling properties of the film. The 25 kGy and 15 kGy exposures rendered films with mechanical integrity. We selected 15 kGy and 25 kGy irradiation as parameters for an *in vivo* dissolution study. It was also advised from industry representatives that we select values within the range of 15 – 40 kGy. We aimed to correlate irradiation of alginate/GMHA films and the *in vivo* dissolution profile. A dissolution study of 48 animals was conducted, with necropsy at 4 weeks. (**Table 7.3**) An extended necropsy date was selected to maximize dissolution time. There were 4 groups with 12 animals in each group. This experiment's groups included a negative control group that was untreated, a positive control group that received the leading commercially available anti-adhesion device, Seprafilm®, and an experimental group with templated LVG/GMHA(11)-blended films with 33% GMHA(11) concentration and 15 kGy irradiation exposure.

177
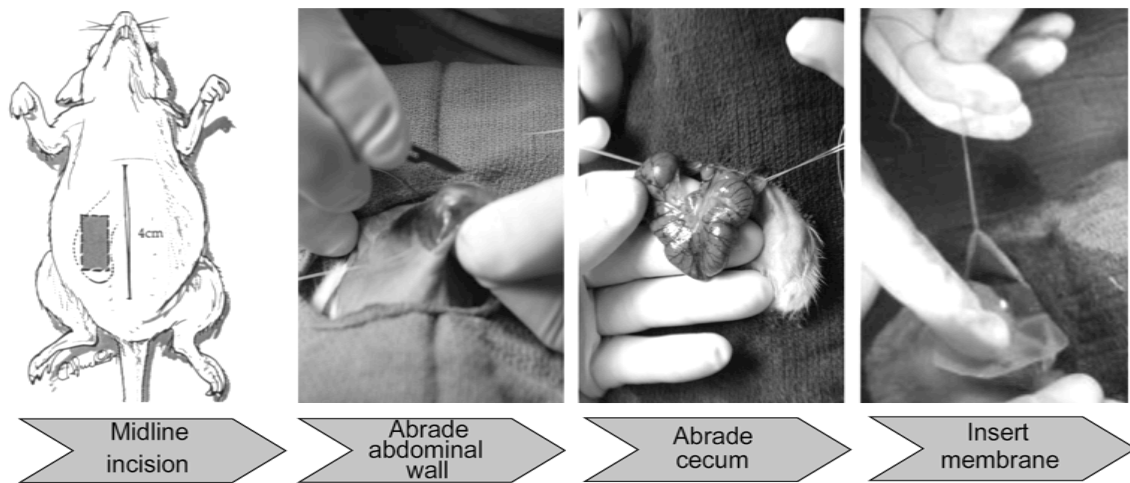
Figure 7.3. Rat cecal/sidewall abrasion model of abdominal adhesions (Harris *et al* 1995). The rat abdominal cavity is opened by midline incision. Then a 1 in^2 section of the abdomen is abraded with a scalpel and the entire surface of the cecum is abraded with sterile gauze. Anti-adhesion efficacy is tested by insertion of test membranes between the cecum and abdominal wall. Without an intervention adhesions form between the cecum and abdominal wall within 3-7 days.
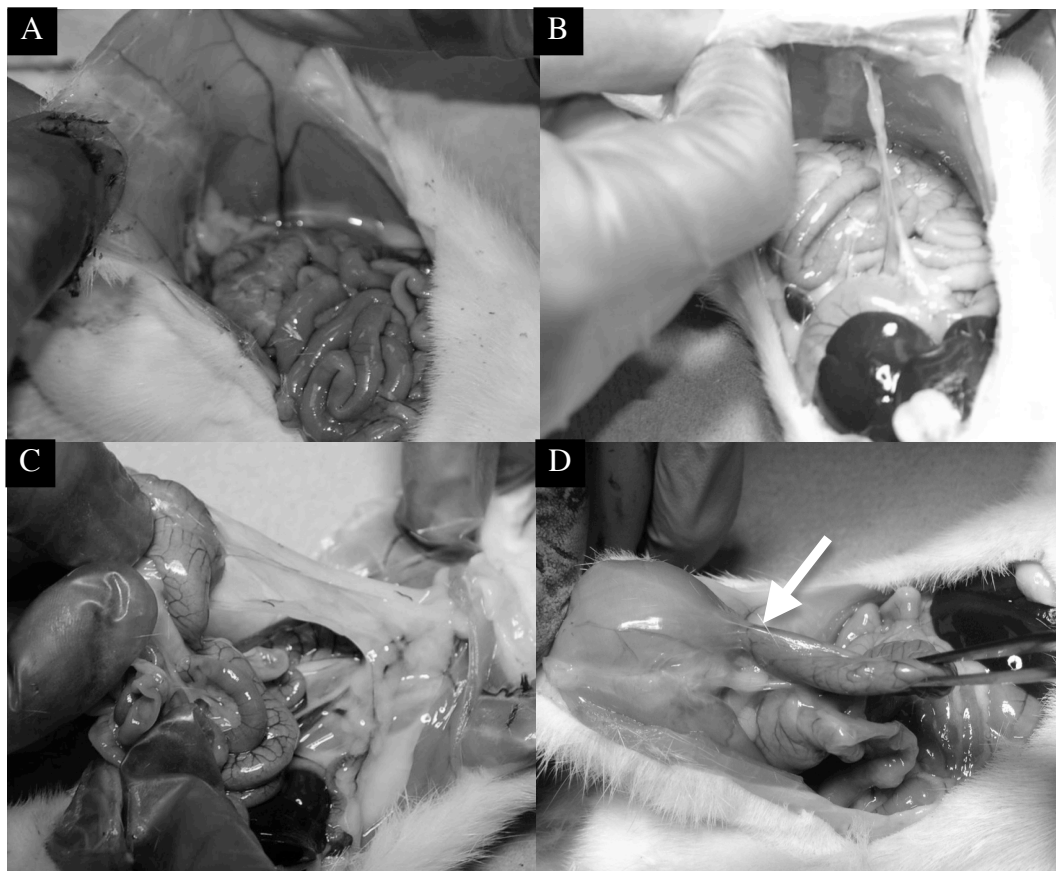
Figure 7.4. Adhesion grading scale (Harris *et al* 1995). A) Grade 0: no adhesions. B) Grade 1: Least severe adhesions, separable by gravity. C) Grade 2: moderate severity adhesions, separable by blunt dissection. D) Grade 3: Severest adhesions, separable only by sharp dissection. Arrow indicates a fibrous adhesion tethering the cecum to the abdominal wall.

	Grade 0	Grade 1	Grade 2	Grade 3	p-value	film found?
Control	1	0	2	7	--	N/A
Sseprafilm®	8	0	1	1	0.002	0
67/33 Alginate/GMHA Templated	9	0	1	0	0.0004	7
LVL/GMHA(11) backfilled	7	0	0	3	0.026	8

Table 7.2. Pilot study results for necropsy at 14 days. Grade 3 adhesions occur between cecum and abdominal wall in untreated rat. Significantly fewer adhesions are found in animals treated with LVG/GMHA(11) barrier. These results represent gross observation results at necropsy. Statistics conducted using pairwise Mann Whitney U tests**.** Films were recovered in 70% of animals treated with LVG/GMHA(11) films. Films were recovered in 80% of animals treated with the backfilled films.

	Grade 0	Grade 1	Grade 2	Grade 3	p-value	film found?
Control	3	0	0	9	--	N/A
Seprafilm®	7	0	1	4	0.07	0
15 kGy	9	0	0	3	0.02	5
25 kGy	5	0	0	7	0.042	6

Table 7.3. *In vivo* **dissolution study with ebeam sterilization (28 days).** Model was successful in causing adhesions in 75% of untreated animals. However, this model may have been too adhesiogenic because Seprafilm® did not statistically prevent unwanted adhesions when compared to the control. Films exposed to 25 kGy irradiation performed the worst compared to the other experimental groups and did not successfully prevent unwanted adhesions when compared to the control. Significantly fewer adhesions are found in animals treated with a film exposed to 15 kGy irradiation. These results represent gross observation results at necropsy. Statistics conducted using pairwise Mann Whitney U tests**.** Films were recovered in 42% of animals treated with LVG/GMHA(11) films exposed to 15 kGy. Films were recovered in 50% of animals treated with LVG/GMHA(11) films exposed to 25 kGy.
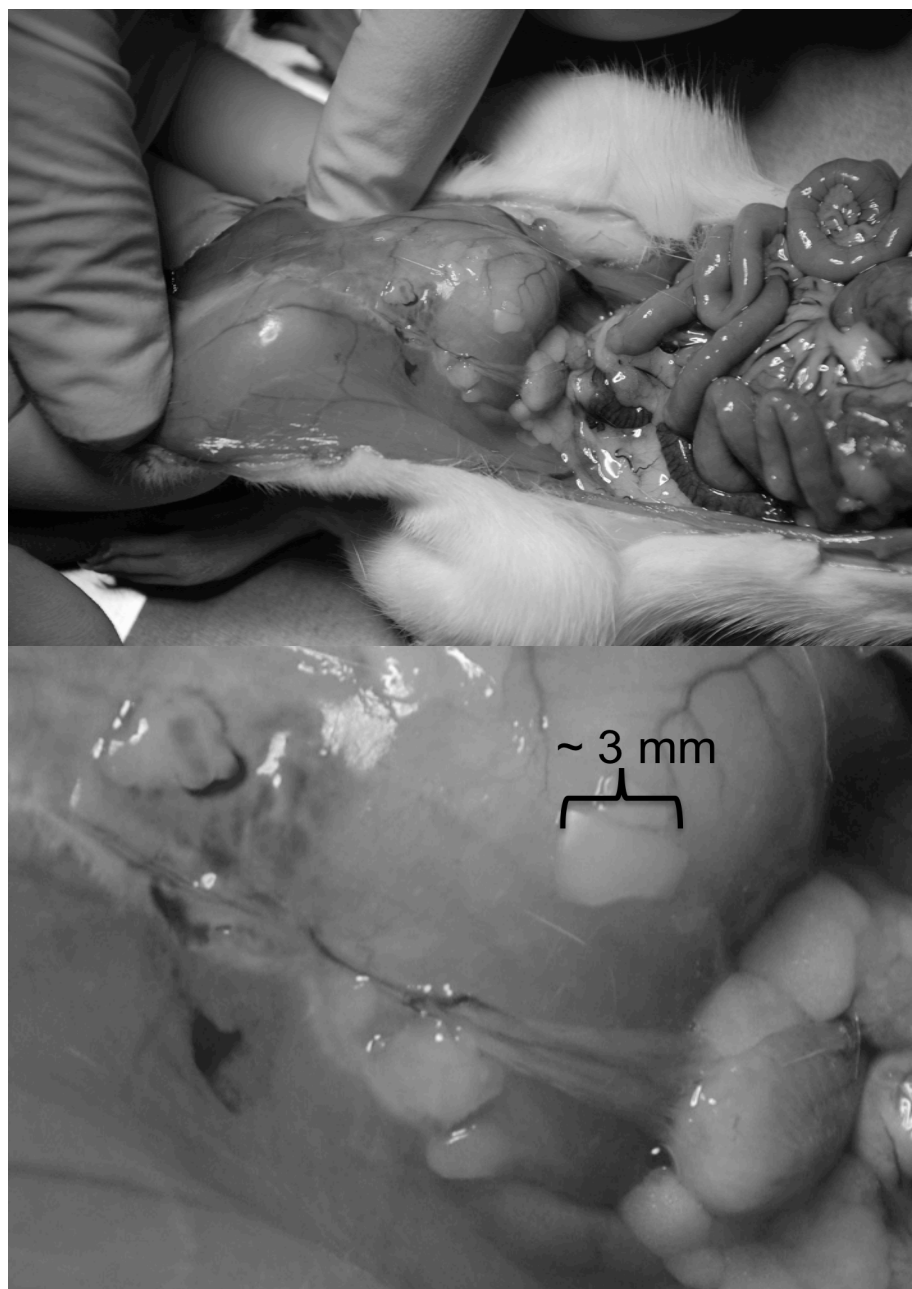
Figure 7.5. Gross observations at 28 days postoperative of e-beam irradiated films.
LVG/GMHA(11) films are broken into pieces 28 days postoperative in the
rat cecal abrasion model, after exposure to 15 kGy e-beam irradiation.

An important observation made during this study was the significant impact that e-beam sterilization had on the mechanical properties of the films. Irradiated films were softer and displayed less plastic deformation before failure, qualitatively. Thus, the improved toughness provided by templating was obscured by the irradiation. The results of the dissolution study also demonstrated that e-beam sterilization contributes to increased dissolution rate of the films, although more investigation is needed.

There were several key conclusions from this dissolution study:

1. Exposure to e-beam irradiation increased the dissolution rate of the films, however, this increase still did not satisfy the requirements of an effective anti-adhesion membrane because small remnants were visible at 4 week postoperative.

2. Higher levels of irradiation may have caused additional or unknown effects on our films. Subsequent *in vivo* studies involved films radiated at 15kGy only.

3. Templated LVG/GMHA(11)-blended films with 33% GMHA(11) concentration sterilized at 15 kGy successfully prevented adhesions.

4. Film pieces were recovered remotely from the injury site, indicating that films had migrated. Therefore, we would need to address the adhesivity.

5. The rat model may be too adhesiogenic and modifications may need to be considered for reduced complications.

7.4.2 *In vivo* chelator study. Tissue adherence is a key differentiator among adhesion barriers. Many pre-formed membranes are ineffective because residence time in the area of injury does not persist throughout the 3 – 5 day critical healing period (Al-Jabri & Tulandi 2011). Predicate materials have failed because they are too stiff, resulting in migration, delayed resorption, and impaired site-specific function. The alginate in our films is ionically crosslinked with calcium. Calcium ions are replaced by sodium ions *in*

vivo (Hunt *et al* 2010) resulting in a slow transition from a nonadhesive- to a mucoadhesive-membrane. As presented in Chapter 4, benchtop dissolution studies were conducted in citrate, a nontoxic calcium chelator. Citrate is a small molecule that binds strongly to calcium ions. The binding of citrate to calcium ions removes the calcium from the gelled alginate. By removing calcium ions citrate reduces the crosslinking density of the film, rendering it less mechanically stable and better able to conform to the contours of the cecum. This transition should promote mucoadhesion. By stripping away calcium ions the chelator also promotes dissolution of the film, as this was the method for dissolution studies presented in Chapter 4. To take advantage of the robust mechanical properties that gelled alginate provides, it was optimal to direct this gel-to-mucinous transition to occur on the surface of the tissues, after implantation and positioning.

A chelator study of 40 animals was conducted, with necropsy at 2 weeks. (**Table 7.4**) All films were exposed to 15 kGy irradiation with e-beam. There were 4 groups with 10 animals in each group. Chelator study groups included a negative control group that was untreated, a positive control group that received Seprafilm®, an experimental group with templated LVG/GMHA(11)-blended films with 33% GMHA(11) concentration, and an experimental group with nontemplated LVG/HA-blended films. Templating was not needed for this application. Lack of templating obviates photopolymerization the HA. As presented in Chapter 4, UV exposure does not contribute to film stability in nontemplated films with HA concentrations below percolation threshold. Therefore, a nontemplated, non-methacrylated alginate/HA film could offer a simpler successful anti-adhesion membrane. Both groups with our films were treated with chelator after film was positioned in the peritoneal cavity. Animals were closed after administration of chelator.

	Grade 0	Grade 1	Grade 2	Grade 3	p-value	film found?
Control	2	0	0	8	--	N/A
Seprafilm®	5	0	1	4	0.22	0
Templated	5	0	2	2	0.15	1
Nontemplated	6	0	0	4	0.09	1

Table 7.4. *In vivo* chelator study at 14 day necropsy. Model was successful in causing adhesions in 80% of untreated animals. However, this model may have been too adhesiogenic because Seprafilm® did not statistically prevent unwanted adhesions when compared to the control. No group statistically prevented unwanted adhesions in this study, however all experimental groups decreased the incidence of adhesions compared to the control. Most importantly, the chelator was successful at increasing the dissolution rate of our films. Only one animal in each film group had visible film. These remnants were very small and wispy. These results represent gross observation results at necropsy. Statistics conducted using pairwise Mann Whitney U tests**.**

The results of the chelator study suggest that adding a chelator to the films was successful at increasing the dissolution rate and mucoadhesivity. There were only two animals with film remnants visible at 2 weeks postoperative. These remnants were small wispy pieces of film.

There were several key conclusions from this chelator study:

1. The untreated control group had fewer animals with grade 3 adhesions than desired (only 8/10 animals). For this reason no treatments were statistically significantly superior compared to the control group.

2. Chelator treatment dramatically improved film bioresorption ($p \ll 0.05$, compared to previous studies). This result validates the chelator strategy.

3. Seprafilm® did not prevent adhesions ($p = 0.22$ compared with the control group)

4. Non-templated films treated with citrate were the most effective treatment for preventing adhesions (6/10 animals were free of adhesions, $p = 0.09$ compared with the control group).

5. Templated films were no more effective for preventing adhesions than non-templated films ($p = 0.30$).

7.5 DISCUSSION

To develop a successful candidate for adhesion prevention, live animal testing is inevitable. The peritoneal healing environment is dynamic, diverse, and cannot be replicated *in vitro*. Furthermore, there is no better way to gain a profound perspective of the requirements instilled upon anti-adhesive devices, than to engage in the process in live animals. Both the complex handling requirements and the even more complex adhesion prevention requirements mandate an animal model for gauging how a device would behave in humans.

That said the rat cecal/sidewall abrasion model, although popular for its adhesiogenicity, is not ideal. The cecum is delicate and easily perforated, greatly challenging consistency from animal to animal. Cecum size is also different from animal to animal, not just by its own regard but also with respect to the larger peritoneal cavity. Thus some animals with small peritoneal cavities have relatively large cecums, while some large cavities have small cecums, at the time of surgery. Because our model dictates abrasion of the entire cecum, the variable cecum size is relevant. In future studies, it might be more successful to abrade an equivalent area on each cecum.

Despite these challenges, ultimately we were able to successfully meet all of the requirements of an adhesion barrier. Our films are mechanically robust, can be rolled up for laparoscopic insertion, can be applied wet, and are repositionable. Upon administration of the chelator the films become very mucoadhesive and are dissolved by 14 days postoperative. We have shown efficacy of our films in the rat cecal abrasion model, however, the efficacy results vary. This inconsistency is more likely a result of the model than the capabilities of the film. In future studies, the film and chelator should be applied to a different model.

7.6 MATERIALS AND METHODS

7.6.1. Materials. Medical grade sodium alginate was purchased from FMC Novamatrix (Sandvika, Norway): Pronova UP LVG: 120 kDa, M/G ratio 0.67; Pronova UP LVM: 120 kDa, M/G ratio 1.5. High molecular weight sodium hyaluronate from *Streptococcus equi* of molecular weight 1.6×10^6 Da was obtained from Sigma-Aldrich (St. Louis, MO). Bacteria-derived high molecular weight sodium hyaluronate was also received from Genzyme, as a generous gift. (1.6×10^6 MDa, Genzyme, Cambridge, MA) Photoinitiator Irgacure 2959 (I2959) was obtained from Ciba Specialty Chemicals (Basel, Switzerland). All other chemicals purchased from Fisher Scientific. All animals were female Sprague-Dawley *Rattus norvegicus* from the Charles River colony, 4-6 weeks old.

7.6.2 Synthesis of a urea-templated calcium alginate/GMHA film for animal testing. A 1% w/v solution of 67% alginate / 33% GMHA(11) (w/v) with 2% w/v urea in ddI water was stirred at room temperature overnight with 0.05% photoinitator. Solution was cast in a 72 mm by 72 mm form. Forms were placed in a temperature and humidity controlled environmental chamber from Cincinnati Sub-Zero (Cincinnati, Oh). Temperature was held at 25 °C and humidity was held at 70% Rh during the casting period of 48 hours. Forms and solutions were kept from light at all times. At 48 hours, nucleation of urea crystallization was conducting by seed crystal. One nucleation point was seeded in the center of the film. Cast films were subjected to UV light from the chamber after completion of crystal propagation. After photocrosslinking, 50 mL of 100 mM calcium chloride solution was pipetted on top of the cast film in the form, in the tissue culture hood. Films were left to crosslink for 30 minutes. Films were removed from molds and transferred to petri dishes with large volumes of ddI water, and rinsed exhaustively for at least 24 hours. Ribbing was cut with sterile scissors and discarded as selvage, and films were cut into 4 equal pieces. Each film piece was about 1.5 in^2 and

was individually used per animal. Films were sterilized either in petri dishes by addition of gentamicin, or in plastic Ziploc bags by e-beam sterilization conducted at the TAMU Electron Beam Facility (College Station, TX) with 15 kGy radiation in one pass. Films were not removed from packaging until time of surgery.

7.6.3. *In vitro* cytocompatibility. Films used for cell studies were sterilized by adding 100μL of gentamicin in sterile ddI water for 24 hours in the hood followed by excessive washing with sterile ddI water. Cytotoxicity studies were conducted with guidance of ISO 10993-5 for *in vitro* cytotoxicity. Briefly, 1.5 in^2 of film was placed in 3 mL (final film concentration of about 0.75% (w/v)) of cell media (DMEM plus 10% FBS and 1:100 PSA) on a rocker at 37°C for 24 hours. Human dermal fibroblasts (Cambrex) were seeded onto 96-well tissue culture polystyrene at 15,000 cells/mL for 12 hours. Cells were then incubated with extractions from leaching media for 24 hours. Cell viability was assessed using celltiter glo luminescent cell viability assay (Promega, Madison WI) or fixed with 4% paraformaldehyde in PBS and stained with 2μM calcein AM and 4μM ethidium homodimer-1 (Life Technologies, Grand Island NY). Studies were conducted in triplicate.

7.6.4. Fibroblast attachment. To assess cell attachment to our films, we conducted a direct-contact test in a custom-built polycarbonate well with rubber gasket (**Figure 7.6**). After assembly, PLL is added to wells without a film. After two hours wells are washed to remove excess PLL. HDF cells are then seeded 20,000/well with 300 μL serum-free media (DMEM and 1:100 PSA). Wells are incubated for 3 hours at 37°C. Cell viability was assessed after fixing with 4% paraformaldehyde in PBS, and staining with 1:400 DAPI in ddI water and 1:300 phalloidin 488 in blocking buffer. Cells were imaged by epifluorescence at 20x magnification. Studies were conducted in triplicate.
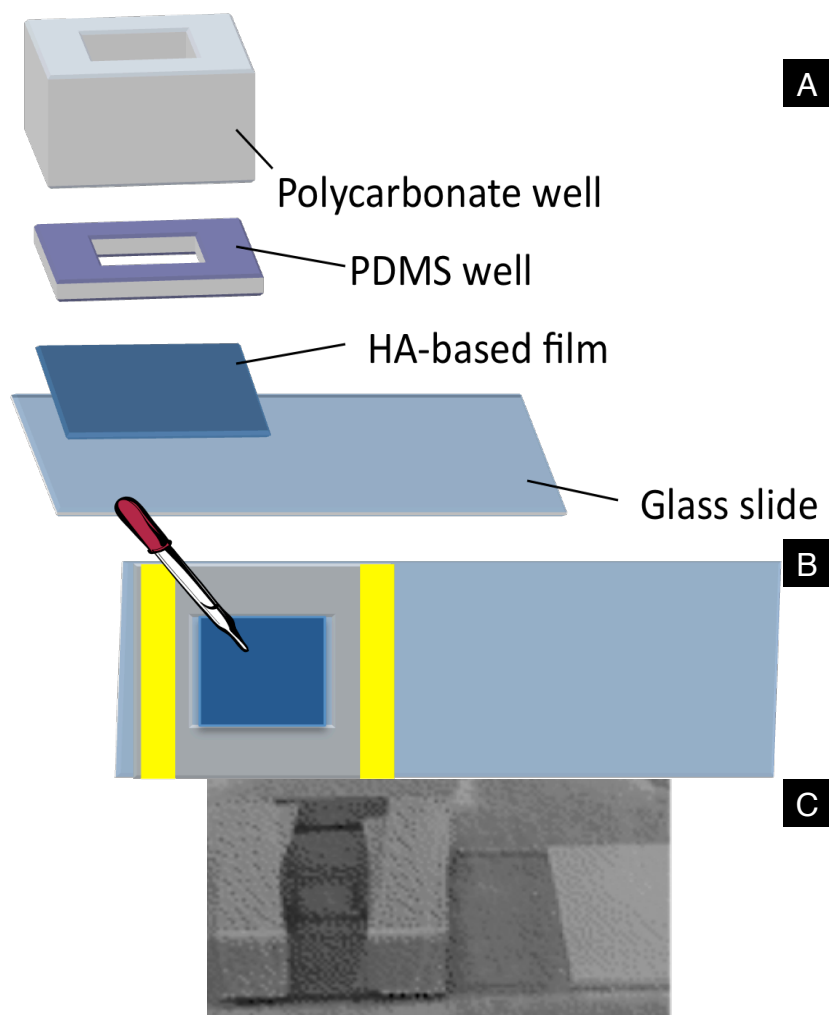
**Figure 7.6. Fibroblast attachment study custom-built well.** A) After fabrication and rinsing, films were placed between a glass slide and a polycarbonate well with a PDMS gasket to prevent leaking. Control wells were treated with PLL. B) Cells and media were exposed to film or control surface through the top of the well. C) Wells and gasket with or without film were held together with electrical tape.

7.6.5. Rat cecal/sidewall abrasion model. All animal testing was conducted at The University of Texas at Austin Animal Research Center (UT-ARC) under the approval of the Institutional Animal Care and Use Committee (IACUC) for protocol AUP-2010-00164. Animals were anesthetized with isoflurane (5% induction, 2% maintenance). A midline laparotomy incision of 4 cm was performed, and the cecum was identified. The entire surface of the cecum was abraded with sterile surgical gauze until area was deserosalized as evidenced by punctuate bleeding without hemostasis. Then, a defect of partial thickness in the abdominal wall was created by #15 scalpel (Bard, Murray Hill, NJ). Approximately 2 cm^2 of parietal peritoneum was removed. Sham surgery animals had no defect or abrasion. Some experimental animals received 1.5 in^2 sodium hyaluronate/carboxymethyl cellulose (Seprafilm® Genzyme Corporation) films, placed between the deserosalized surfaces. Some animals received 4 cm^2 LVG/GMHA(11) films in the same manner. No additional interventions were performed to negative control animals after the approximation of abraded cecum to the abraded abdominal wall. Irrigation with saline or citrate was conducted before closing the animal, depending on the experiment. The abdominal layers and skin incisions were closed separately with interrupted 3.0 vicryl on an SH needle (Ethicon, Somerville, NJ), a nylon monofilament suture in a subcuticular fashion and surgical clips, when necessary. Clips were removed for studies beyond 14 days. Animals were anesthetized, as described previously, for clip removal on day 15. If dehiscence occurred within the first 24 hours of any procedure, animals were anesthetized as previously described, and closed with interrupted 4.0 Ethilon, a nylon monofilament suture, and surgical clips. Animals were only placed under anesthesia for a maximum of two times, except for those animals whose sutures and clips were removed at day 15. For these extended study animals, anesthesia was capped at a total of three times. Pilot and pivotal studies were terminated

191

at 14 days postoperative to evaluate the presence and extent of adhesions. Adhesions were evaluated on a 5-point subjective scale well-described in the literature. Adhesions were evaluated by 3 surgeons, not included in the surgical procedures. Tissues were harvested for histological analysis. The ARC director provided authorization to video-record all necropsy procedures. Adherence was evaluated post-mortem by gross observation, manual manipulation, and irrigation with saline. Furthermore, peritoneal cavity was irrigated with saline and resulting fluid was visually analyzed for film remnant content. Tissue adherence and degradation studies were evaluated for gross observation of adhesion formation as described for the efficacy study. Rats were monitored twice daily to ensure normothermia, satisfactory analgesia, and adequate respiratory function.

7.6.6 Statistical analysis. Kruskal-Wallis pairwise comparison was conducted on R software. All other data are presented as mean ± standard deviation.

Chapter 8: Conclusions

8.1 GLYCIDYL METHACRYLATION OF HYALURONIC ACID

Functionalization of HA via glycidyl methacrylate is not well defined. Conflicting publications suggest a variety of end products. Our spectra suggest that a shift in TEA peaks occur as a result of protonation of the TEA by the carboxylic acid groups on HA (HA-CO2$^-$.HN$^+$Et$_3$). Our conclusion is supported with the strong similarities between the null-methacrylated and GMHA spectra because TEA was the only chemical added to the null-methacrylated HA. However, there is a shift in the peak at 1.2 ppm towards high field that suggests there are impurities. We were not able to confirm what these impurities were. We hypothesize that even at very low degree of methacrylation, glycidyl methacrylation of HA changes the conformation of the HA molecules, which causes a significant and obvious decrease in viscosity. This viscosity later plays a role in the behavior of HA in alginate-rich environments. Future recommendations include using a different method for HA modification such as conjugation with methacrylic anhydride, which results in finer tuning of degree of methacrylation as well as a more stable and straightforward reaction mechanism.

8.2 PERCOLATION THRESHOLD OF HA IN ALGINATE-RICH ENVIRONMENTS

The theory of percolation is applicable to films of alginate/HA blends. Awareness of the percolation threshold at various HA modifications is a powerful tool in understanding the film composition, the processing requirements for film fabrication, and the film's ability to dissolve or to degrade. Based on our findings, HA of varying modification can be retained in alginate films without further crosslinking, as long as the percolation threshold is known. These threshold values can support predictions of other

functionalizations of HA. We suggest that the relationship between the percolation threshold concentration of GMHA and methacrylation is a power law relationship. This type of relationship is plausible because GMHA is too weak to sustain gelled alginate in dilute concentrations. Thus, invalidating a linear relationship. Using a power law relationship one could predict a percolation value for a given amount of alginate and known modification of HA. Furthermore, knowing that release of calcium ions causes dissolution of the alginate-rich films, one could select a modification of HA that best suits a minimum amount of alginate for fastest degradation of a film. Simultaneously, the percolation threshold predicts when a fully interpenetrating network of alginate and HA is established. These concentrations would provide the slowest degrading films requiring both dissolution of alginate and enzymatic degradation of the crosslinked HA network. Although our observations of alginate/GMHA-blended film behavior can be described by the theory of percolation, future recommendations include image-supported documentation of the phase separation between these two polymers. Fluorescent labeling with epifluorescence or confocal imaging of films both before and after calcium gelation would support our conclusion that phase separation happens during the casting process, or during alginate gelation.

8.3 MECHANICAL INTEGRITY OF ALGINATE/GMHA FILMS

Ultimately, mechanical strength is owed to the calcium gelation of the alginate component of blended films. All mechanical properties related to load, such as tensile strength and Young's modulus, follow the trend in alginate composition. Loss of strength is a result of decreased concentration of calcium gelled alginate. However, the ability for the films to stretch farther, with decreased amounts of alginate, suggests that the presence of GMHA allows greater chain movement. GMHA is mucinous when not

photocrosslinked. Strongly bound water to GMHA is responsible for this texture. While we hypothesize that the alginate and GMHA components are phase-separated, the water retention caused by the presence of GMHA may significantly impact alginate chain motility. This motility provides alginate/GMHA-blended films the ability to withstand higher strain prior to tensile failure.

8.4 MECHANICAL INFLUENCE OF CRYSTAL TEMPLATING ON ALGINATE/GMHA FILMS

Crystal templating creates a porous network along side a fibrous network of compressed polymer. Compression of the polymers in an alginate/GMHA-blended film may reduce the concentration of GMHA clusters with a direct path into the free water, thereby increasing polymer retention. This compression also causes increased density of polymer, which decreases the dissolution rate of alginate/GMHA-blended films. The network of pores and fibers contribute to the mechanical properties of templated films. Templated films have greater elongation than nontemplated films. We hypothesize that increased elongation is a result of the porous structure that acts as sacrificial defects, and of the fibrous network that requires greater elongation to decompress and stretch. Templating increases film toughness as a result of increased elongation. However, fiber direction was ultimately difficult to control, and tensile test results varied. High frequency dynamic mechanical analysis indicated that templating decreases gel stability, with fiber alignment playing a role in that stability. These results confirm that there is fiber directionality, which is not clearly demonstrated in large deformation testing. Thus, templated films are tougher, yet more liquid-like. These mechanical property changes allow for improved film handling and increased flexibility, as confirmed by surgeon subjective evaluation.

195

8.5 ALGINATE/HA AS AN ADHESION BARRIER

Despite challenges, we successfully met all of the requirements of an adhesion barrier. Our films are mechanically robust, can be rolled up for laparoscopic insertion, can be applied wet, and are repositionable. Upon administration of the chelator the films become very mucoadhesive and are dissolved by 14 days postoperative. We have shown efficacy of our films in the rat cecal abrasion model, however, the efficacy results vary. This inconsistency is more likely a result of the model than the capabilities of the film. In future studies, the film and chelator should be applied to a different model.

Hyaluronic acid is sensitive to slight changes in hydration, but does not degrade easily. Slight modifications with hydrophobic moieties create conformational changes that dramatically effect the viscosity and behavior of resulting films; however, HA can withstand very high pH environments for extended periods of time without degradation. Therefore HA is effected by access to hydrated environments. Cellular recruitment of HA to areas of injury is to provide hydration. This much-needed hydration supports removal of unwanted debris. Perhaps it is more critical than we currently acknowledge to have HA present at the time of injury. Thus, HA as a component of an anti-adhesion device may be critical to the success of the device.

The ability for alginate to gel in the presence of calcium, and then degel in a sodium-rich environment is unique, and offers a nontoxic and dramatic mechanical property shift. This property, alone, seems tailored for the application of an anti-adhesion membrane. The need to handle a robust membrane for insertion and positioning, and then, on demand, have the device conform to delicate and intricate geometries works synergistically with the mechanics of calcium-alginate films. Alginate provides the

ability to deliver HA to injured tissues in a nontoxic and gentle form. Furthermore, no additional crosslinking of HA is required, making for a simpler device.

8.6 BILAYER CONSTRUCT FOR REGENERATIVE STRATEGIES

Future recommendations include exploration of a bilayer membrane with bifunctional flexibility that is both anti-scarring and pro-regenerative. The aim of this construct will be to promote regeneration and to prevent fibrotic scarring. Strategies for bilayer hydrogels include fibrotic protection in parallel with cellular activation. The synchronization of these parameters has shown to be effective in artificial skin hydrogels (Franco *et al* 2011). The commercially available artificial skin, Integra^{TM}, utilizes silicone for the top protecting layer, and a collagen-glycosaminoglycan bottom layer for cell stimulation and regrowth. Also, commercially available hernia repair meshes have a bilayer strategy including HA-based coatings on synthetic mesh networks (Ventralight^{TM}, Davol, Inc). We recommend the anti-adhesive film presented in this work, comprised of HA and alginate, to serve as the anti-adhesion layer in a bilayer construct. The regenerative layer may be a collagen/alginate substrate that is bound to the anti-adhesive layer via calcium associations. These associations between the alginate in both layers provide mechanical stability. Preliminary studies suggest layer-by-casting is an effective method for bilayer fabrication (**Appendix C**). This bilayer hydrogel can be optimized for the dynamic wound-healing environment to serve as a multi-functioning construct.

APPENDIX A: SURGEON RESPONSE TO GMHA FILMS

13859 Progress Blvd. Suite 100
Alachua, Florida 32615
(386) 462-6841 tel   (386) 462-6803 fax

AxoGen.
Nerve Regeneration

Memo

To: Christine Schmidt (UT-Austin)
From: Curt Deister, Bill Gregory
CC:
Date: May 29, 2009
RE: UT GMHA Film Handling Evaluation Summary

Evaluations:

Three of the six hyaluronic acid films provided by the Schmidt Lab at UT-Austin were evaluated for handling and suturing characteristics in the AxoGen Product Development Lab on May 18th and 22nd. The handling evaluators were E. DeVinney (Clinical Research Director) and C. Deister (PD Engineer). Additionally, C. Simon (PD Engineer), Jon Gatson (PD lab technician) and B. Gregory (Dir PD) observed portions of the handling.

Films were observed and gently handled before hydration. No suturing was attempted. While films appeared somewhat brittle, the evaluators were able to move the film to facilitate hydration. Films were hydrated in either the petri dish that the film was shipped in (1 film) or a silicone dissection pad (2 films) for easier access during suturing and handling. Hydration was performed with a volume of PBS sufficient to completely cover the films. Hydration was determined by a distinct increase in pliability and was very rapid, less than 1 minute. However, the films had a distinct tendency to roll into a tube, 1-2mm in diameter, during hydration (described further below) and, depending on orientation, cracks would propagate. One film split into two separate rolls during hydration as a crack at the edge propagated through the film. This crack was present when the dish was opened and was not a result of handling.

Suturing of the films with 8-0 suture was attempted without success. In most cases the needle itself ripped through the plane of the film generating a gash instead of a hole. This effect required extremely little force (i.e. far below a level that would be common during clinical use). If the film was carefully positioned, the needle could be passed straight through (adjusting for the curvature and avoiding lateral forces) avoiding the "gashing." However, the suture line easily ripped through the film in an analogous manner and pull-out strength was too low to estimate. i.e. it could not be felt by evaluator. The film was capable of supporting its own hydrated weight on a single suture line without tearing.

Serrated forceps quickly and easily caused the film to tear during handling. Non-serrated (i.e. flat) forceps slid along the film and did not provide sufficient grip before also causing a tear or rip, effectively a pressure cut of the film. Using fingers was somewhat more successful but could still induce tears.

198

If the film rolled during hydration, it was extremely difficult to unroll. Most of the film was torn during the process of unrolling and the film continued to re-roll.

The films had excellent gliding properties (were very non-adhesive).

Summary and Recommendations:
- The films must be significantly more durable to be used clinically.
  - The film must be able to withstand handling with serrated forceps without damage.
- A significant pull-out strength, on the order of preferably ~50-100 g minimum, is needed for suturing.
- The "memory" of the device after hydration must be significantly reduced. Unless it can be controlled as an application method, the amount of rolling observed must be reduced. As the films would re-roll after straightening, this likely must be addressed before hydration.

Prepared By: _Curt Lester_   Date: 5/29/09

Small angle x-ray scattering (SAXS) utilizes changes in x-ray scattering intensity to distinguish feature sizes in materials. The more homogenous a material, the less scattering. Changes in density can cause significant changes in scattering intensity. In collaboration with the Texas Materials Institute, Dr. Steve Swinnea conducted SAXS tests on templated and nontemplated alginate-only hydrogel films. The results of these tests are presented in **Figure B.1**. Alginate (LVG) films with 4% (w/v) urea templating show increased density of features compared to nontemplated LVG films. These features are in the range of 5-125 nm. The templated and nontemplated films appear similar for features less than 5 nm. The radius of gyration of alginate in ionic solutions is about 15 nm. (Andersen *et al* 2012) The denser the polymer crosslinks are, the higher the scattering intensity. The significant deviation in intensity at these feature sizes suggests the alginate chains are more densely packed in the fibers than in the nontemplated bulk film.
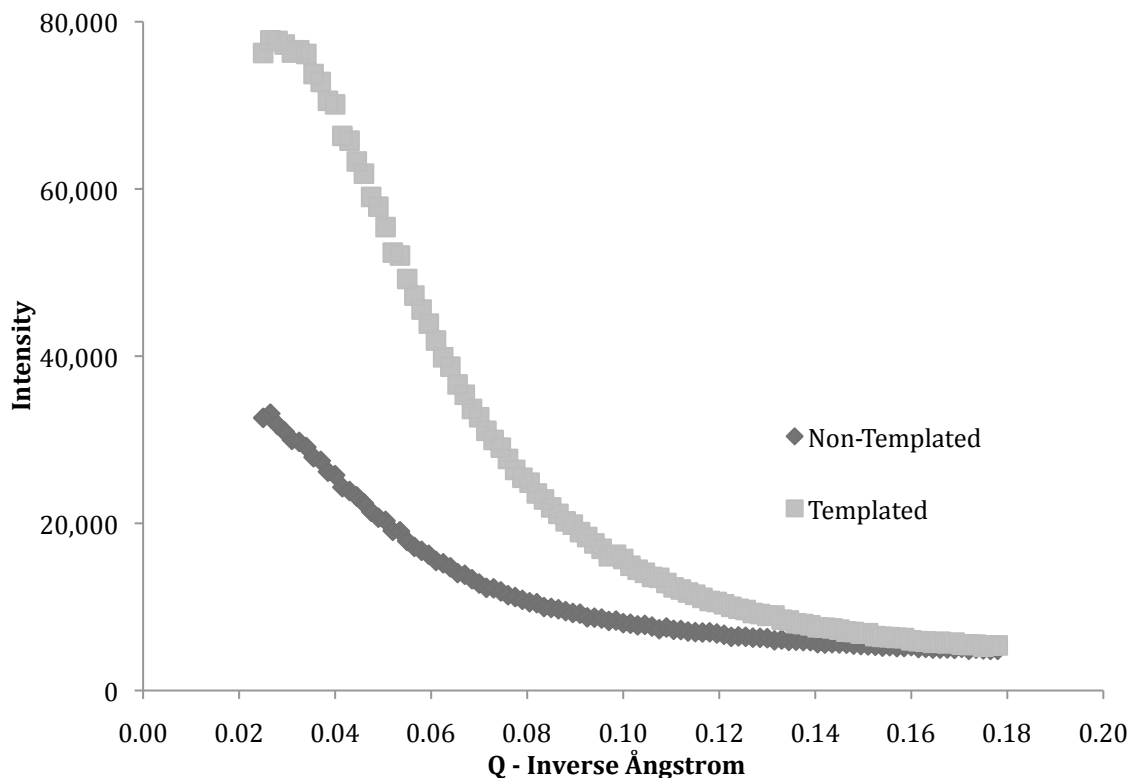
Figure B.1. Small angle x-ray scattering (SAXS) of templated and nontemplated alginate films. Alginate (LVG) films with 4% (w/v) urea templating show increased density of features compared to nontemplated LVG films. These features are in the range of 5-125 nm. The films appear similar for features less than 5 nm. The radius of gyration of alginate in ionic solutions is about 15 nm. The denser the polymer crosslinks are, the higher the scattering intensity. The significant deviation in intensity at these feature sizes suggests the alginate chains are more densely packed in the fibers than in the nontemplated bulk film.

APPENDIX C: BILAYER VERIFICATION

Preliminary results indicate that layer-by-casting is an effective method for bilayer fabrication. For initial investigation, a collagen/alginate substrate was selected for a pro-regenerative layer. A solution of collagen and alginate was cast onto a dehydrated urea-templated membrane of GMHA and alginate. The bilayer was then placed in a 37°C oven for one hour, to allow gelation of collagen fibers. The membrane was then soaked in an aqueous solution of calcium chloride, which ionically crosslinked the two layers. Calcium stabilizes the bilayer membrane for mechanical robustness.

Verification of distinct layers was obtained through SEM (**Figure C.1**). Layers are distinctly visible in microscopy evaluation. To validate these findings, we examined the behavior of human dermal fibroblasts *in vitro* for cellular adherence to the collagenous surface of the membrane, and for anti-adherence to the anti-scarring surface of the membrane. Collagen provides both topographical and chemical cues for cellular adherence. Due to the hydrophilic nature of GMHA and alginate, the anti-scarring surface is resistant to both protein adsorption and cellular adhesion. The experiments were conducted in the custom-built polycarbonate wells and rubber gaskets. The goal of this study was to show that the bilayer construct provides a supportive substrate for cellular adherence only on the pro-regenerative side of the membrane (**Figure C.2**). The results of this study will provide impetus to conduct subsequent studies for optimization of this bilayer construct.
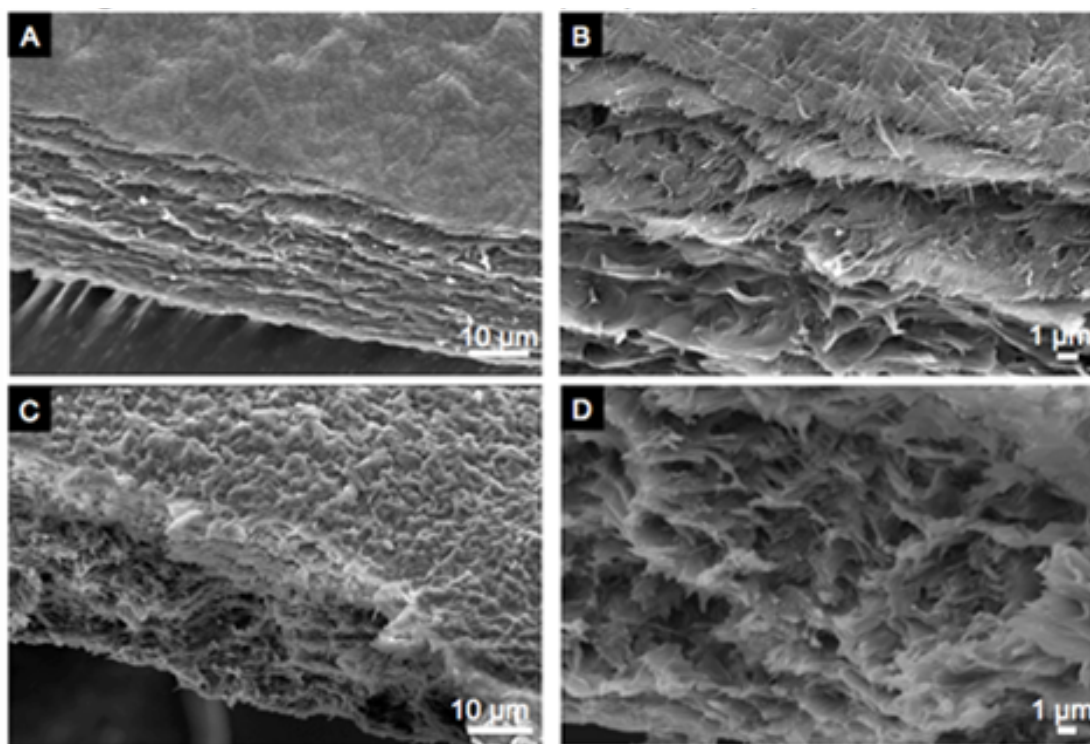
Figure C.1 SEM images of bilayer membrane. (A,B) Top of bilayer membrane with collagenous fibers visible in top layer only. (C,D) Bottom of bilayer membrane with alginate / HA topography visible, void of collagenous fibers found in top layer. All four images are taken of the same membrane.
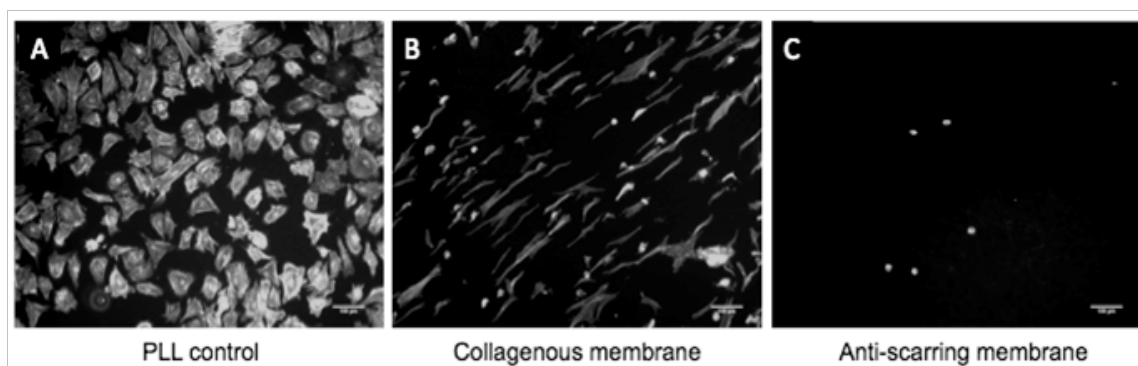
Figure C.2 Fibroblast adherence to collagenous layer. Human dermal fibroblast cells were exposed to (A) a PLL control surface, (B) a fibrous collagenous membrane, and (C) an alginate/GMHA membrane, and stained with DAPI and phalloidin. Fibroblasts spread along the collagen fibers and did not adhere to the anti-scarring surface. All scale bars are 100 μm.

References

1. Abdou, M. Samy, and Russell W. Hardy, Jr. "Epidural fibrosis and the Failed Back Surgery Syndrome: History and physical findings." *Neurological Research* 21.1 (1999): 55-58. Digital file.

2. Adas, Gokhan, et al. "The effect of hyaluronic acide carboxymethyl cellulosis on the healing of colonic anastomosis in rats." *Bratisl Lek Listy* 110.4 (2009): 210-14. Digital file.

3. *Advanced solutions for tendon protection: TenoGlide*. TenoGlide. gif file.

4. Akbar, Umar, et al. "Delivery of temozolomide to the tumor bed via biodegradable gel matrices in a novel model of intracranial glioma with resection." *J Neurooncol* 94 (2009): 203-12. Digital file.

5. Al Jabri, Sheikha, and Togas Tulandi. "Management and Prevention of Pelvic Adhesions." *Seminars in reproductive medicine* 29.2 (2011): 130-37. Print.

6. Allbritton NL, Verret CR, Wolley RC, Eisen HN. "Calcium ion concentrations and DNA fragmentation in target cell destruction by murine cloned cytotoxic T lymphocytes" *J Exp Med* 167 (1988): 514-527. Digital file.

7. Al-Shamkhani, Aymen, and Ruth Duncan. "Radioiodination of Alginate via Covalently-Bound Tyrosinamide Allows Monitoring of Its Fate In Vivo." *Journal of Bioactive and Compatible Polymers* 10 (1995): 4-13. Digital file.

8. Altenhofen da Silva, Mariana, Andrea Cristiane Krause Bierhalz, and Theo Guenter Kieckbusch. "Alginate and pectin composite films crosslinked with Ca2+ ions: Effect of the plasticizer concentration." *Carbohydrate Polymers* 77 (2009): 736-42. Digital file.

9. Alves, Natalia M., Catherine Picart, and Joao F. Mano. "Self Assembling and Crosslinking of Polyelectrolyte Multilayer Films of Chitosan and Alginate Studied by QCM and IR Spectroscopy." *Macromolecular Bioscience* 9 (2009): 776-85. Digital file.

10. Amer, Mohamed I, et al. "Human Amnion as a Temporary Biologic Barrier after Hysteroscopic Lysis of Severe Intrauterine Adhesions: Pilot Study." *Journal of Minimally Invasive Gynecology* 17.5 (2010): 605-11. Digital file.

11. Andersen T, Strand BL, Formo K, Alsberg E, Christensen BE. "Alginates as biomaterials in tissue engineering" *Carbohydrate Chemistry* 37 (2012): 227-258. Digital file.

12. Andradi LN and Hellmann GP. "The percolation limits for two-phase blends of PMMA and copolymers of styrene and MMA" *Polymer* 34.5 (1993): 925-932. Digital file.

13. Anseth KS, Bowman CN, Brandon-Peppas L. "Mechanical properties of hydrogels and their experimental determination" *Biomaterials* 17 (1996): 1647-1657. Review. Digital file.

14. Asi B, Wong E, Prasseril J, Keralapura M, Mobed Miremadi M. "Diffusivity Determination for Alginate-Based Artificial Cells Using Fluorescent Microscopy" BMES 2012 Annual Meeting, Atlanta. (Oct 2012). Poster.

15. Assietti, Roberto, Annarita Mora, and Marco Brayda-Bruno. "Use of Carboxymethylcellulose/Polyethylene Oxide Gel in Microdiscectomy With Interlaminectomy: A Case Series Comparison With Long-term Follow-up." *Spine* 33.16 (2008): 1762-65. Digital file.

16. ASTM Standard D638, 1941 (2010), "Standard Test Method for Tensile Properties of Plastics," ASTM International, West Conshohocken, PA, 2010, DOI: 10.1520/D0638-10, www.astm.org.

17. ASTM Standard D882, 1946 (2012), "Standard Test Method for Tensile Properties of Thin Plastic Sheetng," ASTM International, West Conshohocken, PA, 2012, DOI: 0.1520/D0882-12, www.astm.org.

18. Aufderhorst-Roberts A, Frith WJ, Donald AM. "Micro-scale kinetics and heterogeneity of a pH triggered hydrogel" *Soft Matter* 21 (2012): 5940-5946. Digital file.

19. Baier Jennie Melinda. (2003) Hyaluronic Acid Hydrogel Biomaterials for Soft Tissue Engineering Applications (Doctoral Dissertation). Retrieved from ProQuest Dissertations and Theses. (Accession Order No. [3116256]).

20. Bajpai, S. K., and Shubhra Sharma. "Investigation of swelling/degradation behaviour of alginate beads crosslinked with Ca2þ and Ba2þ ions." *Reactive and Functional Polymers* 59 (2004): 129-40. Digital file.

21. Banerjee A, arha M, Choudhary S, Ashton RS, Bhatia SR, Schaffer DV, Kane RS. "The influence of hydrogel modulus on the proliferation and differentiation of encapsulated neural stem cells" *Biomaterials* 30 (2009): 4695-4699. Digital file.

22. Barbetta, Andrea, et al. "Polysaccharide based scaffolds obtained by freezing the external phase of gas-in-liquid foams." *Soft Matter* 6 (2010): 5213-24. Digital file.

23. Barbucci, Rolando, Marco Consumi, and Agnese Magnani. "Dependence of Water Uptake and Morphology of Hyaluronan- and Alginate-Based Hydrogels on pH and Degree of Crosslinking." *Macromolecular Chemistry and Physics* 203 (2002): 1292-300. Digital file.

24. Barbucci, Rolando, et al. "Inter-penetrating hydrogels (IPHs) as a new class of injectable polysaccharide hydrogels with thixotropic nature and interesting mechanical and biological properties." *Soft matter* 6 (2010): 3524-32. Digital file.

25. Barbucci, R., et al. "Synthesis, chemical and rheological characterization of new hyaluronic acid-based hydrogels." *J Biomater. Sci. Polymer Edn* 11.4 (2000): 383-99. Digital file.

26. Becker, Timothy A., Daryl R. Kipke, and Tedd Brandon. "Calcium alginate gel: A biocompatible and mechanically stable polymer for endovascular embolization." *Journal of Bio Materials* (2000): 76-86. Digital file.

27. Benavides, Sergio, R. Villalobos-Carvajal, and J.E Reyes. "Physical, mechanical and antibacterial properties of alginate film: Effect of the crosslinking degree and oregano essential oil concentration." *Journal of Food Engineering* 110 (2012): 232-39. Digital file.

28. Bencherif, Sidi A. et al. "Influence of the degree of methacrylation on hyaluronic acid hydrogels properties." *Biomaterials* 29 (2008): 1739-49. Digital file.

29. Bienaime, Christophe, Jean-Noel Barbotin, and Jose-Edmundo Nava-Saucedo. "How to build an adapted and bioactive cell microenvironment? A chemical interaction study of the structure of Ca-alginate matrices and their repercussion on confined cells." *Wiley Periodicals, Inc.* (2003): 376-88. Digital file.

30. Boontheekul, Tanyarut, Hyun-Joon Kong, and David J. Mooney. "Controlling alginate gel degradation utilizing partial oxidation and bimodal molecular weight distribution." *Biomaterials* 26 (2005): 2455-65. Digital file.

31. Braccini I, Grasso RP, Perez S. "Conformational and configurational features of acidic polysaccharides and their interactions with calcium ions: a molecular

modeling investigation" *Carbohydrate Research* 317 (1999): 119-130. Digital file.

32. Brannvall, K, et al. "Enhanced Neuronal Differentiation in a Three-Dimensional Collagen-Hyaluronan Matrix." *Journal of Neuroscience Research* 85.10 (2007): 2138-46. Digital file.

33. Brochhausen, Christoph, et al. "Intraperitoneal adhesions — An ongoing challenge between biomedical engineering and the life sciences." *J of Biomed Mat Res* 98A.1 (2011): 143-56. Digital file.

34. Brostow, Witold, Haley E. Hagg Lobland, and Moshe Narkis. "Sliding wear, viscoelasticity, and brittleness of polymers." *J. Mater. Res.* 21.9 (2006): 2422-28. Digital file.

35. Brown, Colin B, et al. "Adept (icodextrin 4% solution) reduces adhesions after laparoscopic surgery for adhesiolysis: a double-blind, randomized, controlled study." *Fertility and Sterility* 88.5 (2007): 1413-26. Digital file.

36. Bu, Huaitian, et al. "Rheological and Structural Properties of Aqueous Alginate during Gelation via the Ugi Multicomponent Condensation Reaction." *Biomacromolecules* 5 (2004): 1470-79. Digital file.

37. Budhavaram, Naresh K., Matthew Stauffer, and Justin R. Barone. "Chemistry between crosslinks affects the properties of peptide hydrogels." *Materials Science and Engineering* C.31 (2011): 1042-49. Digital file.

38. Bulpitt, Paul, and Daniel Aeschlimann. "New strategy for chemical modification of hyaluronic acid: Preparation of functionalized derivatives and their use in the formation of novel biocompatible hydrogels." *J of Biomedical Materials Research* 47.2 (1999): 152-69. Digital file.

39. Burdick, Jason A., and Glenn D. Prestwich. "Hyaluronic Acid Hydrogels for Biomedical Applications." *Advanced Materials* 23 (2011): H41-H56. Digital file.

40. Callister WD. *Materials Science and Engineering: An Introduction* 8th ed. Wiley, New York. (2010). Print.

41. Cao N, Fu Y, He J. "Mechanical properties of gelatin films cross-linked, respectively, by ferulic acid and tannin acid" *Food Hydrocolloids* 21.4 (2007): 575-584. Digital file.

42. Cathell, Matthew D., and Caroline L. Schauer. "Structurally Colored Thin Films of Ca2+-Cross-Linked Alginate." *Biomacromolecules* 8 (2007): 33-41. Digital file.

43. Caykara T, Demirci S, Eroglu MS, Guven O. "Poly(ethylene oxide) and its blends with sodium alginate" *Polymer* 46 (2005): 10750-10757. Digital file.

44. Cekinmez, Melih, et al. "Effects of methyl prednisolone acetate, fibrin glue and combination of methyl prednisolone acetate and fibrin glue in prevention of epidural fibrosis in a rat model." *Neurological Research* 32.7 (2010): 700-05. Digital file.

45. Cemil, Berker, et al. "Use of pimecrolimus to prevent epidural fibrosis in a postlaminectomy rat model." *J Neurosurg: Spine* 11 (2009): 758-63. Digital file.

46. Censi, Roberta, et al. "In Situ Forming Hydrogels by Tandem Thermal Gelling and Michael Addition Reaction between Thermosensitive Triblock Copolymers and Thiolated Hyaluronan." *Macromolecules* 43 (2010): 5771-78. Digital file.

47. Chan, Ariel W., Ralph A. Whitney, and Ronald J. Neufeld. "Kinetic Controlled Synthesis of pH-Responsive Network Alginate." *Biomacromolecules* 9 (2008): 2536-45. Digital file.

48. Chapa, Hector O, et al. "Peritoneal Adhesion Prevention at Cesarean Section." *Journal of Reproductive Medicine* 56.3-4 (2011): 103-09. Print.

49. Chen, J. Paul, and Lin Wang. "CHARACTERIZATION OF A Ca-ALGINATE BASED ION-EXCHANGE RESIN AND ITS APPLICATIONS IN LEAD, COPPER, AND ZINC REMOVAL." *Separation Science and Technology* 36.16 (2001): 3617-37. Digital file.

50. Chen, Po-Hui, et al. "Novel chitosan–pectin composite membranes with enhanced strength, hydrophilicity and controllable disintegration." *Carbohydrate Polymers* 82 (2011): 1236-42. Digital file.

51. Chen, Xu, et al. "Tensile testing of thin films supported on compliant substrates." *Mechanics of Materials* 41 (2009): 839-48. Digital file.

52. Cheung, Jason PY, et al. "Adjuvant Therapy for the Reduction of Postoperative Intra-abdominal Adhesion Formation." *Asian Journal of Surgery* 32.3 (2009): 180-86. Digital file.

53. Cho, Wan Jin, Se Heang Oh, and Jin Ho Lee. "Alginate Film as a Novel Post-Surgical Tissue Adhesion Barrier." *Journal of Biomaterials Science* 21 (2010): 701-13. Digital file.

54. Chou, A. I., S. O. Akintoye, and S. B. Nicoll. "Photo-crosslinked alginate hydrogels support enhanced matrix accumulation by nucleus pulposus cells in vivo." *Osteoarthritis and Cartilage* 17 (2009): 1377-84. Digital file.

55. Chuang, Yi-Chen, et al. "A novel technique to apply a Seprafilm® (hyaluronate–carboxymethylcellulose) barrier following laparoscopic surgeries." *Fertility and Sterility* 90.5 (2008): 1959-63. Digital file.

56. Chueh, Bor-han, et al. "Patterning alginate hydrogels using light-directed release of caged calcium in a microfluidic device." *Biomed Microdevices* 12 (2010): 145-51. Digital file.

57. Ciofani, Gianni, et al. "Magnetic alginate microspheres: system for the position controlled delivery of nerve growth factor." *Biomed Microdevices* 11 (2009): 517-27. Digital file.

58. Cui, Helen, et al. "Reducing post-surgical adhesions utilizing a drug-enhanced device: sodium carboxymethylcellulose aqueous gel/poly(p-dioxanone) and Tranilast." *Biomedical Materials* 4 (2009): 1-10. Digital file.

59. Dahlmann J, Krause A, Moller L, Kensah G, Mowes M, Diekmann A, Martin U, Kirschning A, Gruh I, Drager G. "Fully defined in situ cross-linkable alginate and hyaluronic acid hydrogels for myocardial tissue engineering" *Biomaterials* 34 (2013): 940-951. Digital file.

60. Dainiak, Maria B, et al. "Gelatin–fibrinogen cryogel dermal matrices for wound repair: Preparation, optimisation and in vitro study." *Biomaterials* 31 (2009): 67-76. Digital file.

61. Dais, Photis, et al. "13C Nuclear Magnetic Relaxation Study of Segmental Dynamics of Hyaluronan in Aqueous Solutions." *Biomacromolecules* 6.3 (2005): 1397-404. Digital file.

62. D'Arrigo G, Meo CD, Geissler E, Coviello T, Alhaique F, Matricardi P. "Hyaluronic acid methacrylate derivatives and calcium alginate interpenetrated hydrogel network for biomedical applications: physico-chemical characterization and protein release" *Colloid Polym Sci* 290 (2012): 1575-1582. Digital file.

63. Decher G, and Schlenoff JB. <u>Multilayer thin films</u>. Wiley-VCH, Weinheim (2012). Print.

64. De Vos, P, et al. "Improved biocompatibility but limited graft survival after purification of alginate for microencapsulation of pancreatic islets." *Diabetologia* 40 (1997): 262-70. Digital file.

65. DeWilde, Rudy Leon, and Geoffrey Trew. "Postoperative abdominal adhesions and their prevention in gynaecological surgery. Expert consensus position. Part 2—steps to reduce adhesions." *Gynecol Surg* 4 (2007): 243-53. Digital file.

66. Dhanasingh, Anandhan, et al. "Tailored hyaluronic acid hydrogels through hydrophilic prepolymer cross-linkers." *Soft Matter* 6 (2010): 618-29. Digital file.

67. Diamond, Michael P, et al. "Adhesion Prevention and Reduction: Current Status and Future Recommendations of a Multinational Interdisciplinary Consensus Conference." *Surgical Innovation* 17.3 (2010): 183-88. Digital file.

68. Dietrich, W. Dalton, Coleen M. Atkins, and Helen M. Bramlett. "Protection in Animal Models of Brain and Spinal Cord Injury with Mild to Moderate Hypothermia." *Journal of Neurotrauma* 26 (2012): 301-12. Digital file.

69. DiZerega, Gere S., et al. "Use of Temporary Implantable Biomaterials to Reduce Leg Pain and Back Pain in Patients with Sciatica and Lumbar Disc Herniation." *Materials* 3 (2010): 3331-68. Digital file.

70. DiZerega, Gere S., James Coad, and Jacques Donnez. "Clinical evaluation of endometriosis and differential response to surgical therapy with and without application of Oxiplex/AP* adhesion barrier gel." *Fertility and Sterility* 87.3 (2006): 485-89. Digital file.

71. DiZerega, GS. "Contemporary Adhesion Prevention." *Fertility and Sterility* 61.2 (1994): 219-235. Digital file.

72. Dogan, Seref, et al. "The Effects of Seprafilm® and Interceed TC7 on Epidural Fibrosis in a Rat Hemilaminectomy Model." *Neurosurgery Quarterly* 19.3 (2009): 190-95. Digital file.

73. Dolce, Charles J, et al. "Pushing the envelope in biomaterial research: initial results of prosthetic coating with stem cells in a rat model." *Surg Endosc* 24 (2010): 2687-93. Digital file.

74. Draget, Kurt Ingar, Gudmund Skjafik-Bræk, and Bjørn Torger Stokke. "Similarities and differences between alginic acid gels and ionically crosslinked alginate gels." *Food Hydrocolloids* 20 (2006): 170-75. Digital file.

75. Draget, K. I., G. Skjfik Braek, and O. Smidsrod. "Alginic acid gels: the effect of alginate chemical composition and molecular weight." *Carbohydrate Polymers* 25 (1994): 31-38. Digital file.

76. Dusseault, Julie. "valuation of alginate purification methods: Effect on polyphenol, endotoxin, and protein contamination." *J Biomed Mater Res A* 76.2 (2006): 243-51. Digital file.

77. Eiselt, Petra, et al. "Porous carriers for biomedical applications based on alginate hydrogels." *Biomaterials* 21 (2000): 1921-27. Digital file.

78. Ellis, H., Moran, BJ, Thompson, JN, Parker, MC, Wilson, MS, Menzies, D., McGuire, A., Lower, AM, Hawthorn, RJS, O'Brien, F., Buchan, S., Crowe, AM. "Adhesion-related hospital readmissions after abdominal and pelvic surgery: a retrospective cohort study" LANCET 353.9163 (1999): 1476-1480. Digital file.

79. Ellis H. "Cause and prevention of postoperative intraperitoneal adhesions." *Surgery Gynecology and Obstetrics with International Abstracts of Surgery* 133.3 (1971): 497-511. Digital file.

80. Emmez, Hakan, et al. "Role of Antifibrotic Cytokine Interferon-Y in the Prevention of Postlaminectomy Peridural Fibrosis in Rats." *Neurosurgery* 62.6 (2008): 1351-58. Digital file.

81. Eng, Doris, et al. "Hyaluronan scaffolds: A balance between backbone functionalization and bioactivity." *Acta Biomaterialia* 6 (2010): 2407-14. Digital file.

82. Ersoy, Eren, et al. "Comparison of the Two Types of Bioresorbable Barriers to Prevent Intra-Abdominal Adhesions in Rats." *J Gastrointest Surg* 13 (2009): 282-86. Digital file.

83. Falabella, Christine A., and Weiliam Chen. "Cross-Linked Hyaluronic Acid Films to Reduce Intra-Abdominal Postsurgical Adhesions in an Experimental Model." *Digestive Surgery* 26 (2009): 476-81. Digital file.

84. Falabella, Christine A, et al. "Novel Macromolecular Crosslinking Hydrogel to Reduce Intra-Abdominal Adhesions." *Journal of Surgical Research* 159 (2010): 772-78. Digital file.

85. Farris, Stefano, et al. "Gelatinepectin composite films from polyion-complex hydrogels." *Food Hydrocolloids* 25 (2011): 61-70. Digital file.

86. Feng, Qian, et al. "Self-assembly and characterization of polyelectrolyte complex films of hyaluronic acid/chitosan." *Colloids and Surfaces A* 257–258 (2005): 85-88. Digital file.

87. Ferris CJ, Panhuis M. "Conducting bio-materials based on gellan gum hydrogels" *Soft Matter* 5 (2009): 3430-3437. Digital file.

88. Food and Drug Administration. "Guidance for Resorbable Adhesion Barrier Devices for Use in Abdominal and/or Pelvic Surgery; Guidance for Industry" *CDRH* Document issued on: June 18.2002. Digital file.

89. Fournier, N., and C. J. Doillon. "In Vitro Angiogenesis in Fibrin Matrices Containing Fibronectin or Hyaluronic Acid." *Cell Biology International Reports* 16.12 (1992): 1251-63. Digital file.

90. Friedrich K, Fakirov S, Zhang Z. *Polymer Composites: from nano to macro-scale* Springer, New York. (2005). Print.

91. Fujie T, Matsutani N, Kinoshita M, Okamura Y, Saito A, Takeoka S. "Adhesive, flexible, and robust polysaccharide nanosheets integrated for tissue-defect repair" *Advanced Functional Materials* 19 (2009): 2560-2568. Digital file.

92. Furukawa J. *Physical Chemistry of Polymer Rheology*. Kodansha, 2003. Print.

93. Gago, L. April, et al. "Seprafilm® (modified hyaluronic acid and carboxymethylcellulose) acts as a physical barrier." *Fertility and Sterility* 80.3 (2003): 612-16. Digital file.

94. Gaillard Y, Girard M, Monge G, Burr A, Darque Ceretti E, Felder E. "Superplastic behavior of rosin/beeswax blends at room temperature" *J Applied Polymer Science* 128 (2013): 2713-2719. Digital file.

95. Gamini, Amelia, et al. "Structural Investigations of Cross-linked Hyaluronan." *Biomaterials* 23 (2002): 1161-67. Digital file.

96. Garcia MA, Pinotti A, Martino M, Zaritzky N. "Electrically treated composite FILMS based on chitosan and methylcellulose blends" *Food Hydrocolloids* 23 (2009): 722-728. Digital file.

97. Go, A. K, et al. "PEG-Containing Polymeric Films and Gels as Postoperative Tissue Adhesion Barriers." *Key Engineering Materials*: 373-76. Print.

98. Goetz, Walter. "Curl In Multilayer PA/PE Film." *TAPPI 2002 PLACE Conference*: 1-8. Digital file.

99. Gong JP, Katsuyama Y, Kurokawa T, Osada Y. "Double-network hydrogels with extremely high mechanical strength" *Advanced Materials* 15.14 (2003): 1155-1158. Digital file.

100. Gottlieb HE, Kotlyar V, Nudelman A. "NMR Chemical Shifts of Common Laboratory Solvents as Trace Impurities" *The Journal of Organic Chemistry*. 62 (1997): 7512-7515. Digital file.

101. Grant GT, Morris ER, Rees DA, Smith PJC, Thom D. "Biological interactions between polysaccharides and divalent cations: The egg-box model." *FEBS Letters*. 32.1 (1973): 195-198.

102. Gryczka U, Dondi D, Chmielewski AG, Migdal W, Buttafava A, Faucitano A. "The mechanism of chitosan degradation by gamma and e-beam irradiation" *Radiation Physics and Chemistry* 78 (2009): 543-548. Digital file.

103. Greenawalt, Keith E, et al. "A Membrane Slurry Reduces Postoperative Adhesions in Rat Models of Abdominal Surgery." *Journal of Surgical Research* 168 (2011): e25-e30. Digital file.

104. Guida, Maurizio, et al. "Effectiveness of auto-crosslinked hyaluronic acid gel in the prevention of intrauterine adhesions after hysteroscopic surgery: a prospective, randomized, controlled study." *Human Reproduction* 19.6 (2004): 1461-64. Digital file.

105. Haney, A. F., and Elissa Doty. "A barrier composed of chemically crosslinked hyaluronic acid (Incert) reduces postoperative adhesion formation." *Fertility and Sterility* 70.1 (1998): 145-51. Digital file.

106. Haque MA, Kurokawa T, Gong JP. "Super tough double network hydrogels and their application as biomaterials" *Polymer* 53 (2012): 1805-1822. Digital file.

107. Harding, Stephen E. "Some observations on the effects of bioprocessing on biopolymer stability." *Journal of Drug Targeting* 18.10 (2010): 732-49. Digital file.

108. Harris, Elizabeth S., Raymond F. Morgan, and George T. Rodeheaver. "Analysis of the kinetics of peritoneal adhesion formation in the rat and evaluation of potential antiadhesive agents." *Surgery* 117.6 (1995): 663-69. Digital file.

109. Harris, ML. "The use of silver foil to prevent adhesions in brain surgery." *JAMA* 42 (1904): 763-765. Digital file.

110. Haug A and Smidsrod O. "The effect of divalent metals on the properties of alginate solutions. II. Comparison of different metal ions." *Acta Chemica Scandinavica* 19 (1965): 341-351.

111. Haug A and Larsen B."Quantitative determination of the uronic acid composition of alginates." *Acta Chem Scand* 16 (1962): 1908-18. Digital file.

112. Henry, Francis P, et al. "Improving electrophysiologic and histologic outcomes by photochemically sealing amnion to the peripheral nerve repair site." *Surgery* 145.3 (2008): 313-21. Digital file.

113. Herington, Jennifer L, et al. "Development and prevention of postsurgical adhesions in a chimeric mouse model of experimental endometriosis." *Fertility and Sterility* 95.4 (2011): 1295-302. Digital file.

114. Hillberg, Anna L., Christina A. Holmes, and Maryam Tabrizian. "Effect of genipin cross-linking on the cellular adhesion properties of layer-by-layer assembled polyelectrolyte films." *Biomaterials* 30 (2009): 4463-70. Digital file.

115. Himeda, Y, et al. "Adhesion Preventive Effect of a Novel Hyaluronic Acid Gel Film in Rats." *Journal of International Medical Research* 31 (2003): 509-16. Digital file.

116. Holmdahl L, Risberg B, Beck DE, Burns JW, Chegini N, diZerega GS, Ellis H. Adhesions: pathogenesis and prevention-panel discussion and summary. *Eur J Surg Suppl*. 1997;(577):56-62. Review. Digital File.

117. Hori, Yuki, Amy M. Winans, and Darrell J. Irvine. "Modular injectable matrices based on alginate solution/microsphere mixtures that gel in situ and co-deliver immunomodulatory factors." *Acta Biomaterialia* 5 (2009): 969-82. Digital file.

118. Hsu, Shan-hui, et al. "Evaluation of Chitosan-alginate-hyaluronate Complexes Modified by an RGD-containing Protein as Tissue-engineering Scaffolds for Cartilage Regeneration." *Artificial Organs* 28.8 (2004): 693-703. Digital file.

119. Hu J, Hiwatashi K, Kurokawa T, Liang SM, Wu ZL, Gong JP. "Microgel-reinforced hydrogel films with high mechanical strength and their visible mesoscale fracture structure" *Macromolecules* 44 (2011): 7775-7781. Digital file.

120. Hunt, N. C, et al. "Encapsulation of fibroblasts causes accelerated alginate hydrogel degradation." *Acta Biomaterialia* 6 (2010): 3649-56. Digital file.

121. Ibrahim, S. "Characterization of glycidyl methacrylate – Crosslinked hyaluronan hydrogel scaffolds incorporating elastogenic hyaluronan oligomers." *Acta Biomaterialia* 7 (2011): 653-65. Digital file.

122. Ibrahim, Samir, Qian K. Kang, and Anand Ramamurthi. "The impact of hyaluronic acid oligomer content on physical, mechanical, and biologic properties of divinyl sulfone-crosslinked hyaluronic acid hydrogels." *Journal of Biomedical Materials Research Part A* (2009): 353-70. Digital file.

123. Ip, W. Y., et al. "ADHESION FORMATION AFTER NERVE REPAIR: AN EXPERIMENTAL STUDY OF EARLY PROTECTED MOBILIZATION IN THE RABBIT." *Journal of Hand Surgery* 25.6 (2000): 582-84. Digital file.

124. ISO 10993-5:2009. "Biological evaluation of medical devices – Part 5: Tests for *in vitro* cytotoxicity". AAMI. Single license. Digital file.

125. Ito, Taichi, et al. "The prevention of peritoneal adhesions by in-situ cross-linking hydrogels of hyaluronic acid and cellulose derivatives." *Biomaterials* 28.6 (2007): 975-83. Digital file.

126. Jansson, A., and F. Thuvander. "Influence of thickness on the mechanical properties for starch films." *Carbohydrate Polymers* 56.4 (2004): 499-503. Digital file.

127. Jeon O, Song SJ, Lee KJ, Park MH, Lee SH, Hahn SK, Kim S, Kim BS. "Mechanical properties and degradation behaviors of hyaluronic acid hydrogels crosslinked at various crosslinking densities" *Carbohydrate Polymers* 70 (2007): 251-257. Digital file.

128. Jeon, Oju, et al. "Photocrosslinked alginate hydrogels with tunable biodegradation rates and mechanical properties." *Biomaterials* 30 (2009): 2724-34. Digital file.

129. Jeans, L. A., T. Gilchrist, and D. Healy. "Peripheral nerve repair by means of a flexible biodegradable glass fibre wrap: A comparison with microsurgical

epineurial repair." *Journal of Plastic, Reconstructive & Aesthetic Surgery* 60 (2006): 1302-08. Digital file.

130. Julian TN, Radebaugh GW, Wisniewski SJ. "Permeability characteristics of calcium alginate films" *JCR* 7 (1988): 165-169. Digital file.

131. Kadi, Shirin, et al. "Alkylamino Hydrazide Derivatives of Hyaluronic Acid: Synthesis, Characterization in Semidilute Aqueous Solutions, and Assembly into Thin Multilayer Films." *Biomacromolecules* 10 (2010): 2875-84. Digital file.

132. Kasada R, Lee SG, Isselin J, Lee JH, Omura T, Kimura A, Okuda T, Inoue M, Ukai S, Ohnuki S, Fujisawa T, Abe F. "Anisotropy in tensile and ductile-brittle transition behavior of ODS ferritic steels" *J of Nuclear Materials* 417.1-3. (2011): 180-184. Digital file.

133. Kasimcan, Mustafa Omur, et al. "Effectiveness of the biophysical barriers on the peridural fibrosis of a postlaminectomy rat model: An experimental research." *Injury* 42 (2011): 778-81. Digital file.

134. Kayaoglu HA, Ozkan N, Hazinedaroglu SM, et al. "An assessment of the effects of two types of bioresorbable barriers to prevent postoperative intra-abdominal adhesions in rats." *Surg Today* 35 (2005): 946. Digital file.

135. Khan TA, Peh KK and Ch'ng HS. "Mechanical, Bioadhesive Strength and Biological Evaluations of Chitosan Films for Wound Dressing". *J. Pharm. Pharmaceut. Sci.*, 3.3 (2000)**:** 303-311. Digital file.

136. Kim, Jong Oh, et al. "Development of Clindamycin-Loaded Wound Dressing with Polyvinyl Alcohol and Sodium Alginate." *Biological Pharmaceutical Bulletin* 31.12 (2008): 2277-82. Digital file.

137. Kim, Yoo-Joo, Kee-Jong Yoon, and Sohk-Won Ko. "Preparation and Properties of Alginate Superabsorbent Filament Fibers Crosslinked with Glutaraldehyde." *Journal of Applied Polymer Science* (2000): 1797-804. Digital file.

138. Klock, Gerd, et al. "Production of purified alginates suitable for use in immunoisolated transplantation." *Applied Microbiology and Biotechnology* 40 (1994): 638-43. Digital file.

139. Kolarik J, Fambri L, Pegoretti A, Penati A. "Ternary Polymer Blends: Prediction of mechanical properties for various phase structures". *Polymer for Advanced Technologies* 11 (2000): 75-81. Digital file.

140. Kurt, G, et al. "Comparison of Oxiplex and Gore-Tex effectivity in an experimental peridural fibrosis model." *Neurocingia* 20 (2009): 360-66. Digital file.

141. Lalountas, Miltiadis A, et al. "Preventing intraperitoneal adhesions with atorvastatin and sodium hyaluronate/carboxymethylcellulose: a comparative study in rats." *The American Journal of Surgery* 200 (2010): 118-23. Digital file.

142. Lauder, Chris IW, Andrew Strickland, and Guy J. Maddern. "Abdominal adhesion prevention, time to change our everyday practice?ans_5273 306..311." *ANZ Journal of Surgery* 80.5 (2010): 306-07. Digital file.

143. Leach, Jennie B., and Christine E. Schmidt. "Characterization of protein release from photocrosslinkable hyaluronic acid-polyethylene glycol hydrogel tissue engineering scaffolds." *Biomaterials* 26.2 (2005): 125-35. Digital file.

144. Leach, Jennie Baier, et al. "Photocrosslinked Hyaluronic Acid Hydrogels: Natural, Biodegradable Tissue Engineering Scaffolds." *Biotechnology and Bioengineering* 82.5 (2003): 578-89. Digital file.

145. Lee, Jin W., Richard D. Ashby, and Donald F. Day. "Role of acetylation on metal induced precipitation of alginates." *Carbohydrate Polymers* 29 (1996): 337-45. Digital file.

146. Lee, Yuhan, et al. "Thermo-sensitive, injectable, and tissue adhesive sol–gel transition hyaluronic acid/ pluronic composite hydrogels prepared from bio-inspired catechol-thiol reaction." *Soft Matter* 6 (2010): 977-83. Digital file.

147. Leiss, Michael, et al. "The role of integrin binding sites in fibronectin matrix assembly in vivo." *Cell Biology* 20 (2008): 502-07. Digital file.

148. Levine, Mario M, et al. "ostoperative intra-abdominal collections using a sodium hyaluronate-carboxymethylcellulose (HA-CMC) barrier at the time of laparotomy for ovarian, fallopian tube, or primary peritoneal cancers." *Gynecologic Oncology* 115 (2009): 204-08. Digital file.

149. Li Q, Wang D, Elisseeff JH. Heterogeneous-Phase Reaction of Glycidyl Methacrylate and Chondroitin Sulfate: Mechanism of Ring-Opening-Transesterification Competition. *Macromolecules* 36 (2003): 2556-2562. Digital file.

150. Lin WC, Fan W, Marcellan A, Hourdet D, Creton C. "Large strain and fracture properties of poly(dimethylacrylamide)/silica hybrid hydrogels" *Macromolecules* 43 (2010): 2554-2563. Digital file.

151. Lindenhayn K, Perka C, Spitzer RS, Heilmann HH, Pommerening K, Mennicke J, Sittinger M. "Retention of hyaluronic acid in alginate beads: Aspects for in vitro cartilage engineering". *J Biomed Mater Res* 44 (1999): 149-155. Digital file.

152. Liu, Danqing, et al. "Single-composition three-dimensionally morphing hydrogels." *Soft Matter* 9.588 (2013): n. pag. Digital file.

153. Liu, Jun, et al. "Mitomycin C-polyethylene glycol controlled-release film inhibits collagen secretion and induces apoptosis of fibroblasts in the early wound of a postlaminectomy rat model." *The Spine Journal* 10 (2010): 441-47. Digital file.

154. Liu, Yanchun, et al. "Crosslinked hyaluronan hydrogels containing mitomycin C reduce postoperative abdominal adhesions." *Fertility and Sterility* 83.1 (2005): 1275-83. Digital file.

155. Livnat, Maya, Rafael Beyar, and Dror Seliktar. "Endoluminal hydrogel films made of alginate and polyethylene glycol: Physical characteristics and drug-eluting properties." *J Biomed Mater Res A* 75.3 (2005): 710-22. Digital file.

156. Lo, Hsien-Yi, Hsuan-Ting Kuo, and Yi-You Huang. "Application of Polycaprolactone as an Anti-Adhesion Biomaterial Film." *Artificial Organs* 34.8 (2010): 648-53. Digital file.

157. Lodge, Andrew J, et al. "A Novel Bioresorbable Film Reduces Postoperative Adhesions After Infant Cardiac Surgery." *Ann Thorac Surg* 86 (2008): 614-21. Digital file.

158. Lord, Megan S., et al. "Protein adsorption on derivatives of hyaluronic acid and subsequent cellular response." *Journal of Biomedical Materials Research Part A* (2009): 635-46. Digital file.

159. Luo, Yi, Kelly R. Kirker, and Glenn D. Prestwich. "Cross-linked hyaluronic acid hydrogel films: new biomaterials for drug delivery." *Journal of Controlled Release* 69.1 (2000): 169-84. Digital file.

160. Macleod GS, Fell JT and Collett JH. "Studies on the Physical Properties of Mixed Pectin/Ethylcellulose Films Intended for Colonic Drug Delivery." *Int. J. Pharm.,* 157 (1997): 53-60. Digital file.

161. Malladi DP, Scherer JR, Kint S, Bailey GF. "Water in polymer membranes. 3. Water sorption and pore volume in cellulose-acetate films" *J Membrane Science* 19.2 (1984): 209-231. Digital file.

162. Martin A, Bustamante P and Chun AHC. Physical Pharmacy. (Fourth ed.). Lippincott Williams & Wilkins, Philadelphia, (2001): 556-594. Print.

163. Massie, Jennifer B, et al. "Topical high molecular weight hyaluronan reduces radicular pain post laminectomy in a rat model." *The Spine Journal* 5.5 (2005): 494-502. Digital file.

164. McMaster LP. Aspects of liquid-liquid phase transition phenomena in multicomponent polymeric systems. Copolymers, Polyblends and Composites Chapter 5. *Advances in Chemistry* 142 (1975): 43-65. Print.

165. Menard, Kevin. *Dynamic Mechanical Analysis: A Practical Introduction*. CRC Press. Boca Raton. (2008). Print.

166. Menard, Martin, et al. "Role of Protein Contaminants in the Immunogenicity of Alginates." *Journal of Biomedical Materials Research Part B: Applied Biomaterials* (2009): 333-40. Digital file.

167. Mensitieri, M, et al. "Viscoelastic properties modulation of a novel autocrosslinked hyaluronic acid polymer." *Journal of Materials Science: Materials in Medicine* 7 (1996): 695-98. Digital file.

168. Menzies D, and Ellis H. "Intestinal obstruction from adhesions--how big is the problem?" *Ann R Coll Surg Engl*. 72.1 (1990) 60–63.

169. Meyers, M.A., et al. "Biological materials: A materials science approach." *Journal of the Mechanical Behavior of Biomedical Materials* (2010): 1-32. Digital file.

170. Mi, Fwu-Long, et al. "In vivo biocompatibility and degradability of a novel injectable-chitosan-based implant." *Biomaterials* 23 (2002): 181-91. Digital file.

171. Mjahed, Hajare, et al. "Micro-stratified architectures based on successive stacking of alginate gel layers and poly(L-lysine)–hyaluronic acid multilayer films aimed at tissue engineering." *Soft Matter* 4 (2008): 1422-29. Digital file.

172. Mosehebi, Afshin, et al. "A Novel Use of Alginate Hydrogel as Schwann Cell Matrix." *Tissue Engineering* 7.5 (2001): 525-34. Digital file.

173. Mosesson, Michael W., Kevin R. Siebenlist, and David A. Meh. "The Structure and Biological Features of Fibrinogen and Fibrin." *Annals New York Academy of Sciences* (2001): 11-30. Digital file.

174. Murano, Erminio, et al. "Hyaluronan: From Biomimetic to Industrial Business." *Natural Product Communications* 6.4 (2011): 555-72. Digital file.

175. Na, Seung Yeon, et al. "Hyaluronic acid/mildly crosslinked alginate hydrogel as an injectable tissue adhesion barrier." *J Mater Sci: Mater Med* (2012): n. pag. Digital file.

176. Nagahama K, Shimizu K, Ichimura S, Takahashi A, Ouchi T, Ohya Y. "Biodegradable stereocomplex materials of polylactide-grafted dextran exhibiting soft and tough properties in dry and wet states" *J Polymer Sci Part A: Polym Chem* 50 (2012): 2669-2676. Digital file.

177. Nagarsenker MS and Hegde DD. "Optimization of the Mechanical Properties and Water-Vapor Transmission Properties of Free Films of Hydroxypropylmethylcellulose." *Drug Dev. Ind. Pharm.,* 25.1 (1999): 95-98. Digital file.

178. Namba, Jiro, et al. "Modulation of Peritendinous Adhesion Formation by Alginate Solution in a Rabbit Flexor Tendon Model." *Journal of Biomedical Materials Research Part B* (2006): 273-79. Digital file.

179. Napier M, and Hadler NM. "Effect of calcium on structure and function of a hyaluronic acid matrix: Carbon-13 nuclear magnetic resonance analysis and the diffusional behavior of small solutes" *Proc. Natl. Acad. Sci* 75.5 (1978): 2261-2265. Digital file.

180. Nishimura K, Blume P, Ohgi S, Sumpio BE. "Effect of different frequencies of tensile strain on human dermal fibroblast proliferation and survival". *Wound Repair and Regeneration*. 15 (2007): 646-656. Digital file.

181. Oerther, Sandra, et al. "Hyaluronate-alginate combination for the preparation of new biomaterials: investigation of the behaviour in aqueous solutions." *Biochimica et Biophysica Acta* 1426 (1999): 185-94. Digital file.

182. Oerther, Sandra, et al. "Hyaluronate-Alginate Gel as a Novel Biomaterial: Mechanical Properties and Formation Mechanism." *Biotechnology and Bioengineering* 63.2 (1999): 206-15. Digital file.

183. Ossipov, Dmitri A, et al. "Functionalization of Hyaluronic Acid with Chemoselective Groups via a Disulfide-Based Protection Strategy for In Situ Formation of Mechanically Stable Hydrogels." *Biomacromolecules* 11 (2010): 2247-54. Digital file.

184. Ozdemir, Ozgur, et al. "Topical use of colchicine to prevent spinal epidural fibrosis in rats." *Neurological Research* 32.10 (2010): 1117-20. Digital file.

185. Park, Jun Seok, et al. "An Assessment of the Effects of a Hyaluronan-Based Solution on Reduction of Postsurgical Adhesion Formation in Rats: A Comparative Study of Hyaluronan-Based Solution and Two Film Barriers." *Journal of Surgical Research* (2009): 1-7. Digital file.

186. Park, Si-Nae, et al. "Preparation and characterization of biodegradable anti-adhesive membrane for peritoneal wound healing." *J Mater Sci: Mater Med* 18 (2007): 475-82. Digital file.

187. Park, Won Seo, et al. "Anti-adhesive Effect and Safety of Sodium Hyaluronate and Sodium Carboxymethyl Cellulose Solution in Thyroid Surgery." *Asian Journal of Surgery* 33.1 (2010): 25-30. Digital file.

188. Paul DR and Bucknall CB. *Polymer Blends*. Wiley, New York. (2000). Print.

189. Pawde SM and Deshmukh K. "Characterization of polyvinyl alcohol/gelatin blend hydrogel films for biomedical applications" *J Appl Polym Sci* 109 (2008): 3431-3437. Digital file.

190. Periera R, Carvalho A, Vaz DC, Gil MH, Mendes A, Bartolo P. "Development of novel alginate based hydrogel films for wound healing applications" *Int J of Biological Macromolecules* 52 (2013): 221-230. Digital file.

191. Piana, Stefano, Manijeh Reyhani, and Julian D. Gale. "Simulating micrometre-scale crystal growth from solution." *Nature* 438.3 (2005): 70-73. Digital file.

192. Picart C., *et al*. "Molecular basis for the explanation of the exponential growth of polyelectrolyte multilayers." *Proc. Natl. Acad. Sci.* 99.20 (2002): 12531-12535. Digital file.

193. Pitarresi, G, et al. "Crosslinked hyaluronan with a protein-like polymer: Novel bioresorbable films for biomedical applications." *Journal of Biomedical Materials Research Part A* (2007): 413-24. Digital file.

194. Prestwich, Glenn D., and Jing-wen Kuo. "Chemically-Modified HA for Therapy and Regenerative Medicine." *Current Pharmaceutical Biotechnology* 9 (2008): 242-45. Digital file.

195. Preul, Mark C, et al. "Application of a new hydrogel dural sealant that reduces epidural adhesion formation: evaluation in a large animal laminectomy model." *J Neurosurg: Spine* 12 (2010): 381-90. Digital file.

196. Price, Richard D., M. G. Berry, and Harshad A. Navsaria. "Hyaluronic acid: the scientific and clinical evidence." *Journal of Plastic, Reconstructive & Aesthetic Surgery* 60 (2007): 1110-19. Digital file.

197. Quinn FX, Kampff E, Smyth G, McBrierty VJ. "Water in Hydrogels. 1. A study of water in poly (N-vinyl-2-pyrrolidone/methyl methacrylate) copolymer." *Macromolecules* 21 (1988): 3191.3198. Digital file.

198. Rajab, Taufiek Konrad, et al. "A Direct Comparison of Seprafilm®, Adept, Intercoat, and Spraygel for Adhesion Prophylaxis1." *Journal of Surgical Research* 161 (2010): 246-49. Digital file.

199. Raz, Neta, et al. "Microgels with an Interpenetrating Network Structure as a Model System for Cell Studies." *Macromolecules* 43 (2010): 7277-81. Digital file.

200. Reed, Karen L., Arthur F. Stucchi, and James M. Becker. "The Peritoneal Fibrinolytic Response to Conventional and Prolonged Surgery Is Similar." *Journal of Surgical Research* 152 (2009): 175-77. Digital file.

201. Reijnen, M. M. P. J., R. P. Bleichrodt, and H. Van Goor. "Pathophysiology of intra-abdominal adhesion and abscess formation, and the effect of hyaluronan." *British Journal of Surgery* 90.5 (2003): 533-41. Digital file.

202. Reijnen, Michel M P J, et al. "Polyanionic Polysaccharides Reduce Intra-abdominal Adhesion and Abscess Formation in a Rat Peritonitis Model1." *Journal of Surgical Research* 101 (2001): 248-53. Digital file.

203. Reis AV, Fajardo AR, Schuquel ITA, Guilherme MR, Vidotti GJ, Rubira AF, Muniz EC. "Reaction of Glycidyl Methacrylate at the Hydroxyl and Carboxylic Groups of Poly(vinyl alcohol) and Poly(acrylic acid): Is This Reaction Mechanism Still Unclear?" *JOC* 74 (2009): 3750-3757. Digital file.

204. Riall TS, et al. "Resection Benefits Older Adults with Locoregional Pancreatic Cancer Despite Greater Short-Term Morbidity and Mortality" *JOURNAL OF THE AMERICAN GERIATRICS SOCIETY* 59.4 (2011): 647-654.

205. Rinaudo, M. "Properties and degradation of selected polysaccharides: hyaluronan and chitosan." *Corrosion Engineering, Science and Technology* 42.4 (2007): 324-34. Digital file.

206. Roberts, Meredith Colleen. "NEW IN SITU CROSSLINKING CHEMISTRIES FOR HYDROGELATION." Diss. The University of Utah, 2008. Print.

207. Roger S, Talbot D, Bee A. "Preparation and effect of Ca^{2+} on water solubility, particle release and swelling properties of magnetic alginate films" *J Magnetism and Magnetic Materials* 305 (2006): 221-227. Digital file.

208. Ropes,M.W., Robertson,W.B., Rossmeisl, E.C., Peabody,R. B. & Bauer, W. *Acta Med. Scand. Suppl.* 196 (1947): 700- 744. Print.

209. Rubert M, Alonso-Sande M, Monjo M, Ramis JM. "Evaluation of alginate and hyaluronic acid for their use in bone tissue engineering" *Biointerphases* 7.1-4 (2012): 44. Digital file.

210. Rubin, Mark G. "Quantifying Facial Volumizing." *Dermatol Surg* 36 (2010): 329-30. Digital file.

211. Sahoo, Sujata, et al. "Hydrolytically Degradable Hyaluronic Acid Hydrogels with Controlled Temporal Structures." *Biomacromolecules* 9 (2008): 1088-92. Digital file.

212. Sartori C, Finch DS, Ralph B. "Determination of the cation content of alginate thin films by *FT*i.r. spectroscopy" *Polymer* 38.1 (1997): 43-51. Digital file.

213. Sakai, Shinji, and Koei Kawakami. "Synthesis and characterization of both ionically and enzymatically cross-linkable alginate." *Acta Biomaterialia* 3 (2007): 495-501. Digital file.

214. Sawhney, Amarpreet S, et al. "Optimization of photopolymerize bioerodible hydrogen properties for adhesion prevention." *Journal of Biomedical Materials Research* 28 (1994): 831-38. Digital file.

215. Schanté, Carole E, et al. "Chemical modifications of hyaluronic acid for the synthesis of derivatives for a broad range of biomedical applications." *Carbohydrate Polymers* 85 (2011): 469-89. Digital file.

216. Schnüriger, Beat, et al. "Prevention of postoperative peritoneal adhesions: a review of the literature." *The American Journal of Surgery* 201.1 (2011): 111-21. Digital file.

217. Schonmann, Ron, et al. "Intercoat Gel (Oxiplex): Efficacy, Safety, and Tissue Response in a Laparoscopic Mouse Model." *Journal of Minimally Invasive Gynecology* 16.2 (2009): 188-94. Digital file.

218. Schug-PaB, Christine, et al. "Does the additional application of a polylactide film (SurgiWrap) to a lightweight mesh (TiMesh) reduce adhesions after laparoscopic intraperitoneal implantation procedures? Experimental results obtained with the laparoscopic porcine model." *Surg Endosc* 22(2008): 2433-39. Digital file.

219. Schultz KM, Baldwin AD, Kiick KL, Furst EM. "Measuring the modulus and reverse percolation transition of a degrading hydrogel" *ACS Macro Letters* 1 (2012): 706-708. Digital file.

220. Seidlits, Stephanie K. et al. "The effects of hyaluronic acid hydrogels with tunable mechanical properties on neural progenitor cell differentiation." *Biomaterials* 31 (2010): 3930-40. Digital file.

221. Sevag, M. G. "Eine neue physikalische Enteiweissungsmethode zur Darstellung biologisch wirksamer Substanzen. Isolierung von Kohlenhydraten aus Huhnereiweiss und Pneumococcen." *Biochemische zeitschrift* 273.273 (1934): 419-29. Print.

222. Sezer AD, Hatipoglu F, Cevher E, Ogurtan Z, Bas AL and Akbuga J. "Chitosan Film Containing Fucoidan as a Wound Dressing for Dermal Burn Healing: Preparation and *In vitro/In vivo* Evaluation." *AAPS PharmSciTech*, 8.2 (2007): E1- E8. Digital file.

223. Sheehan JK, Arundel C, Phelps CF. "Effect of the cations sodium, potassium and calcium on the interaction of hyaluronate chains – a light-scattering and viscometric study" *International Journal of Biological Macromolecules* 5.4 (1983): 222-228. Digital file.

224. Siggia ED. Late stages of spinal decomposition in binary-mixtures. *Physical Review A* 20.2 (1979): 595-605. Digital file.

225. Singh, Milind, et al. "Chondrogenic differentiation of neonatal human dermal fibroblasts encapsulated in alginate beads with hydrostatic compression under

hypoxic conditions in the presence of bone morphogenetic protein-2." *Journal of Biomedical Materials Research A* A.00 (2011): 1-13. Digital file.

226. Siri, Shalu, and Christine E. Schmidt. "Photopatterned collagen–hyaluronic acid interpenetrating polymer network hydrogels." *Acta Biomaterialia* 5 (2009): 2385-97. Digital file.

227. Skardal, Aleksander, et al. "Photocrosslinkable Hyaluronan-Gelatin Hydrogels for Two-Step Bioprinting." *Tissue Engineering: Part A* 16.8 (2010): 2675-85. Digital file.

228. Skulason, S, et al. "Evaluation of polymeric films for buccal drug delivery." *PHarmazie* 64 (2009): 197-201. Digital file.

229. Smeds, Kimberly A., and Mark W. Grinstaff. "Photocrosslinkable polysaccharides for in situ hydrogel formation." *Journal of Biomedical Materials Research* 54 (2001): 115-21. Digital file.

230. Smidsrod O. and Haug A. "The effect of divalent metals on the properties of alginate solutions." *Acta Chemica Scandinavica* 19 (1965): 329-340. Digital file.

231. Smidsrod O. and Haug A. "Dependence upon the gel-sol state of the ion-exchange properties of alginates.' *Acta Chemica Scandinavica* 26 (1972): 2063-2074. Digital file.

232. Song, Hyung Jun, et al. "Effects of Three Different Types of Anti-adhesive Agents in a Rat Abdominal Wall Defect Model." *J Korean Surg Soc* 77 (2009): 7-14. Digital file.

233. Stauffer D and Aharony A. *Introduction to Percolation Theory,* 2nd edition. Taylor & Francis e-Library. London: 1994. Print.

234. Stern R. "Devising a pathway for hyaluronan catabolism: are we there yet?" *Glycobiology* 13 (2003): 105R–15R. Digital file.

235. Sufiyarov IF. "Experimental validation for the use of a film on the basis of modified hyaluronic acid for prevention of postoperative peritoneal adhesions". *Bulletin of Experimental Biology and Medicine* 144.2 (2007): 269-271.

236. Sulaiman, Hassan, et al. "Presence and Distribution of Sensory Nerve Fibers in Human Peritoneal Adhesions." *Annals of Surgery* 234.2 (2001): 256-61. Digital file.

237. Sun, Guoming, Xian-Zheng Zhang, and Chih-Chang Chu. "Formulation and characterization of chitosan-based hydrogel films having both temperature and pH sensitivity." *Journal of Materials Science* 18 (2007): 1563-77. Digital file.

238. Sun JY, Zhao X, Illeperuma WRK, Chaudhuri O, Oh KH, Mooney DJ, Vlassak JJ, Suo Z. "Highly stretchable and tough hydrogels" Nature 133 (2012): 133-136. Digital file.

239. Sun F and Zhitomirsky I. "Electrochemical deposition of composite biopolymer films" *Surface Engineering* 26.7 (2010): 546-551. Digital file.

240. *SurgiWrap: Bioresorbable Adhesion Barrier Film*. San Diego, CA: MAST Biosurgery, 2006. pdf file.

241. Tan, Annie, et al. "The Use of Sodium Hyaluronate–Carboxymethylcellulose (HA-CMC) Barrier in Gynecologic Malignancies: A Retrospective Review of Outcomes." *Annals of Surgical Oncology* 16 (2009): 499-505. Digital file.

242. Tan, Rongwei, et al. "In vitro and in vivo degradation of an injectable bone repair composite" *Polymer Degradation and Stability* 95 (2010): 1736-42. Digital file.

243. Taub, Amy Forman, et al. "Effect of Multisyringe Hyaluronic Acid Facial Rejuvenation on Perceived Age." *Dermatol Surg* 36 (2010): 322-28. Digital file.

244. Thomas, R.C. [speaker], C.E. Schmidt. "Three-Dimensional Hyaluronic Acid Hydrogels Templated by Self-Assembled Poragen Architecture". TERMIS-North America 2011 Conference and Exposition, Houston, TX, December 13, 2011.

245. Thomas, S. "Alginate dressings in surgery and wound management- part 1." *Journal of Wound Care* 9.2 (2000): 56-60. Digital file.

246. Thomas, S. "Alginate dressings in surgery and wound management- part 2." *Journal of Wound Care* 9.3 (2000): 115-119. Digital file.

247. Thomas, S. "Alginate dressings in surgery and wound management- part 3." *Journal of Wound Care* 9.4 (2000): 163-166. Digital file.

248. Tomihata, Kenji, and Yoshito Ikada. "Crosslinking of hyaluronic acid with water-soluble carbodiimide." *Journal of Biomedical Materials Research Part A* (1998): 243-51. Digital file.

249. Tominaga, Taiki, et al. "Thermodynamic Interactions in Double-Network Hydrogels." *J. Phys. Chem. B* 112 (2008): 2903-3909. Digital file.

250. Vallee, Frederic, et al. "Synthesis and rheological properties of hydrogels based on amphiphilic alginate-amide derivatives." *Carbohydrate Research* 344 (2009): 223-28. Digital file.

251. Van der Wal, J B C, et al. "Adhesion Prevention During Laparotomy Long-Term Follow-up of a Randomized Clinical Trial." *Annals of Surgery* 256.6 (2011): 1118-21. Digital file.

252. Vanderhooft, Janssen L., Brenda K. Mann, and Glenn D. Prestwich. "Synthesis and Characterization of Novel Thiol-Reactive Poly(ethylene glycol) Cross-Linkers for Extracellular-Matrix-Mimetic Biomaterials." *Biomacromolecules* 8 (2007): 2883-89. Digital file.

253. Wakeland S, Martinez R, Grey JK, Luhrs CC. "Production of graphene from graphite oxide using urea as expansion-reduction agent" *Carbon* 48.12 (2010): 3463-3470. Digital file.

254. Wang J, Lin L, Cheng Q, Jiang L. "A strong bio-inspired layered PNIPAM-clay nanocomposite hydrogel" *Angewandte Communications* 51 (2012): 4676-4680. Digital file.

255. Wang, L. "Evaluation of sodium alginate for bone marrow cell tissue engineering." *Biomaterials* 24 (2003): 3475-81. Digital file.

256. Wang, Ling Chong, et al. "Biological evaluation of a novel chitosan-PVA-based local delivery system for treatment of periodontitis." *Journal of Biomedical Materials Research Part A* (2008): 1065-76. Digital file.

257. Wang Y and Rahmatalla S. "Human head-neck models in whole-body vibration: effect of posture" *Journal of Biomechanics* 46 (2013): 702-710. Digital file.

258. Wang, Yingjun, et al. "A study on the performance of hyaluronic acid immobilized chitosan film." *Biomedical Materials* 4 (2009): 1-7. Digital file.

259. Ward, Brian C., and Alyssa Panitch. "Abdominal Adhesions: Current and Novel Therapies." *Journal of Surgical Research* 165 (2011): 91-111. Digital file.

260. Way, Tzong-Der, et al. "Preparation and characterization of branched polymers as postoperative anti-adhesion barriers." *Applied Surface Science* 256 (2010): 3330-63. Digital file.

261. Wei, Chang-Zheng, et al. "A thermosensitive chitosan-based hydrogel barrier for post-operative adhesions' prevention." *Biomaterials* 30 (2009): 5534-40. Digital file.

262. Wei, Y. T, et al. "Hyaluronic acid hydrogels with IKVAV peptides for tissue repair and axonal regeneration in an injured rat brain." *Biomedical Materials* 2 (2007): S142-S146. Digital file.

263. Weinstein, Jason S, et al. "The safety and effectiveness of a dural sealant system for use with nonautologous duraplasty materials." *J Neurosurg* 112 (2010): 428-33. Digital file.

264. Wierzbicka-Patynowski, Iwona, and Jean E. Schwarzbauer. "The ins and outs of fibronectin matrix assembly." *Journal of Cell Science* 116 (2003): 3269-326. Digital file.

265. Wiseman, David M. Letter. *Fertility and Sterility* (2005): 771. Digital file.

266. Wiseman, David M, et al. "Evaluation of a fibrin preparation containing tranexamic acid (Adhexil) in a rabbit uterine horn model of adhesions with and without bleeding and in a model with two surgical loci." *Fertility and Sterility* 93.4 (2010): 1045-51. Digital file.

267. Wong, Joyce Y., Jennie B. Leach, and Xin Q. Brown. "Balance of chemistry, topography, and mechanics at the cell–biomaterial interface: Issues and challenges for assessing the role of substrate mechanics on cell response." *Surface Science* 570 (2004): 119-33. Digital file.

268. Xu J, Bai H, Wang M, Xia W, Liu X. "Properties of hyaluronan/PVA-SbQ composite films processed by casting" *Polymers & Polymer Composites* 21.1 (2013): 55-60. Digital file.

269. Xu, Shanshan, et al. "Chemical crosslinking and biophysical properties of electrospun hyaluronic acid based ultra-thin fibrous membranes." *Polymer* 50 (2009): 3762-69. Digital file.

270. Yanagida, Hiroshi, et al. "Cell adhesion and tissue response to hydroxyapatite nanocrystal-coated poly(L-lactic acid) fabric." *Journal of Bioscience and Bioengineering* 108.3 (2009): 235-43. Digital file.

271. Yang, Chiung L., et al. "A novel fibrin gel derived from hyaluronic acid-grafted fibrinogen." *Biomedical Materials* 6 (2011): 1-11. Digital file.

272. Yeo, Yoon, et al. "In situ cross-linkable hyaluronic acid hydrogels prevent post-operative abdominal adhesions in a rabbit model." *Biomaterials* 27.27 (2006): 4698-705. Digital file.

273. Yeo, Yoon, et al. "In Situ Cross-linkable Hyaluronan Hydrogels Containing Polymeric Nanoparticles for Preventing Postsurgical Adhesions." *Annals of Surgery* 245.5 (2007): 819-24. Digital file.

274. Yeo, Yoon, et al. "Prevention of peritoneal adhesions with an in situ cross-linkable hyaluronan hydrogel delivering budesonide." *Journal of Controlled Release* 120 (2007): 178-85. Digital file.

275. Yeo, Yoon, and Daniel S. Kohane. "Polymers in the prevention of peritoneal adhesions." *European Journal of Pharmaceutics and Biopharmaceutics* 68 (2008): 57-66. Digital file.

276. Yoon, Diana M., et al. "Addition of Hyaluronic Acid to Alginate Embedded Chondrocytes Interferes with Insulin-like Growth Factor-1 Signaling In Vitro and In Vivo." *Tissue Engineering: Part A* 15.11 (2009): 3449-59. Digital file.

277. Zawaneh, Peter N., and David Putnam. "Materials in Surgery: A Review of Biomaterials in Postsurgical Tissue Adhesion and Seroma Prevention." *Tissue Engineering: Part B* 14.4 (2008): 377-91. Digital file.

278. Zawko, Scott Andrew, PhD. (2008) Hyaluronic Acid Hydrogel Materials. (Doctoral dissertation). Retrieved from ProQuest Dissertations and Theses. (Accession Order No. [3467798]).

279. Zawko, Scott A., and Christine E. Schmidt. " Crystal templating dendritic pore networks and fibrillar microstructure into hydrogels" *Acta Biomaterials* 6 (2010): 2415-21. Digital file.

280. Zawko, SA, Suri S, Truong Q, Schmidt CE. "Photopatterned anisotropic swelling of dual-crosslinked hyaluronic acid hydrogels"*Acta Biomaterialia* 5.1 (2009): 14-22. Digital file.

281. Zhang, Jing, and Nicholas A. Peppas. "Synthesis and Characterization of pH- and Temperature-Sensitive Poly(methacrylic acid)/Poly(N-isopropylacrylamide)

Interpenetrating Polymeric Networks." *Macromolecules* 33.1 (2002): 102-07. Digital file.

282. Zhang, Qiqiang, et al. "Efficacy and Safety of Seprafilm® for Preventing Postoperative Abdominal Adhesion: Systematic Review and Meta-analysis." *World J Surg* 31 (2007): 2125-31. Digital file.

283. Zhang, Zheng, et al. "Blood compatibility of surfaces with superlow protein adsorption." *Biomaterials* 29 (2008): 4285-91. Digital file.

284. Zhao, W, Jin, X, Cong Y, Liu Y, Fu J. "Degradable natural polymer hydrogels for articular cartilage tissue engineering" *J Chem Technol Biotechnol* 88 (2013): 327–339. Digital file.

285. Zhao, Xihong, et al. "Preparation and Properties of Sodium Carboxymethyl Cellulose-Hyaluronic Acid-Carboxymethyl Chitosan Blend." *Applied Mechanics and Materials* 20-23 (2010): 1157-61. Digital file.

286. Zinther, Nellie Bering, Jens Fedder, and Hans Friis-Andersen. "Noninvasive detection and mapping of intraabdominal adhesions: a review of the current literature." *Surg Endosc* 24 (2010): 2681-86. Digital file.

287. Zohar-Perez, C., I. Chet, and A. Nussinovitch. "Irregular textural features of dried alginate–filler beads." *Food Hydrocolloids* 18 (2004): 249-58. Digital file.